Late Transition Metals Supported by Aryl Ethers and Phenoxides Bearing Pendant Phosphines: Mechanistic Insights Relevant to Ether C-O Bond Cleavage

Thesis by
Guy Anthony Edouard

In Partial Fulfillment of the Requirements
for the Degree of Doctor of Philosophy

CALIFORNIA INSTITUTE OF TECHNOLOGY
Division of Chemistry and Chemical Engineering
Pasadena, California
2015
(Defended on December 17, 2015)

To Mom and Dad

"All things are possible to him who believes."

Mark 9:23

"For me, giving up's way harder than trying."

-Kanye West

ACKNOWLEDGEMENTS

I would like to start by thanking my family for giving me the opportunity to study chemistry at the California Institute of Technology. Thank you, Mom and Dad, for sacrificing for my education and encouraging me through a decade of study since leaving home. You have allowed me to grow and mature while allowing me the freedom to make mistakes and find my way in life – I can never fully repay you for your love and support. To my brother Alan, though I have not been in touch, thank you for being my role model. I look forward to reconnecting with you in the years to come. I consider my friends to be my extended family. To my friends, thank you for supporting me throughout this endeavor. If you are not specifically named here, please know that I appreciate everything you have done for me and consider myself blessed to have such incredible people in my life.

Prof. Theodor Agapie, thank you for taking me into your group, for your instruction, and for your mentorship. When I was looking to join a group in my first months at CalTech, your enthusiasm and passion were both welcoming and inspiring. I recall watching you retrieve multiple powerpoint slides to present during our first meeting together as well as patiently allowing me to present some of my undergraduate research at the chalkboard. If memory serves, our meeting ran over our allotted time, but you graciously made more time for us to complete our discussion. This was not a rare occurrence and speaks to your dedication to supporting our science, which I am grateful for. I walked out of our meeting confident that this was the research group that I wanted to join, one in which my advisor would be accessible to students, involved in

project and experimental design, and an advocate and supporter for science education. I am grateful that I had the opportunity to participiate directly in a collaboration between our group and Beyond Petroleum (BP) and the King Fahd University of Petroleum and Minerals (KFUPM). I learned a great deal from these experiences. Thank you for being generous with your time. Thank you for teaching me how to be a more dedicated scholar, a better experimentalist, and a more responsible professional.

Prof. Jonas Peters, thank you for chairing my thesis committee and being a great mentor over the years. Profs. Dennis Dougherty and Robert Grubbs, thank you for serving on my thesis committee. Your feedback in our meetings has been insightful and formative. Thank you for helping me see the forest through the trees on multiple occasions.

Thank you, Prof. Daniel Kahne and Prof. Greg Tucci for encouraging me to go to graduate school when I was not sure I could graduate from college. Thank you, Prof. Ted Betley for inspiring me to pursue a Ph. D. in chemistry. A young scientist could not ask for a better mentor, and I could never repay you for your guidance through the years and to this day. Thanks to your research group for being a great environment to develop as a chemist. To your first student, Dr. Evan King, thank you for being a great mentor and friend to me.

Thank you to all members of the Agapie Group, past and present. To my cohort in the group, thank you for your support and friendship. Justin Henthorn, thanks for great discussions and always speaking with intelligence and humility. Thank you especially for standing with me at times when I feared that we would not complete

our studies. Josh Wiensch, thanks for teaching me how to run and being our great tinkerer. Kyle Horak, thanks for being a dedicated co-worker and colleague – I look forward to working with you for years to come!

To the graduate students who joined the group before me, thanks for paving the way for our studies and being such incredible teachers. Paul Kelley, thanks for being a great project partner and friend, listening to me for years, and traveling the globe with me. I hope you learned from me a fraction of what I learned from you. Sibo Lin, it was great to work with you, thanks for your patience and training. Emily Tsui, thanks for your tireless interest and support of everyone's projects and organizing so many great trips further than Lake Ave. Madalyn Radlauer, thanks for teaching me many techniques, how to be a safety officer, fun conversations on a regular basis, and lending your husband to us for our basketball team. Steven Chao, thanks for being a pleasant coworker. Jacob Kanady, thanks for being a great friend and conversation about science as well as honest conversation on how to interact with people and manage the lab. Sandy Suseno, thanks for always being so positive, introducing me to the best food in the San Gabriel Valley, and being a great labmate. I look forward to working with you in the future! Davide Lionetti, thanks for being our great social manager and conversations about football and science.

To the post-doctoral researchers that I have worked with, thanks for sharing your skills and expertise with us. Dave Herbert, thanks for your mentorship early on in my career and continued support of my research – I consider myself lucky to have had a chance to work directly with such a fantastic scientist. Po-Heng Lin, you had a

great, optimistic attitude throughout your time here, thanks for keeping us motivated – first drinks on me when I visit Taiwan. Graham de Ruiter, thanks for being a great friend. One of my fondest memories in graduate school is receiving a phone call from you after sleeping in past my alarm just to check if I was ill or needed anything and ultimately to encourage me to get of bed! Thanks for bringing your work ethic and positivity to the lab. Alejo Lifschitz, thanks for being a great officemate and your incredible scientific insight. Gyeonsghin Choi, thanks for being a great project partner and friend. Zhiji Han, thanks for always be pleasant and helpful to me. Thanks Siti Riduan for great conversations, reading an overwhelming amount of this thesis in the form of rough drafts, and being our "Claire Huxtable."

To the students who started their Ph. D. studies after me, your excitement about chemistry has always been refreshing. Thank you for the energy you bring to the laboratory with each class. Joshua Buss, thanks for being tireless in synthesis, building and maintaining equipment, and helping students. You are truly an all-star. Marcus Low, Jessica Sampson, and Heui Beom Lee, thanks for helpful discussions and being such supportive labmates. Chris Reed, Ryan Ribson, and Nate Hirscher, thanks for listening to me rant as your officemate, hoodmate, and boxmate respectively. I look forward to the great things you will all do. Thanks to all the undergraduate students I have spent time working with – Kurtis Carsch, Bogan Dimitriu, Ruomeng Wan, Jeffrey Rosenberg, Aya Buckley, Chung-Sun Chen, Christine Cheng, Michael Desanker, Jennifer Karolewski, Daniel Kim, Nadia Lara, Katherine Lee, Eva Nichols, and Agnes Thorarinsdotter. Thanks to the visiting scholars as well – Aimee Bryan, Yuji Nishii,

and Jihae Park. It is impossible to do thesis research alone, and I am glad that I have been able to complete my research alongside all of you.

I am grateful to the members of the Division of Chemistry and Chemical Engineering who I have had the pleasure of interacting with – faculty, students, and researchers. This is truly a special place to be a scientist, and I have greatly enjoyed being part of such a great community. Though I acknowledge here a few whom I have had specific interactions with, I truly feel that I could list all the names of the department if I had the space. Thanks Bruce Brunschwig and Jay Winkler for allowing me to be a teaching assistant for the Chemistry 3x course and for being so kind and supportive since. Thanks Prof. John Bercaw for being a great instructor and mentor. To Prof. Sarah Resiman, Prof. Bercaw, Jay Labinger, Prof. Peters, and the late Dr. Mike Day, thank you for being such great instructors. Years after your classes I find myself referring to notes and references you first presented to me which is one of the many signs of your incredible talents as educators. Thanks to Ian Tonks, Taylor Lenton, Rachel Klet, Tom Teets, Aaron Sattler, Keith Steelman, and the Bercaw Group for truly being a wealth of knowledge for our young group. Thanks to John Anderson, Henry Fong, Jon Rittle, Sid Creutz, and many others in the Peters Group for helpful discussions. John and Henry, thanks for captaining our intramural basketball teams and getting me back out on the court after years away! Thanks to Oliver Shafaat, Jeff Warren, Wes Sattler, and the Gray Group for helpful discussions as well. The Resiman and Stoltz groups have been great to interact with on athletic fields and courts as well as in scientific discourse, I'm grateful for all of our

interactions. Thank you Prof. Harry Gray for making our lecture series so enjoyable to attend. Thanks to Ariel Furst, Alyson Weidmann, Joey Varghese, Ryan Henning, Adam Neilander, Kyra Lee, and all our downstairs neighbors in the Barton, Heath, and Lewis Groups for pleasant conversations in the Noyes hallways and great evenings outside of the lab as well. Thanks to Connie Wang and the Miller Group for making it out to the basketball court with us many times. Thank you Professors Thomas Miller and Brian Stoltz for always taking the time to greet me and ask me about my progress, you cultivate a fantastic environment on this campus and I deeply appreciate it. Thanks to Andrew Wang, Matt Griffin, Helen Yu and the Hsieh-Wilson group and thanks to Nick Swisher, Brendan Quigley, Keith Keitz, Chris Daeffler Pablo Guzman, and the Grubbs' Group for being great colleagues.

Our staff at Caltech has been phenomenal to interact with. Thank you, Mona Shahgholi, Nassem Torian, David VanderVelde, Larry Henling, and Mike Takase. David, you have always been willing to share your wealth of knowledge with all of the students here, thanks for running a world-class NMR laboratory and for allowing me to serve as a graduate assistant in the facility. Larry, thank you for being so incredibly meticulous and perservant with samples that I have brought to you for X-ray diffraction. Thank you for your advancement of our research and your friendship. Thank you, Rick Gerhart, for solving the many crises I inadvertently caused by breaking glassware. Thank you, Agnes Tong, for dedication to the students of the department and their well-being. Thank you, Joe Drew, for your dedication as well. There was never a leak or crack too small or too big for you too help us to repair,

thanks for maintaining the high standards of our facilities. And thank you to the Caltech Center for Diversity and its staff, it has greatly enriched my last few years and I regret not connecting with it sooner.

Thanks to everyone who helped me outside of the lab. I will acknowledge here specifically my roommates: Johnny Chapman, Khai Xiong, Christoph Merz, Daniel Baeriswyl, and Brad Hulse. You guys have been incredible friends, I'm lucky to have met you. Generally, thanks to all my friends outside of CCE. *L'union fait la force!*

To close, I thank my best friend, Jane Ni. In the words of a dear friend, I feel truly at home when I am with you.

PREFACE

Parts of this thesis have been adapted from articles co-written by the author.

The following articles were reproduced in part with permission from the American Chemical Society:

"Nickel-Mediated Hydrogenolysis of C–O Bonds of Aryl Ethers: What Is the Source of the Hydrogen?" Paul Kelley, Sibo Lin, Guy A. Edouard, Michael W. Day, Theodor Agapie. *J. Am. Chem. Soc.* 2012, *134* (12), 5480-5483.

"Molybdenum Catalyzed Ammonia Borane Dehydrogenation: Oxidation Specific Mechanisms." Joshua A. Buss, Guy A. Edouard, Christine Cheng, Jade Shi, Theodor Agapie. *J. Am. Chem. Soc.* 2014, *136* (32), 11272-11275.

"Aryl Ether Cleavage by Group 9 and 10 Transition Metals: Stoichiometric Studies of Selectivity and Mechanism." Guy A. Edouard, Paul Kelley, David E. Herbert, Theodor Agapie. *Organometallics* 2015, *34* (21), 5254-5277.

RESPECTIVE CONTRIBUTIONS

The work in this thesis is the result of collaborative efforts; general comments outlining these efforts are provided here.

Studies of carbon–oxygen bond activation were conducted in close collaboration with Dr. Paul Kelley, who completed studies of this transformation with Ni using the –NMe_2 substituted terphenyl diphoshpine methyl–aryl ether **1b** and aryl–aryl ether **1c** in Chapter 2. Dr. Sibo Lin complimented this work with studies of a related catalytic system and provided computational insight throughout our investigations. Dr. David E. Herbert processed all single crystal X-ray diffraction (XRD) data and provided finalized solid state structures. The late Dr. Michael W. Day solved some of the solid state structures presented earlier on this work. Mr. Larry Henling and Mr. Joshua A. Buss aided in solving the solid state structure of compound **26a**.

In Appendix A, Dr. Gyeongshin Choi synthesized 1-iminoquinolyl-3-tert-butyl-5-triphenylsilyl-phenol and completed half of the ethylene oligomerization/polymerization reactions reported in Table A.1. Salicylaldehyde precursors **41** and **42** were prepared with Ms. Jessica Sampson and Dr. Choi; precursors, particularly Neigishi coupling partners, were shared and purified for common use.

In Appendix B, molybdenum compounds ***57*** and ***58*** were first prepared by Mr. Jade Shi. Optimization of my preparations of molybdenum compounds ***57-59***, their characterization, and the completion of the determination of their solid states

structures was accomplished by Mr. Buss. Processing of single crystal X-ray diffraction data and determination of solid structures in the case of the molybdenum compounds was completed by Mr. Buss; for all other compounds, this work was done by Larry Henling and the late Dr. Day.

ABSTRACT

Terphenyl diphosphines bearing pendant ethers were prepared to provide mechanistic insight into the mechanism of activation of aryl C–O bonds with Group 9 and Group 10 transition metals. Chapters 2 and 3 of this dissertation describe the reactivity of compounds supported by the model phosphine and extension of this chemistry to heterogenous C–O bond activation.

Chapter 2 describes the synthesis and reactivity of aryl-methyl and aryl-aryl model systems. The metallation of these compounds with Ni, Pd, Pt, Co, Rh, and Ir is described. Intramolecular bond activation pathways are described. In the case of the aryl-methyl ether, aryl C–O bond activation was observed only for Ni, Rh, and Ir.

Chapter 3 outlines the reactivity of heterogenous Rh and Ir catalysts for aryl ether C–O bond cleavage. Using Rh/C and an organometallic Ir precursor, aryl ethers were treated with H_2 and heat to afford products of hydrogenolysis and hydrogenation. Conditions were modified to optimize the yield of hydrogenolysis product. Hydrogenation could not be fully suppressed in these systems.

Appendix A describes initial investiagtions of bisphenoxyiminoquinoline dichromium compounds for selective C_2H_4 oligomerization to afford α-olefins. The synthesis of monometallic and bimetallic Cr complexes is described. These compounds are compared to literature examples and found to be less active and non-selective for production of α-olefins.

Appendix B describes the coordination chemistry of terphenyl diphosphines, terphenyl bisphosphinophenols, and biphenyl phosphinophenols proligands with

molybdenum, cobalt, and nickel. Since their synthesis, terphenyl diphosphine molybdenum compounds have been reported to be good catalysts for the dehydrogenation of ammonia borane. Biphenyl phosphinophenols are demonstrated provide both phosphine and arene donors to transition metals while maintaining a sterically accessible coordination sphere. Such ligands may be promising in the context of the activation of other small molecules.

Appendix C contains relevant NMR spectra for the compounds presented in the preceeding sections.

TABLE OF CONTENTS

LIST OF FIGURES

LIST OF SCHEMES

LIST OF TABLES

CHAPTER 1

General Introduction

This dissertation deals primarily with the synthesis, metallation, and reactivity of terphenyl diphosphines and monophosphines with mid- to late-transition metals. An emphasis is placed on aryl C–O bond activation of terphenyl diphosphines bearing pendant methyl and aryl ethers. Efforts towards the synthesis of bisphenoxyiminoquinoline dichromium complexes tethered by a rigid terphenyl linker for selective oligomerization of ethylene are also described.

Aryl C–O bond activation is of interest in the context of conversion of biomass to hydrocarbons as well as aromatic compounds that are useful precursors in the preparation of pharmaceuticals and commodity chemicals. It is also a fundamental transformation in the elaboration of arene rings (e.g., through cross-coupling reactions). In aryl–alkyl ethers, the aryl C–O is stronger than the alkyl C–O bond; thus, engendering selectivity for catalytic aryl bond activation is an ongoing topic of research.

Our group has investigated terphenyl diphosphines which enfore metal-arene interactions. In the literature, computational studies had identified a nickel-arene interaction proximal to an aryl C–O bond as a key intermediate on the pathway of aryl C–O bond cleavage. We prepared a series of terphenyl diphosphines bearing pendant alkyl and aryl ethers which position transition metals in close proximity to aryl C–O bonds. With Ni, a mechanism for reductive cleavage of aryl-alkyl ether C–O without the addition of exogenous reductant was elucidated through a stoichiometric study with our terphenyl model system. This mechanism was shown to be relevant to a catalytic system. These stoichiometric studies were extended to Group 9 and Group 10 transition metals; Rh and Ir were found to activate the aryl C–O bond of our model system in the presence of an alkyl C–O bond (Chapter 2).

Having demonstrated that mechanisms determined in our stoichiometric system were operative in reported Ni-catalyzed C–O bond cleavage technology, we attempted to design new Rh- and Ir-catalyzed methodologies for selective aryl ether C–O bond cleavage (Chapter 3). In the absence of exogenous ligand, Rh/C and organometallic Rh and Ir precursors were found to be precatalysts for reactions which yielded hydrogenolysis and hydrogenation products of aryl ethers in the presence of neat aryl ether, heating, and H_2. Although reaction conditions were optimized for hydrogenolysis product, hydrogenation was observed all reactions.

From there, this dissertation continutes with a discussion of efforts towards the synthesis of terphenyl bisphenoxyiminoquinoline dichromium complexes envisioned to be precatalysts for selective olefin oligomerization (Appendix A). Activities are an order of magnitude less than those reported in the literature for monometallic phenoxyiminoquinoline Cr compounds. A distribution of α-olefins is observed in this reaction. Optimization of the described reaction conditions and substitution of the phenoxyiminoquinoline proligand is suggested as a strategy towards engendering higher activity and selectivity in this system.

Lastly, terphenyl, terphenyl phenoxide, and biphenylphenoxide complexes of mid- to late-transition metals are dicussed in an appendix (Appendix B). These compounds display hemilabile metal-arene interactions, hard and soft donors, and open coordination sites which are attractive design principles for the activation of small molecules (e.g., CO_2, H_2, N_2) by low-coordinate, low-valent transition metal complexes.

CHAPTER 2

Aryl Ether Cleavage by Group 9 and 10 Transition Metals: Stoichiometric Studies of Selectivity and Mechanism

Published in part as:

Kelley, P.; Lin, S.; Edouard, G. A.; Day, M. W.; Agapie, T. *J. Am. Chem. Soc.* 2012, *134*, 5480-5483.

Edouard, G. A.; Kelley, P.; Herbert, D. E.; Agapie, T. *Organometallics* 2015, *34*, 5254-5277.

ABSTRACT

The reactivity of terphenyl diphosphines bearing aryl–methyl ether or aryl–aryl ether moieties with M^0 (M = Ni, Pd, Pt), M'^0 (M′ = Co, Rh, Ir), or M^{II} centers was investigated to gain mechanistic insight into intramolecular aryl–ether bond cleavage in structurally related metal complexes. Rh^I converts the aryl–methyl ether moiety to an aryl C–H bond. This is similar to reactivity previously observed at Ni^0 that involves C–O oxidative addition, β-H elimination liberating CH_2O, reductive elimination of an aryl C–H bond, and decarbonylation of CH_2O. Ir^I leads to unselective aryl and alkyl C–O bond activation. In the presence of excess CO, Rh^I and Ir^I display a shift in selectivity and reactivity and cleave the alkyl C–O bond. Co^I does not perform C–O cleavage. Alkyl C–O bond activation was observed with M^{II}–halide complexes with loss of MeCl via a Lewis acid–base mechanism. Pd^0 and Pt^0 cleave selectively the O–Me bond via oxidative addition. With a diaryl ether moiety, Pd^0 and Pt^0 are found to be capable of performing aryl C–O bond activation. Various levels of interactions between the central arene and the metal center were observed, and these were correlated with trends in bond activation. Overall, selective cleavage of the stronger aryl ether C–O bond was observed only with Ni^0 and Rh^I. Pd^0 and Pt^0 can perform aryl ether C–O cleavage, but if available, they will cleave the weaker O–Me bond. This study provides insight into the relative reactivity of group 9 and 10 metal centers with aryl ether bonds and suggests future directions for designing systems for metal-catalyzed cleavage of ether C–O bonds in synthetic methodology as well as lignin deoxygenation.

INTRODUCTION

Cleavage of aryl C–O bonds mediated by transition metals is of significant current interest for organic methodology[1] and biomass conversion.[2] A variety of cross-coupling reactions that utilize phenol-derived electrophiles has been developed.[1] Reductive cleavage has been employed as a deprotection strategy for aryl ethers used as removable directing groups.[3] Given the prevalence of aryl ether linkages in lignin,[4] strategies for the conversion of biomass to liquid fuel and other value- added products have been invoked on the basis of activation of the ether moieties.[2] Although C–O bond cleavage of phenol derivatives has been demonstrated using group 9 (Co,[5] Rh,[5a,6] Ir[7]) and 10 (Ni,[1,3,5d,6e,8] Pd,[1b,6b,6e,9] Pt[9a,10]) transition-metal complexes, the activation of the stronger aryl ether C–O bond is less common.[1a,1b,3,6b,6e,6f,7d,8a,8c-f] We have investigated the mechanism of aryl C–O bond cleavage at Ni by using a diphosphine ligand tethered to a pendant aryl methyl ether (Scheme 1.1).[11] That stoichiometric model provides insight into the mechanism of aryl C–O bond conversion to a C–H moiety. In a prior example, a Rh complex supported by a pincer ligand precursor shows analogous aryl ether C–O activation, but the reaction is arrested at the cyclometalated species due to the stability of the resulting pincer complex, without full conversion of the C–O bond to a C–H bond.[6b,6c] The overall conversion for the Ni system allowed for mapping out of a full pathway of potential relevance to catalytic systems. Indeed, we performed isotopic labeling studies of a Ni–NHC catalytic system[8d,11] that were consistent with the mechanism elucidated with the stoichiometric system, indicating that β-H moieties in the alkyl group of the substrate can provide the reducing equivalents necessary for C–O to C–H conversion. We have extended our stoichiometric studies to investigate the mechanism of C–O cleavage with group 9 and 10 metals in different oxidation states. Intermediates displaying η^2 interactions between Ni^0 and the double bonds

adjacent to the oxygen atoms of phenol derivatives have been found computationally to precede aryl C–O bond activation.[12] The *m*-terphenyl diphosphine motif predisposes group 9 and 10 metals toward interaction with the alkoxy or aryloxy substituents at the 2′-positions of the central rings of ligands **1a-d**. These studies revealed metal-dependent selectivity for aryl C–O versus alkyl C–O bonds and evidence for several different mechanisms of C–O bond activation, providing mechanistic insight for the design of potential catalytic systems using group 9 and 10 transition metals.

Scheme 2.1. Aryl C–O Bond Activation of Ar–O–Me Ether by Ni^0.

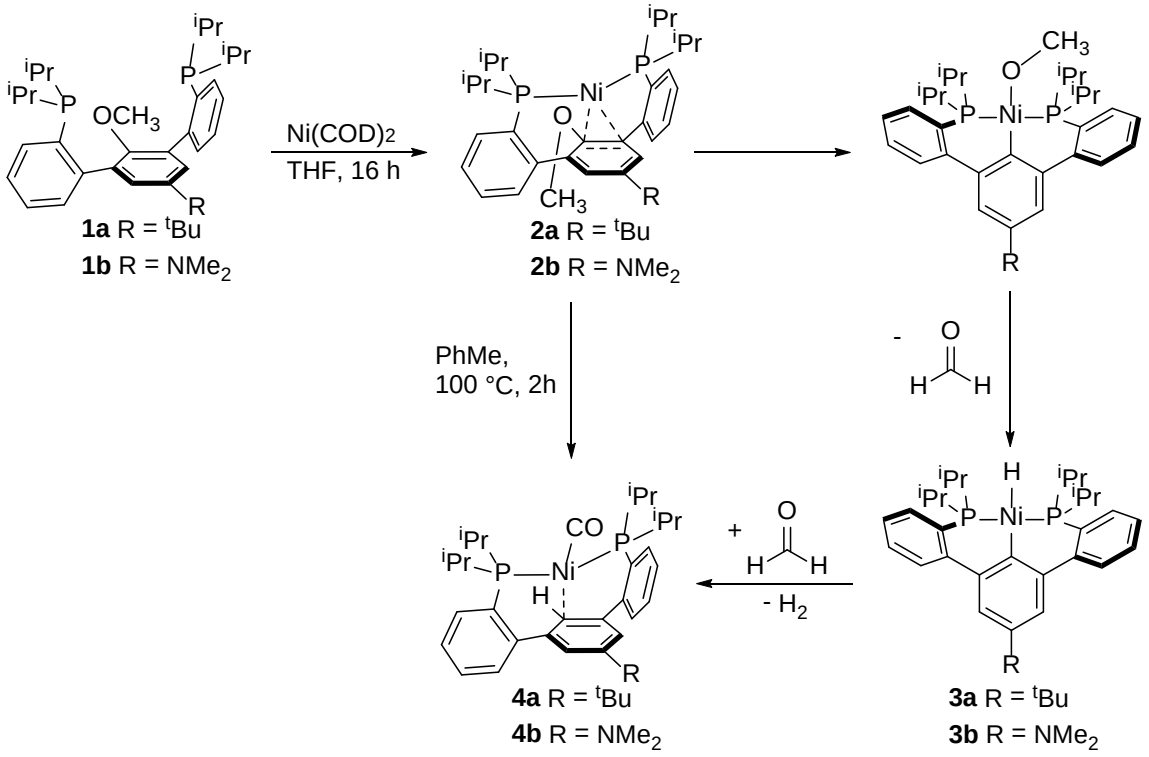

We have previously reported[11] that treatment of diphosphines **1a,b** bearing a pendant ether with Ni(COD)$_2$ (COD = 1,5-cyclooctadiene) at 20 °C afforded the Ni^0 complexes **2a,b** (Scheme 2.1). ^{1}H NMR spectroscopic analysis of the Ni adducts showed a significant shift in the resonance of the protons of the central arene of the ligand upon binding to Ni (**1a**, 7.11 ppm; **1b**, 6.73 ppm; **2a**, 6.31 ppm; **2b**, 5.84 ppm; C_6D_6). These

observations are consistent with strong back-bonding interactions between Ni^0 and the aromatic π systems of the terphenyl diphosphine ligands. The solid-state structures of **2a,b** show the metal center interacting with two carbons of the central arene, with short Ni–C distances (1.96−2.09 Å) and partial localization of the double bonds within the central ring.

Heating solutions of complexes **2a,b** in toluene to 100 °C led to the formation of **4a,b** (Scheme 2.1). In the final products **4a,b**, the central arene bears a hydrogen in place of the methoxy substituent of **2a,b** and a CO ligand was found bound to Ni. Characterization of intermediates, including **3a,b**, by multinuclear NMR spectroscopy, IR spectroscopy, single-crystal X-ray diffraction (XRD), and mechanistic studies revealed that oxidative addition of the aryl C–O bond is followed by β-hydride elimination to afford Ni^{II}–hydride intermediates (**3a,b**) and liberate formaldehyde. Decarbonylation of formaldehyde and reductive elimination of a C–H bond then affords **4a,b** with concomitant release of a molecule of H_2.

RESULTS AND DISCUSSION

2.1 Bond Activation by Oxidative Addition

2.1a Alkyl C–O Bond Activation by Pd^0 and Pt^0

Pd^0 and Pt^0 complexes of diphosphine **1a** were targeted for comparison of reactivity with the Ni complex **2a**. Reduction of a mixture of $Pd(COD)Cl_2$ (COD = 1,5-cyclooctadiene) and **1a** with cobaltocene (2.4 equiv.) over 12 h resulted in clean conversion to a single new species, **5a** (Scheme 2.2). The resonance observed by ^{1}H NMR spectroscopy that can be assigned to the hydrogens of the central arene (7.01 ppm) is shifted relative to that of diphosphine **1a** but not as significantly upfield as was observed for complex **2a**, potentially indicating a weaker metal–arene interaction. In addition, a resonance attributable to an intact methoxy group (3.16 ppm, C_6D_6) was also observed by ^{1}H NMR spectroscopy. Assuming reduction of Pd^{II}, both Pd^0 and dinuclear Pd^I species could be consistent with the sharp, diamagnetic NMR spectra observed for **5a**. The identity of compound **5a** was confirmed by single-crystal XRD (Figure 2.1). The metal coordination sphere consists of the two phosphines and an η^1 interaction with the central arene (Pd(1)–C(1) = 2.495(2) Å). No localization of the double-bond character within the central arene ring was observed (C–C = 1.394(3) – 1.408(3) Å; average C–C = 1.399 Å, standard deviation 0.006 Å). Furthermore, the aryl C–O distance for **5a** (C(1)–O(1) = 1.376(3) Å) is shorter than that of **2a** (C(1)–O(1) = 1.406(2) Å; see Figure 2.1), consistent with more π delocalization in the aryl ether moiety of the Pd complex. These bond metrics are consistent with an aryl ether–metal interaction that lacks a strong metal π back-bonding component but is adjacent to the aryl C–O bond, potentially predisposing this bond toward activation.

Scheme 2.2. Alkyl C–O Bond Activation of Ar–O–Me Ether by Pd^0 and Pt^0.

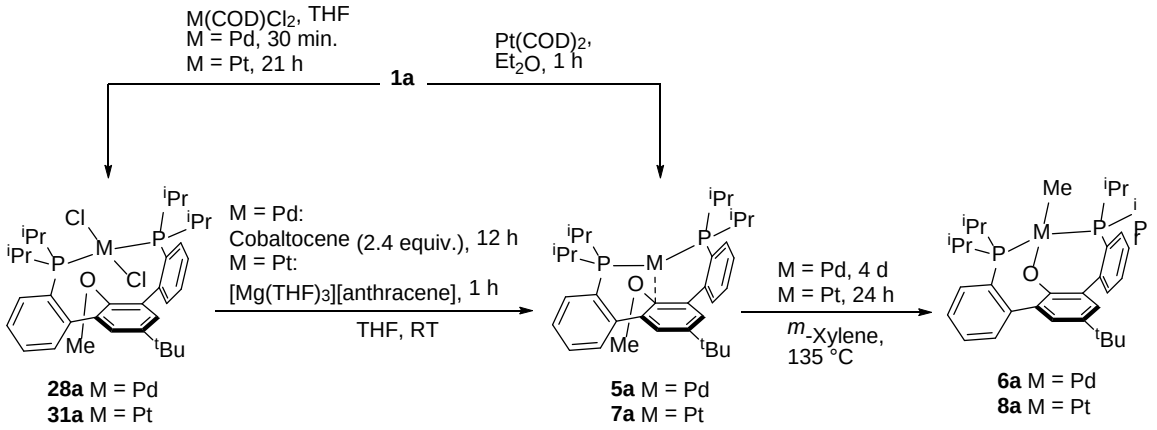

Heating of compound **5a** in *m*-xylene at 135 °C for 4 days resulted in clean conversion to a new complex (**6a**) on the basis of the ^{31}P NMR spectrum (29.76 ppm, C_6D_6; Scheme 2.2). The upfield shift relative to **5a** is consistent with those observed for group 10 M^{II} complexes supported by **1a** (see *Alkyl C–O Bond Cleavage at Ni*^{II} and *Alkyl C–O Bond Cleavage at Pd*^{II} *and Pt*^{II}). A resonance attributable to the protons of the methoxy group of **1a** was not observed in the ^{1}H NMR spectrum of **6a**. However, a triplet at 0.26 ppm (C_6D_6) integrating to 3H was assigned to a Pd–CH_3 moiety.[13] Taken together, these observations support oxidative addition of the methyl–oxygen bond of the aryl ether to generate the square-planar Pd^{II} complex **6a**.

Thus, in contrast to aryl C–O bond activation observed for Ni^0 upon heating compound **2a**, alkyl C–O bond activation was observed with Pd^0. The reasons behind the change in selectivity are not clear but may be related to the different strengths of the metal–arene interactions in the reduced precursors. In addition to the weaker interaction with the arene, the larger Pd center may more easily approach the more distant methyl group.

Figure 2.1. Solid-State Structures of 5a (top) and 8a (bottom). Shown with thermal ellipsoids at the 50% probability level. Hydrogen atoms are omitted for clarity. Bond distances are given in Å.

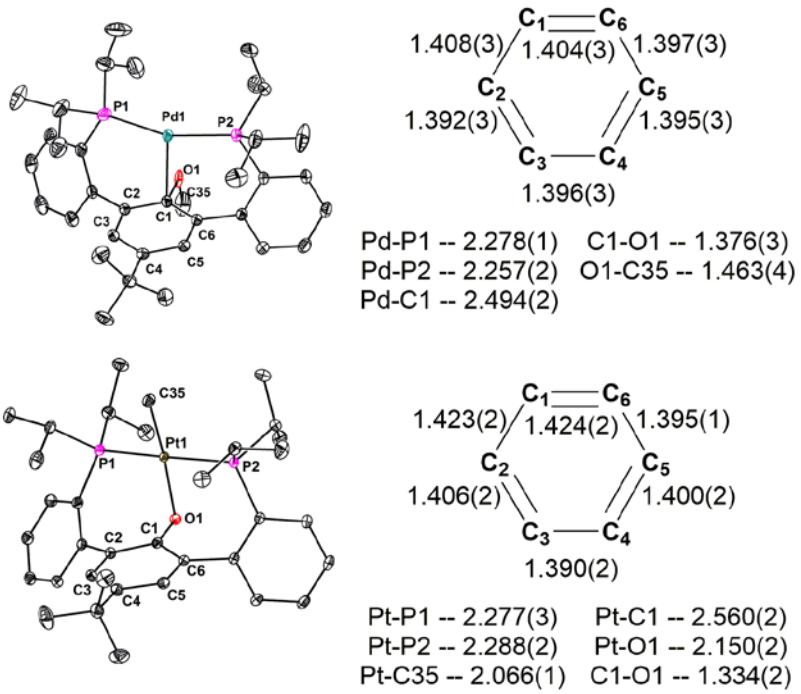

It is notable that the activation of the alkyl C–O bond (ca. 65 kcal/mol for anisole) by Pd^0 is slower than cleavage of the aryl C–O bond (ca. 100 kcal/mol for anisole) by Ni^0.[14] It is notable that the activation of the alkyl C–O bond (ca. 65 kcal/mol for anisole) by Pd^0 is slower than cleavage of the aryl C–O bond (ca. 100 kcal/mol for anisole) by Ni^0.[14] The more compact first-row transition metal Ni forms a tighter η^2 interaction with the central arene, which may prevent the Ni^0 center from coming into close proximity with the weaker alkyl C–O bond.

For comparison, a Pt^0 complex of **1a** was prepared. Treatment of a solution of $Pt(COD)Cl_2$ and **1a** with activated magnesium turnings did not result in conversion to a Pt^0 species. Reduction using magnesium anthracenide afforded a new complex (**7a**) with J_{PtP} = 4730 Hz consistent with related Pt^0 diphosphine complexes[15] (Scheme 2.2). However,

purification attempts were frustrated by persistent anthracene impurities. Clean metalation to **7a** was achieved upon treatment of **1a** with $Pt(COD)_2$.[16] The NMR features of **7a** are reminiscent of **5a**, suggesting a similar structure, with a weak metal–arene interaction.

Heating a solution of **7a** in *m*-xylene at 135 °C for 24 h resulted in conversion to complex **8a**. The Pt–P coupling (J_{PtP} = 3089 Hz) is similar to those observed for related cis-diphosphine Pt^{II}–Me species[17] and smaller than that for Pt^0 precursor **7a**. A resonance assigned to the protons of the methoxy group was not observed in the ^{1}H NMR spectrum of **8a**. Instead, a triplet integrating for three hydrogen atoms was observed at 0.67 ppm, consistent with a Pt–C*H*$_3$ species.[17b,18] Pt satellites were also observed for this peak, corroborating the assignment of **8a**. The structural assignment was confirmed by single-crystal XRD (Figure 2.1). The nearly linear angle ∠C(35)–Pt(1)–O(1) (174.01(5)°) shows that the trans-spanning *m*-terphenyl framework is capable of supporting a slightly distorted square planar (∠C(35)–Pt(1)–P(1) = 91.88(4)°; ∠O(1)–Pt(1)–P(1) = 87.26(3)°) geometry. A *trans* isomer of phenoxide and methyl donors for a diphosphine-supported Pt^{II} is unusual, with the only example characterized in the solid state being reported for a perfluorophenoxide diphenylphosphine.[18] As for the analogous Pd chemistry and in contrast to the Ni analogue **2a**, oxidative addition of the alkyl C–O rather than the aryl C–O bond of the ether occurs with Pt^0. With the cases of both Pd^{II} and Pt^0 activating the weaker alkyl C–O bond of an aryl alkyl ether, it remained unclear whether Pd^0 and Pt^0 could activate any aryl C–O in the present system. To address this question, a diphosphine with a pendant diaryl ether moiety was prepared.

2.1b Aryl C–O Bond Activation at Pd^0 and Pt^0

The reactivity of Ni^0, Pd^0, and Pt^0 with the diaryl ether diphosphines **1c,d** was investigated to determine if these metal centers could activate aryl C–O bonds and their

resultant selectivity (Scheme 2.3). These experiments were designed to test if an aryl C–O bond could be cleaved by Pd and Pt even though oxidative addition of the alkyl C–O bond is observed in complexes **5a** and **7a**. Determining whether the aryl C–O bond proximal or distal to the terphenyl moiety of the diphosphine was cleaved would reveal if the distance from the Pd^0 and Pt^0 centers to the central arene relative to the Ni^0 center prevents the larger metals from cleaving the C–O bond closer to the terphenyl moiety.

The Ni^0 (**9c**), Pd^0 (**10d**), and Pt^0 (**11d**) compounds were synthesized by treatment of diphosphine **1c** with $Ni(COD)_2$, and treatment of diphosphine **1d** with $Pd(COD)Cl_2$ and cobaltocene (2.1 equiv.), or $Pt(COD)_2$ using procedures previously developed for the metalation of **1a** (Scheme 2.3).

Scheme 2.3. C–O Bond Activation of Ar–O–Ar Ether by Pd^0 and Pt^0.

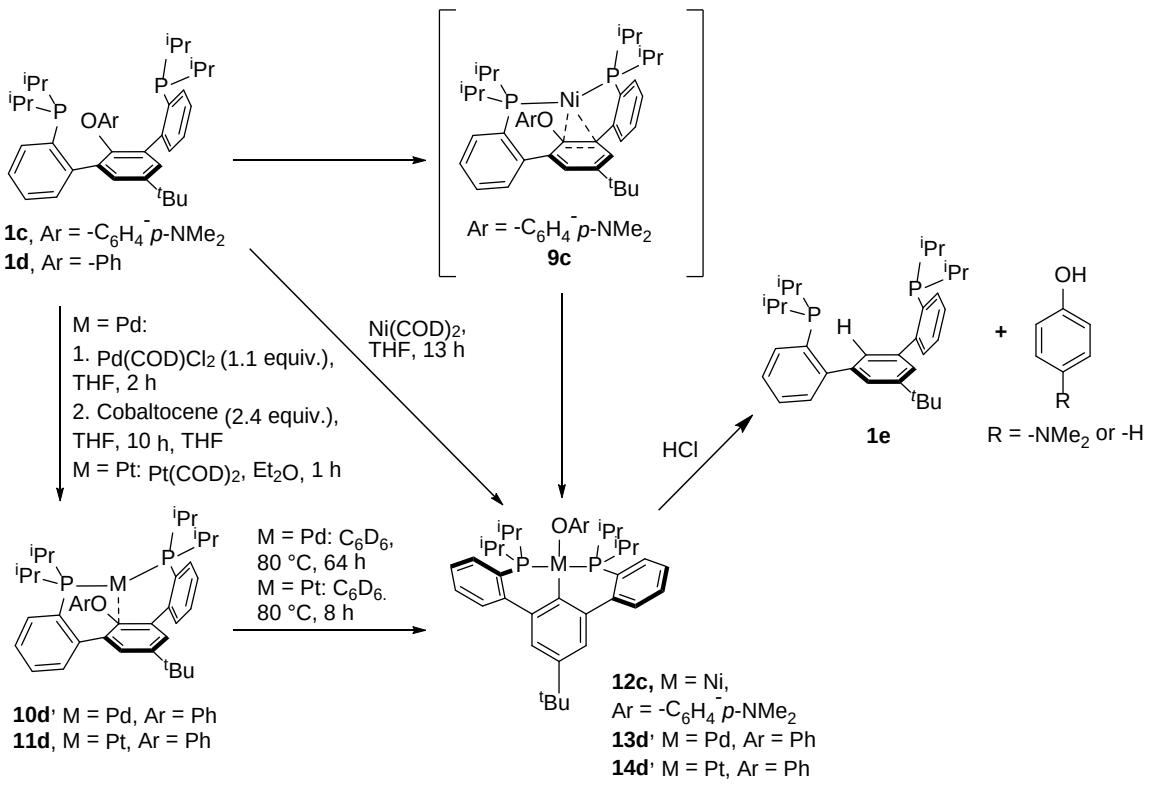

Varying the substitution of the diaryl ether diphosphine aided in the preparation of compounds with solubilities amenable to isolation in moderate yields. All products showed resonances by ^{31}P NMR spectroscopy (**9c**, 41.56 ppm; **10d**, 32.45 ppm; **11d**, 55.92 ppm; C_6D_6) similar to the complexes supported by **1a**, consistent with the formation of structurally similar compounds.

Complex **9c** was observed as an intermediate in the reaction of **1c** and Ni(COD)$_2$ at room temperature and converted to the new species **12c** over the course of 13 h. Complexes **10d** and **11d**, however, required heating at 80 °C in C_6D_6 for conversion to the new species **13d** and **14d**, respectively. Treatment of each reaction mixture with HCl followed by extraction in hexanes and analysis by mass spectrometry (MS) showed the formation of *p*-dimethylaminophenol or phenol (GC-MS) and diphosphine **1e** (ESI-MS) (Scheme 2.3). The cleavage of the terphenyl aryl C–O bond with Ni, even when two are available, indicates that there is a preference for activation of the arene that the metal coordinates to, in the present case biased via phosphine chelation. It is notable that both Pd^0 and Pt^0 lead to selective cleavage of the aryl C–O bond that is likely closer to the metal due to phosphine coordination. These data demonstrate that Pd^0 and Pt^0 centers are neither limited to oxidative addition of the C–O bond distal to the terphenyl diphosphine moiety nor incapable of cleaving stronger aryl C–O bonds. Instead, in the case of **5a** and **7a**, selective alkyl C–O bond cleavage may be a result of a weaker η^1 interaction allowing for access to and cleavage of the weaker, distal bond. Although activation of the same aryl C–O bond is observed, the reaction of Ni complex **9c** is significantly faster than that of the Pd and Pt analogues, a fact that correlates with a stronger metal–arene interaction for Ni, as shown in the solid-state structures with **1a**.

2.1c Aryl C–O Bond Activation at Rh

Given the precedent for aryl C–O bond activation by oxidative addition from Rh^{I},[6b,6c,6f] metalations of **1a** with Rh^{I} precursors were performed (Scheme 2.4). Upon addition of **1a** to 0.5 equiv. of $(Rh(COD)Cl)_2$ in THF a new species, **15a**, was generated (*ca.* 70% conversion, ^{31}P NMR spectroscopy) featuring a singlet near that of the free ligand (-4.04 ppm, C_6D_6) and a doublet shifted significantly downfield of **1a** (59.97 ppm, J_{RhP} = 145 Hz) of equal integration. This species was assigned as a Rh^{I} monophosphine with one phosphine of **1a** bound to Rh and one phosphine unbound (compare to **27a**; see *Aryl C–O Bond Activation at Ir*[I] and Scheme 2.7). Treatment of $(Rh(COE)_2Cl)_2$ (COE = cyclooctene) with **1a** led to the formation of two new major species displaying resonances by ^{31}P NMR spectroscopy at 35.48 and 38.31 ppm within 30 min in C_6D_6 (Scheme 2.4), indicating that diphosphine **1a** is able to displace the monodentate COE at room temperature more rapidly than the bidentate, chelating COD ligand. The peak at 35.48 ppm is assigned to a Rh^{III}–OMe species (**17a**) on the basis of the corresponding ^{1}H NMR spectrum. The peak at 38.31 ppm corresponds to a species that displays a doublet of triplets in the ^{1}H NMR spectrum at -23.28 ppm (J_{PH} = 13.0 Hz, J_{RhH} = 48 Hz) consistent with a Rh–hydride (**18a**), coupled to two equivalent ^{31}P nuclei and one ^{103}Rh center. Selective ^{31}P heteronuclear decoupling allowed for observation of a doublet for this resonance. Additionally, a doublet of doublets was observed by ^{31}P NMR spectroscopy (J_{RhP} = 116 Hz). These data are consistent with the phosphine nuclei coupling to one hydride and one ^{103}Rh center. **18a** does not display a peak corresponding to the CH_3–O group. Stirring compound **18a** at room temperature for an additional 11.5 h resulted in full conversion to a new species (**19a**) with a resonance observed by ^{31}P NMR spectroscopy (35.77 ppm, broad) downfield of that observed for **18a**. No spectroscopic evidence of a hydride was

observed, suggesting reductive elimination had occurred to form a C–H bond and afford a $Rh^{I}Cl$ species. A single-crystal XRD study of **19a** confirmed the formation of a Rh^{I}–chloride species, with the phosphines and the arene π system completing the metal coordination sphere. (Figure 2.2). Two crystallographically distinct species were observed in the solid state. One displayed an η^1 interaction (**19a-η^1**) with the central arene, whereas the other displayed an η^2 interaction (**19a-η^2**). The central arene C–C distances in **19a-η^2** are indicative of disruption of aromaticity, with alternating short and long bonds suggesting partial localization of single and double C–C bond character. These distances are similar to those observed for η^2-arene binding with Ni (**2a**) and Co (**38a**; see Figure 2.6). The presence of both η^1 and η^2 binding modes in the solid state and the observation of a single set of NMR resonances in solution for compound **19a** indicate facile interconversion of the isomers. Similar to the case for Rh^{I} in **19a**, Ni^{0} complexes supported by *m*-terphenyldiphosphines show both η^1- and η^2-arene binding.[19] In the absence of an additional ligand, the η^2-coordination mode is observed, with Ni^{0} coordinating two phosphine donors and the arene. Upon binding of CO or acetonitrile, the arene coordination shifts to η^1. For example, the Ni–C distances shift from 1.973(2) Å (Ni(1)–C(1)) and 2.133(2) Å (Ni(1)–C(2)) to 2.089(1) Å (Ni(1)–C(1)) and 2.427(1) Å (Ni(1)–C(2)) upon coordination of acetonitrile (Figure 1.3). By comparison, the structural parameters of **19a-η^2** show a more symmetric interaction with the two carbon centers, suggesting a higher propensity for Rh^{I} to interact with a double-bond moiety of the arene.

Compound **19a** is proposed to form via a pathway (Scheme 1.4) similar to that for the Ni reactivity (Scheme 1.1). Rh^{I} is proposed to coordinate to the two phosphines and the

arene upon substitution of COE, followed by oxidative addition of the aryl C–O bond and β-H elimination.

Scheme 2.4. Aryl C–O Bond Activation of Ar–O–Me Ether by Rh^{I} (this work).

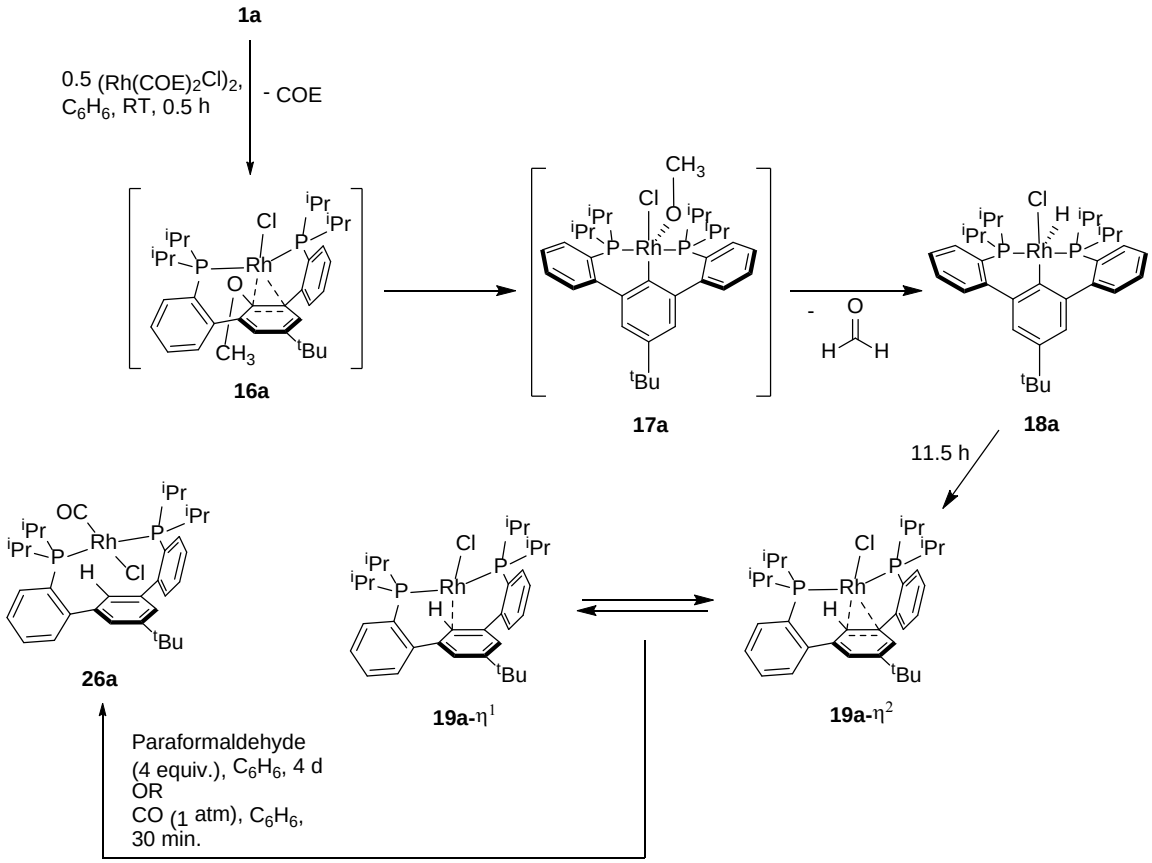

This mechanism is similar to that proposed for C–O cleavage observed for a related diphosphine (**1e**) bearing a pendant methyl ether reported by Milstein and co-workers upon metalation with $(Rh(COE)_2Cl)_2$.[6b,6e] Notably, the aryl ether cleavage reported by Milstein is significantly slower, with only 20% conversion to the analogous Rh^{III}–hydride–aryl species after 24 h at room temperature (Scheme 2.5).

Figure 2.2. Solid-State Structures of 19a-η^1 (top) and 19a-η^2 (bottom). Shown with thermal ellipsoids at the 50% probability level. Hydrogen atoms are omitted for clarity. Bond distances are given in Å.

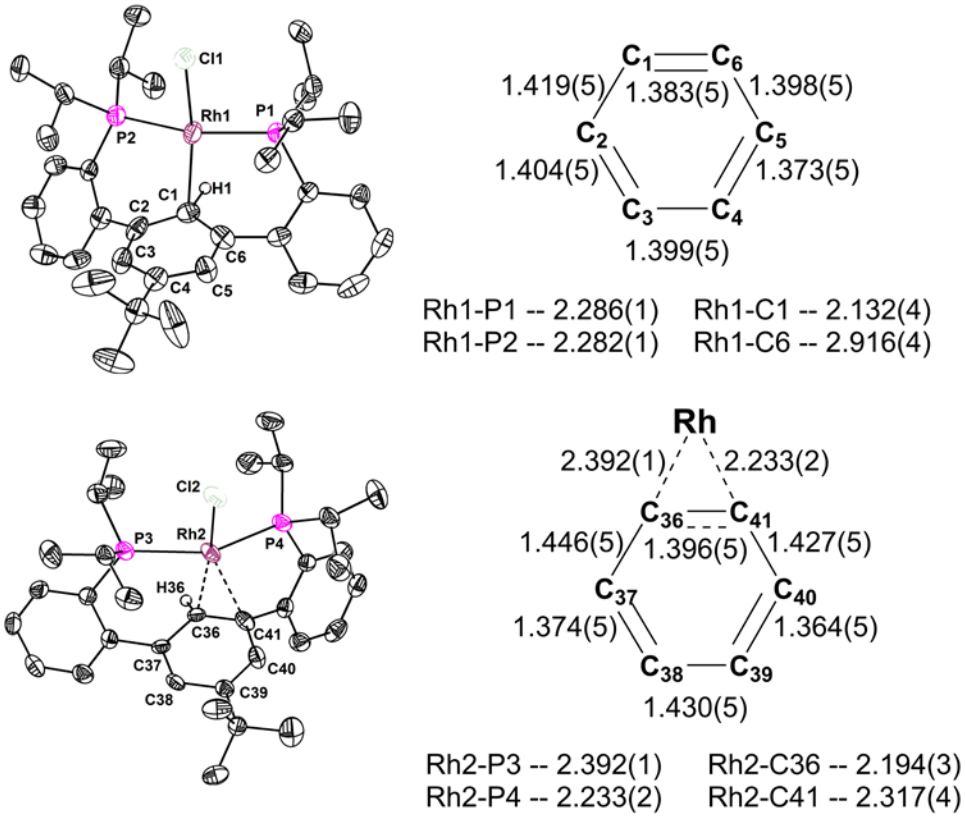

This difference in reactivity could be due to the smaller phosphine substituents and the ability of **1a** to more readily lead to a diphosphine–arene chelate from which aryl C–O activation is facile. In the case of complex **21e** (Scheme 2.5) prepared by Milstein et al., reductive elimination of the aryl C–H bond was not observed, likely due to the high stability offered by the two five-membered chelates of the PCP pincer ligand (**1e**). In contrast, complex **18a** undergoes facile C–H reductive elimination within hours at room temperature. This is likely a consequence of the two six-membered chelates, each strained by the presence of a biphenyldiyl moiety, strain that is relieved by reductive elimination.

Figure 2.3. Solid-State Structural Parameters of the *m*-Terphenyldiphosphine Ni^0 Complex (left) and Its Related Acetonitrile Adduct (right). Bond distances are given in Å.

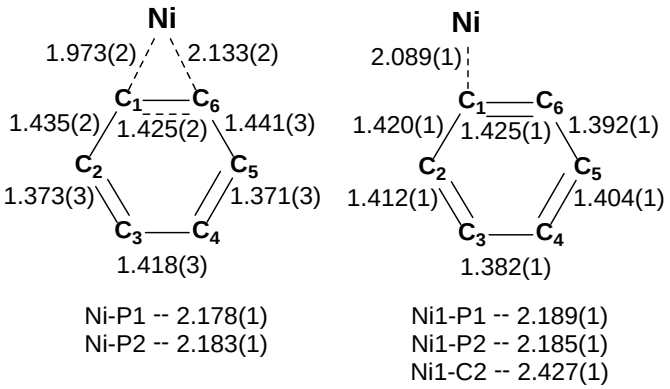

Scheme 2.5. Aryl C–O Bond Activation of Ar–O–Me Ether by Rh^I (Milstein et al.).[6b,6e]

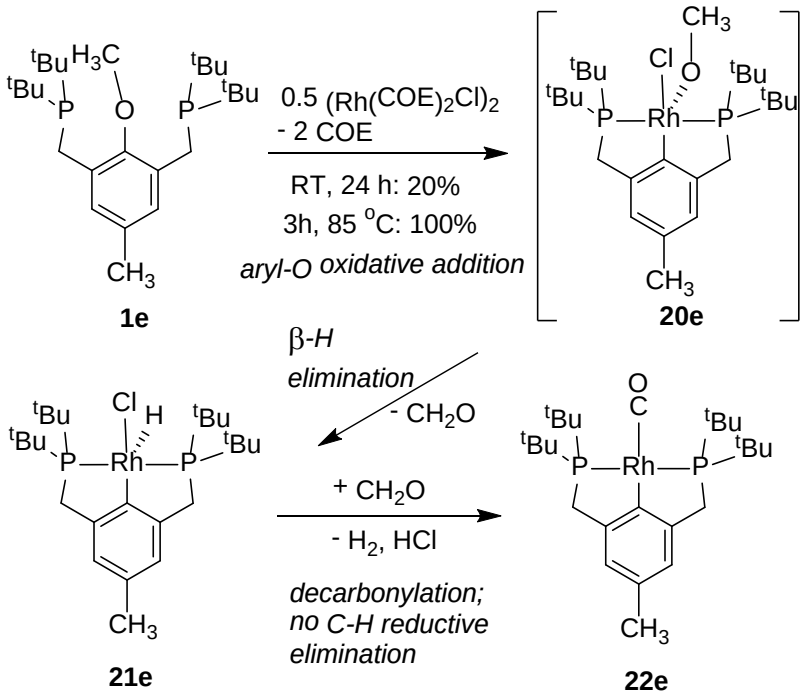

To further compare our system to the Milstein system, the CO adduct of species **19a** was targeted (Scheme 2.6). Coordination of CO to **19a** can be effected by stirring a solution of **19a** and paraformaldehyde over 4 days, a slower reaction in comparison with

21e. Alternatively, adding CO (1 atm) to a degassed solution of **19a** affords **26a** within 30 min (Scheme 2.4). Trace amounts of **26a** (ca. 5% or less) are also detected in crude reaction mixtures of **1a** and $(Rh(COE)_2Cl)_2$ (^{1}H NMR spectroscopy).

Scheme 2.6. Alkyl C–O Bond Activation of Ar–O–Me Ether by Rh^I.

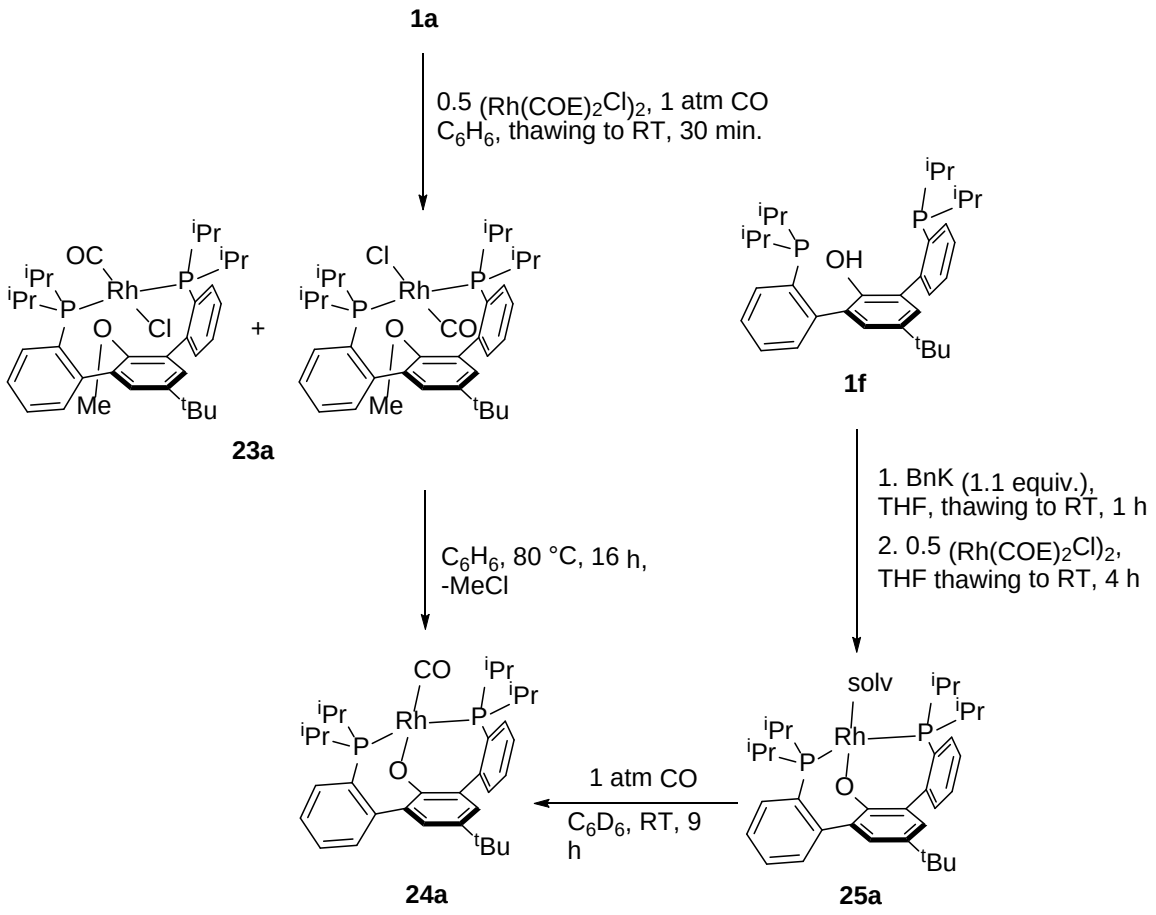

Compound **26a** displays a new resonance by ^{31}P NMR spectroscopy at 38.71 ppm (d, J_{RhP} = 123 Hz) and an IR stretch consistent with a Rh–CO moiety (ν_{CO} 1942 cm^{-1}). In comparison to the broad resonances observed in the ^{1}H NMR spectrum for **19a**, resonances for **26a** are sharp and a triplet (8.82 ppm) and doublet (7.23 ppm) are assigned to the central arene. These upfield-shifted resonances are consistent with little or no back-bonding to the central arene from Rh^I upon coordination of the π-acidic CO ligand. An XRD study confirmed

the assignment of **26a** as a pseudo-square-planar diphosphine $Rh^{I}(CO)Cl$ complex (Figure 2.4). The structure of a similar square-planar $Rh^{I}(CO)Cl$ species has been reported.[20] Four crystallographically distinct molecules were observed in the asymmetric unit. For each molecule, the distance between Rh and the *ipso* carbon of the central arene (2.817(7) – 2.845(6) Å) is consistent with no interaction. The distances between Cl and the calculated position of the *ipso* C*H* (2.430−2.461 Å) suggest a possible H-bonding interaction between the Cl and *ipso* CH of **26a**.[21] This interaction may explain why a single coordination isomer is observed (compare to **23a** and **29a**) in the solid-state structure and the major product by NMR spectroscopy.

Figure 2.4. Solid-State Parameters of 26a. Shown with thermal ellipsoids at the 50% probability level. Hydrogen atoms are omitted for clarity. One of four crystallographically distinct molecules in the asymmetric unit cell is shown. Bond distances are given in Å.

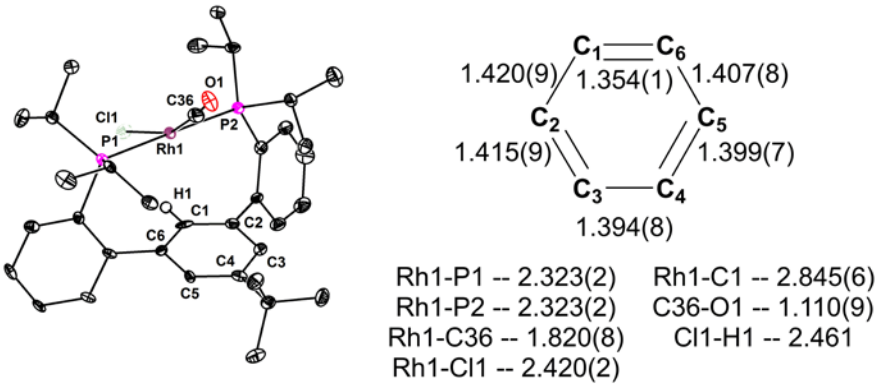

The effect of CO on bond activation chemistry was further studied. Treatment of **1a** with 0.5 equiv. of $(Rh(COE)_2Cl)_2$ under an atmosphere of CO affords a new species (**23a**) as a mixture of isomers displaying two doublets by $^{31}P\{^{1}H\}$ NMR spectroscopy (major, 39.73 ppm, J_{RhP} = 127 Hz; minor, 35.08 ppm, J_{RhP} = 127 Hz; Scheme 2.6). Resonances at 3.07 ppm (major isomer) and 3.02 ppm (minor isomer) in the ^{1}H NMR spectrum are

attributable to the –OC*H*$_3$ substituent of **1a** remaining intact in **23a**, assigned as a diphosphine Rh(Cl)(CO) species with an IR stretch assigned to Rh–CO (ν_{CO} = 1957 cm^{-1}) comparable to those reported in the literature for similar compounds.[20,22] Heating a solution of **23a** in a sealed J. Young tube affords the new compound **24a** with a new resonance observed by ^{31}P NMR spectroscopy (43.34 ppm) and an IR stretch (ν_{CO} = 1942 cm^{-1}) comparable to those of previously reported phenoxide diphosphine RhCl species.[23] In the ^{1}H NMR spectrum, a resonance consistent with a –OC*H*$_3$ group was no longer observed and MeCl was detected. This is consistent with alkyl C–O bond cleavage. The identity of the final Rh species was confirmed by independent synthesis from diphosphine **1f** (Scheme 2.6). Thus, in the presence of an excess of a π-acidic ligand (CO) other than the central arene of **1a**, aryl C–O bond activation is suppressed in favor of cleavage of the weaker alkyl C–O bond. This transformation likely proceeds through an acid–base mechanism involving coordination of Rh^{I}–CO to the O atom of **1a**. This observation indicates that an electron-rich metal center is required for activation of the aryl C–O bond. The complete shift in selectivity upon CO addition is notable. In putative catalytic systems, CO poisoning of the metal center and a shift in reactivity could occur.

The reductive elimination for **18a** is faster than for the Ni complex **3a**, which requires heating to 100 °C and the addition of formaldehyde or other donors. The Ni complex is proposed to undergo slow conversion due to the *trans* orientation of the aryl and hydride moieties. Assuming *cis* positioning of these moieties in the five-coordinate Rh complex **18a**,[6b,6e,24] they are poised to undergo reductive elimination more readily than in **3a**. The Rh product **19a** does not display CO coordination, in contrast to the Ni (**4a,b**) case, suggesting that a potential Rh catalyst for the deoxygenation of aryl alkyl ethers may be less prone to deactivation by aldehydes or CO.

2.1d Aryl C–O Bond Activation at Ir^{I}

An Ir^{I} species was targeted to continue the investigation of the series of group 9 metals with the aryl alkyl ether **1a** (Scheme 2.7). As with Rh, the commercially available Ir^{I} compounds $(Ir(COD)Cl)_2$ and $(Ir(COE)_2Cl)_2$ were tested as precursors. Broad resonances near those of **1a** were observed by ^{31}P NMR spectroscopy upon stirring of **1a** with 0.5 equiv of $(Ir(COE)_2Cl)_2$ in THF at room temperature after 4 h and remained mostly unchanged after 48 h. No signals consistent with ether bond cleavage were observed by ESI-MS, although a signal consistent with **1a** and Ir (m/z 741) was observed. Treatment of **1a** with $(Ir(COD)Cl)_2$ in THF for 0.5 h, however, afforded a new species, **27a**, that displayed a pair of resonances in its $^{31}P\{^{1}H\}$ NMR spectrum in a 1:1 ratio: one at a chemical shift (-4.01 ppm) close to that observed for the free diphosphine **1a** and one further downfield (47.37 ppm, C_6D_6) (Scheme 2.8). The ^{1}H NMR spectrum displays resonances consistent with bound COD (3.04–3.36 ppm, 8H; 5.31 ppm, 4H) and an intact methoxy group (2.90 ppm). These spectra are consistent with coordination of a single phosphine donor to the Ir(COD)Cl fragment, without loss of the olefin ligand. In contrast to metalation of **1a** with Rh, Ir does not show olefin substitution with phosphine at room temperature, probably due to the stronger metal–olefin interaction in the case of Ir. This reactivity is consistent with the literature; the reaction of phosphine and $(Ir(COD)Cl)_2$ under mild conditions typically results in dimer dissociation to afford four-coordinate mono-phosphine Ir(COD)Cl species.[25] Examples of the use of heat[26] or hydrogenation[27] to dissociate COD have been reported in the case of electron-deficient[26] or bulky[27] phosphines. In contrast, the Rh analogues undergo substitution at room temperature in the absence of H_2.[6b,6e,28] The

faster reaction with $(Ir(COD)Cl)_2$ in comparison to $(Ir(COE)_2Cl)_2$ may be due to the smaller steric profile of one COD vs two COE ligands, although the COE adduct is typically more reactive than the chelating COD ligand.[25]

Scheme 2.7. Nonselective C–O Bond Activation of Ar–O–Me Ether by Ir^I.

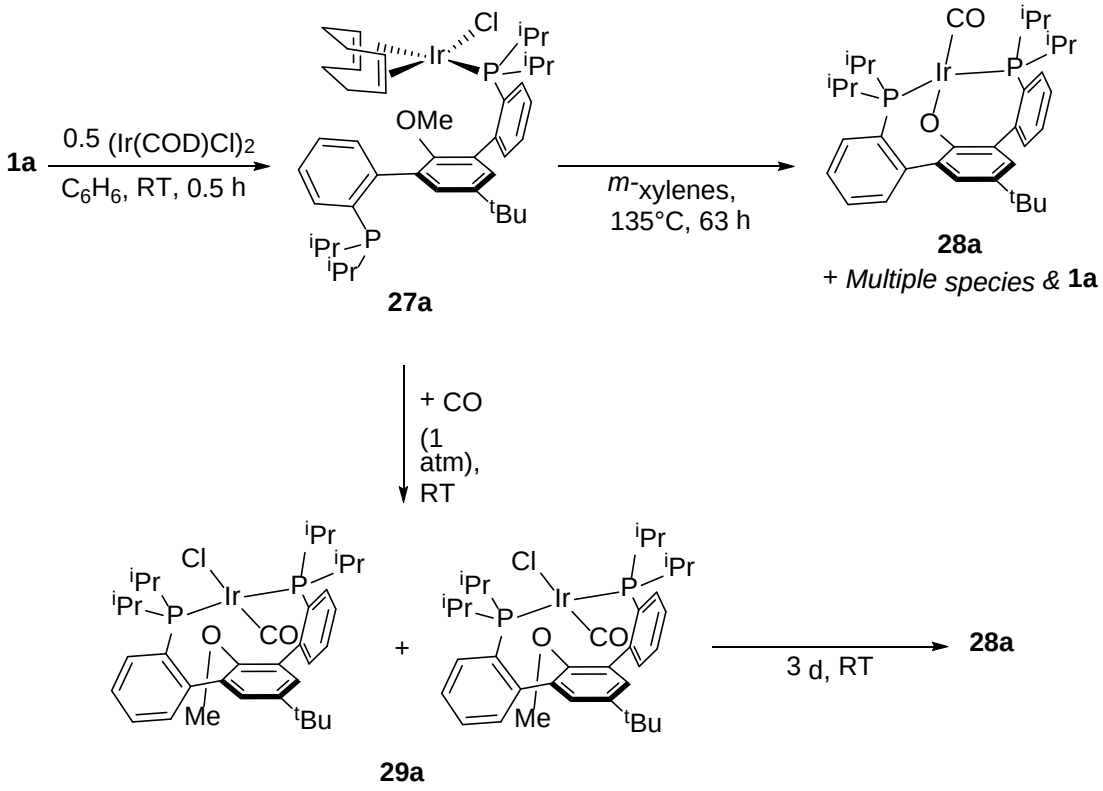

Compound **27a** is stable in solution at room temperature for extended periods (^{1}H and ^{31}P NMR spectroscopy, ESI-MS) of time. However, heating a slurry of compound **27a** at 135 °C in *m*-xylene for 63 h affords a new major species, **28a**, in *ca.* 50% NMR yield with a new resonance observed by ^{31}P NMR spectroscopy at 38.57 ppm (*m*-xylene), a minor species with an upfield 144.63 ppm resonance, and multiple other minor species with resonances downfield of **1a** (14.08–36.41 ppm, ca. seven species). Masses consistent with both aryl and alkyl bond cleavage were observed by ESI-MS upon treatment of an aliquot

of this reaction mixture with HCl. Thus, C–O bond activation is observed at Ir^{I} but not selectively.

Upon isolation of compound **28a** in analytically pure form, characterization by ^{1}H NMR spectroscopy did not reveal a signal consistent with a methoxy resonance, suggesting that ether bond cleavage had occurred. MeCl was detected among the volatile components by ^{1}H NMR spectroscopy (2.28 ppm, C_6D_6) consistent with cleavage of the alkyl–O ether bond. Characterization by IR spectroscopy revealed a band (1931 cm^{-1}) consistent with the CO stretch of related diphosphine Ir^{I}–CO adducts.[23a,29] Furthermore, the ^{13}C NMR spectrum shows a resonance at 176.98 ppm (C_6D_6) that corroborates the IR data. The assignment of 28a as an Ir^{I}-phenoxide-CO complex was confirmed by independent synthesis through two routes (Scheme 2.8). Treatment of diphosphine **1f** with benzylpotassium (BnK) followed by addition of 0.5 equiv of $(Ir(COD)Cl)_2$ in THF afforded new species with ^{31}P resonances downfield of those for the free ligand, assigned as an Ir^{I} species supported by a POP-pincer, and another ligand (e.g., solvent or COD) similar to the case for **25a** (see Scheme 2.6). Subsequent treatment of this intermediate species with 1 atm of CO resulted in near-quantitative conversion to a compound with ^{1}H and ^{31}P NMR spectroscopic features identical with those of **28a**. Another synthetic route involved placing a solution of **27a** in C_6H_6 under 1 atm of CO at room temperature. Again, near-quantitative conversion to compound **28a** was observed over the course of 3 days. Here, CO is proposed to displace COD, facilitating diphosphine chelation and MeCl elimination. An intermediate, compound **29a**, was observed by NMR spectroscopy in the conversion of **27a** to **28a** and is assigned as a mixture of diphosphine $Ir^{I}(CO)Cl$ isomers (Scheme 1.7; compare to the Rh^{I} example **23a**; Scheme 2.6). Two singlets are observed for **29a** by $^{31}P\{^{1}H\}$ NMR spectroscopy (major isomer, 31.82 ppm; minor isomer, 26.43 ppm).

Resonances consistent with an intact –OCH_3 moiety are detected by ^{1}H NMR spectroscopy as well (major, 3.01 ppm; minor, 2.97 ppm). The observed Ir–O stretch (ν_{CO} = 1937 cm^{-1}) is consistent with examples in the literature,[30] including another square-planar Ir^I(CO)Cl complex (in this case, dinuclear) supported by a trans-spanning diphosphine, for which both coordination isomers were also observed.[30a]

Scheme 2.8. Mechanism of Nonselective C–O Bond Activation by Ir^I.

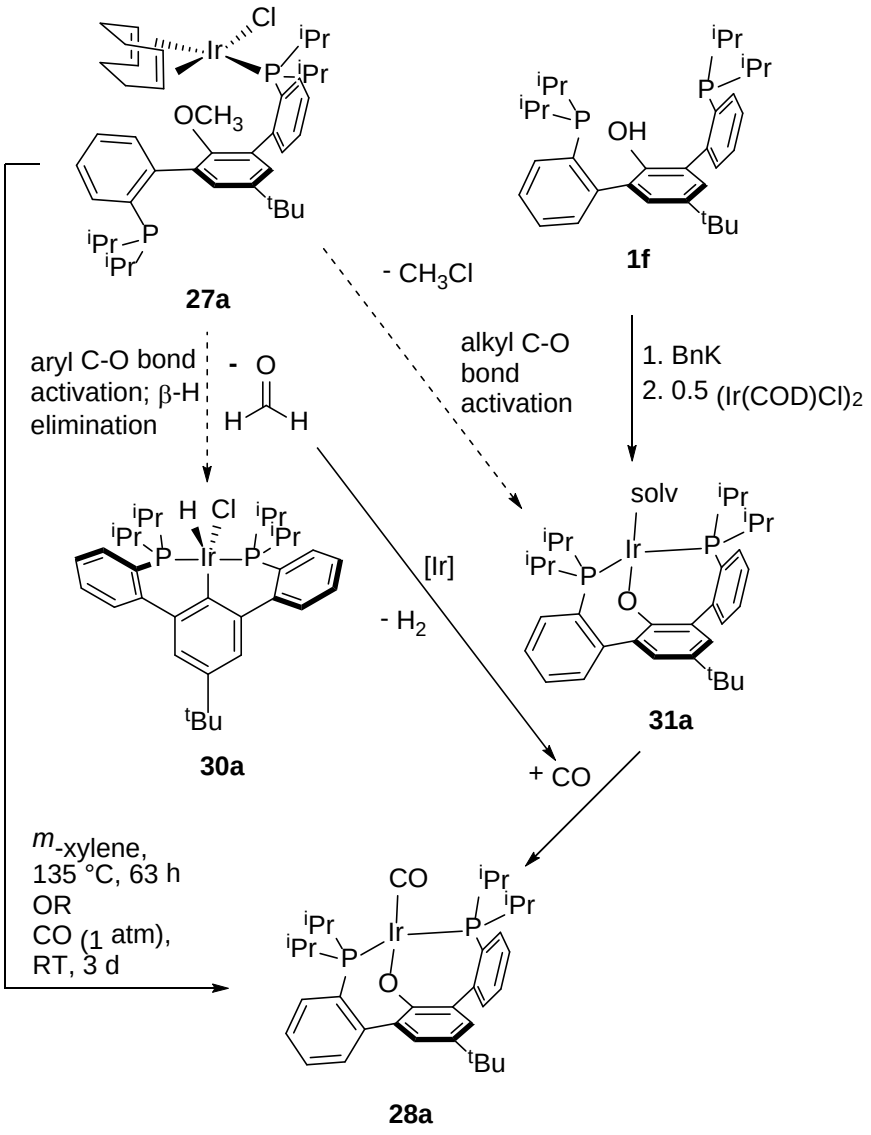

Direct confirmation of the structure of **28a** came from a single-crystal XRD study of the compound (Figure 2.5a). The coordination about Ir deviates only slightly from square

planar (∠C(35)–Ir(1)–P(1) = 92.00(3)°; ∠O(1)–Ir(1)–P(1) = 90.88(2)°, ∠P(1)–Ir(1)–P(2) = 172.56(2)°, ∠O(1)–Ir(1)–C(35) = 176.18(4)°). The Ir(1)–O(1) bond distance (2.089(1) Å) is similar to that reported by Milstein and coworkers (2.083(5) Å) for an Ir^{III}-hydride-chloride supported by the phenoxide version of diphosphine **1e**, although that example is six-coordinate.[28b] Milstein and co-workers have also isolated a six-coordinate Ir^{I} species supported by a diphosphine tethered to a phenoxium cation.[28a] For that complex, Ir(1)–C(1) and Ir(1)–O(1) distances of 2.189(5) and 2.061(3) Å, respectively, are consistent with η^2 coordination to the phenoxium moiety. In the case of **28a**, the longer Ir(1)–C(1) distance (2.514(1) Å) is consistent with η^1-coordination to the O atom of a phenoxide moiety.

The formation of complex **28a** suggests that both aryl and alkyl C–O bond activation occurs with Ir. Alkyl C–O bond activation with Ir^{I} may occur via several mechanisms to generate MeCl and a POP-pincer Ir^{I} species (**31a**), presumably with one additional ligand (Scheme 2.8). The Ir^{I} center can act as a Lewis acid, as described for Rh^{I} (see *Aryl C–O Bond Activation at Rh*) and Ni^{II} (see *Alkyl C–O Bond Activation at Ni*^{II}). Recently, Ir has also been reported to activate aryl ethers, upon coordination to the π system of the arene, toward alkyl C–O bond cleavage by intermolecular attack of a nucleophile.[7d] Similar to the case for Pd^{0} and Pt^{0} (Scheme 2.2) Ir^{I} can react via oxidative addition of the C–O bond to generate an Ir^{III}-methyl-chloride-phenoxide species that undergoes reductive elimination of MeCl. Ir has also been reported to perform alkyl C–O cleavage of ethers via initial C–H activation at the alkyl group.[7b,7e] From either reaction pathway, the resulting Ir^{I} complex (**27a**) coordinates CO to form **28a**. A CO moiety could be generated from the methyl aryl ether in a fashion similar to that with Ni^{0} (Scheme 2.1) and Rh^{I} (Scheme 1.4) via aryl C–O bond activation, followed by β-H elimination to generate

formaldehyde, which then is decarbonylated by Ir. The Ir complexes resulting from aryl C–O bond activation could not be isolated but were detected by ESI-MS. The yield of formation of **28a**, at *ca.* 50%, is consistent with aryl and alkyl C–O bond activation occurring in approximately a 1:1 ratio.

As discussed for Rh^{I} reactivity in the presence and absence of CO, the more Lewis acidic CO-ligated Ir center likely facilitates C–O bond activation via a Lewis acid-base mechanism. A redox mechanism involving oxidative addition of the O–Me bond followed by reductive elimination of MeCl cannot be ruled out. However, the π back-bonding interaction between Ir^{I} and CO lowers the propensity of the Ir^{I} center to undergo oxidative addition. With a related phosphine ligand, CO bonding to the Ni^{0} center leads to a longer metal-arene interaction, consistent with decreased back-bonding into the antibonding orbitals of the arene.[19] Therefore, the coordination of CO is expected to increase the Lewis acidity of the Ir center by π back-bonding, which increases the rate of alkyl C–O bond activation and decreases the rate of aryl C–O bond activation. The CO stretching frequencies of the Rh and Ir compounds mirror their reactivity toward C–O bond activation. The IR stretches for the diphosphine M(CO)Cl complexes **23a** (M = Rh, ν_{CO} = 1957 cm^{-1}) and **29a** (M = Ir, ν_{CO} = 1937 cm^{-1}) and diphosphine phenoxide M(CO) complexes **24a** (M = Rh, ν_{CO} = 1942 cm^{-1}) and **28a** (M = Ir, ν_{CO} = 1929 cm^{-1}) indicate more π back-bonding to CO from Ir in comparison to that from Rh. This correlates with the faster conversion of **1a** to the alkyl C–O bond activation product **28a** (Scheme 1.7) with Ir versus the conversion of **1a** to **24a** (Scheme 2.6) with Rh.

The reactivity observed for Ir^{I} suggests that Ir may be an attractive candidate for catalyst design. It is capable of cleaving ether C–O bonds, and even in the presence of CO it performs the conversion, although by activating the weaker alkyl C–O bond.

2.2 Bond Activation by Lewis Acid-Base Pathways

2.2a Alkyl C–O Bond Activation at Ni^{II}

Treatment of diphosphine **1a** with group 10 $M^{II}X_2$ (X = Cl) salts was conducted to determine if ether C–O bond cleavage could be effected using a more oxidized metal center. Addition of 1 equiv. of Ni(DME)Cl_2 (DME = dimethoxyethane) to diphosphines **1a,b** at 20 °C gave rise to the new species **32a,b**, respectively, which displayed resonances in ^{31}P NMR spectra (**32a**, 13.74 ppm; **32b**, 14.04 ppm; C_6D_6) significantly upfield of signals observed for the related Ni^{0} complexes **2a,b** (**2a**, 41.04 ppm; **2b**, 40.65 ppm; C_6D_6). In further contrast, the signals assigned to the protons of the central arene resonate downfield in comparison with those of the free phosphine in the ^{1}H NMR spectrum of **32a,b** (**32a**, 7.53 ppm; **32b**, 6.99 ppm; C_6D_6) (Scheme 2.9). In addition, no signals attributable to the –OC*H*$_3$ group were observed. These data suggest cleavage of the ether but no strong metal-arene interaction in the product. To determine the fate of the methyl group and chloride, the reaction was run in a sealed reaction vessel in C_6D_6 and the volatiles were vacuum-transferred to a J. Young tube. A singlet at 2.28 ppm (C_6D_6) in the ^{1}H NMR spectrum indicates the formation of MeCl, as confirmed by comparison against a spectrum of an authentic sample. Formation of MeCl indicates alkyl C–O cleavage to generate a Ni-phenoxide species. A single-crystal XRD study confirmed the assignment of **32b** as a Ni chloride supported by a POP phenoxide (Figure 2.5a) ligand. Two crystallographically distinct molecules were observed with different orientations of the dimethylamino

substituents. Average *cis* L–M–L angles (90.31(5)°, standard deviation 3.4) and *trans* L–M–L angles (∠P(1)–Ni(1)–P(2) = 168.72(3)°; ∠P(3)–Ni(2)–P(4) = 167.73(3)°) are consistent with a square-planar geometry. The angles between the planes defined by the carbons of the central arene (C(1) through C(6); C(33) through C(38)) and the dimethylamino substituents (C(19), C(20), and N(1); C(52), C(53), and N(2)) of the molecules are quite different (16.41, 65.88°). The dimethylamino substituent in one molecule is nearly in plane with the central arene, and a shorter N(2)–C(36) distance (1.383(4) Å) versus N(1)–C(4) in the other molecule (1.432(4) Å) suggests possible stabilization of an iminoquinone-like moiety; however, neither localization of double-bond character of the central arene nor contraction of the phenolic C–O bond is observed (Figure 2.5a). Thus, for both crystallographically distinct molecules, solid-state structural metrics are most consistent with a Ni–phenoxide–chloride–diphosphine. The solid-state structure of **32b** is unusual, as it displays metal coordination to oxygen with an Ni–O vector perpendicular (∠C(1)–O(1)–Ni(1) = 95.03(2)°; ∠C(33)–O(2)–Ni(2) = 90.58(2)°) to the plane of the phenoxide; typical Ni–O–aryl angles for Ni phenoxides range from 111 to 130°.[31]

Ni^{II}-mediated cleavage of the alkyl C–O bond is proposed to occur via a Lewis acid-base mechanism. Donation of electron density from the oxygen atom in **1a,b** to the Lewis acidic Ni^{II} weakens both O–CH_3 and Ni–Cl bonds. Elimination of MeCl affords the Ni–phenoxide–chloride product. A related mechanism could involve initial dissociation of chloride, followed by nucleophilic attack by an outer-sphere halide at the methoxy carbon of the diphosphine. Milstein and co-workers have reported cleavage of the methyl C–O bond of the aryl/methyl ether of a related diphosphine upon treatment of that ligand with group 10 $M^{II}X_2$ precursors (two examples, M = Pd, X = OTf; M = Ni, X = I) to afford a

$M^{II}X$ fragment supported by a POP-pincer ligand.[6b,6e,8g] Examples of intramolecular methyl C–O bond cleavage by elimination of MeCl have been reported for Fe^{II},[32] Ru^{II},[33] Ni^{II},[6e,8g] Pd^{II},[6c,9a,9b,28b] Pt^{II},[9a,10a] and Rh^{III}.[6a,6c] In addition, intramolecular C–O bond cleavage in related diphosphine systems through a mechanism involving nucleophilic attack of a ligand on the methyl group of a transition-metal-coordinated methoxy moiety has been reported for Ru^{II},[34] Rh^{I},[35] Ir^{I},[35] and Pd.[9b] The absence of evidence of phosphonium at the end of the reaction to afford **32a,b** is inconsistent with that alternate reaction mechanism.

Figure 2.5a. (top to bottom) **Solid-state parameters of 28a and 29a** (two crystallographically distinct molecules observed in the asymmetric unit, both shown). Shown with thermal ellipsoids at the 50% probability level. Hydrogen atoms are omitted for clarity. Bond distances are given in Å.

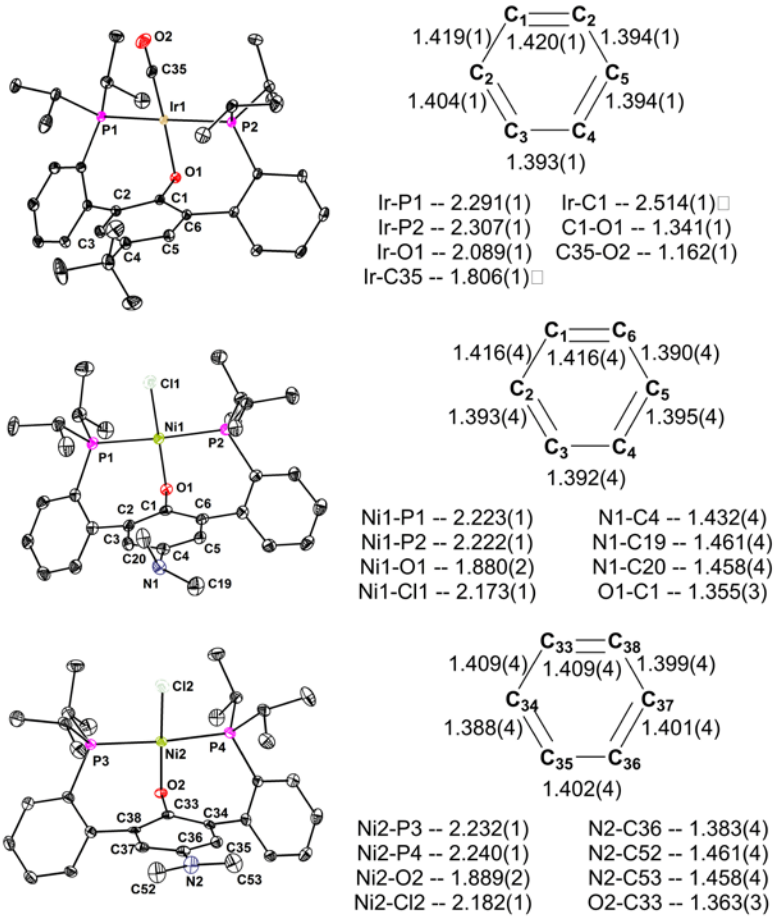

Figure 2.5b. Solid-state parameters of 31a (two crystallographically distinct molecules observed in the asymmetric unit cell, both shown) shown with thermal ellipsoids at the 50% probability level. Hydrogen atoms are omitted for clarity. Bond distances are given in Å.

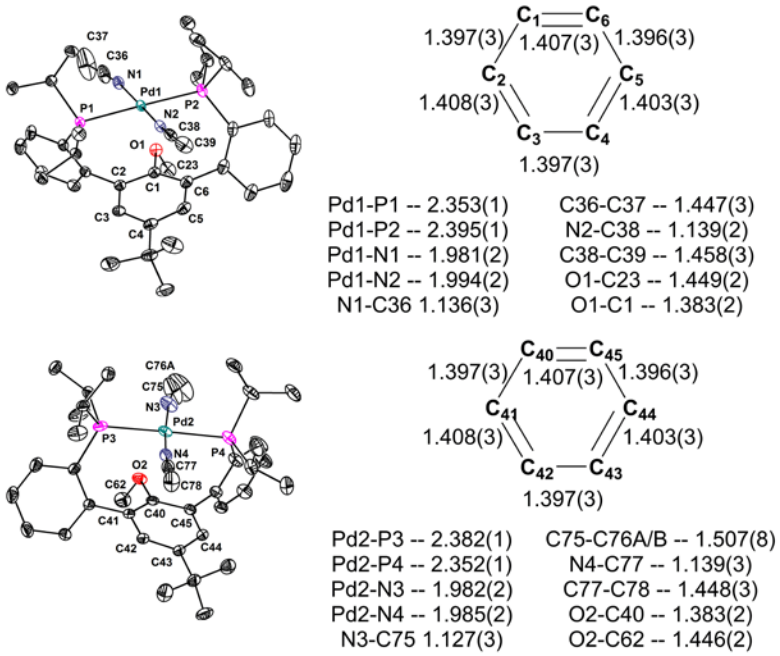

2.2b Alkyl C–O Bond Activation at Pd^{II} and Pt^{II}

Ether activation with Pd^{II} was tested by treatment of **1a** with 1 equiv. of Pd(COD)Cl$_2$ (Scheme 2.9) ^{31}P{^{1}H} NMR spectroscopy revealed the formation of a new major species, **33a**, in 90% NMR yield over the course of 1 h with a resonance observed by ^{31}P{^{1}H} NMR spectroscopy upfield of the resonance for the free ligand (**33a**; 26.28 ppm, C_6D_6). In contrast to the Ni^{II} compounds **32a,b** a resonance assigned to the protons of a methoxy group in compound **32a** (3.07 ppm, C_6D_6) was observed by ^{1}H NMR spectroscopy at room temperature, near the resonance of the protons assigned to the methoxy group of **1a** (3.02 ppm, C_6D_6).

These observations are consistent with substitution of COD by diphosphine **1a** to afford a square-planar Pd^{II} species with two *trans* chloride ligands and a *trans*-spanning diphosphine. Attempts to characterize this compound by crystallography have been unsuccessful, but X-ray diffraction quality crystals were obtained for a related species.

To confirm the binding motif proposed for **33a**, diphosphine **1a** was treated with 1 equiv. of $[Pd(MeCN)_4][(BF4)_2]$ to afford the new species **34a** with a resonance observed by ^{31}P NMR spectroscopy at 38.38 ppm (CD_3CN). Protons assigned to a methoxy group (3.09 ppm, CD_3CN) were observed by ^{1}H NMR spectroscopy. A resonance observed by ^{19}F NMR spectroscopy (-149.28 ppm) was assigned to outer-sphere BF_4 anions. These data suggest the formation of square-planar Pd^{II} species with the two phosphines and MeCN coordinated to the metal center. A single-crystal XRD study of **34a** (Figure 2.5b) shows two crystallographically distinct molecules, both with two MeCN molecules coordinating to Pd in a *trans* fashion, and **1a** acting as a *trans*-spanning diphosphine ligand. The Pd(1)–C(1) and Pd(2)–C(40) distances are 2.874(2) and 2.872(2) Å, respectively. These bond distances indicate that there is no interaction between the metal center and the ether and arene moieties. On the basis of these structural data and the similarity of the NMR spectra to those of **33a**, we assign compound **33a** as a square-planar Pd^{II} species bearing two *trans* chloride ligands.

Heating **1a** and $Pd(COD)Cl_2$ in an 80 °C oil bath in a sealed vessel over the course of 4 h in C_6H_6 resulted in full conversion to species **35a**. The ^{1}H NMR spectrum of **35a** is similar to that of Ni^{II} compound **32a**, with a diagnostic shift of the resonance of the protons of the central arene downfield (7.31 ppm, C_6D_6) of free phosphine and no resonance that could be assigned to an intact methoxy substituent. On the basis of these spectroscopic

features, the product was assigned as analogous to **32a**, with cleavage of the alkyl C–O bond.

The reactivity of **1a** with a Pt^{II} complex was explored. Treatment of **1a** with 1 equiv. of $Pt(COD)Cl_2$ gave 50% conversion from free ligand to afford the new major species **36a** ($^{31}P\{^1H\}$ NMR spectroscopy: 17.96 ppm, C_6D_6) in 40% NMR yield over the course of 12 h (notably, a reaction time longer than that required with either $Ni(DME)Cl_2$ or $Pd(COD)Cl_2$) and unidentified products with resonances observed by ^{31}P NMR spectroscopy upfield of free phosphine **1a** (Scheme 2.9). Similar to the case for compound **33a**, resonances assigned to the protons of a methyl group in compound **36a** (3.08 ppm) were observed by ^1H NMR spectroscopy, near the resonance of the protons assigned to the methoxy group of compound **1a** (3.02 ppm). These observations are consistent with substitution of COD by the phosphine **1a**. On the basis of the spectroscopic similarities to compound **33a**, we assign **36a** as an isostructural square-planar Pt^{II} species.

Heating **1a** and $Pt(COD)Cl_2$ in an 80 °C oil bath in a sealed vessel over the course of 4 h in C_6H_6 resulted in full conversion to compound **37a**. The ^1H NMR spectrum of **37a** is similar to that of compounds **32a** and **35a**, with a diagnostic shift of the resonance of the protons of the central arene downfield (7.33 ppm, C_6D_6) of free ligand and no resonance consistent with a methoxy substituent remaining intact, consistent with the assignment of this compound as a diphosphine Pt^{II} chloride phenoxide. Phenoxide PtCl compounds supported by *trans*-spanning diphosphines are rare in the literature; the observed Pt–P coupling (**36a**, J_{PtP} = 2609 Hz, C_6D_6; **37a**, J_{PtP} = 2812 Hz, C_6D_6) for both Pt^{II} chloride species is smaller than that reported for a salicylaldiminato $Pt^{II}Cl$ in the literature with *trans*-phenoxide and chloride ligands.[36]

Scheme 2.9. Alkyl C–O Bond Activation of Ar–O–Me Ether by Group 10 Metals.

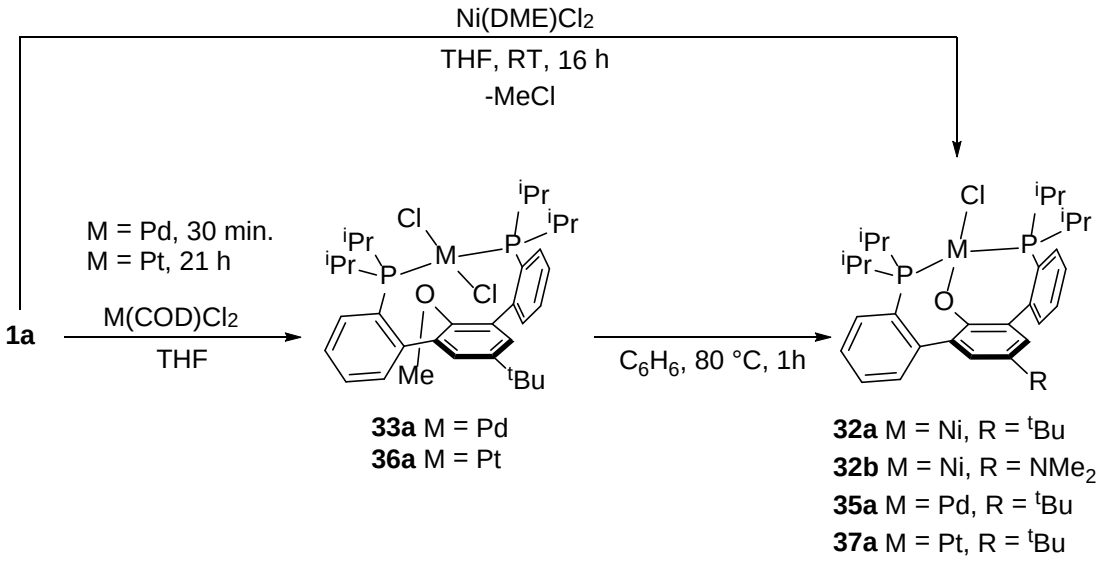

In contrast to Ni^{II}, both Pd^{II} and Pt^{II} diphosphine dihalides are isolable at room temperature. This is consistent with the decrease in Lewis acidity upon descending a group. Whereas alkyl C–O bond activation is observed at room temperature with Ni^{II}, heating is required to drive the less Lewis acidic metals to activate the alkyl C–O bond of diphosphine **1a**.

2.2c Alkyl C–O Bond Activation at Rh^{I} and Ir^{I}

As discussed under *Aryl C–O Bond Activation at Rh^{I}* and *Aryl C–O Bond Activation at Ir^{I}*, the cleavage of the alkyl C–O bond by Rh^{I} and Ir^{I} in the presence of CO is proposed to occur via a Lewis acid-base mechanism, but a redox mechanism cannot be ruled out.

2.3 No Ether C–O Bond Activation at Co^{I}

Reduction of an *in situ* generated THF adduct of $CoBr_2$ in the presence of diphosphine **1a** with cobaltocene in a nonpolar solvent (toluene) afforded the new species

38a. Reduction in nonpolar solvent following addition of metal halide to phosphine in THF has been previously employed in the synthesis of low-valent late transition-metal complexes.[37] Compound **38a** displays paramagnetically shifted peaks from ca. -10.00 to 55.00 ppm in the ^{1}H NMR spectrum and no detectable resonance by ^{31}P NMR spectroscopy.

Figure 2.6. Solid-state parameters of 2a and 38a. Shown with thermal ellipsoids at the 50% probability level. Hydrogen atoms are omitted for clarity. Bond distances are given in Å.

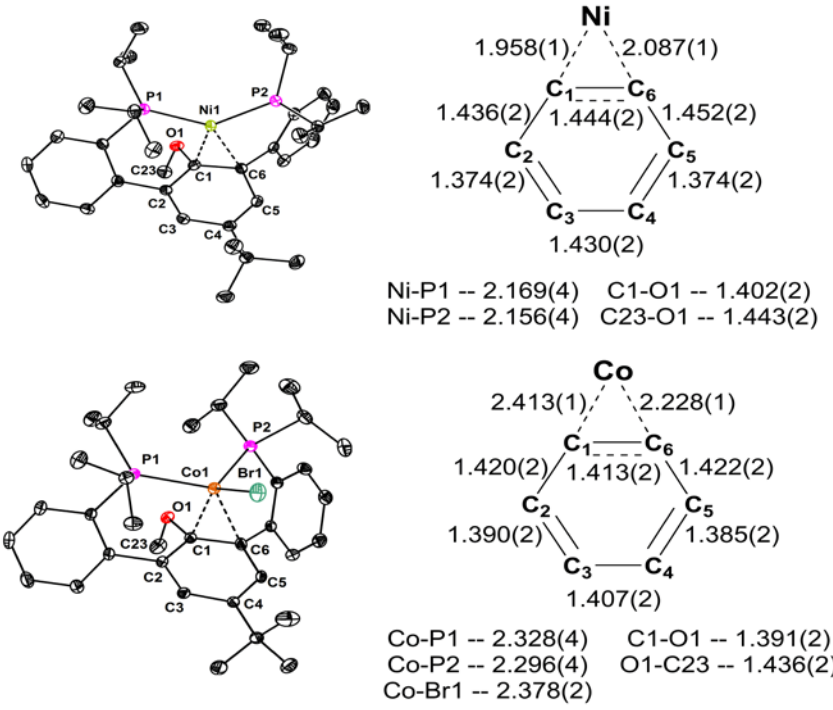

A single-crystal XRD study confirmed the assignment of **38a** (Figure 2.6). In the solid state, the Co^{I} compound is pseudo-tetrahedral, with coordination of the two phosphines, a bromide, and part of the ligand arene π system. As with **2a**, an η^2 interaction between Co and two carbons of the central arene was observed (Co–C(1) = 2.413(1) Å; Co–C(6) = 2.228(1) Å), similar to that seen with the Ni^{0} species **2a,b** (Ni–C(1) = 1.958(1) Å;

Ni–C(6) = 2.087(1) Å). The longer Co–C distances are consistent with the longer covalent radius of high-spin Co (1.50 Å) vs low-spin Ni (1.24 Å).[38] A shorter bond distance is observed between the two carbons bound η^2 to Co in **38a** (C(1)–C(6) = 1.413(2) Å) versus those bound to Ni in **2a** (C(1)–C(6) = 1.444(2) Å). Furthermore, longer C–C bonds are observed between the carbons displaying partially localized double-bond character in the central arene ring in **38a** (C(2)–C(3) = 1.390(2) Å, C(4)–C(5) = 1.385(2) Å) in comparison with **2a** (C(2)–C(3) = 1.374(2) Å, C(4)–C(5) = 1.374(2) Å), consistent with more limited disruption of aromaticity arising from the metal-arene interaction in the case of **38a** versus **2a**.

As **38a** was found to be stable in solution at room temperature (^{1}H and ^{31}P NMR spectroscopy, ESI-MS), a solution of the Co^I compound was heated to determine if ether bond activation could be induced at higher temperatures. Heating compound **38a** at 80 °C in C_6D_6 for 12 h afforded a black insoluble precipitate and free phosphine **1a** with no ether bond activation products observed by NMR spectroscopy or ESI-MS. Although activation of the O–Me bond was observed with Ni^{II}, also a d^8 metal center, lack of ether cleavage with **38a** is likely due to the lower Lewis acidity of Co^I vs Ni^{II}. More reduced Co complexes, isoelectronic with Ni^0 species **2a,b** known to perform ether activation, were targeted. However, attempts to reduce **38a** over Na/Hg amalgam afforded primarily free phosphine and black precipitate. To access a halide-free version of **38a**, treatment with TlOTf (OTf = trifluoromethanesulfonate) afforded a new, diamagnetic complex. On the basis of an upfield shift of the protons of the central arene, the interaction between the metal center and the arene remains strong. However, heating this compound at 80 °C in C_6D_6 for 12 h only afforded a black insoluble precipitate and free phosphine **1a** (^{1}H and ^{31}P NMR

spectroscopy, ESI-MS). Thus, C–O bond activation was not observed at Co^{I} supported by **1a**.

CONCLUSIONS

Scheme 2.10. Summary of Aryl Ether Bond Activation Reactivity.

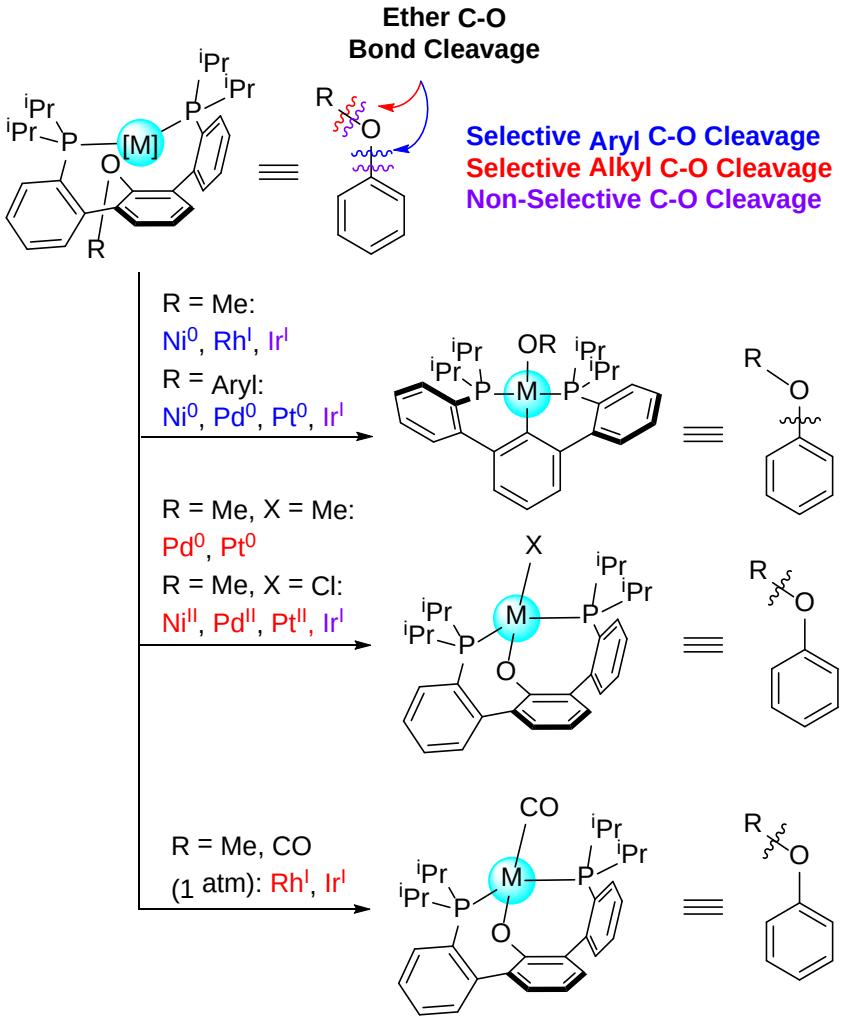

Several modes of ether CO bond cleavage have been observed for aryl alkyl and diaryl ethers bearing pendant phosphines (Scheme 2.10). Ni^0 and Rh^I are both selective for the cleavage of the stronger aryl C–O bond in aryl alkyl ethers. Moreover, conversion of the C–O bond to C–H is observed, modeling the full conversion desirable in the context of substrate deoxygenation, particularly important for lignin cleavage and conversion to fine chemicals or fuels. Activation by Rh^I occurs under very mild conditions of room temperature within 3 h and is significantly faster than that by Ni^0. CO coordination is

observed at Ni^0, but not the major Rh^I product, suggesting that potential catalyst poisoning is less likely with Rh^I. Ni^0 and Rh^I react by a redox mechanism involving oxidative addition of the C–O bond, β-H elimination, and C–H reductive elimination. Ni^{II}, Pd^{II}, Pt^{II}, Pd^0, and Pt^0 perform the selective cleavage of the alkyl C–O bond of aryl alkyl ethers. Ni^{II}, Pd^{II}, and Pt^{II} are proposed to facilitate the transformation via a Lewis acid-base mechanism. Cleavage of the Me–O bond by Ni^{II} demonstrates that the metal center can access that position; therefore, the selective activation of the aryl C–O bond is not a matter of steric accessibility. Pd^0 and Pt^0 activate the alkyl C–O bond by oxidative addition. Studies with a diaryl ether moiety show that both Pd^0 and Pt^0 can cleave the aryl C–O bond, indicating that for aryl alkyl ethers these prefer the weaker but more distant alkyl C–O bond, unlike Ni^0. The stronger metal–arene interaction observed with Ni^0 and Rh^I correlates with selective and fast cleavage of the aryl C–O bond. Ir^I is unselective, cleaving the aryl C–O bond concurrently with the alkyl C–O bond. In the presence of CO, however, selective cleavage of the alkyl C–O bond was observed for both Rh^I and Ir^I, a notable change in mechanism. Overall, the present studies have provided a thorough and systematic comparison of the reactivity of group 9 and 10 metals when presented with a sterically proximal ether C–O activation. On the basis of these model studies, Ni^0 and Rh^I are particularly well suited for catalysis, as they could undergo complete C–O to C–H conversion; indeed, Ni-based catalysts have already been reported. Depending on the nature of the substrate and desired outcome, Ni^0, Pd^0, Pt^0, Rh^I, and Ir^I are all potential candidates for the development of catalysts for the cleavage of aryl ether C–O bonds.

EXPERIMENTAL SECTION:

General considerations

Unless otherwise indicated, reactions performed under inert atmosphere were carried out in oven-dried glassware in a glovebox under a nitrogen atmosphere purified by circulation through RCI-DRI 13X-0408 Molecular Sieves 13X, 4x8 Mesh Beads and BASF PuriStar® Catalyst R3-11G, 5x3 mm (Research Catalysts, Inc.). Solvents for all reactions were dried by Grubbs' method.[39] Acetonitrile-d_3, benzene-d_6, chloroform-d_1, and dichloromethane-d_2 were purchased from Cambridge Isotope Laboratories. Benzene-d_6 was vacuum distilled from sodium benzophenone ketyl. Acetonitrile-d_3 and dichloromethane-d_2 were vacuum distilled from calcium hydride. Alumina and Celite were activated by heating under vacuum at 200 °C for 24 h. 1,3-bis(2'-diisopropylphosphinophenyl)-5-tert-butyl-2-methoxybenzene (**1a**),[11] 1,3-bis(2'-diisopropylphosphinophosphino)-5-dimethylamino-2-methoxybenzene (**1b**),[11] bis(1,5-cyclooctadiene)platinum,[16] 1-(*tert*-butyl)-3,5-diiodobenzene,[40] 4-(tert-butyl)-2,6-diiodophenol,[41] chloromethyl methyl ether,[42] and benzyl potassium[43] were synthesized following literature procedures. [(4-nitrophenyl)(phenyl)iodonium] [trifluoromethanesulfonate][44] was synthesized by the method of Olofsson and co-workers and matched previously reported spectra.[45] All other materials were used as received. ^{1}H, ^{13}C, ^{19}F, and ^{31}P NMR spectra were recorded on Varian or Bruker spectrometers at ambient temperature unless denoted otherwise. Chemical shifts are reported with respect to internal solvent for ^{1}H and ^{13}C NMR data, respectively: 1.94 ppm and 118.26 and 1.32 ppm (CD_3CN); 7.16 ppm and 128.06 ppm (C_6D_6); 7.26 ppm and 77.16 ppm ($CDCl_3$); 5.32 ppm and 53.84 ppm (CD_2Cl_2).[46] ^{19}F and ^{31}P NMR chemical shifts are reported with respect to an external standard of C_6F_6 (-164.9 ppm) and 85% H_3PO_4 (0.0 ppm), respectively, unless

denoted otherwise. Apparent triplets are denoted: "app t". For apparent triplets, the reported coupling constant represents average of coupling to two phosphorous nuclei. IR measurements were obtained on a Bruker Alpha spectrometer equipped with a diamond ATR probe. Fast atom bombardment-mass spectrometry (FAB-MS) analysis was performed with a JEOL JMS-600H high resolution mass spectrometer. Elemental analysis (EA) was conducted by Robertson Microlit Laboratories, Inc. (Ledgewood, NJ). NMR data are provided for all newly reported compounds. In the following complexes, the carbons of the terphenyl backbone are assigned using the following schemes:

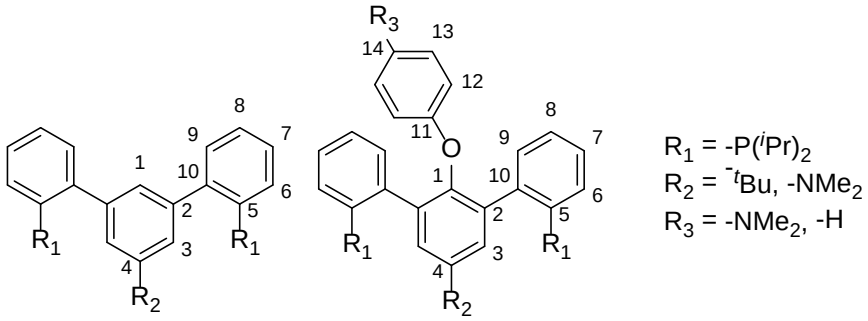

Synthesis of [1,3-bis(2'-diisopropylphosphinophenyl)-5-tert-butyl-2-methoxybenzene]-palladium(0) (5a).

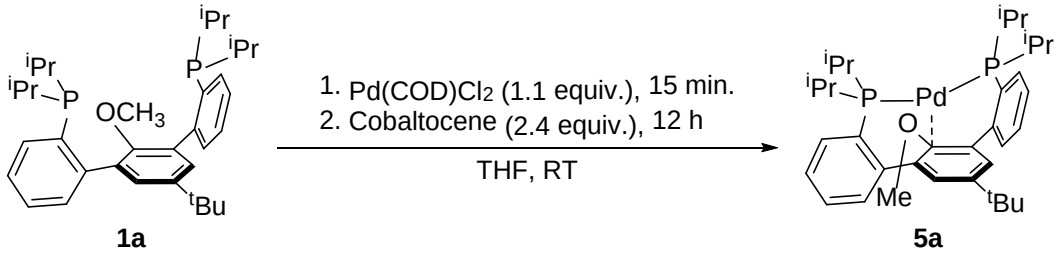

1a **5a**

In the glovebox, a 20 mL scintillation vial was charged with a magnetic stir bar, $Pd(COD)Cl_2$ (0.172 g, 0.601 mmol, 1.10 equiv.), and THF (4 mL). A yellow solution was observed. A pale yellow solution of diphosphine **1a** (0.300 g, 0.547 mmol, 1.00 equiv.) in THF (4 mL) was added dropwise to the solution of $Pd(COD)Cl_2$. After 15 min., an orange homogenous solution was observed. A dark purple solution of

cobaltocene (0.248 g, 1.312 mmol, 2.4 equiv.) in THF was added dropwise to the reaction mixture. A dark yellow brown solution was observed after 1 h. After 12 h, the reaction mixture was filtered and the solvent removed under reduced pressure to afford a yellow-brown powder. This powder was washed on a fritted glass funnel three times with pentane (6 mL) then extracted three times with C_6H_6 (4 mL). The portions of the C_6H_6 filtrate were combined and the volatiles were lyophilized under reduced pressure to afford **5a** (0.223 g, 0.387 mmol, 70.6%) as a yellow-brown powder. ^{1}H NMR (300 MHz, C_6D_6) δ 7.47 (m, 2H, Ar-*H*$_6$), 7.38 (m, 2H, Ar-*H*$_9$), 7.19 (m, 4H, Ar-*H*$_6$& Ar-*H*$_7$), 7.01 (t, 2H, Ar-*H*$_3$), 3.16 (s, 3H, -OC*H*$_3$), 2.18 (m, 2H, -C*H*$(CH_3)_2$), 1.91 (m, 2H, -C*H*$(CH_3)_2$), 1.44 (dd, 6H, -CH(C*H*$_3)_2$), 1.36 (s, 9H, -C(C*H*$_3)_3$), 1.25 (dd, 6H, -CH(C*H*$_3)_2$), 1.12 (dd, 6H, -CH(C*H*$_3)_2$), 0.96 (dd, 6H, -CH(C*H*$_3)_2$). ^{13}C{^{1}H} NMR (101 MHz, C_6D_6) δ 148.83 (app t, Ar-*C*$_{10}$, J_{PC} = 2.5 Hz), 142.61 (s, Ar-*C*$_4$), 140.34 (s, Ar-*C*$_1$), 137.50 (app t, Ar-*C*$_5$, J_{PC} = 11.6 Hz), 135.21 (app t, Ar-*C*$_2$, J_{PC} = 4.0 Hz), 132.12 (app t, Ar-*C*$_9$, J_{PC} = 1.0 Hz), 130.88 (app t, Ar-*C*$_6$, J_{PC} = 2.5 Hz), 128.40 (s, br, Ar-*C*$_7$ or Ar-*C*$_8$), 126.93 (app t, Ar-*C*$_7$ or Ar-*C*$_8$), 126.70 (app t, Ar-*C*$_3$), 59.92 (s, -O*C*H_3), 34.44 (s, -*C*$(CH_3)_3$), 31.74 (s, -C(*C*$H_3)_3$), 28.21 (app t, -*C*$H(CH_3)_2$, J_{PC} = 5.6 Hz), 23.24 (app t, -*C*$H(CH_3)_2$, J_{PC} = 7.1 Hz), 21.37 (app t, -CH(*C*$H_3)_2$, J_{PC} = 5.1 Hz), 20.68 (app t, -CH(*C*$H_3)_2$, J_{PC} = 9.1 Hz), 20.47 (app t, -CH(*C*$H_3)_2$, J_{PC} = 6.1 Hz), 18.78 (app t, -CH(*C*$H_3)_2$, J_{PC} = 1.0 Hz). ^{31}P{^{1}H} NMR (121 MHz, C_6D_6) δ 33.17 (s). Anal. calcd. for $C_{35}H_{50}OP_2Pd$ (%): C, 64.17; H, 7.69. Found: C, 63.90; H, 7.68.

Synthesis of [2,6-bis(2'-diisopropylphosphinophenyl)-4-tert-butyl-phenoxide]palladium(II)methyl (6a).

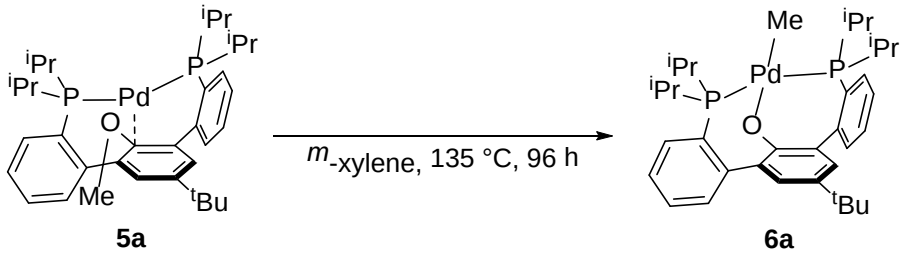

5a **6a**

In the glovebox, a 100 mL Schlenk tube fitted with a Teflon screw cap was charged with a yellow solution of **5a** (0.050 g, 0.076 mmol) in *m*-xylene (4 mL), sealed, removed from the glovebox and placed in an oil bath preheated to 135 °C. The solution was heated and stirred for 96 h. The Schlenk tube was removed from the oil bath and a yellow solution was observed. This solution was filtered through Celite in the glovebox and solvent removed under reduced pressure. The resulting yellow oil was dissolved in a minimum of C_6H_6 and volatiles were lyophilized under reduced pressure to afford **6a** (0.0387 g, 0.059 mmol, 77.4%) as a yellow solid. ^{1}H NMR (400 MHz, C_6D_6) δ 7.34 (s, 2H, Ar-*H*$_5$), 7.28-7.21 (m, 4H, Ar-*H*$_6$), 7.19-7.13 (m, 2H, Ar-*H*$_9$), 7.05 (m, 2H, Ar-*H*$_7$), 2.24 (m, 2H, -C*H*$(CH_3)_2$), 2.08 (m, 2H, -C*H*$(CH_3)_2$), 1.51 (s, 9H, -C(C*H*$_3)_3$), 1.47 (dd, 6H, -CH(C*H*$_3)_2$), 1.25 (dd, 6H, -CH(C*H*$_3)_2$), 0.85 (dd, 6H, -CH(C*H*$_3)_2$), 0.71 (dd, 6H, -CH(C*H*$_3)_2$), 0.26 (t, 3H, Pd-C*H*$_3$, J_{PH} = 6.0 Hz). ^{13}C{^{1}H} NMR (101 MHz, C_6D_6) δ 152.34 (app t, Ar-*C*$_2$, J_{PC} = 1.5 Hz), 150.65 (t, Ar-*C*$_1$, J_{PC} = 7.6 Hz), 136.73 (s, Ar-*C*$_4$), 133.84 (app t, Ar-*C*$_8$, J_{PC} = 4.0), 131.36 (app t, Ar-*C*$_6$, J_{PC} = 2.0), 131.26 (app t, Ar-C$_5$, J_{PC} = 1.5), 130.56 (app t, Ar-C$_9$, J_{PC} = 1.0 Hz), 129.00 (s, Ar-*C*$_3$), 124.91 (app t, Ar-*C*$_7$, J_{PC} = 3.0 Hz), 124.64 (app t, Ar-*C*$_{10}$, J_{PC} = 21.7 Hz), 34.15 (s, -*C*$(CH_3)_3$), 32.28 (s, -C(*C*$H_3)_3$), 23.95 (app t, -*C*$H(CH_3)_2$, J_{PC} = 10.61 Hz), 20.84 (app t, -*C*$H(CH_3)_2$, J_{PC} = 10.61 Hz), 19.66 (app t, -CH(*C*$H_3)_2$, J_{PC} = 3.5 Hz), 19.39 (app t, -

CH(CH$_3$)$_2$, J_{PC} = 4.0 Hz), 18.62 (app t, -CH(CH$_3$)$_2$, J_{PC} = 3.0 Hz), 15.52 (app t, -CH(CH$_3$)$_2$, J_{PC} = 2.0), -13.03 (t, Pd-CH$_3$, J_{PC} = 7.6 Hz). ^{31}P{^{1}H} NMR (121 MHz, C$_6$D$_6$) δ 29.76 (s). Anal. calcd. for C$_{35}$H$_{50}$OP$_2$Pd (%): C, 64.17; H, 7.69. Found: C, 63.93; H, 7.53.

Synthesis of [1,3-bis(2'-diisopropylphosphinophenyl)-5-tert-butyl-2-methoxybenzene]-platinum(0) (7a).

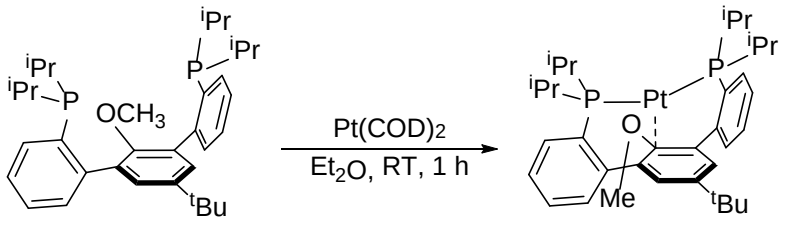

1a **7a**

In the glovebox, a 20 mL scintillation vial was charged with a magnetic stir bar and Pt(COD)$_2$[16] (0.027 g, 0.066 mmol, 1.00 equiv.) as a solution in Et$_2$O (1 mL). Diphosphine **1a** (0.036 g, 0.066 mmol, 1.00 equiv.) was added to this vial as a solution in Et$_2$O (2 mL). After 1 h, a yellow solution was observed. The yellow solution was filtered through Celite and volatiles were removed from the filtrate under reduced pressure. A pale yellow solid was observed. This solid was washed with three times with pentane (1 mL) and extracted with three portions of Et$_2$O (1 mL). Volatiles were removed under reduced pressure from this Et$_2$O solution to afford **7a** (0.012 g, 0.016 mmol, 24.7%) as an off-white solid. ^{1}H NMR (500 MHz, C$_6$D$_6$) δ 7.47 (m, 2H, Ar-H_6), 7.31 (m, 2H, Ar-H_9), 7.18 (m, 4H, Ar-H_7 & Ar-H_8), 7.02 (s, Ar-H_3), 3.28 (s, 3H, -OCH_3), 2.28 (m, 2H, -CH(CH$_3$)$_2$), 2.03 (m, 2H, -CH(CH$_3$)$_2$), 1.51 (dd, 6H, -CH(CH_3)$_2$), 1.37 (s, 9H, -C(CH_3)$_3$), 1.30 (dd, 6H, -CH(CH_3)$_2$), 1.13 (dd, 6H, -CH(CH_3)$_2$), 0.95 (dd, 6H, -CH(CH_3)$_2$). ^{13}C{^{1}H} NMR (126 MHz, C$_6$D$_6$) δ 148.92 (app t, Ar-C_5, J_{PC} = 8.5 Hz), 142.93 (s, Ar-C_1), 141.42 (s, Ar-C_4), 135.77 (app t, Ar-C_2, J_{PC} = 2.4

Hz), 135.29 (app t, Ar-C_{10}, J_{PC} = 16.9 Hz), 132.20 (app t, Ar-C_9, J_{PC} = 1.8 Hz), 131.38 (app t, Ar-C_6, J_{PC} = 3.0 Hz), 128.61 (app t, Ar-C_7 or Ar-C_8, J_{PC} = 128.61), 127.28 (s, Ar-C_3), 126.84 (app t, Ar-C_7 or Ar-C_8, J_{PC} = 2.4 Hz), 59.14 (s, -OCH$_3$), 34.48 (s, -C(CH$_3$)$_3$), 31.65 (s, -C(CH$_3$)$_3$), 28.93 (app t, -CH(CH$_3$)$_2$, J_{PC} = 11.5 Hz), 24.74 (app t, -CH(CH$_3$)$_2$, J_{PC} = 14.5 Hz), 20.83 (app t, -CH(CH$_3$)$_2$, J_{PC} = 3.0 Hz), 20.56 (app t, -CH(CH$_3$)$_2$, J_{PC} = 4.8 Hz), 20.24 (app t, -CH(CH$_3$)$_2$, J_{PC} = 3.6 Hz), 18.74 (s, br, -CH(CH$_3$)$_2$). ^{31}P{^{1}H} NMR (121 MHz, C_6D_6) δ 56.68 (J_{PtP} = 4729.9 Hz). Anal. calcd. for $C_{35}H_{50}OP_2Pt$, 56.52; H, 6.78. Found: C, 56.72, H, 6.58.

Synthesis of [2,6-bis(2'-diisopropylphosphinophenyl)-4-tert-butyl-phenoxide]-platinum(II)methyl (8a).

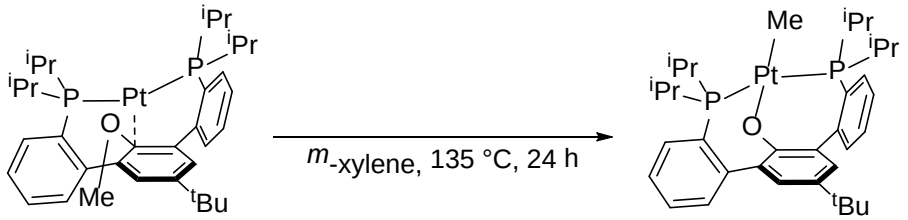

7a **8a**

Method A: In the glovebox, a J. Young tube was charged with a colorless solution of **7a** (0.020 g, 0.026 mmol) in *m*-xylene (*ca.* 0.6 mL), sealed, removed from the glovebox, and placed in an oil bath preheated to 135 °C for 24 h to afford a colorless solution of **8a** (NMR yield: quantitative).

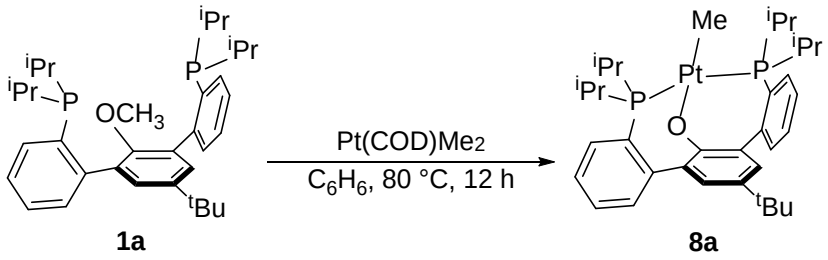

1a **8a**

Method B: In the glovebox, a Schlenk tube fitted with a Teflon screw cap was charged with a stir bar, diphosphine **1a** (0.200 g, 0.365 mmol, 1.00 equiv.) as a solution in C_6H_6 (4 mL), and Pt(COD)Me_2 (0.122 g, 0.365 mmol, 1.00 equiv.) as a solution in C_6H_6 (2 mL). The Schlenk tube was removed from the glovebox, placed in an oil bath preheated to 80 ºC, and heated while stirring. After 12 h, the Schlenk tube was removed from the oil bath and bought into the glovebox. A pale yellow solution was observed. This C_6H_6 solution was filtered through Celite and volatiles removed under reduced pressure to afford an off white solution. Diffusion of hexanes into a concentrated solution of this off-white solid in C_6H_6 afforded **8a** (0.048 g, 0.064 mmol, 17.6%) as a white precipitate. ^{1}H NMR (300 MHz, C_6D_6) δ 7.33 (s, 2H, Ar-*H*$_3$), 7.12-7.29 (m, 4H, Ar-*H*$_6$ & Ar-*H*$_9$), 7.15 (obscured by solvent residual, detected by HSQC, 2H, Ar-*H*$_7$ or Ar-*H*$_8$), 7.07 (m, 2H, Ar-*H*$_7$ or Ar-*H*$_8$), 2.35 (m, 2H, -C*H*$(CH_3)_2$), 2.26 (m, 2H, -C*H*$(CH_3)_2$), 1.50 (s, 9H, -C(C*H*$_3)_3$), 1.47 (dd, 6H, -CH(C*H*$_3)_2$), 1.29 (dd, 6H, -CH(C*H*$_3)_2$), 0.87 (dd, 6H, -CH(C*H*$_3)_2$), 0.70 (dd, 6H, -CH(C*H*$_3)_2$), 0.67 (t, 3H, Pt-C*H*$_3$, J_{PH} = 12.0 Hz). ^{13}C{^{1}H} NMR (101 MHz, C_6D_6) δ 151.48 (s, Ar-*C*$_1$), 149.79 (app t, Ar-*C*$_5$, J_{PC} = 7.1 Hz), 137.22 (s, Ar-*C*$_4$), 134.02 (app t, Ar-*C*$_6$ or Ar-*C*$_9$), 131.67 (app t, Ar-*C*$_6$ or Ar-*C*$_9$, J_{PC} = 7.5 Hz), 131.16 (s, Ar-*C*$_2$), 130.46 (app t, Ar-*C*$_7$ or Ar-*C*$_8$, 1.0 Hz), 128.93 (s, Ar-*C*$_3$), 125.07 (app t, Ar-*C*$_7$ or Ar-*C*$_8$, J_{PC} = 3.5), 122.61 (app t, Ar-*C*$_{10}$, J_{PC} = 25.3 Hz), 34.23 (s, -*C*$(CH_3)_3$), 32.20 (s, -C(*C*$H_3)_3$), 24.88 (app t, -*C*H$(CH_3)_2$, J_{PC} = 15.2 Hz), 20.16

(app t, -*C*H(CH$_3$)$_2$, J_{PC} = 14.1 Hz), 19.24 (app t, -CH(*C*H$_3$)$_2$, J_{PC} = 2.5 Hz), 18.84 (app t, -CH(*C*H$_3$)$_2$, J_{PC} = 3.0 Hz), 18.09 (app t, -CH(*C*H$_3$)$_2$, J_{PC} = 2.0 Hz), 15.61 (app t, -CH(*C*H$_3$)$_2$, J_{PC} = 1.5 Hz), -30.15 (t, Pt-*C*H$_3$, J_{PC} = 7.1 Hz). ^{31}P{^{1}H} NMR (121 MHz, C$_6$D$_6$) δ 29.24 (J_{PtP} = 3089.1 Hz). Anal. calcd. for C$_{35}$H$_{50}$OP$_2$Pt (%): C, 56.52; H, 6.78. Found: C, 56.28; H, 6.55.

Synthesis of 5-(tert-butyl)-1,3-diiodo-2-(4-nitrophenoxy)benzene.

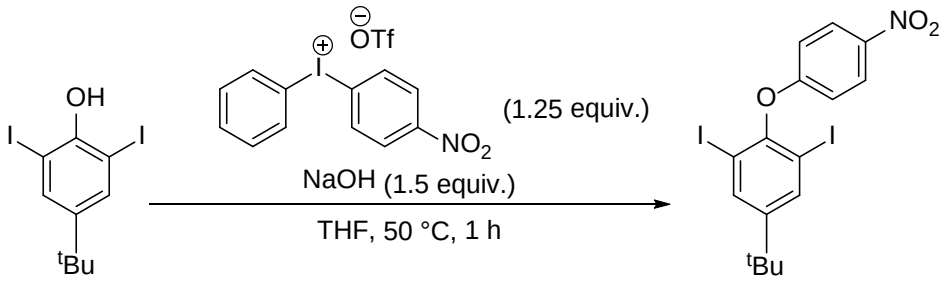

5-(tert-butyl)-1,3-diiodo-2-(4-nitrophenoxy)benzene was synthesized using a modification of the procedure reported by Olofsson and co-workers for the arylation of malonates with diaryl iodonium salts.[47] In a round bottom flask in the fume hood, NaOH (0.406 g, 10.2 mmol, 1.50 equiv.) and 4-(tert-butyl)-2,6-diiodophenol[41] (2.720 g, 6.8 mmol, 1.00 equiv.) were stirred in THF (20 mL). To this slurry was added [(4-nitrophenyl)(phenyl)iodonium][trifluoromethanesulfonate][44-45] (4.020 g, 8.5 mmol, 1.25 equiv.). This dark brown mixture was heated to 50 °C for 1 h, then solvent was removed under reduced pressure. The resulting residue was dissolved in a 90:10 hexanes:Et$_2$O (50 mL) mixture. A yellow solid precipitated from solution. The precipitate was collected via filtration affording 5-(tert-butyl)-1,3-diiodo-2-(4-nitrophenoxy)benzene (1.193 g, 2.3 mmol, 33.7%) as a yellow solid. ^{1}H NMR (400 MHz, CDCl$_3$) δ 8.22 (d, 2H, Ar-*H*, J_{HH} = 8.0 Hz), 7.85 (s, 2H, Ar-*H*), 6.89 (d, 2H, Ar-*H*, J_{HH} = 8.0 Hz), 1.33 (s, 9H, -C(C*H*$_3$)$_3$). ^{13}C{^{1}H} NMR (101 MHz, CDCl$_3$) δ 161.19 (s,

Ar-*C*), 153.29 (Ar-*C*), 150.73 (Ar-*C*), 143.04 (s, Ar-*C*), 137.87 (s, Ar-*C*H), 126.20 (s, Ar-*C*H), 116.02 (s, Ar-*C*H), 90.20 (s, Ar-*C*), 34.68 (s, -*C*(CH_3)$_3$), 31.32 (s, -C(*C*H_3)$_3$). MS (m/z) calcd. for $C_{16}H_{15}I_2NO_3$: 523.9220 (M+H). Found 523.9227 (FAB+, M+H).

Synthesis of 1,3-bis(2'-bromophenyl)-2-(4'-nitrophenoxy)-5-tert-butyl-benzene.

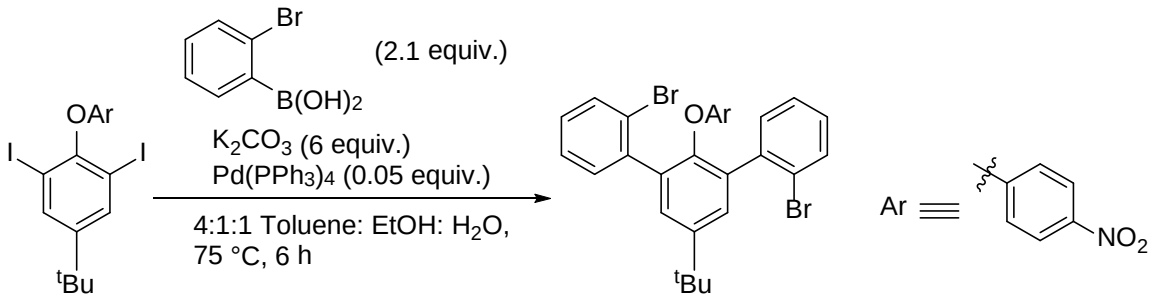

1,3-bis(2'-bromophenyl)-2-(4'-nitrophenoxy)-5-tert-butyl-benzene was synthesized using a modification of the procedure reported by Albrecht and co-workers for the Suzuki coupling of aryl halides with boronic acids.[48] In the fume hood, a 500 mL Schlenk flask fitted with a Teflon screw cap was charged with 5-(tert-butyl)-1,3-diiodo-2-(4-nitrophenoxy)benzene (1.193 g, 2.28 mmol, 1.00 equiv.), 2-bromo-phenylboronic acid (1.008 g. 5.02 mmol, 2.20 equiv.), K_2CO_3 (1.891 g, 13.68 mmol, 6.00 equiv.), 140 mL toluene, 40 mL EtOH, and 40 mL deionized H_2O. On the Schlenk line, the mixture was degassed by three freeze-pump-thaw cycles, after which $Pd(PPh_3)_4$ (0.132 g, 0.114 mmol, 0.05 equiv.) was added as a solid with a counterflow of nitrogen. The reaction vessel was then placed in an oil bath pre-heated to 75 °C. After stirring for 6 h, the reaction mixture was removed from the oil bath, allowed to cool to room temperature, concentrated via rotary evaporation, and diluted with 200 mL H_2O. The solution was extracted with three portions of CH_2Cl_2 (75 mL). The combined organic fraction were dried over $MgSO_4$, filtered and concentrated via rotary evaporation to afford a dark red oil. The crude 1,3-

bis(2'-bromophenyl)-2-(4'-nitrophenoxy)-5-tert-butyl-benzene was reduced without purification. ^{1}H NMR (300 MHz, $CDCl_3$) δ 7.86 (d, 2H, Ar-H_{13}, J_{HH} = 9.0 Hz), 7.54 (m, 2H, Ar-*H*), 7.44 (s, 2H, Ar-H_8), 7.35 – 7.14 (m, 4H, Ar-*H*), 7.09 (m, 2H, Ar-*H*), 6.61 (d, 2H, Ar-H_{12}, J_{HH} = 9.0 Hz), 1.41 (s, 9H, -C(CH_3)$_3$).

Synthesis of 1,3-bis(2'-bromophenyl)-2-(4'-aminophenoxy)-5-tert-butyl-benzene.

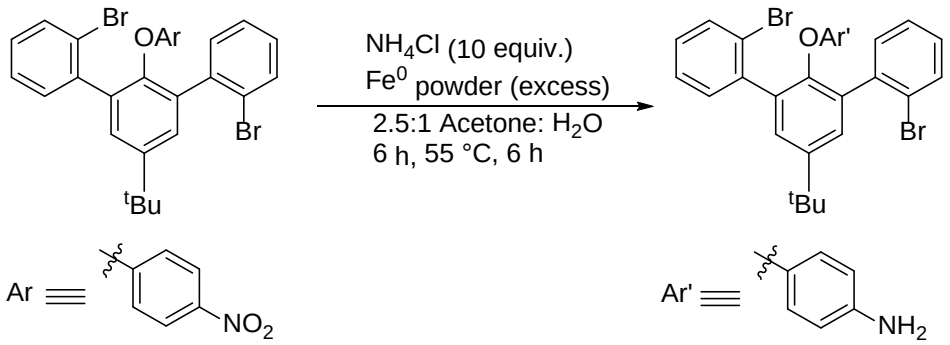

1,3-bis(2'-bromophenyl)-2-(4'-aminophenoxy)-5-tert-butyl-benzene was synthesized from 1,3-bis(2'-bromophenyl)-2-(4'-nitrophenoxy)-5-tert-butyl-benzene using a literature procedure.[49] The crude 1,3-bis(2'-bromophenyl)-2-(4'-aminophenoxy)-5-tert-butyl-benzene was methylated without purification. ^{1}H NMR (300 MHz, $CDCl_3$) δ 7.54 (m, 2H, Ar-*H*), 7.36 (s, 2H, Ar-H_8), 7.31 (m, 2H, Ar-*H*), 7.18 (m, 2H, Ar-*H*), 7.07 (m, 2H, Ar-*H*), 6.28 (m, 4H, Ar-H_{12} and Ar-H_{13}), 3.26 (s, br, 2H, -NH_2), 1.38 (s, 9H, -C(CH_3)$_3$).

Synthesis of 1,3-bis(2'-bromophenyl)-2-(4'-dimethylaminophenoxy)-5-tert-butyl-benzene.

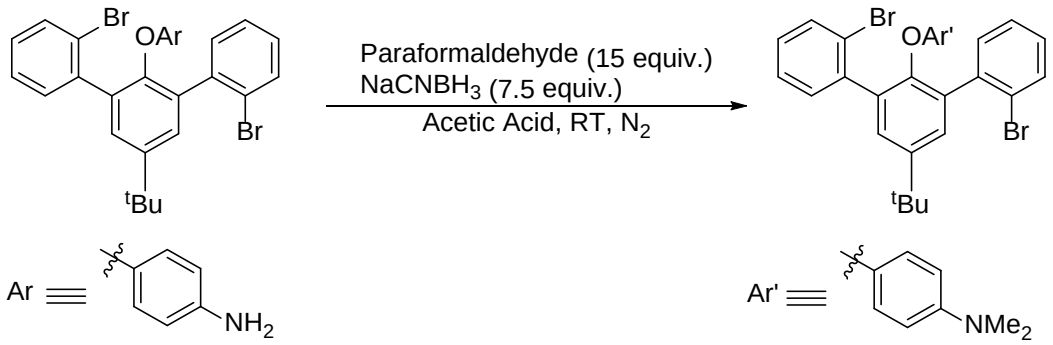

1,3-bis(2'-bromophenyl)-2-(4'-dimethylaminophenoxy)-5-tert-butyl-benzene was synthesized from 1,3-bis(2'-bromophenyl)-2-(4'-aminophenoxy)-5-tert-butyl-benzene using a literature procedure.[50] The product was purified by flash chromatography (CH_2Cl_2) and isolated as a colorless solid. Yield: 33.8 %. 1,3-bis(2'-bromophenyl)-2-(4'-dimethylaminophenoxy)-5-tert-butyl-benzene of this purity was used in a subsequent phosphination (via lithium-halogen exchange and dialkyl chlorophosphine quench) without further purification. ^{1}H NMR (300 MHz, C_6D_6) δ 7.59 (s, 2H Ar-*H*), 7.45 (m, 2H, Ar-*H*), 7.41 (m, 2H, Ar-*H*), 6.83 (m, br, 2H Ar-*H*), 6.68 (m, 2H, Ar-*H*), 6.61 (m, 2H, Ar-*H*), 6.26 (d, 2H, Ar-*H*), 2.29 (s, 6H, -N(C*H*$_3$)$_2$), 1.29 (s, 9H, -C(C*H*$_3$)$_3$).

Synthesis of 1,3-bis(2'-diisopropylphosphinophenyl)-5-tert-butyl-2-(4'-dimethylamino-phenoxy)benzene (1c).

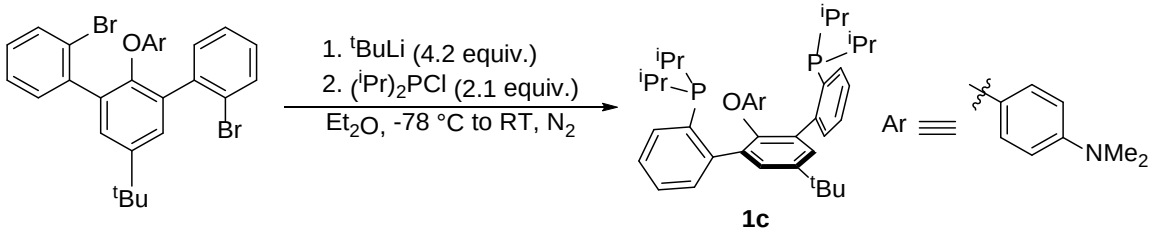

1c

In a glovebox, a 100 mL Schlenk tube was charged with a colorless solution of 1,3-bis(2'-bromophenyl)-2-(4'-dimethylaminophenoxy)-5-tert-butyl-benzene (50.1 mg, 0.11 mmol, 1.00 equiv.) in Et_2O (30 mL) and a stir bar. The Schlenk tube was removed

from the glovebox and cooled to -78 °C in a dry ice/acetone bath. Under N_2, ^{t}BuLi in pentane (1.5 M, 303.5 µL, 0.46 mmol, 4.20 equiv.) was added via syringe slowly to the cold solution. The resulting dark yellow mixture was stirred for 1 h at -78 °C. After 1 h, chlorodiisopropylphosphine (36.5 µl, 0.23 mmol, 2.10 equiv.) was added to the cold solution slowly via syringe. After addition, the reaction mixture was allowed to warm to room temperature and stirred at room temperature for 8 h. The volatile materials were then removed under vacuum and the pale yellow/white residue was mixed in hexanes and filtered through Celite. The volatiles were removed from the filtrate *in vacuo*, and the resulting pale yellow oil was mixed in pentane and stirred with alumina. The mixture was filtered through a bed of alumina and the alumina was rinsed with toluene. Removal of volatile materials under vacuum yielded 1,3-bis(2'-diisopropylphosphino)-4-dimethylamino-2-phenoxybenzene (**1c**) as a white solid. (0.53 g, 0.83 mmol, 92.9% yield) ^{1}H NMR (500 MHz, C_6D_6, 25 °C) δ 7.73 (s, br, 1H, Ar-*H*), 7.43 (s, 2H, Ar-*H*), 7.39 (m, br, 3H, Ar-*H*), 7.03 (m, 5H. Ar-*H*), 6.61 (m, 2H, Ar-*H*), 6.24 (m, 2H, Ar-*H*), 2.35 (s, 6H, -N(C*H*$_3$)$_2$), 2.11 (s, br, 1H, -C*H*(CH$_3$)$_2$), 1.93 (m, 3H, -C*H*(CH$_3$)$_2$), 1.42 & 1.39 (s, 9H, -C(C*H*$_3$)$_3$), 1.25 – 0.97 (m, 20H, -CH(C*H*$_3$)$_2$), 0.90 (m, 4H, -CH(C*H*$_3$)$_2$). ^{1}H NMR (C_6D_6, 500 MHz, 70 °C) δ 7.59 (br s, 2H, Ar-*H*), 7.46 (s, 2H, Ar-*H*), 7.43 (m, 2H, Ar-*H*), 7.04 (m, 4H, Ar-*H*), 6.58 (m, 2H, Ar-*H*), 6.26 (d, 2H, Ar-*H*), 2.40 (s, 6H, N(C*H*$_3$)$_2$), 1.97 (s, br, 4H, C*H*(CH$_3$)$_2$), 1.41 (s, 9H, C(C*H*$_3$)$_3$), 1.33 – 0.85 (m, br, 24H, CH(C*H*$_3$)$_2$). ^{13}C{^{1}H} NMR (126 MHz, C_6D_6, 25 °C) δ 152.22 (s, Ar-*C*$_1$), 151.31 (s, Ar-*C*$_1$), 148.63 (s, Ar-*C*$_{10}$), 147.79 (s, Ar-*C*$_{10}$), 147.47 (s, Ar-*C*$_2$), 147.23 (s, Ar-*C*$_2$), 145.91 (s, O*Ar*), 145.62 (s, O*Ar*), 145.42 (s, O*Ar*), 145.09 (s, Ar-*C*$_4$), 136.98 (m, Ar-*C*$_5$), 136.74 (s, Ar-*C*$_5$), 132.24 (m, Ar-*C*$_{6\text{-}9}$), 131.89 (s, Ar-*C*$_{6\text{-}9}$), 130.99 (s, Ar-*C*$_{6\text{-}9}$), 130.21 (s, Ar-*C*$_3$), 130.01 (s, Ar-*C*$_3$), 128.35 (s, Ar-*C*$_{7\text{-}8}$), 126.80 (s, Ar-*C*$_{7\text{-}8}$),

117.36 (s, O*Ar*), 116.61 (s, O*Ar*), 114.29 (s, O*Ar*), 114.03 (m, O*Ar*), 41.23 (m, Ar-N(CH$_3$)$_2$), 34.64 (s, C(CH$_3$)$_3$), 31.79 (s, C(CH$_3$)$_3$), 26.84 (m, CH(CH$_3$)$_2$), 26.00 (m, CH(CH$_3$)$_2$), 24.83 (m, CH(CH$_3$)$_2$), 21.32 – 20.37 (m, CH(CH$_3$)$_2$), 19.90 (s, br, CH(CH$_3$)$_2$). ^{31}P{^{1}H} NMR (121 MHz, C$_6$D$_6$, 25 °C) δ -2.61 (s), -3.98 (s). MS (m/z) calcd. for C$_{42}$H$_{57}$NOP$_2$: 653.3915 (M+). Found 653.3904 (FAB+, M+).

Synthesis of 1,3-bis(2'-bromophenyl)-2-phenoxy-5-tert-butyl-benzene.

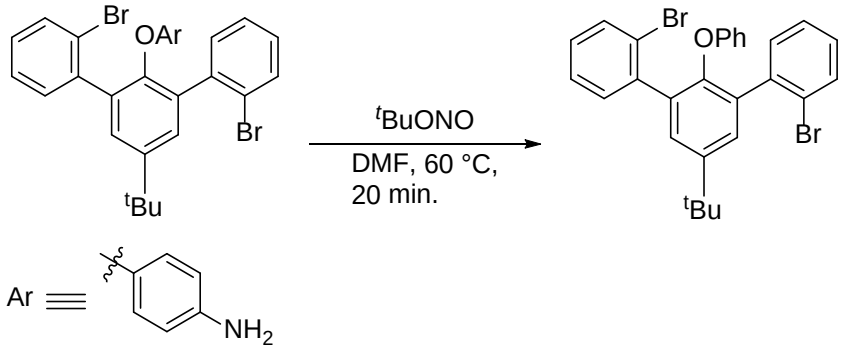

1,3-bis(2'-bromophenyl)-2-phenoxy-5-tert-butyl-benzene was synthesized from 1,3-bis(2'-bromophenyl)-2-(4'-aminophenoxy)-5-tert-butyl-benzene using a literature procedure for the conversion of Ar-NO$_2$ substituents to Ar-H substituents.[40] A 100 mL round bottom flask was charged with 1,3-bis(2'-bromophenyl)-2-(4'-aminophenoxy)-5-tert-butyl-benzene (2.05 g, 3.72 mmol, 1.00 equiv.) as a solution in dimethylformamide (20 mL), a stir bar, and *tert*-butyl nitrite (0.38 g, 3.72 mmol, 1.00 equiv.). The round bottom flask was capped loosely and placed in an oil bath pre-heated to 60 °C for 20 min. After 20 min., the reaction mixture was removed from the oil bath and the solution was poured into EtOAc (70 mL). This solution was washed three times with *ca.* 70 mL brine. The combined aqueous washes were then extracted twice with 70 mL EtOAc. The combined organic layers were dried were dried over MgSO$_4$, filtered and concentrated via rotary evaporation to afford the desired compound in good purity as

a brown oil. Analytically pure compound was isolated by adding MeOH (20 mL) to this oil, stirring vigorously and concentrating via rotary evaporation. An additional portion of MeOH (20 mL) was added, the mixture was sonicated, and the precipitate collected on a fritted glass funnel to afford 1,3-bis(2'-bromophenyl)-2-phenoxy-5-tert-butyl-benzene as a white solid (0.65 g, 1.22 mmol, 32.7%). ^{1}H NMR (400 MHz, $CDCl_3$) δ 7.53 (m, 2H, Ar-H_6 or Ar-H_9), 7.39 (s, 2H, Ar-H_3), 7.31 (m, 2H, Ar-H_6 or Ar-H_9), 7.17 (m, 2H, Ar-H_7 or Ar-H_8), 7.06 (m, 2H, Ar-H_7 or Ar-H_8), 6.92 (m, 2H, Ar-H_{13}), 6.68 (t, 1H, Ar-H_{14}, J_{HH} = 8.0 Hz), 6.50 (d, 2H, Ar-H_{12}, J_{HH} = 8.0 Hz), 1.39 (s, 9H, -C(CH_3)$_3$). ^{13}C{^{1}H} NMR (101 MHz, $CDCl_3$) δ 158.32 (s, Ar-C_{11}), 147.48 (s, Ar-C_{12}), 146.87 (s, Ar-C_4), 139.01 (s, Ar-C_{10}), 134.41 (s, Ar-C_1), 132.75 (s, Ar-C_6 or Ar-C_9), 132.04 (s, Ar-C_6 or Ar-C_9), 129.19 (s, Ar-C_3), 128.82 (s, Ar-C_7 or Ar-C_8), 128.70 (s, Ar-C_{13}), 126.73 (s, Ar-C_7 or Ar-C_8), 123.91 (s, Ar-C_5), 121.18 (s, Ar-C_{14}), 116.27 (s, Ar-C_{12}), 34.87 (s, -C(CH$_3$)$_3$), 31.57 (s, -C(CH$_3$)$_3$). MS (m/z) calcd. for $C_{28}H_{24}Br_2O$: 536.0173 (M+). Found 536.0170 (FAB+, M+).

Synthesis of 1,3-bis(2'-diisopropylphosphinophenyl)-5-tert-butyl-2-phenoxy-benzene (1d).

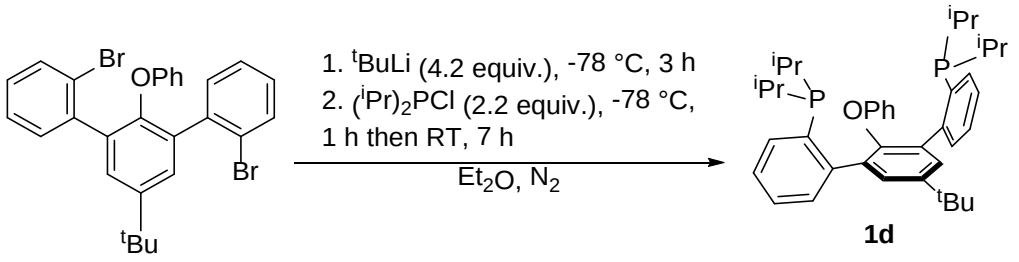

1d

In a glovebox, a 100 mL Schlenk tube was charged with a colorless solution of 1,3-bis(2'-bromophenyl)-2-phenoxy-5-tert-butyl-benzene (0.316 g, 0.59 mmol, 1.00 equiv.) in Et_2O (25 mL). The Schlenk tube was removed from the glovebox and cooled to -78 °C in a dry ice/acetone bath. Under N_2, ^{t}BuLi (1.7 M in pentane, 2.48 mmol, 1.46 mL,

4.20 equiv.) was added via syringe to the solution. The resulting yellow-orange mixture was stirred for 3 h at -78 °C. After 3 h, chlorodiisopropylphosphine (0.198 g, 0.21 mL, 1.30 mmol, 2.20 equiv.) was added to the cold solution slowly via syringe. After addition, the reaction mixture was stirred 1 h at -78 °C. After 1 h, the reaction mixture was allowed to warm to room temperature and stirred at room temperature for 7 h. The volatile materials were removed under reduced pressure. In the glovebox, the pale yellow residue was extracted with three portions of pentane (20 mL each) and the combine organic layer was filtered through Celite. The volatiles were removed from the filtrate under reduced pressure and a pale yellow oil was observed. In a glovebox containing degassed protic solvents under N_2 atmosphere, the pale yellow oil was dissolved in MeOH (10 mL) and stirred for 4 h. A white precipitate was observed. The precipitate was collected on a fritted funnel and washed with two portions of MeOH (2 mL each) to afford diphosphine **1d** (0.104 g, 0.17 mmol, 28.8 %). (Note: Diphosphine **1d** was dried while heating on a Schlenk line under reduced pressure before further manipulation under N_2 atmosphere in a glovebox free of protic solvents.) ^{1}H NMR (400 MHz, $CDCl_3$) δ 7.49 (m, 2H, Ar-$H_{6\text{-}9}$), 7.41 (m, 1H, Ar-$H_{6\text{-}9}$), 7.28 (s, 2H, Ar-H_3, minor isomer), 7.25 (s, 2H, Ar-H_3, major isomer), 7.21 (m, 4H, Ar-$H_{6\text{-}9}$), 7.08 (m, 1H, Ar-$H_{6\text{-}9}$), 6.99 – 6.82 (m, 2H, Ar-H_{13}), 6.69 (m, 1H, Ar-H_{14}, minor isomer), 6.61 (m, 1H, Ar-H_{14}, major isomer), 6.47 (m, 2H, Ar-H_{12}), 2.09 (m, 2H, -CH(CH_3)$_2$), 1.98 (m, 2H, -CH(CH_3)$_2$), 1.39 (s, 9H, -C(CH_3)$_3$), 1.18 – 0.91 (m, 20H, -CH(CH_3)$_2$), 0.70 (m, 4H, -CH(CH_3)$_2$). ^{1}H NMR (300 MHz, C_6D_6) δ 7.71 – 7.63 (m, br, 1H, Ar-H), 7.50 (s, 2H, Ar-H_3), 7.36 (m, 2H, Ar-H), 7.28 (m, 1H, Ar-H), 7.12 – 6.88 (m, 4H, Ar-H), 6.83 – 6.72 (m, 3H, Ar-H), 6.66 – 6.48 (m, 2H, Ar-H), 2.08 (s, br, 2H, -CH(CH_3)$_2$, minor isomer), 1.90 (m, 4H, -CH(CH_3)$_2$, major isomer; m, 2H, -

C*H*(CH_3)$_2$, minor isomer), 1.42 (s, 9H, -C(C*H*$_3$)$_3$, minor isomer), 1.39 (s, 9H, -C(C*H*$_3$)$_3$, major isomer), 1.34 – 1.24 (m, 3H, -CH(C*H*$_3$)$_2$), 1.23 – 0.95 (m, 18H, -CH(C*H*$_3$)$_2$), 0.84 (m, 3H, -CH(C*H*$_3$)$_2$). ^{1}H NMR (400 MHz, C_6D_6, 70 °C) δ 7.45 (s, 2H, Ar-*H*$_3$), 7.43 – 7.38 (m, br, 2H, Ar-*H*$_6$), 7.03 (m, br, 4H, Ar-*H*$_{7\text{-}9}$), 6.78 (m, 2H, Ar-*H*$_{13}$), 6.61 (m, br, 2H, Ar-*H*$_{12}$), 6.54 (m, 1H, Ar-*H*$_{14}$), 1.97 (s, br, 4H, -C*H*(CH_3)$_2$), 1.40 (s, 9H, -C(C*H*$_3$)$_3$), 1.27 – 0.73 (s, br, 24H, -CH(C*H*$_3$)$_2$); Ar-*H* (2H) not detected. ^{13}C{^{1}H} NMR (101 MHz, $CDCl_3$) δ 159.24 (s, Ar-*C*$_{11}$, minor isomer), 158.23 (s, Ar-*C*$_{11}$, major isomer), 146.86 (s, Ar-*C*), 146.43 (d, Ar-*C*, J_{PC} = 30.3 Hz), 145.26 (s, Ar-*C*$_4$), 136.27 (d, Ar-*C*, J_{PC} = 8.1 Hz), 135.98 (m, br, Ar-*C*), 132.20 – 131.94 (m, Ar-*C*$_{6\text{-}9}$), 131.46 (d, Ar-*C*$_{6\text{-}9}$, J_{PC} = 5.1 Hz), 130.59 (s, Ar-*C*$_{6\text{-}9}$), 129.71 (m, br, Ar-*C*$_{6\text{-}9}$), 129.59 (d, Ar-*C*$_{6\text{-}9}$, J_{PC} = 4.0 Hz), 128.56 (s, Ar-*C*$_{13}$, minor isomer), 128.48 (s, Ar-*C*$_{13}$, major isomer), 127.32 (s, Ar-*C*$_{6\text{-}9}$), 126.47 (s, Ar-*C*$_{6\text{-}9}$), 120.34 (s, Ar-*C*$_{14}$, minor isomer), 120.19 (s, Ar-*C*$_{14}$, major isomer), 116.38 (s, Ar-*C*$_{12}$, major isomer), 116.05 (s, Ar-*C*$_{12}$, minor isomer), 34.64 (s, -*C*(CH_3)$_3$, major isomer), 34.58 (s, -*C*(CH_3)$_3$, minor isomer), 31.76 (s, -C(*C*H$_3$)$_3$, major isomer), 31.63 (s, -C(*C*H$_3$)$_3$, minor isomer), 26.65 (d, -*C*H(CH_3)$_2$, J_{PC} = 15.2 Hz, major isomer), 25.89 – 25.71 (m, br, -*C*H(CH_3)$_2$, minor isomer), 24.59 (d, -*C*H(CH_3)$_2$, J_{PC} = 13.1 Hz, major isomer), 24.34 – 24.19 (m, br, -*C*H(CH_3)$_2$, minor isomer), 21.11 – 20.22 (m, -CH(*C*H$_3$)$_2$), 19.84 (m, br, -CH(*C*H$_3$)$_2$). ^{13}C{^{1}H} NMR (101 MHz, C_6D_6, 70 °C) δ 147.18 (d, Ar-*C*, J_{PC} = 31.3 Hz), 145.97 (m, br, Ar-*C*), 137.46 (m, br, Ar-*C*), 136.99 (s, Ar-*C*), 132.32 (m, Ar-*C*$_6$), 131.50 (s, br, Ar-*C*), 130.18 (app t, Ar-*C*H, J_{PC} = 1.5 Hz), 126.87 (s, Ar-*C*H), 126.83 (s, Ar-*C*H), 120.85 (s, Ar-*C*H), 116.78 (m, Ar-*C*H), 34.71 (s, -*C*(CH_3)$_3$), 31.78 (s, -C(*C*H$_3$)$_3$), 27.47 – 23.47 (m, br, -*C*H(CH_3)$_2$), 21.13 – 20.50 (m, br, -CH(*C*H$_3$)$_2$). ^{31}P{^{1}H} (121 MHz, $CDCl_3$) δ -1.92 (s), -2.88 (s). ^{31}P{^{1}H} (121

MHz, C_6D_6) δ -2.17 (s), -3.52 (s). $^{31}P\{^1H\}$ (162 MHz, C_6D_6, 70 °C, referenced to solvent lock) δ -0.42 - -2.47 (s, br). MS (m/z) calcd. for $C_{40}H_{52}OP_2$: 611.3572 (M+H). Found: 611.3549 (FAB+, M+H).

Synthesis of [1,3-bis(2'-diisopropylphosphinophenyl)-5-tert-butyl-2-phenoxy-benzene]-palladium(0) (10d).

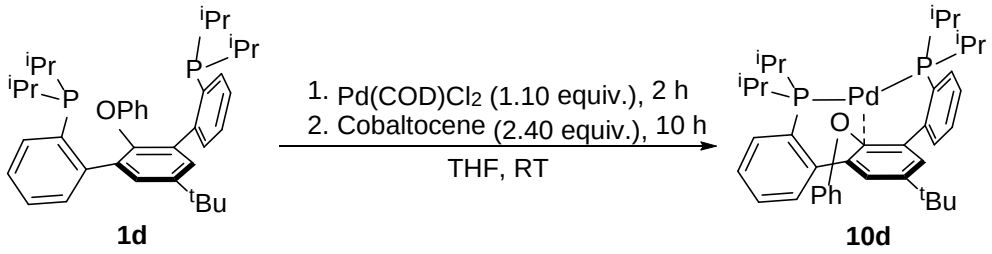

In the glovebox, a 20 mL scintillation vial was charged with a magnetic stir bar, $Pd(COD)Cl_2$ (0.0149 g, 0.072 mmol, 1.10 equiv.), and THF (2 mL). A yellow solution was observed. A colorless solution of diphosphine **1d** (0.040 g, 0.066 mmol, 1.00 equiv.) in THF (1 mL) was added dropwise to the solution of $Pd(COD)Cl_2$. After 15 min., an orange homogenous solution was observed. The mixture was stirred for a total of 2 h. A dark purple solution of cobaltocene (0.030 g, 0.157 mmol, 2.40 equiv.) in THF (1 mL) was added dropwise to the reaction mixture. A dark yellow brown solution was observed after 1 h. After 10 h, the reaction mixture was filtered and the solvent removed under reduced pressure to afford a brown powder. The powder was washed three times with pentane (1 mL) and three times with hexanes (1 mL). The powder was then extracted three times with Et_2O (1 mL) and three times with C_6H_6 (1 mL). Volatiles were removed from the combined Et_2O and C_6H_6 solutions under reduced pressure to afford intermediate **10d** (0.027 g, 0.038 mmol, 57.7%) as a yellow powder. ^1H NMR (400 MHz, C_6D_6) δ 7.30 (m, 2H, Ar-*H*$_6$), 7.23 (m, 2H, Ar-*H*$_9$), 7.11 (s, 2H, Ar-*H*$_3$), 7.00 (m, 2H, Ar-*H*$_7$), 6.91 (m, 2H, Ar-*H*$_8$), 6.74 (m, 2H, Ar-*H*$_{13}$), 6.53

(m, 1H, Ar-H_{14}), 6.48 (m, 2H, Ar-H_{12}), 2.19 (m, 2H, -CH(CH_3)$_2$), 1.94 (m, 2H, -CH(CH_3)$_2$), 1.50 (dd, 6H, -CH(CH_3)$_2$), 1.39 (s, 9H, -C(CH_3)$_3$), 1.38 (dd, 6H, -CH(CH_3)$_2$), 1.13 (dd, 6H, -CH(CH_3)$_2$), 0.93 (dd, 6H, -CH(CH_3)$_2$). ^{13}C{^{1}H} NMR (101 MHz, C_6D_6) δ 159.49 (s, Ar-C_{11}), 147.27 (app t, Ar-C_5, J_{PC} = 12.1 Hz), 145.03 (s, Ar-C_4), 136.46 (t, Ar-C_1, J_{PC} = 12.1 Hz), 136.35 (app t, Ar-C_{10}, J_{PC} = 4.5 Hz), 134.48 (s, Ar-C_2), 131.88 (s, Ar-C_6), 130.79 (app t, Ar-C_9, J_{PC} = 2.5 Hz), 128.90 (s, Ar-C_{13}), 128.22 (obscured by solvent residual, detected by HSQC, Ar-C_8), 127.09 (app t, Ar-C_7, J_{PC} = 1.5 Hz), 126.78 (s, Ar-C_3), 120.74 (s, Ar-C_{14}), 116.20 (s, Ar-C_{12}), 34.66 (s, -C(CH_3)$_3$), 31.70 (s, -C(CH$_3$)$_3$), 28.10 (app t, -CH(CH_3)$_2$, J_{PC} = 5.6 Hz), 23.49 (app t, -CH(CH_3)$_2$, J_{PC} = 7.6 Hz), 21.70 (app t, -CH(CH_3)$_2$, J_{PC} = 6.1 Hz), 20.62 (app t, -CH(CH_3)$_2$, J_{PC} = 9.1 Hz), 20.43 (app t, -CH(CH_3)$_2$, J_{PC} = 6.1 Hz), 18.14 (s, -CH(CH$_3$)$_2$). ^{31}P{^{1}H} NMR (121 MHz, C_6D_6) δ 32.45 (s).

Synthesis of [1,3-bis(2'-diisopropylphosphinophenyl)-5-tert-butyl-2-phenoxy-benzene]-platinum(0) (11d).

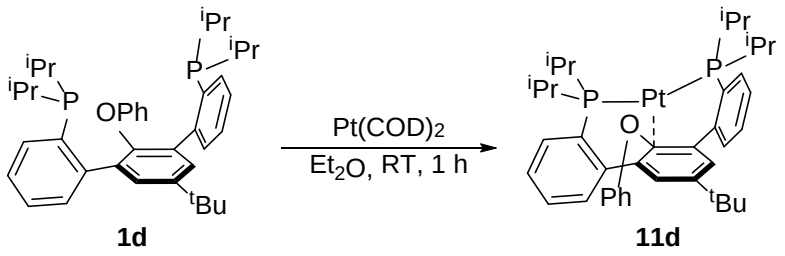

1d **11d**

In the glovebox, a 20 mL scintillation vial was charged with a magnetic stir bar, Pt(COD)$_2$[16] (0.027 g, 0.025 mmol, 1.00 equiv.), and Et$_2$O (1 mL). A light brown solution was observed. A colorless solution of diphosphine **1d** (0.040 g, 0.025 mmol, 1.00 equiv.) in Et$_2$O (2 mL) was added dropwise to the solution of Pt(COD)$_2$ and allowed to stir. After 15 min. a brown solution was observed. After 1 h, volatiles were removed under reduced pressure. The resulting brown solid was extracted with three

portions of pentane (1 mL each) to afford intermediate **11d** (0.044 g, 0.054 mmol, 82.6%) as an off-white solid with an impurity of **14d** (22% conversion by NMR). ^{1}H NMR (400 MHz, C_6D_6) δ 7.27 – 7.20 (m, 4H, Ar-*H*$_6$ & Ar-*H*$_9$), 7.11 (s, 2H, Ar-*H*$_3$), 7.01 (m, 2H, Ar-*H*$_7$ or Ar-*H*$_8$), 6.91 (m, 2H, Ar-*H*$_7$ or Ar-*H*$_8$), 6.75 (m, 2H, Ar-*H*$_{13}$), 6.55 (m, 1H, Ar-*H*$_{14}$), 6.49 (m, 2H, Ar-*H*$_{12}$), 2.30 (m, 2H, -C*H*(CH$_3$)$_2$), 2.07 (m, 2H, -C*H*(CH$_3$)$_2$), 1.56 (dd, 6H, -CH(C*H*$_3$)$_2$), 1.44 (dd, 6H, -CH(C*H*$_3$)$_2$), 1.39 (s, 9H, -C(C*H*$_3$)$_3$), 1.15 (dd, 6H, -CH(C*H*$_3$)$_2$), 0.91 (dd, 6H, -CH(C*H*$_3$)$_2$). ^{13}C{^{1}H} NMR (101 MHz, C_6D_6) δ 159.21 (s, Ar-*C*$_{11}$), 147.25 (app t, Ar-*C*$_{10}$, J_{PC} = 9.1 Hz), 144.18 (s, Ar-*C*$_4$), 137.33 (app t, Ar-*C*$_2$, J_{PC} = 3.0 Hz), 136.34 (s, Ar-*C*$_1$), 134.34 (app t, Ar-*C*$_5$, J_{PC} = 18.1 Hz), 131.97 (app t, Ar-*C*$_6$ or Ar-*C*$_9$, J_{PC} = 1.5 Hz), 131.18 (app t, Ar-*C*$_6$ or Ar-*C*$_9$, J_{PC} = 3.5 Hz), 128.88 (app t, Ar-*C*$_{13}$, J = 5.6 Hz), 128.25 (obscured by solvent residual, detected by HSQC, Ar-*C*$_7$ or Ar-*C*$_8$), 127.32 (s, br, Ar-*C*$_3$), 127.06 (app t, Ar-*C*$_7$ or Ar-*C*$_8$, J_{PC} = 2.5 Hz), 120.61 (s, Ar-*C*$_{14}$), 116.52 (s, Ar-*C*$_{12}$), 34.80 (s. -*C*(CH$_3$)$_3$), 31.56 (s, -C(*C*H$_3$)$_3$), 28.88 (app t, -*C*H(CH$_3$)$_2$, J_{PC} = 11.6 Hz), 25.03 (app t, -*C*H(CH$_3$)$_2$, J_{PC} = 15.2 Hz), 21.11 (app t, -CH(*C*H$_3$)$_2$, J_{PC} = 3.5 Hz), 20.53 (app t, -CH(*C*H$_3$)$_2$, J_{PC} = 5.1 Hz), 20.12 (app t, -CH(*C*H$_3$)$_2$, J_{PC} = 3.0 Hz), 18.21 (s, -CH(*C*H$_3$)$_2$). ^{31}P{^{1}H} NMR (121 MHz, C_6D_6) δ 55.92 (J_{PtP} = 4743.2 Hz).

Synthesis of [1,3-bis(2'-diisopropylphosphinophenyl)-5-tert-butyl-phenyl]nickel(II)(4'-dimethyl-amino phenoxide) (12c).

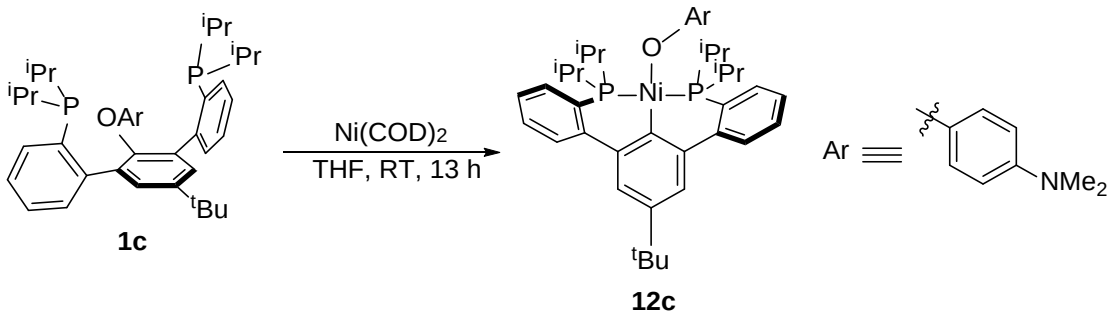

In the glovebox, a colorless solution of diphosphine **1c** (0.111 g, 0.170 mmol) in THF (5 ml) was added to a yellow slurry of $Ni(COD)_2$ (0.047 g, 0.170 mmol) in THF (3 ml) at RT. A color change to orange was observed. The mixture was stirred for 13 h. Volatiles were removed under reduced pressure. An orange solid was observed. Washing the crude solid with hexanes and Et_2O afforded **12c** (0.116 g, 0.163 mmol, 97.8%) as an orange solid. ^1H NMR (C_6D_6, 500 MHz) δ 7.74 (d, 2H, Ar-*H*), 7.43 (m, 2H, Ar-*H*), 7.27 (mm, 2H, Ar-*H*), 7.26 (s, 2H, Ar-H_3), 7.18 (mm, 2H, Ar-*H*), 7.01 (mm, 2H, Ar-*H*), 6.81 (mm, 2H, Ar-*H*), 2.68 (s, 6H, N(CH_3)$_2$), 2.18 (m, 2H, C*H*(CH_3)$_2$), 1.59 (m, 2H, C*H*(CH_3)$_2$), 1.50 (mm, 6H, CH(CH_3)$_2$), 1.25 (mm, 9H, C(CH_3)$_3$), 0.88 (mm, 12H, CH(CH_3)$_2$) 0.71 (mm, 6H, CH(CH_3)$_2$). $^{13}C\{^1H\}$ NMR (C_6D_6, 126 MHz) δ 163.57 (s, Ar-C_{11}), 152.51 (app t, Ar-C_{10}, J_{PC} = 6.9 Hz), 149.53 (app t, Ar-C_4, J_{PC} = 1.9 Hz), 147.41 (app t, Ar-C_2, J_{PC} = 6.3 Hz), 140.47 (app t, Ar-C_5, J_{PC} = 32.1 Hz), 140.38 (s, Ar-C_{14}), 130.69 (s, Ar-*C*H), 129.92 (app t, Ar-*C*H, J_{PC} = 1.3 Hz), 128.20 (m, Ar-*C*), 126.94 (app t, Ar-*C*H, J_{PC} = 2.5 Hz), 126.52 (t, Ar-C_1, J_{PC} = 15.1 Hz), 124.47 (app t, Ar-C_3, J_{PC} = 2.5 Hz), 120.27 (s, Ar-C_{12}), 117.56 (Ar-C_{13}), 43.72 (s, -N(*C*H_3)$_2$), 34.16 (s, -*C*(CH_3)$_3$), 31.54 (s, -C(*C*H_3)$_3$), 23.34 (m, br, -C*H*(CH_3)$_2$), 20.9f0 (app t, -C*H*(CH_3)$_2$, J_{PC} = 9.5 Hz), 20.42 (s, -CH(C*H*$_3$)$_2$), 19.17 (s, -CH(C*H*$_3$)$_2$), 18.98 (s, -

CH(C*H*$_3$)$_2$), 17.94 (s, -CH(C*H*$_3$)$_2$). ^{31}P{^{1}H} NMR (C_6D_6, 121 MHz) δ 29.73 (s). Anal. calcd. for $C_{42}H_{57}NNiOP_2$ (%): C, 70.80; H 8.06; N 1.97. Found: C, 70.95; H, 7.98; N, 1.96.

Synthesis of [1,3-bis(2'-diisopropylphosphinophenyl)-5-tert-butyl-phenyl]palladium(II)-phenoxide (13d).

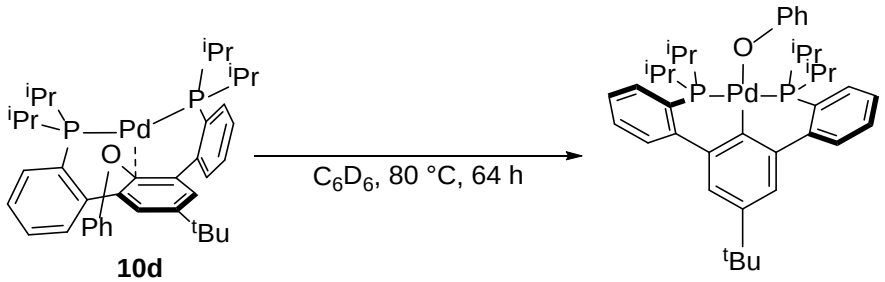

10d **13d**

In the glovebox, a J. Young tube fitted with a Teflon screw cap was charged with **10d** (0.015 g, 0.021 mmol) as a solution C_6D_6 (ca. 0.6 mL). The J. Young tube was removed from the glovebox and placed in an oil bath preheated to 80 °C. After 64 h, the J. Young tube was removed from the oil bath and brought into the glovebox. A pale yellow solution was observed. The solution was transferred to a 20 mL scintillation vial. Volatiles were removed under reduced pressure and the resulting yellow residue was extracted three times with 1 mL portions of pentane. This pentane solution was filtered through Celite and volatiles removed under reduced pressure to afford a yellow residue. This yellow residue was dissolved in a minimum of pentane, filtered once more through Celite, and stored at -35 ºC. Compound **13d** (0.011 g, 0.015 mmol, 72.7%) was isolated as a semi-crystalline yellow precipitate. ^{1}H NMR (400 MHz, C_6D_6) δ 7.70 (m, 2H, Ar-*H*$_9$), 7.43 (s, 2H, Ar-*H*$_3$), 7.34 (m, 2H, Ar-*H*$_8$), 7.26 (m, 4H, Ar-*H*$_6$& Ar-*H*$_{13}$), 7.13 (m, 2H, Ar-*H*$_7$), 7.01 (m, 2H, Ar-*H*$_{12}$), 6.71 (m, 1H, Ar-*H*$_{14}$), 2.31 (s, br, 2H, -C*H*(CH$_3$)$_2$), 1.73 (s, br, 2H, -C*H*(CH$_3$)$_2$, 1.56 (s, br, 6H, -CH(C*H*$_3$)$_2$),

1.28 (s, 9H, -C(C*H*$_3$)$_3$), 0.94 (s, br, 6H, -CH(C*H*$_3$)$_2$), 0.79 (s, br, -CH(C*H*$_3$)$_2$), 0.62 (s, br, 6H, -CH(C*H*$_3$)$_2$). ^{13}C{^{1}H} NMR (101 MHz, C_6D_6) δ 171.60 (s, Ar-*C*$_{11}$), 153.87 (app t, Ar-*C*$_2$, J_{PC} = 8.1 Hz), 149.55 (s, Ar-*C*$_4$), 145.55 (app t, Ar-*C*$_5$ or Ar-*C*$_{10}$, J_{PC} = 7.1 Hz), 138.56 (t, Ar-*C*$_1$, J_{PC} = 7.6 Hz), 130.43 (s, Ar-*C*$_8$), 129.86 (app t, Ar-*C*$_5$ or Ar-*C*$_{10}$, J_{PC} = 1.5 Hz), 129.39 (app t, Ar-*C*$_9$, J_{PC} = 4.0 Hz), 129.13 (s, Ar-*C*$_6$ or Ar-*C*$_{13}$), 128.59 (s, Ar-*C*$_6$ or Ar-*C*$_{13}$), 126.80 (app t, Ar-*C*$_7$, J_{PC} = 2.5 Hz), 126.01 (s, Ar-*C*$_3$), 120.55 (s, Ar-*C*$_{12}$), 112.25 (s, Ar-*C*$_{14}$), 34.33 (s, -*C*(CH$_3$)$_3$), 31.52 (s, -C(*C*H$_3$)$_3$), 23.87 (s, br, -C*H*(CH$_3$)$_2$), 22.10 (s, br, -CH(C*H*$_3$)$_2$), 20.58 (s, br, -CH(C*H*$_3$)$_2$), 17.93 (s, br, -CH(C*H*$_3$)$_2$). ^{31}P{^{1}H} NMR (121 MHz, C_6D_6) δ 34.70 (s). Anal. calcd. for $C_{40}H_{52}OP_2Pd$ (%): C, 66.99; H, 7.31. Found: C, 66.21; H, 6.81. Low in carbon and hydrogen despite multiple syntheses.

Synthesis of [1,3-bis(2'-diisopropylphosphinophenyl)-5-tert-butyl-phenyl]platinum(II)-phenoxide (14d).

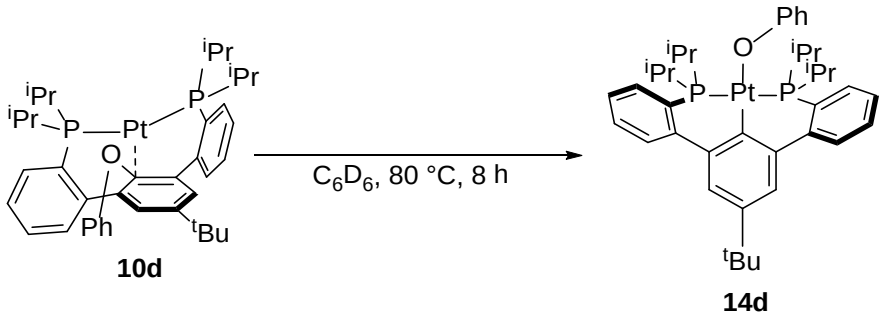

10d **14d**

In the glovebox, a J. Young tube fitted with a Teflon screw cap was charged with **11d** (0.015 g, 0.019 mmol) as a colorless solution C_6D_6 (ca. 0.6 mL). The J. Young tube was removed from the glovebox, placed in an oil bath preheated to 80 ºC, and heated while stirring. After 8 h, the J. Young tube was removed from the oil bath and bought into the glovebox. A colorless solution was observed. The solution was transferred to a 20 mL scintillation vial. Volatiles were removed under reduced pressure and the

resulting yellow residue was washed three times with 1 mL portions of pentane. Compound **14d** (0.009 g, 0.012 mmol, 62.7%) was isolated as a white solid. ^{1}H NMR (500 MHz, C_6D_6) δ 7.74 (m, 2H, Ar-*H*$_9$), 7.45 (s, 2H, Ar-*H*$_3$), 7.36 (m, 2H, Ar-*H*$_8$), 7.27 (m, 2H, Ar-*H*$_{13}$), 7.23 (m, 2H, Ar-*H*$_6$), 7.13 (m, 2H, Ar-*H*$_7$), 7.10 (m, 2H, Ar-*H*$_{12}$), 6.74 (m, 1H, Ar-*H*$_{14}$), 2.41 (s, br, 2H, -C*H*$(CH_3)_2$), 1.91 (s, br, 2H, -C*H*$(CH_3)_2$), 1.72 – 1.45 (s, br, 6H, -CH(C*H*$_3)_2$), 1.30 (s, 9H, -C(C*H*$_3)_3$), 1.08 – 0.51 (s, br, 18H, -CH(C*H*$_3)_2$). ^{13}C{^{1}H} NMR (101 MHz, C_6D_6) δ 171.31 (s, Ar-*C*$_{11}$), 154.15 (app t, Ar-*C*$_{10}$, J_{PC} = 6.9 Hz), 148.76 (s, Ar-*C*$_4$), 144.91 (s, Ar-*C*$_2$), 130.71 (s, Ar-*C*$_8$), 129.49 (app t, Ar-*C*$_9$, J_{PC} = 3.8 Hz), 129.19 (s, br, Ar-*C*$_6$), 128.94 (s, Ar-*C*$_{13}$), 126.74 (m, br, Ar-*C*$_5$), 126.74 (app t, Ar-*C*$_7$), 125.93 (s, Ar-*C*$_3$), 124.88 (t, Ar-*C*$_1$, 9.5 Hz), 120.18 (s, Ar-*C*$_{12}$), 113.23 (s, Ar-*C*$_{14}$), 34.32 (s, -*C*$(CH_3)_3$), 31.51 (s, -C(*C*H$_3)_3$), 23.52 (s, br, -*C*H$(CH_3)_2$), 21.54 (s, br, -*C*H$(CH_3)_2$), 20.11 (s, br, -CH(*C*H$_3)_2$), 18.48 (s, br, -CH(*C*H$_3)_2$). ^{31}P{^{1}H} NMR (121 MHz, C_6D_6) δ 33.23 (J_{PP} = 2773.3 Hz).

Synthesis of [1,3-bis(2'-diisopropylphosphinophenyl)-5-tert-butyl-2-methoxybenzene]-rhodium(I)(1,5-cyclooctadiene)chloride (15a).

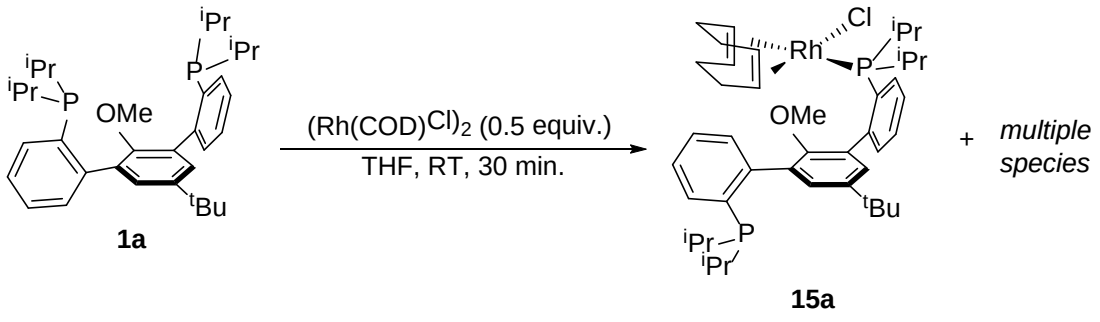

In the glovebox, a 20 mL scintillation vial was charged with $(Rh(COD)Cl)_2$ (0.011 g, 0.023 mmol, 0.50 equiv.), THF (2 mL), and a magnetic stir bar. Diphosphine **1a** (0.025 g, 0.046 mmol, 1.00 equiv.) was added as a solution in THF (1 mL). After 5 min., a red-orange solution was observed. After 30 min., volatiles were removed under

reduced pressure to afford a gummy orange solid (mixture of species; **15a**, NMR yield: 74%). ^{1}H NMR (400 MHz, C_6D_6) δ 7.87 (m, 1H, Ar-*H*), 7.42 (m, 1H, Ar-*H*), 7.35 (m, 1H, Ar-*H*), 7.28 (m, 2H, Ar-*H*), 7.25 (m, 1H, Ar-*H*), 7.20 (m, 1H, Ar-*H*), 7.01 (m, 1H, Ar-*H*), 6.92 (m, 2H, Ar-*H*), 5.79 – 5.61 (m, br, 3H, COD, -C*H*$_2$), 5.58 (s, 1H, COD, -C*H*$_2$), 3.50 – 3.26 (m, 4H, COD, -C*H*), 2.89 (s, 3H, -OC*H*$_3$), 2.58 – 2.36 (m, 2H, -C*H*(CH$_3$)$_2$), 2.03 (m, 1H, -C*H*(CH$_3$)$_2$), 1.90 (m, 1H, -C*H*(CH$_3$)$_2$), 1.80 – 1.52 (m, 9H, -CH(C*H*$_3$)$_2$), 1.16 – 1.05 (m, 3H, -CH(C*H*$_3$)$_2$), 1.28 (s, 9H, -C(C*H*$_3$)$_3$), 1.04 – 0.94 (m, 6H, -CH(C*H*$_3$)$_2$), 0.88 – 0.77 (m, 6H, -CH(C*H*$_3$)$_2$). ^{13}C{^{1}H} NMR (101 MHz, C_6H_6) δ 152.12 (s, Ar-*C*$_1$), 147.94 (d, Ar-*C*, J_{PC} = 32.3 Hz), 144.46 (s, Ar-*C*), 144.06 (s, Ar-*C*), 136.81 (d, Ar-*C*, J_{PC} = 6.1 Hz), 136.25 – 135.49 (m, Ar-*C*), 135.78 (d, Ar-*C*H, J_{PC} = 19.2 Hz), 133.46 (d, Ar-*C*H, J_{PC} = 5.1 Hz), 132.76 (d, Ar-*C*H, J_{PC} = 4.0 Hz), 131.15 (d, Ar-*C*H, J_{PC} = 6.1 Hz), 129.99 (s, Ar-*C*H), 128.82 (s, Ar-*C*H), 127.68 (detected by HSQC, obscured by solvent residual, Ar-*C*H), 127.56 (detected by HSQC, obscured by solvent residual, Ar-*C*H), 127.00 (s, Ar-*C*H), 125.12 (d, Ar-*C*H, J_{PC} = 12.1 Hz), 102.41 (m, COD, -*C*H), 101.87 (m, COD, -*C*H), 71.99 (d, COD, -*C*H$_2$, J_{RhC} = 15.2 Hz), 69.27 (d, COD, -*C*H$_2$, J_{RhC} = 13.1), 59.79 (s, -O*C*H$_3$), 34.37 (s, -*C*(CH$_3$)$_3$), 34.17 (d, -*C*H(CH$_3$)$_2$, J_{PC} = 3.0 Hz), 32.00 (d, -*C*H(CH$_3$)$_2$, J_{PC} = 2.0 Hz), 31.44 (s, -C(*C*H$_3$)$_3$), 29.81 (d, -*C*H(CH$_3$)$_2$, J_{PC} = 2.0 Hz), 28.17 (s, br, -*C*H(CH$_3$)$_2$), 24.44 (d, -CH(*C*H$_2$)$_3$, J_{PC} = 9.1 Hz), 22.56 (d, -CH(*C*H$_2$)$_3$, J_{PC} = 4.0 Hz), 21.32 – 20.20 (m, -CH(*C*H$_3$)$_2$), 20.07 – 19.67 (m, -CH(*C*H$_3$)$_2$), 17.79 (s, br, -CH(*C*H$_3$)$_2$). ^{31}P{^{1}H} NMR (121 MHz, C_6D_6) δ 59.97 (d, J_{RhP} = 145.2 Hz), -4.04 (s). ^{1}H NMR (300 MHz, CD_2Cl_2) δ 7.68 (m, 1H, Ar-*H*), 7.60 – 7.52 (m, 1H, Ar-*H*), 7.41 – 7.22 (m, 5H, Ar-*H*), 7.18 – 7.12 (m, 1H, Ar-*H*), 7.09 (m, 1H, Ar-*H*), 5.27 – 5.02 (m, COD, -C*H*), 3.36 – 3.17 (m, COD, -C*H*$_2$), 2.93 (s, -

OC*H*$_3$), 2.29 (m, 2H, -C*H*(CH$_3$)$_2$), 1.87 (m, 1H, -C*H*(CH$_3$)$_2$), 1.76 (m, 1H, -C*H*(CH$_3$)$_2$), 1.41 – 1.18 (m, 12H, -CH(C*H*$_3$)$_2$), 1.29 (s, -C(C*H*$_3$)$_3$), 1.15 – 0.99 (m, 6H, -CH(C*H*$_3$)$_2$), 0.92 – 0.72 (m, 6H, -CH(C*H*$_3$)$_2$). ^{13}C{^{1}H} NMR (101 MHz, CD_2Cl_2) δ 151.99 (s, Ar-*C*), 147.86 (d, Ar-*C*, J_{PC} = 32.32 Hz), 143.92 (d, Ar-*C*, J_{PC} = 39.41, Ar-*C*), 136.65 (d, Ar-*C*, J_{PC} = 8.1 Hz), 136.18 – 135.10 (m, Ar-*C*), 135.81 (d, Ar-*C*$_6$, J_{PC} = 17.2 Hz), 133.69 (d, Ar-*C*H, J_{PC} = 5.1 Hz), 132.76 (d, Ar-*C*H, J_{PC} = 3.0 Hz), 131.34 (d, Ar-*C*H, J_{PC} = 6.1 Hz), 130.17 (s, Ar-*C*H), 128.87 – 127.59 (m, Ar-*C*H & Ar-*C*), 126.96 (s, Ar-*C*H), 125.23 (d, Ar-*C*H, J_{PC} = 12.1 Hz), 102.39 – 101.96 (m, COD, -*C*H), 101.59 – 101.19 (m, COD, -*C*H), 73.02 (d, COD, -*C*H$_2$, J_{PC} = 15.2 Hz), 69.76 (d, COD, -*C*H$_2$, J_{PC} = 13.1 Hz), 59.91 (s, -O*C*H$_3$), 34.54 (s, -*C*(CH$_3$)$_3$), 33.78 (d, -C*H*(CH$_3$)$_2$, J_{PC} = 3.0 Hz), 32.13 (d, -C*H*(CH$_3$)$_2$, J_{PC} = 2.0 Hz), 31.48 (s, -C(*C*H$_3$)$_3$), 29.52 (s, br, -C*H*(CH$_3$)$_2$), 28.39 (d, -C*H*(CH$_3$)$_2$, J_{PC} = 3.0 Hz), 22.11 (d, -CH(*C*H$_3$)$_2$, J_{PC} = 4.0 Hz), 21.38 – 20.29 (m, -CH(*C*H$_3$)$_2$), 19.91 (d, -C*H*(CH$_3$)$_2$, J_{PC} = 2.0 Hz), 19.73 (d, -C*H*(CH$_3$)$_2$, J_{PC} = 5.1 Hz), 18.58 (s, br, -C*H*(CH$_3$)$_2$). ^{31}P{^{1}H} NMR (121 MHz, CD_2Cl_2) δ 59.11 (d, J_{RhP} = 143.99 Hz), -4.06 (s).

Synthesis of [1,3-bis(2'-diisopropylphosphinophenyl)-5-tert-butyl-benzene]rhodium(I)-chloride (19a).

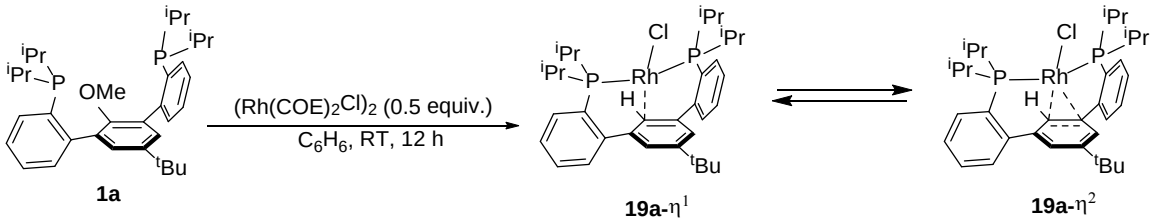

1a **19a-η^1** **19a-η^2**

Method A: In the glovebox, a 20 mL scintillation vial was charged with a magnetic stir bar and (Rh(COE)$_2$Cl)$_2$ (0.162 g, 0.225 mmol, 0.50 equiv.) as a slurry in C_6H_6 (2 mL). Diphosphine **1a** (0.247 g, 0.450 mmol, 1.00 equiv.) was added as a solution in C_6H_6 (1

mL) and the solution was stirred. After 10 min., a dark purple solution was observed. After 26 h, volatiles were removed under reduced pressure to afford a dark purple residue. Hexanes (10 mL) was added and the resulting slurry was stirred for 10 min. then allowed to stand at room temperature for 10 min. The heterogeneous solution was filtered through Celite and the resulting purple precipitate was extracted with 3 portions of Et_2O (3 mL). Volatiles were removed under reduced pressure and afforded **19a** (ca. 95% NMR yield, isolated with **26a**, 5 % by NMR). Crystals suitable for X-ray diffraction were grown from a saturated solution of **19a** in hexanes at -35 ºC. ^{1}H NMR (300 MHz, C_6D_6, 25 °C) 7.35 – 7.23 (m, br, Ar-*H*), 7.11 (m, br, 2H, Ar-*H*), 7.09 (m, 1H, Ar-*H*), 7.03 (m, 2H, Ar-*H*), 3.09 (s, br, 2H, -C*H*$(CH_3)_2$), 2.42 (s, br, 2H, -C*H*$(CH_3)_2$), 1.56 (m, br, 6H, -CH(C*H*$_3)_2$), 1.37 – 1.19 (m ,br, 6H, -CH(C*H*$_3)_2$), 1.28 (s, 9H, -C(C*H*$_3)_3$), 1.00 (m, br, 12H, -CH(C*H*$_3)_2$). ^{1}H NMR (300 MHz, C_6D_6, 70 °C) δ 7.35 (m, br, 2H, Ar-*H*), 7.27 (m, br, 2H, Ar-*H*), 7.21-7.07 (m, br, Ar-*H*, obscured by solvent residual), 6.98 (s, br, 2H, Ar-*H*), 3.05 (s, br, 2H, -C*H*$(CH_3)_2$), 2.54 (s, br, 2H, -C*H*$(CH_3)_2$), 1.56 (m, br, 6H, -CH(C*H*$_3)_2$), 1.28 (m, br, 6H, -CH(C*H*$_3)_2$; s, 9H, -C(C*H*$_3)_3$), 1.03 (m, br, 12H, -CH(C*H*$_3)_2$). ^{13}C{^{1}H} NMR (101 MHz, C_6D_6, 70°C) δ 155.82 (s, Ar-*C*$_2$), 152.78 (app t, Ar-*C*$_{10}$, J_{PC} = 11.6 Hz), 146.26 (s, Ar-*C*$_4$), 138.35 (m, br, detected by HMBC, Ar-*C*), 130.66 (s, Ar-*C*$_6$), 130.11 (s, Ar-*C*$_9$), 129.91 (app t, Ar-*C*H, J_{PC} = 4.6 Hz), 128.29 (Ar-*C*H, obscured by solvent residual, observed by HMBC), 127.12 (app t, Ar-*C*H, J_{PC} = 2.0 Hz), 125.11 (s, Ar-*H*$_3$), 34.21 (s, -*C*$(CH_3)_3$), 30.91 (s, -C(*C*H$_3)_3$), 24.96 (app t, -*C*H$(CH_3)_2$, J_{PC} = 12.6 Hz), 22.90 (app t, -*C*H$(CH_3)_2$, J_{PC} = 9.6 Hz), 20.19 (app t, -CH(*C*H$_3)_2$, J_{PC} = 2.5 Hz), 19.67 (s, -CH(*C*H$_3)_2$), 19.54 (s, -CH(*C*H$_3)_2$), 17.83 (s, -CH(*C*H$_3)_2$). ^{31}P{^{1}H} NMR (121 MHz, C_6D_6, 25 °C) δ 36.28 (s, br).

$^{31}P\{^{1}H\}$ NMR (162 MHz, C_6D_6, 70 °C, referenced with respect to internal solvent lock) δ 36.48 (d, J_{RhP} = 115.0 Hz).

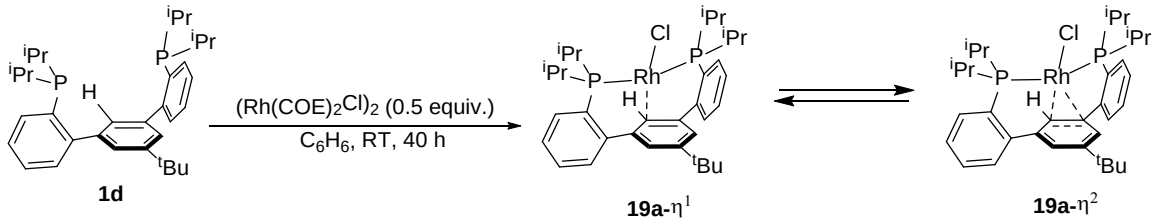

Method B: In the glovebox, a 20 mL scintillation vial was charged with a magnetic stir bar and $(Rh(COE)_2Cl)_2$ (0.069 g, 0.096 mmol, 0.50 equiv.) as a slurry in C_6H_6. Diphosphine **1d** (0.100 g, 0.193 mmol, 1.00 equiv.) was added as a solution in C_6H_6 (1 mL) and the solution was stirred. After 15 min., a dark purple solution was observed. After 40 h, voatiles were removed under reduced pressure to afford a dark purple residue. Hexanes (2 mL) was added and the residue was triturated. Volatiles were removed under reduced pressure to afford a purple powder. This powder was washed with three portions of pentane (*ca.* 1 mL) and three portions of Et_2O (*ca.* 1 mL each). This powder was dissolved in C_6H_6 (2 mL), filtered through Celite, and volatiles were removed under reduced pressure to afford **19a** (0.013 g, 0.019 mmol, 10.1 % yield). Anal. calcd. for $C_{34}H_{48}ClP_2Rh$ (%):C, 62.15; H, 7.38. Found: C, 61.06; H, 7.00. Low in carbon despite multiple analyses.

Synthesis of 1,3-bis(2'bromophenyl)-5-*tert*-butyl-benzene

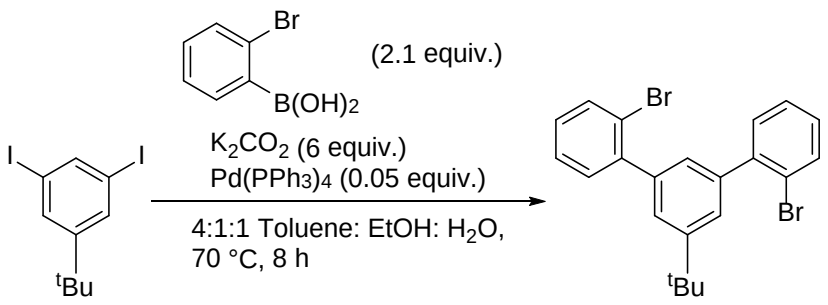

1,3-bis(2'-bromophenyl)-5-*tert*-butyl-benzene was synthesized using a modification of the procedure reported by Albrecht and co-workers for the Suzuki coupling of aryl halides with boronic acids.[48] In the fume hood, a large Schlenk tube fitted with a Teflon screw cap was charged with 1-(*tert*-butyl)-3,5-diiodobenzene (1.812 g, 4.694 mmol, 1.00 equiv.), 2-bromophenylboronic acid (1.980 g, 9.858 mmol, 2.10 equiv.), K_2CO_3 (3.892 g, 28.165 mmol, 6.00 equiv.), toluene (160 mL), EtOH, (40 mL), deionized H_2O (40 mL), and a stir bar. On the Schlenk line, the reaction mixture was degassed via three freeze-pump-thaw cycles. With N_2 backflow, $Pd(PPh_3)_4$ (0.271 g, 0.235 mmol, 0.05 equiv.) was added, providing a yellow biphasic solution. The reaction was stirred at 70 °C for 8 h at which time the reaction mixture was transferred to a round bottom flask and concentrated under reduced pressure to a total volume of *ca.* 100 mL. This mixture was transferred to a separatory funnel and extracted with CH_2Cl_2 (*ca.* 75 mL) three times. The combined organics were washed with brine and dried over $MgSO_4$. The volatiles were removed under reduced pressure, providing an orange oil. Biphenyl impurities were distilled from the crude reaction mixture using a Kugelrohr apparatus (10 mTorr, 90 °C) to afford a gummy orange solid and the distillate was discarded. Under a counter-flow of N_2 on the Schlenk line, this gummy orange solid was transferred as a THF (15 mL) solution to an oven-dried 100 mL

Schlenk flask fitted with a Teflon screw cap charged with a stir bar which had been previously evacuated on the Schlenk line. CaH_2 (*ca.* 500 mg) was added as a solid under a counter-flow of N_2 and sealed. The heterogeneous mixture was stirred vigorously for 3 h, then brought in the glovebox and filtered through a pad of alumina. The alumina pad was rinsed twice with portions of THF (5 mL each). Removal of volatiles from the filtrate afforded 1,3-bis(2'-bromophenyl)-5-*tert*-butyl-benzene (2.006 g, 4.535 mmol, 88.5%) as a gummy yellow solid. Material of this purity was used in a subsequent phosphination (via lithium-halogen exchange and dialkyl chlorophosphine quench) without further purification. ^{1}H NMR (300 MHz, C_6D_6) δ 7.60 (d, 2H Ar-*H*$_3$), 7.52 (m, 2H, Ar-*H*$_{6\text{-}9}$), 7.26 (t, 1H, Ar-*H*$_1$), 7.19 (m, 2H, Ar-*H*$_{6\text{-}9}$), 6.94 (m, 2H, Ar-*H*$_{6\text{-}9}$), 6.75 (m, 2H, Ar-*H*$_{6\text{-}9}$), 1.27 (s, 9H, -C(C*H*$_3$)$_3$). ^{1}H NMR (400 MHz, $CDCl_3$) δ 7.69 (m, 2H, Ar-*H*$_{6\text{-}9}$), 7.48 (d, 2H, Ar-*H*$_3$), 7.42 (m, 2H, Ar-*H*$_{6\text{-}9}$), 7.37 (m, 2H, Ar-*H*$_{6\text{-}9}$), 7.28 (t, 1H, Ar-*H*$_1$), 7.20 (m, 2H, Ar-*H*$_{6\text{-}9}$), 1.40 (s, 9H, -C(C*H*$_3$)$_3$). ^{13}C{^{1}H} NMR (101 MHz, $CDCl_3$) δ 150.41 (s, Ar-*C*$_1$), 142.88 (s, Ar-*C*$_2$), 140.36 (s, Ar-*C*$_{10}$), 133.36 (s, Ar-*C*$_{6\text{-}9}$), 131.64 (s, Ar-*C*$_{6\text{-}9}$), 128.77 (s, Ar-*C*$_{6\text{-}9}$), 127.57 (s, Ar-*C*$_{6\text{-}9}$), 127.52 (s, Ar-*C*$_1$), 126.12 (s, Ar-*C*$_3$), 122.87 (s, Ar-*C*$_5$), 35.06 (s, -*C*(CH$_3$)$_3$), 31.52 (s, -C(*C*H$_3$)$_3$).

Synthesis of 1,3-bis(2'-diisopropylphosphinophenyl)-5-tert-butyl-benzene (1e)

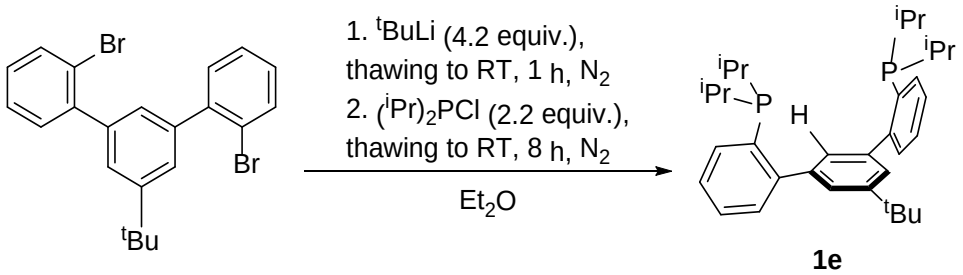

1e

In a glovebox, a 250 mL round bottom flask was charged with a yellow solution of 1,3-bis(2'-bromophenyl)-5-*tert*-butyl-benzene (1.810 g, 4.08 mmol, 1.00 equiv.) in Et_2O (80

mL) and a stir bar. A 20 mL scintillation vial was charged with a solution of ^{t}BuLi in pentane (1.7 M, 17.11 mmol, 10.1 mL, 4.20 equiv.). The two vessels were placed in a liquid N_2 chilled cold well. The vessels were removed from the cold well such that a just-thawed solution of ^{t}BuLi was added to a thawing solution of 1,3-bis(2'-bromophenyl)-5-*tert*-butyl-benzene. The mixture was allowed to warm to room temperature over the course of 1 h. An orange solution was observed. A 20 mL scintillation vial was charged with (^{i}Pr)$_2$PCl (1.368 g, 8.96 mmol, 2.20 equiv.) and pentane (2 mL). The reaction vessel and solution of (^{i}Pr)$_2$PCl in pentane were placed in a liquid N_2 chilled cold well. The vessels were removed from the cold well such that a just-thawed solution of (^{i}Pr)$_2$PCl in pentane was added to the thawing solution in the reaction vessel. After 1 h, a yellow-orange solution was observed. After 8 h, volatiles were removed under reduced pressure to afford an orange solid. This solid was extracted with four portion (20 mL each) of pentane. This organic layer was filtered through alumina and volatiles were removed under reduced pressure to afford an orange oil. Trituration of this orange oil with 5 mL of CH_3CN afforded an off-white solid. This solid was washed three times with three portions of CH_3CN (5 mL each) to afford 1,3-bis(2'-diisopropylphosphino)-5-*tert*-butyl-benzene (1.375 g, 2.65 mmol, 65.1% yield) as an off-white solid. ^{1}H NMR (300 MHz, C_6D_6) δ 7.59 (m, 2H, Ar-*H*$_9$), 7.52-7.47 (m, 2H, Ar-*H*$_6$), 7.45 (t, 1H, Ar-*H*$_1$), 7.44-7.41 (m, 2H, Ar-*H*$_8$), 7.15 (m, 4H, Ar-*H*$_3$ & Ar-*H*$_7$), 1.89 (m, 4H, -C*H*$(CH_3)_2$), 1.39 (s, 9H, -C(*C*$H_3)_3$), 0.95 (m, 24H, -CH(C*H*$_3)_2$). ^{13}C{^{1}H} NMR (101 MHz, C_6D_6) δ 151.60 (d, Ar-*C*$_{10}$, J_{PC} = 27.3 Hz), 148.66 (s, Ar-*C*$_4$), 142.05 (d, Ar-*C*$_2$, J_{PC} = 6.1 Hz), 135.59 (d, Ar-*C*$_5$, J_{PC} = 24.2 Hz), 132.84 (s, Ar-*C*$_8$), 130.95 (d, Ar-*C*$_6$, J_{PC} = 5.1 Hz), 130.53 (t, Ar-*C*$_1$, J_{PC} = 3.0 Hz), 128.67 (s, Ar-*C*$_3$ or Ar-*C*$_7$), 127.62 (d, Ar-*C*$_9$, J_{PC} = 7.1 Hz), 126.72 (s, Ar-*C*$_3$ or Ar-*C*$_7$), 34.89 (s, -

C(CH_3)$_3$), 31.65 (s, -C(*C*H_3)$_3$), 25.15 (d, -*C*H(CH_3)$_2$), J_{PC} = 16.2 Hz), 20.62 (d, -CH(*C*H_3)$_2$, J_{PC} = 20.2 Hz), 20.13 (d, -CH(*C*H_3)$_2$, J_{PC} = 12.1 Hz). $^{31}P\{^1H\}$ NMR (121 MHz, C_6D_6) δ -3.62 (s). ^1H NMR (300 MHz, $CDCl_3$) δ 7.58 (m, 2H, Ar-*H*$_6$), 7.43-7.32 (m, 6H, Ar-*H*$_7$, Ar-*H*$_8$ & Ar-*H*$_9$), 7.30 (s, 2H, Ar-*H*$_3$), 7.06 (s, br, 1H, Ar-*H*$_1$), 2.03 (m, 4H, -C*H*(CH_3)$_2$), 1.37 (s, 9H, -C(C*H*$_3$)$_3$), 1.01 (m, 12H, -CH(C*H*$_3$)$_2$), 0.93 (m, 12H, -CH(C*H*$_3$)$_2$). $^{13}C\{^1H\}$ NMR (101 MHz, $CDCl_3$) δ 151.18 (d, Ar-*C*$_{10}$, J_{PC} = 27.3 Hz), 148.19 (s, Ar-*C*$_4$), 141.43 (d, Ar-*C*$_2$, J_{PC} = 6.1 Hz), 135.28 (d, Ar-*C*$_5$, J_{PC} = 23.2 Hz), 132.64 (d, Ar-*C*$_6$, J_{PC} = 2.0 Hz), 130.53 (d, Ar-*C*$_8$ or Ar-*C*$_9$, J_{PC} = 5.1 Hz), 129.60 (t, Ar-*C*$_1$, J_{PC} = 2.5 Hz), 128.22 (s, Ar-*C*$_8$ or Ar-*C*$_9$), 127.01 (d, Ar-*C*$_3$, J_{PC} = 6.1 Hz), 126.35 (s, Ar-*C*$_7$), 34.80 (s, -*C*(CH_3)$_3$), 31.58 (s, -C(*C*H_3)$_3$), 24.96 (d, -C*H*(CH_3)$_2$, J_{PC} = 15.1 Hz), 20.46 (d, -CH(*C*H_3)$_2$, J_{PC} = 20.2 Hz), 20.01 (d, -CH(*C*H_3)$_2$, J_{PC} = 12.1 Hz). $^{31}P\{^1H\}$ NMR (121 MHz, $CDCl_3$) δ -3.26 (s). MS (m/z) calcd. for $C_{34}H_{48}P_2$: 519.3310 (M+H). Found: 519.3333 (FAB+, M+H).

Synthesis of [1,3-bis(2'-diisopropylphosphinophenyl)-5-tert-butyl-2-methoxybenzene]-rhodium(I) (carbonyl)chloride (23a).

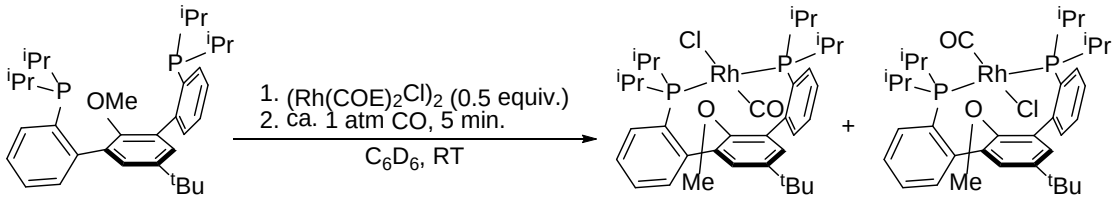

1a **23a**

In the glovebox, a 20 mL scintillation vial was charged with diphosphine **1a** (0.020 g, 0.036 mmol, 1.00 equiv.) as a solid and $(Rh(COE)_2Cl)_2$ (0.013 g, 0.018 mmol, 0.50 equiv.) as a solid. The vial was quickly charged with *ca.* 0.6 mL C_6D_6, the solution was transferred to a J. Young Tube, and the J. Young tube was brought out of the glovebox and frozen in a dry ice/acetone cold bath on the Schlenk line. The solution was

degassed via 3 freeze-pump-thaw cycles, then the reaction was placed under *ca.* 1 atm CO. Upon inverting the tube several times over the course of 5 min., a yellow solution of **23a** (mixture of isomers; 75%, major isomer; 25%, minor isomer; NMR yield: quantitative) was observed. ^{1}H NMR (300 MHz, C_6D_6) δ 7.51 (m, 4H, Ar-*H*, minor isomer), 7.42 (m, Ar-H_6, major isomer), 7.36 (m, Ar-H_9, major isomer), 7.24 (s, 2H, Ar-H_3), 7.19 (m, Ar-*H*), 7.12 (m, Ar-*H*), 3.49 (m, 2H, -C*H*$(CH_3)_2$), minor isomer), 3.07 (s, 3H, -OCH_3, major isomer), 3.02 (s, 3H, -OCH_3, minor isomer), 3.00 (m, 2H, -C*H*$(CH_3)_2$, major isomer), 2.44 (m, 2H, -C*H*$(CH_3)_2$, major isomer), 2.31 (m, 2H, -C*H*$(CH_3)_2$, minor isomer), 1.65 (m, 12H, -CH(CH_3)$_2$, minor isomer), 1.35 – 1.53 (m, -CH(CH_3)$_2$), 1.42 (s, 9H, -C(CH_3)$_3$, major isomer), 1.30 (s, 9H, -C(CH_3)$_3$, minor isomer), 1.23 – 1.32 (m, -CH(CH_3)$_2$), 1.02 – 1.07 (m, -CH(CH_3)$_2$). ^{13}C{^{1}H} NMR (101 MHz, C_6D_6) δ 187.91 (dt, Rh-*C*O, J_{RhC} = 72.72 Hz, J_{PC} = 16.9 Hz), 152.81 (s, Ar-C_1, minor isomer), 151.24 (s, Ar-C_1, major isomer), 146.73 (app t, Ar-*C*, J_{PC} = 7.6 Hz), 145.52 (m, Ar-*C*), 144.91 (s, Ar-C_4, major isomer), 143.91 (s, Ar-C_4, minor isomer), 135.84 (app t, Ar-*C*, J_{PC} = 21.2 Hz), 135.35 (app t, Ar-*C*, J_{PC} = 2.5 Hz), 134.10 (app t, Ar-*C*, J_{PC} = 16.2 Hz), 132.08 (s, Ar-*C*H), 131.69 – 131.91 (m, Ar-*C*H), 130.34 (s, Ar-*C*H), 129.43 (s, Ar-*C*H), 129.96 – 129.17 (m, Ar-C_3, major isomer), 127.02 (app t, Ar-*C*H, J_{PC} = 3.0 Hz), 126.60 (app t, Ar-*C*H, J_{PC} = 2.5 Hz), 34.50 (s, -*C*$(CH_3)_3$, major isomer), 34.30 (s, -*C*$(CH_3)_3$, minor isomer), 31.69 (s, -C(*C*H_3)$_3$, major isomer), 31.44 (s, -C(*C*H_3)$_3$, minor isomer), 29.53 (m, -C*H*$(CH_3)_2$), 26.63 – 27.08 (m, -C*H*$(CH_3)_2$), 21.38 (app t, -CH(*C*H_3)$_2$, J_{PC} = 2.0 Hz), 21.21 (s, -CH(*C*H_3)$_2$), 20.99 (app t, -CH(*C*H_3)$_2$, J_{PC} = 3.5 Hz), 20.43 (s, br, -CH(*C*H_3)$_2$), 20.24 (s, -CH(*C*H_3)$_2$), 20.18 (s, -CH(*C*H_3)$_2$), 19.41 (s, br, -CH(*C*H_3)$_2$). ^{31}P{^{1}H} NMR (121 MHz, C_6D_6) δ 39.73 (d, J_{RhP} = 127.1 Hz, minor isomer), 35.08 (d, J_{RhP} = 127.1 Hz, major isomer). ν_{CO} = 1957 cm^{-1} (solid, film).

Synthesis of [2,6-bis(2'-diisopropylphosphinophenyl)-4-tert-butyl-phenoxide]rhodium(I)carbonyl (24a).

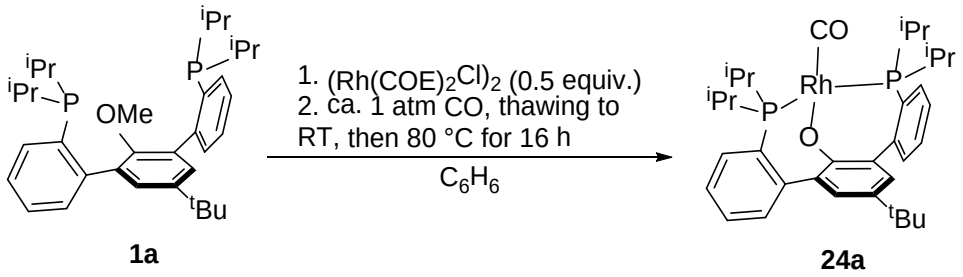

1a **24a**

Method A: In the glovebox, a 100 mL Schlenk tube fitted with a Teflon screw cap was charged with a stir bar and diphosphine **1a** (0.200 g, 0.364 mmol, 1.00 equiv.) as a solution in C_6H_6 (2 mL). This solution was frozen in a liquid N_2-chilled cold well. A layer of C_6H_6 was added to the Schlenk tube and frozen in the cold well. A slurry of $(Rh(COE)_2Cl)_2$ (0.131 g, 0.182 mmol, 0.50 equiv.) was added to the Schlenk tube and frozen in the cold well. The Schlenk tube was sealed, quickly removed from the glovebox, and placed in a dry ice/acetone cold bath. On the Schlenk line, the headspace of the Schlenk tube was evacuated and backfilled with 1 atm CO. The Schlenk tube was removed from the dry ice/acetone cold bath and allowed to thaw to room temperature over the course of 1 h with stirring. A yellow solution was observed. The Schlenk tube was then placed in an oil bath preheated to 80 °C and heated while stirring. After 16 h, the Schlenk tube was removed from the oil bath, brought into the glovebox, and the yellow C_6H_6 solution was filtered through Celite. Volatiles were removed under reduced pressure to afford **24a** (0.219 g, 0.330 mmol, 90.5 %) as a yellow powder. ^{1}H NMR (600 MHz, C_6D_6) δ 7.29 (s, 2H, Ar-*H*), 7.25 (m, 2H, Ar-*H*), 7.21 (m, 2H, Ar-*H*), 7.14 (t, 2H, Ar-*H*), 7.07 (t, 2H, Ar-*H*), 2.30 (s, br, 2H, -C*H*$(CH_3)_2$), 2.12 (sept, 2H, -C*H*$(CH_3)_2$), 1.48 (s, 9H, -C(C*H*$_3)_3$), 1.41 (m, 12H, -CH(C*H*$_3)_2$), 1.05 (dd, 6H, -CH(C*H*$_3)_2$), 0.75 (dd, 6H, -CH(C*H*$_3)_2$). ^{13}C{^{1}H} NMR (101

MHz, C_6D_6) δ 193.71 (dt, Rh-*C*O, J_{PC} = 16.9 Hz, J_{RhC} = 71.7 Hz), 149.86 (app t, Ar-C_5, J_{PC} = 8.1 Hz), 144.13 (s, Ar-C_1), 139.03 (s, Ar-C_4), 134.31 (s, Ar-C_2), 133.58 (app t, Ar-C_6, J_{PC} = 4.0 Hz), 131.73 (s, Ar-C_9), 130.62 (s, Ar-C_8), 129.01 (s, Ar-C_3), 125.49 (app t, Ar-C_7, J_{PC} = 2.5 Hz), 125.16 (app t, Ar-C_{10}, J_{PC} = 20.2 Hz), 34.29 (s, -*C*$(CH_3)_3$), 32.08 (s, -C(*C*$H_3)_3$), 27.54 (app t, -*C*H$(CH_3)_2$, J_{PC} = 12.6 Hz), 24.10 (app t, -*C*H$(CH_3)_2$, J_{PC} = 17.7 Hz), 19.88 (app t, -CH(*C*$H_3)_2$, J_{PC} = 4.0 Hz), 19.44 (app t, -CH(*C*$H_3)_2$, J_{PC} = 3.0 Hz), 19.27 (app t, -CH(*C*$H_3)_2$, J_{PC} = 3.0 Hz), 16.21 (s, -CH$(CH_3)_2$). $^{31}P\{^1H\}$ NMR (121 MHz, C_6D_6) δ 43.34 (d, J_{RhP} = 133.1 Hz). ν_{CO} = 1942 cm^{-1} (solid, film). Anal. calcd. for $C_{35}H_{47}O_2P_2Rh$ (%): C, 63.25; H, 7.13. Found: C, 63.08; H, 7.05.

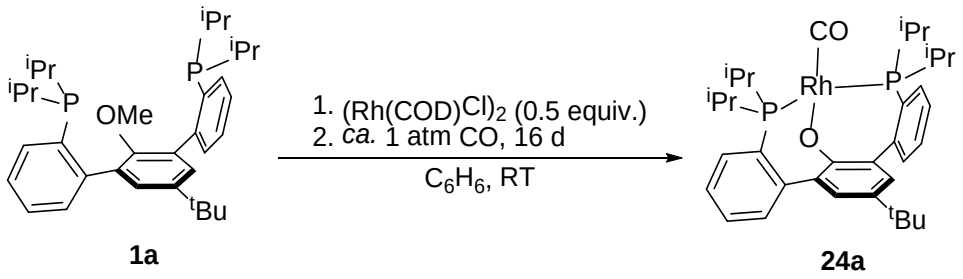

1a **24a**

Method B: In the glovebox, a 20 mL scintillation vial was charged with diphosphine **1a** (0.020 g, 0.036 mmol, 1.00 equiv.) and $(Rh(COD)Cl)_2$ (0.090 g, 0.018 mmol, 0.50 equiv.). C_6D_6 (ca. 0.6 mL) was added to afford a homogenous orange solution. This solution was transferred to a J. Young tube. The J. Young tube was capped and removed from the glovebox. On the Schlenk line, the J. Young Tube was degassed via three freeze-pump-thaw cycles using an ice water bath and ca. 1 atm CO was added. The tube was inverted ten times and left standing for 16 d. **24a** (NMR yield: quantitative) was observed as the only product by NMR.

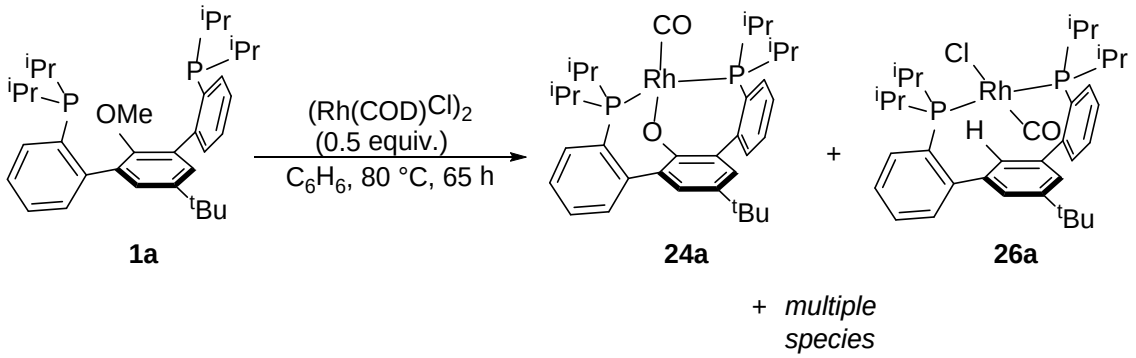

1a **24a** **26a**

Method C: In the glovebox, a 20 mL scintillation vial was charged with diphosphine **1a** (0.020 g, 0.036 mmol, 1.00 equiv) and $(Rh(COD)Cl)_2$ (0.090 g, 0.036 mmol, 0.50 equiv.). C_6D_6 (ca. 0.6 mL) was added to afford a homogenous orange solution. This solution was transferred to a J. Young tube. The J. Young tube was capped, removed from the glovebox, and placed in an oil bath pre-heated to 80 °C. After 65 h of heating, the tube was removed from the oil bath and a mixture of species (NMR Yield: **24a**, 32%; **26a**, 11%) was observed by NMR.

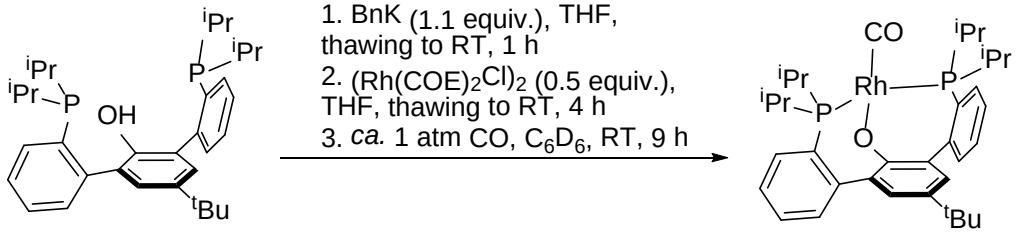

1f **24a**

Method D: In the glovebox, a 20 mL scintillation vial was charged with a magnetic stir bar, diphosphine **1f** (0.050 g, 0.094 mmol, 1.00 equiv.). and THF (2 mL). A pale yellow solution was observed. A separate vial was charged with BnK[43] (0.015 g, 0.112 mmol, 1.20 equiv.) and THF (1 mL). A red-orange solution was observed. Both vials were frozen in a liquid N_2-chilled cold well. The just-thawed solution of BnK was then added dropwise to a thawing solution of **1f** while stirring. At the start of addition, a red-orange color was observed with the addition of each drop but dissipated quickly.

Towards the end of the addition, the red-orange color persisted. A red-orange color was observed upon completion of the addition and the mixture was allowed to warm to room temperature while stirring over the course of 1 h. Volatiles were removed under reduced pressure to afford an orange residue. Hexanes (1 mL) was added, the residue was triturated, and volatiles were removed to afford an orange solid. This orange solid was extracted with three portions of C_6H_6 (1 mL), the portions of C_6H_6 were combined, and the C_6H_6 solution was filtered through Celite. Volatiles were removed under reduced pressure and an orange solid (0.041 g, 0.071 mmol) was observed. Again using a liquid N_2-chilled cold well, a just-thawed solution of this orange solid in THF (1 mL) was added to a thawing slurry of $(Rh(COE)Cl)_2$ (0.026 g, 0.036 mmol) in THF (1 mL) in a 20 mL scintillation vial charged with a magnetic stir bar. The mixture was allowed to warm to room temperature while stirring over the course of 4 h. Volatiles were removed under reduced pressure to afford an orange residue. Hexanes (1 mL) was added, the residue was titurated, volatiles were removed to afford an orange solid. This orange solid was extracted with C_6D_6 (1 mL). The C_6D_6 solution was filtered through Celite and transferred to a J. Young tube. The J. Young Tube was sealed and removed from the glovebox. On the Schlenk line, the solution was degassed via three freeze-pump-thaw cycles using a dry ice/acetone cooling bath and *ca.* 1 atm CO was added. The tube was inverted 10 times and left standing at room temperature. After 9 h, **24a** (NMR yield: quantitative) was observed by NMR.

Synthesis of 5-(tert-butyl)-1,3-diiodo-2-(methoxymethoxy)benzene.

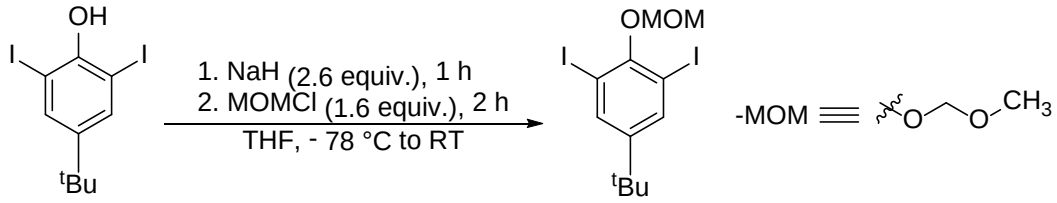

CAUTION: MOMCl is a known carcinogen. 5-(*tert*-butyl)-1,3-diiodo-2-(methoxymethoxy)benzene was synthesized using a modification of the procedure reported by Berliner and co-workers for the protection of phenols with chloromethyl methyl ether.[42] In the fume hood using Schlenk technique, a 500 mL round-bottom Schlenk flask was charged with NaH (3.000 g, 125.0 mmol, 2.6 equiv.), THF (200 mL), and a large stir bar. The flask was placed in a dry ice/acetone bath and cooled to -78 °C. With rapid stirring, a solution of 4-(*tert*-butyl)-2,6-diiodophenol[41] (19.300 g, 48.0 mmol, 1.0 equiv.) in dry THF (50 mL) was added dropwise via cannula. Bubbling was observed and the white slurry turned slightly yellow. Following the addition of 4-(tert-butyl)-2,6-diiodophenol, the flask was removed from the cold bath and allowed to stir at room temperature for 1 h. At this time, the reaction mixture was once again cooled to -78 °C and *ca.* 2.1 M MOMCl in toluene[42] (36 mL, 75.6 mmol, 1.6 equiv.) was added dropwise via syringe. Following the addition of MOMCl, the Schlenk flask was removed from the cold bath and stirred for 2 h at room temperature. Deionized H_2O was slowly added to the flask. Once the excess NaH was fully quenched, the reaction mixture was transferred to a separatory funnel and extracted with Et_2O (*ca.* 60 mL) three times. The combined organics were washed with brine and dried over $MgSO_4$. The volatiles were removed under reduced pressure affording 5-(*tert*-butyl)-1,3-diiodo-2-(methoxymethoxy)benzene as a light brown oil (21.000 g, 47.0 mmol,

98.0%). The crude 5-(*tert*-butyl)-1,3-diiodo-2-(methoxymethoxy)benzene was used in a Suzuki coupling with (2-bromophenyl)boronic acid without further purification. ^{1}H NMR (300 MHz, $CDCl_3$) δ 7.75 (s, 2H, Ar-*H*), 5.11 (s, 2H, -OC*H*$_2$OCH$_3$), 3.75 (s, 3H, -OCH$_2$OC*H*$_3$), 1.27 (s, 9H, -C(C*H*$_3$)$_3$). ^{13}C NMR (101 MHz, $CDCl_3$) δ 153.91 (s, Ar-*C*), 151.38 (s, Ar-*C*), 137.44 (s, Ar-*C*), 100.03 (s, -O*C*H$_2$OCH$_3$), 91.25 (s, Ar-*C*), 58.96 (s, -OCH$_2$O*C*H$_3$), 34.30 (s, -*C*(CH$_3$)$_3$), 31.29 (s, -C(*C*H$_3$)$_3$).

Synthesis of 1,3-bis(2'-bromophenyl)-5-tert-butyl-2-(methoxymethoxy)benzene.

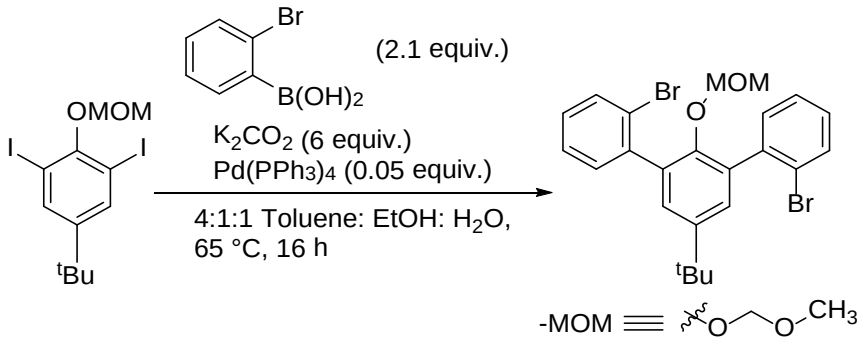

1,3-bis(2'-bromophenyl)-5-tert-butyl-2-(methoxymethoxy)benzene was synthesized using a modification of the procedure reported by Albrecht and co-workers for the Suzuki coupling of aryl halides with boronic acids.[48] In the fume hood, a large Schlenk tube fitted with a Teflon screw cap was charged with 5-(tert-butyl)-1,3-diiodo-2-(methoxymethoxy)benzene (10.600 g, 23.8 mmol, 1.00 equiv.), 2-bromophenylboronic acid (10.000 g, 49.8 mmol, 2.10 equiv.), K_2CO_3 (19.600 g, 141.8 mmol, 6.00 equiv.), toluene (540 mL), EtOH (130 mL), deionized H_2O (130 mL), and a stir bar. On the Schlenk line, the reaction mixture was degassed via three freeze-pump-thaw cycles. With N_2 backflow, $Pd(PPh_3)_4$ (1.37 g, 1.19 mmol, 0.05 equiv.) was added, providing a yellow biphasic solution. The reaction was stirred at 65 °C for 16 h at which time it was concentrated under reduced pressure to a total volume of *ca.* 100 mL. This mixture

was transferred to a separatory funnel and extracted with CH_2Cl_2 (*ca.* 100 mL) three times. The combined organics were washed with brine and dried over $MgSO_4$. The volatiles were removed under reduced pressure, providing a tacky red/brown oil. MeOH (*ca.* 30 mL) was added to the oil, which was then stirred at 60 °C, precipitating an orange powder. Collecting the solids via vacuum filtration and washing with methanol (*ca.* 3 mL x 3) provided 1,3-bis(2'-bromophenyl)-5-tert-butyl-2-(methoxymethoxy)benzene as a pale yellow solid (9.800 g, 19.4 mmol, 82.0%). 1,3-bis(2'-bromophenyl)-5-tert-butyl-2-(methoxymethoxy)benzene of this purity was used in a subsequent phosphination (via lithium-halogen exchange and dialkyl chlorophosphine quench) with acid workup and neutralization without further purification. ^{1}H NMR (300 MHz, $CDCl_3$) δ 7.69 (m, 2H, Ar-*H*), 7.52-7.45 (m, 2H, Ar-*H*), 7.37 (m, 2H, Ar-*H*), 7.31 (s, 2H, Ar-*H*), 7.21 (m, 2H, Ar-*H*), 4.35 (s, 2H, Ar-OC*H*$_2$OCH$_3$), 2.61 (s, 3H, Ar-OCH$_2$OC*H*$_3$), 1.36 (s, 9H, -C(C*H*$_3$)$_3$).

Synthesis of 2,6-bis(2'-diisopropylphosphinophenyl)-4-tert-butyl-phenol (1f).

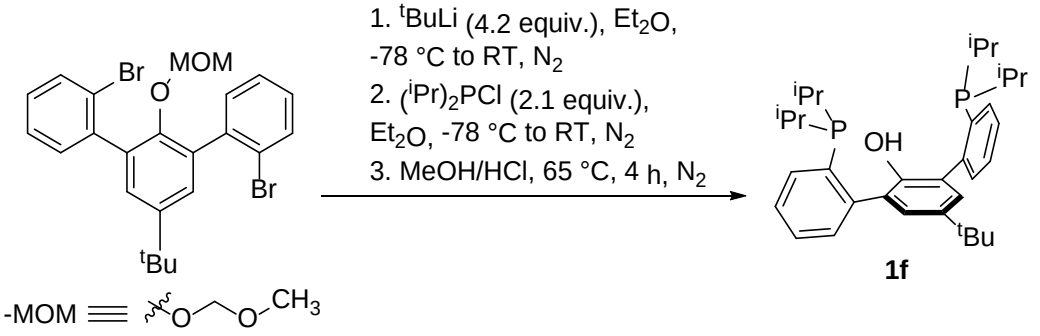

In the glovebox, a large Schlenk tube fitted with a Teflon screw cap was charged with 1,3-bis(2'-bromophenyl)-5-tert-butyl-2-(methoxymethoxy)benzene (12.0 g, 23.8 mmol) and a large stir bar. The Schlenk tube was sealed and removed from the glovebox. The pale yellow powder was dried under active vacuum (5-10 mm Hg) in an oil bath pre-

heated to 80 °C for 6 h. At this time, the flask was cooled to room temperature, and 250 mL of Et_2O was added via cannula, providing a pale yellow homogeneous solution. The flask was placed in a dry ice/acetone bath and cooled to -78 °C. With stirring, a solution of 1.7 M ^{t}BuLi in pentane (57.4 mL, 97.6 mmol) was added dropwise via syringe. The flask was allowed to warm to room temperature at which point it was left to stir for 1 h. Once more, the reaction was cooled to -78 °C and chlorodiisopropylphosphine (1.4 mL, 8.34 mmol) was added slowly via syringe. The flask was stirred at room temperature for 2 h, during which time an off-white precipitate formed. The volatiles were removed under reduced pressure. In an N_2 filled "wetbox" (no exclusion of water), concentrated aqueous HCl (20 mL) and methanol (80 mL) were added to the flask. The resulting mixture was heated to 65 °C for 4 h, providing a homogenous orange solution. Volatiles were once more removed under reduced pressure. In the "wetbox," the resulting orange residue was taken up in CH_2Cl_2 (200 mL) and washed with saturated aqueous solutions of K_2CO_3 (100 mL x 3) and NH_4Cl (100 mL x 3). The volatiles were removed under reduced pressure and the resulting orange oil was triturated with methanol (150 mL), precipitating an off-white solid. The solid was collected via vacuum filtration, yielding **1f** (8.4 g, 15.6 mmol, 66 %) as a mixture of interconverting atropisomers. ^{1}H NMR (400 MHz, C_6D_6, 25 °C) δ 7.57-7.32 (m, 6H, Ar-*H*), 7.20-7.09 (m, 4H, Ar-*H*), 5.79 & 5.05 (s, 1H, -O*H*), 2.11-1.80 (m, 4H, -C*H*(CH_3)$_2$), 1.37 (s, 9H, -C(C*H*$_3$)$_3$), 1.18-0.85 (m, 24H, -CH(C*H*$_3$)$_2$). ^{1}H NMR (400 MHz, C_6D_6, 70 °C) δ 7.50-7.38 (m, 4H, Ar-*H*), 7.33 (s, 2H, Ar-*H*), 7.21-7.10 (m, 4H, Ar-*H*), 5.18 (s, br, 1H, -O*H*), 1.97 (s, br, 4H, -C*H*(CH_3)$_2$), 1.38 (s, 9H, -C(C*H*$_3$)$_3$), 0.79-1.19 (m, 24H, -CH(C*H*$_3$)$_2$). ^{13}C{^{1}H} NMR (101 MHz, C_6D_6, 70 °C) δ 147.80 (s, Ar-*C*), 141.73 (s, Ar-*C*), 137.04 (m, Ar-*C*), 132.70 (s, Ar-*C*), 131.82 (s, Ar-

C), 130.76 (s, br, Ar-*C*), 129.42 (s, Ar-*C*), 127.10 (s, Ar-*C*), 34.34 (s, -*C*(CH_3)$_3$), 31.87 (s, -C(*C*H_3)$_3$), 26.66-23.51 (s, br, -*C*H(CH_3)$_2$), 21.26-19.48 (m, -CH(*C*H_3)$_2$). $^{31}P\{^1H\}$ NMR (121 MHz, C_6D_6, 25 °C) δ -1.04 (s, br). $^{31}P\{^1H\}$ NMR (162 MHz, C_6D_6, 25 °C, referenced to solvent residual) δ -1.54, -1.63. $^{31}P\{^1H\}$ NMR (162 MHz, C_6D_6, 70 °C, referenced to solvent residual) δ 0.04. MS (m/z) calcd. for $C_{34}H_{48}OP_2$: 535.3259 (M+H). Found: 535.3263 (FAB+, M+H).

Synthesis of [1,3-bis(2'-diisopropylphosphinophenyl)-5-tert-butyl-benzene]rhodium(I)-(carbonyl) chloride (26a).

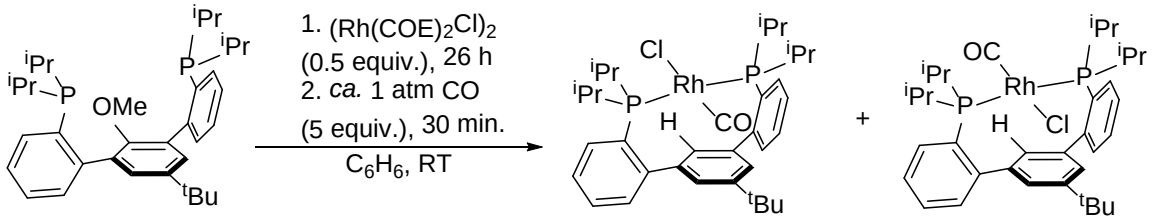

1a **26a**

Method A: In the glovebox, a 20 mL scintillation vial was charged with a magnetic stir bar and (Rh(COE)$_2$Cl)$_2$ (0.165 g, 0.230 mmol, 0.50 equiv.) as a slurry in C_6H_6 (4 mL). Diphosphine **1a** (0.252 g, 0.460 mmol, 1.00 equiv.) was added as a solution in C_6H_6 (1 mL) and the solution was stirred. After 10 min., a dark purple solution was observed. After 26 h, the solution was transferred to a 20 mL Schlenk flask fitted with a Teflon screw cap. The Schenk flask was removed from the glovebox. On the Schlenk line, the solution was frozen in a dry ice/acetone cooling bath, placed under reduced pressure and thawed. The solution was further degassed with two additional freeze-pump-thaw cycles. The reaction mixture was then placed under an atmosphere of CO and stirred for 30 min. A color change to yellow was observed. The Schlenk flask was brought back into the glovebox and the reaction mixture was filtered through Celite. A yellow residue was observed. This yellow residue was washed with three portions of pentane

(*ca.* 1 mL each) and three portions of hexanes (*ca.* 1 mL each). The residue was then extracted with three portions of Et_2O (*ca.* 1 mL each) and three portions of C_6H_6 (*ca.* 1 mL each). The Et_2O and C_6H_6 solutions were combined and volatiles were removed under reduced pressure to afford **26a** (0.185 g, 0.270 mmol, 58.6% yield) as a yellow powder. Crystals suitable for X-ray diffraction were grown from a saturated pentane solution of **26a** at -35 °C. ^{1}H NMR (300 MHz, C_6D_6) δ 8.82 (m, 1H, Ar-*H*$_1$), 7.42 (m, 2H, Ar-*H*$_6$), 7.25 (m, 2H, Ar-*H*$_9$), 7.23 (d, 2H Ar-*H*$_3$, J_{HH} = 3.0 Hz), 7.09 (m, 4H, Ar-*H*$_7$ & Ar-*H*$_8$), 2.97 (m, 2H, -C*H*(CH$_3$)$_2$), 2.15 (m, 2H, -C*H*(CH$_3$)$_2$), 1.81 (dd, 6H, -CH(C*H*$_3$)$_2$), 1.50 (dd, 6H, -CH(C*H*$_3$)$_2$), 1.34 (s, 9H, -C(C*H*$_3$)$_3$), 1.01 (dd, 6H, -CH(C*H*$_3$)$_2$), 0.92 (dd, 6H, -CH(C*H*$_3$)$_2$). ^{13}C{^{1}H} NMR (101 MHz, C_6D_6) δ 188.67 (dt, Rh-*C*O, J_{RhC} = 77.8 Hz, J_{PC} = 14.6 Hz), 149.03 (s, Ar-*C*$_4$), 148.73 (app t, Ar-*C*$_2$, J_{PC} = 7.1 Hz), 142.88 (app t, Ar-*C*$_{10}$, J_{PC} = 2.5 Hz), 133.13 (app t, Ar-*C*$_5$, J_{PC} = 17.7 Hz), 132.54 (s, br, Ar-*C*$_6$), 131.89 (app t, Ar-*C*$_7$, J_{PC} = 3.5 Hz), 129.53 (s, br, Ar-*C*$_8$), 126.80 (m, Ar-*C*$_7$), 126.47 (s, Ar-*H*$_3$), 124.70 (s, Ar-*C*$_1$), 34.77 (s, -*C*(CH$_3$)$_3$), 31.56 (s, -C(*C*H$_3$)$_3$), 29.52 (m, -*C*H(CH$_3$)$_2$), 25.97 (app t, -*C*H(CH$_3$)$_2$, J_{PC} = 12.1 Hz), 22.69 (app t, -CH(*C*H$_3$)$_2$, J_{PC} = 2.0 Hz), 20.70 (app t, -CH(*C*H$_3$)$_2$, J_{PC} = 2.5 Hz), 20.32 (m, -CH(*C*H$_3$)$_2$, 18.25 (s, br, -CH(*C*H$_3$)$_2$). ^{31}P{^{1}H} NMR (121 MHz, C_6D_6) δ 38.71 (d, J_{RhP} = 123.4 Hz). ν_{CO} = 1945 cm^{-1} (solid, film).

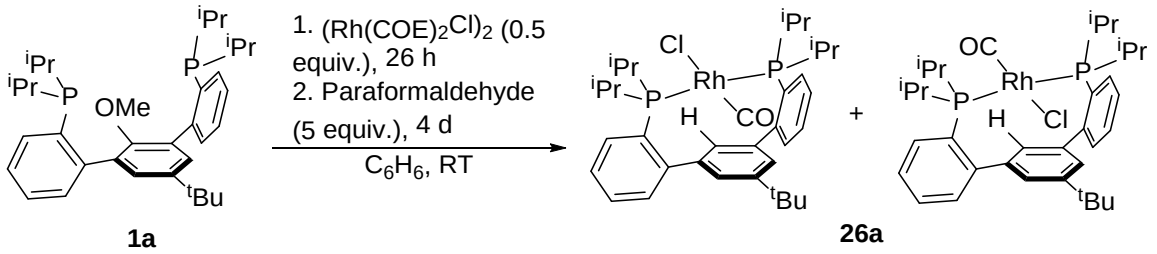

1a **26a**

Method B: In the glovebox, a 20 mL Schlenk flask was charged with a magnetic stir bar and $(Rh(COE)_2Cl)_2$ (0.100 g, 0.091 mmol, 0.50 equiv.) as a slurry in C_6H_6 (2 mL). Diphosphine **1a** (0.100 g, 0.182 mmol, 1.00 equiv.) was added as a solution in C_6H_6 (1 mL) and the solution was stirred. After 10 min., a dark purple solution was observed. After 26 h, volatiles were removed under reduced pressure to afford a purple powder. To 0.020 mg of this powder, paraformaldehyde (0.005 g, 0.152 mmol, 5.00 equiv.) was added and the mixture was stirred for 4 d. After 4 d, volatiles were removed under reduced pressure and the resulting red residue dissolved in C_6D_6. **26a** (NMR yield: **26a**, 48%) was observed in a mixture of species by NMR.

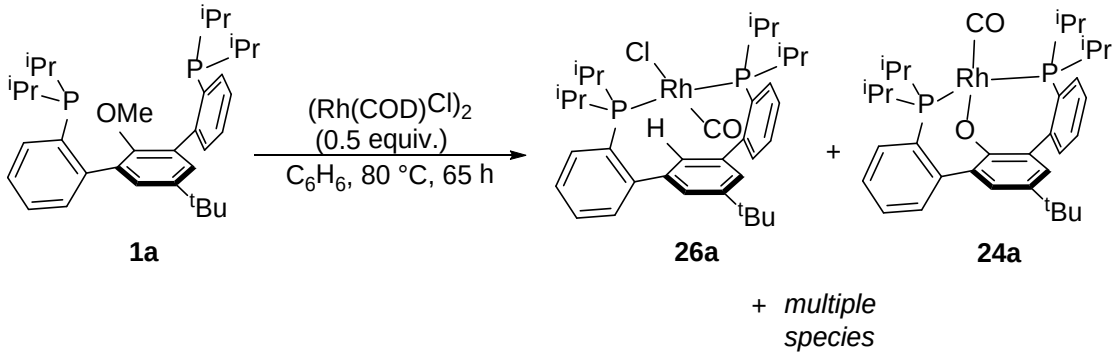

1a **26a** **24a**

Method C: In the glovebox, a 20 mL scintillation vial was charged with diphosphine **1a** (0.020 g, 0.018 mmol, 1.00 equiv) and $(Rh(COD)Cl)_2$ (0.090 g, 0.018 mmol, 0.50 equiv.). C_6D_6 (ca. 0.6 mL) was added to afford a homogenous orange solution. This solution was transferred to a J. Young tube. The J. Young tube was capped, removed from the glovebox, and placed in an oil bath pre-heated to 80 °C. After 65 h of

heating, the tube was removed from the oil bath and a mixture of species (NMR Yield: **24a**, 32%; **26a**, 11%) was observed by NMR.

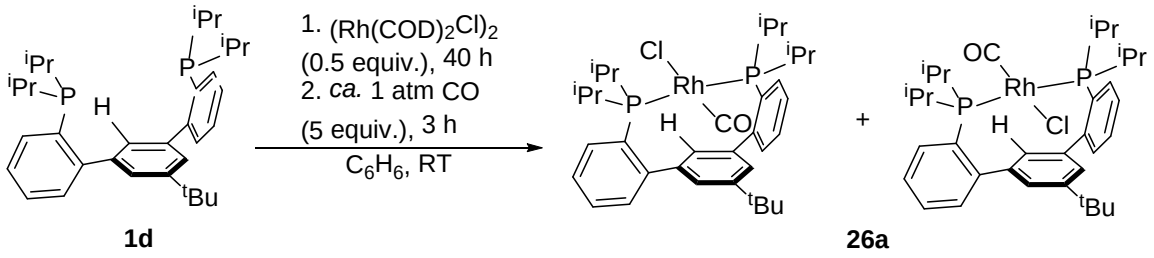

Method D: In the glovebox, a 20 mL scintillation vial was charged with a magnetic stir bar and $(Rh(COD)_2Cl)_2$ (0.048 g, 0.096 mmol, 0.5 equiv.) as an orange solution in C_6H_6 (1 mL). Diphosphine **1d** (0.100 g, 0.193 mmol, 1.0 equiv.) was added as a solution in C_6H_6 (2 mL) and the solution was stirred. An orange homogenous solution was observed upon addition. After 40 h, the solution was transferred to a 20 mL Schlenk flask fitted with a Teflon screw cap. The Schlenk flask was removed from the glovebox. On the Schlenk line, the solution was frozen in a dry ice/acetone cooling bath, placed under reduced pressure, and thawed. The reaction mixture was then placed under an atmosphere of CO and stirred for 3 h. A color change to yellow was observed. The Schlenk flask was placed under reduced pressure, brought back into the glovebox, and the reaction mixture was filtered through Celite. Volatiles were removed under reduced pressure to afford a yellow powder. This powder was washed with three portions of pentane (*ca.* 1 mL) and three portions of Et_2O (*ca.* 1 mL each). This powder was dissolved in C_6H_6 (2 mL), filtered through Celite, and volatiles were removed under reduced pressure to afford **26a** (0.049 g, 0.071 mmol, 36.9 % yield) as yellow powder. Anal. calcd. for $C_{35}H_{48}ClOP_2Rh$ (%): C, 61.36 ; H, 7.06. Found: C, 60.14; H, 6.89. Low in carbon despite multiple analyses.

Synthesis of [1,3-bis(2'-diisopropylphosphinophenyl)-5-tert-butyl-2-methoxybenzene]-iridium(I)(1,5-cyclooctadiene)chloride (27a).

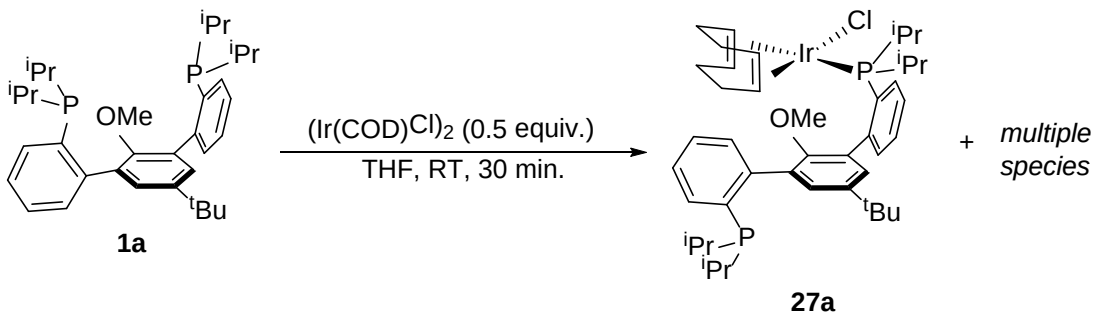

In the glovebox, a 20 mL scintillation vial was charged with $(Ir(COD)Cl)_2$ (0.012 g, 0.023 mmol, 0.50 equiv.), THF (2 mL), and a magnetic stir bar. Diphosphine **1a** (0.025 g, 0.046 mmol, 1.00 equiv.) was added as a solution in THF (1 mL). After 5 min., an orange solution was observed. After 30 min., volatiles were removed under reduced pressure to afford a gummy orange solid (mixture of species; NMR yield: **27a**, 72%). ^{1}H NMR (300 MHz, C_6D_6) δ 7.92 (m, 1H, Ar-*H*), 7.42 (m, 1H, Ar-*H*), 7.34 (m, 1H, Ar-*H*), 7.30 (m, 1H, Ar-*H*), 7.28 (m, 1H, Ar-*H*), 7.25 – 7.18 (m, 2H, Ar-*H*), 7.03 (m, 1H, Ar-*H*), 6.93 (m, 2H, Ar-*H*), 5.31 (s, br, 4H, COD, -C*H*), 3.36 (m, 2H, COD, -C*H*$_2$), 3.22 (m, 4H, COD, -C*H*$_2$), 3.04 (m, 2H, COD, -C*H*$_2$), 2.90 (s, 3H, -OC*H*$_3$), 2.36 (m, 1H, -C*H*$(CH_3)_2$), 2.10 (m, 2H, -C*H*$(CH_3)_2$), 1.88 (m, 1H, -C*H*$(CH_3)_2$), 1.70 – 1.54 (m, 6H, -CH(C*H*$_3)_2$), 1.52 – 1.39 (m, 3H, -CH(C*H*$_3)_2$), 1.26 (s, 9H, -C(C*H*$_3)_3$), 1.15 – 1.07 (m, 3H, -CH(C*H*$_3)_2$), 1.06 -0.92 (m, 6H, -CH(C*H*$_3)_2$), 0.85 – 0.76 (m, 3H, -CH(C*H*$_3)_2$). ^{13}C{^{1}H} NMR (101 MHz, C_6D_6) δ 152.05 (s, Ar-*C*), 147.93 (d, Ar-*C*, J_{PC} = 32.3 Hz), 144.41 (d, Ar-*C*, J_{PC} = 23.2 Hz), 136.78 (d, Ar-*C*, J_{PC} = 6.1 Hz), 136.42 – 135.82 (m, Ar-*C*), 133.35 (d, Ar-*C*H, J_{PC} = 5.1 Hz), 132.75 (d, Ar-*C*H, J_{PC} = 4.0 Hz), 131.16 (d, Ar-*C*H, J_{PC} = 6.1 Hz), 130.02 (s, Ar-*C*H), 129.09 (detected by HSQC, obscured by solvent residual, Ar-*C*H), 128.96 (detected by HSQC, obscured by

solvent residual, Ar-*C*H), 128.84 (s, Ar-*C*H), 127.00 (s, Ar-*C*H), 126.73 (s, Ar-*C*), 126.45 (s, Ar-*C*), 124.93 (d, Ar-*C*H, J_{PC} = 11.1 Hz), 90.00 (d, COD, -*C*H, J_{PC} = 13.1 Hz), 89.56 (d, COD, -*C*H, J_{PC} = 15.2 Hz), 59.79 (s, -O*C*H_3), 54.60 (s, COD, -*C*H_2), 52.64 (s, COD, -*C*H_2), 34.86 (d, -*C*H(CH_3)$_2$, J_{PC} = 4.0 Hz), 34.36 (s, -*C*(CH_3)$_3$), 32.11 (d, -*C*H(CH_3)$_2$, J_{PC} = 3.0 Hz), 31.40 (s, -C(*C*H_3)$_3$), 30.63 (d, -*C*H(CH_3)$_2$, J_{PC} = 2.0 Hz), 23.84 (d, -CH(*C*H_3)$_2$, J_{PC} = 7.1 Hz), 22.01 (m, -CH(*C*H_3)$_2$), 21.19 – 20.10 (m, -CH(*C*H_3)$_2$), 19.96 (s, -CH(*C*H_3)$_2$), 19.77 (d, -CH(*C*H_3)$_2$, J_{PC} = 5.1 Hz), 18.61 (m, -CH(*C*H_3)$_2$), 17.75 (s, br, -CH(*C*H_3)$_2$). $^{31}P\{^1H\}$ NMR (121 MHz, C_6D_6) δ 47.37 (s), -4.01 (s). ^1H NMR (400 MHz, CD_2Cl_2) δ 7.71 (m, 1H, Ar-*H*), 7.56 (m, 1H, Ar-*H*), 7.44 – 7.23 (m, 5H, Ar-*H*), 7.20 – 7.05 (m, 3H, Ar-*H*), 4.71 (m, 4H, COD, -C*H*$_2$), 3.05 – 2.81 (m, 10H, COD, -C*H*), 2.95 (s, 3H, -OC*H*$_3$), 2.11 (m, 1H, -C*H*(CH_3)$_2$), 1.88 (m, 1H, -C*H*(CH_3)$_2$), 1.68 (m, 1H, -C*H*(CH_3)$_2$), 1.50 (m, 1H, -C*H*(CH_3)$_2$), 1.43 – 1.03 (m, 5H, -CH(C*H*$_3$)$_2$), 1.29 (s, 9H, -C(C*H*$_3$)$_3$), 0.96 – 0.72 (m, 3H, -CH(C*H*$_3$)$_2$. $^{13}C\{^1H\}$ NMR (101 MHz, CD_2Cl_2) δ 151.96 (s, Ar-*C*$_1$), 147.86 (d, Ar-*C*, J_{PC} = 33.3 Hz), 144.52 (d, Ar-*C*, J_{PC} = 2.0 Hz), 144.01 (d, Ar-*C*, J_{PC} = 14.1 Hz), 136.66 (d, Ar-*C*, J_{PC} = 6.1 Hz), 136.26 (d, Ar-*C*H, J_{PC} = 17.2 Hz), 136.12 (d, Ar-*C*H, J_{PC} = 11.1 Hz), 133.60 (d, Ar-*C*H, J_{PC} = 6.1 Hz), 135.53 (d, Ar-*C*, 1.0 Hz), 132.76 (d, Ar-*C*H, J_{PC} = 4.0 Hz), 131.35 (d, Ar-*C*H, J_{PC} = 6.1 Hz), 130.21 (s, Ar-*C*H), 128.44 (m, Ar-*C*H), 128.16 (m, Ar-*C*H), 126.98 (s, Ar-*C*H), 126.04 (d, Ar-*C*, J_{PC} = 31.3 Hz), 125.01 (s, Ar-*C*H), 89.63 (d, COD, -*C*H, J_{PC} = 12.1 Hz), 88.60 (d, COD, -*C*H, J_{PC} = 15.1 Hz), 59.93 (s, -O*C*H_3), 55.77 (s, COD, -*C*H), 53.22 (detected by HSQC, obscured by solvent residual, COD, -*C*H), 34.55 (s, -*C*(CH_3)$_3$), 34.33 (d, -C*H*(CH_3)$_2$, J_{PC} = 4.0 Hz), 32.19 (d, -C*H*(CH_3)$_2$, J_{PC} = 2.0 Hz), 31.46 (s, -C(*C*H_3)$_3$), 30.20 (d, -C*H*(CH_3)$_2$, J_{PC} = 2.0 Hz), 28.71 (d, -C*H*(CH_3)$_2$, J_{PC} = 1.0 Hz), 23.62 (d, -CH(*C*H_3)$_2$, J_{PC} = 7.1 Hz), 23.01 (d, -CH(*C*H_3)$_2$, J_{PC} = 14.1 Hz), 21.66 (d, -CH(*C*H_3)$_2$, J_{PC} = 2.0 Hz),

20.98 (d, -CH(CH_3)$_2$, J_{PC} = 17.2 Hz), 20.56 – 20.09 (m, -CH(CH_3)$_2$), 18.65 (m, -CH(CH_3)$_2$), 17.80 (d, -CH(CH_3)$_2$, J_{PC} = 2.0 Hz). $^{31}P\{^1H\}$ NMR (121 MHz, CD_2Cl_2) δ 46.84 (s), -3.99 (s).

Synthesis of [2,6-bis(2'-diisopropylphosphinophenyl)-4-tert-butyl-phenoxide]-iridium(I)carbonyl (28a).

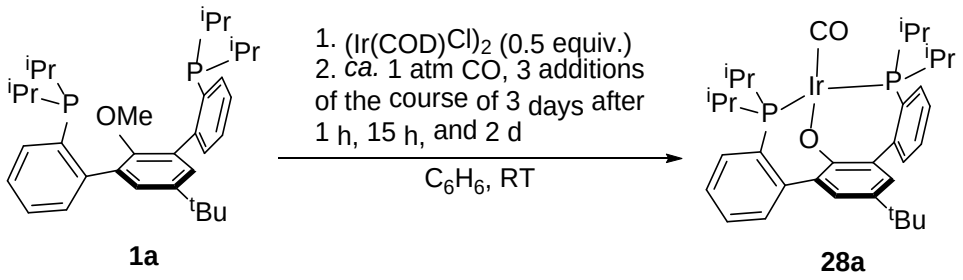

1a **28a**

Method A: In the glovebox, a 100 mL Schlenk tube fitted with a Teflon screw cap was charged with a stir bar, diphosphine **1a** (0.250 g, 0.456 mmol, 1.00 equiv.) as a solution in C_6H_6 (2 mL) and $(Ir(COD)Cl)_2$ (0.153 g, 0.228 mmol, 0.50 equiv.) as a solution in C_6H_6 (4 mL). An orange solution was observed. The Schlenk tube was sealed and removed from the glovebox. On the Schlenk line, the solution was degassed via three freeze-pump-thaw cycles using a dry ice/acetone cooling bath and *ca.* 1 atm CO was added. After 5 min., a yellow solution was observed. The mixture was stirred for 1 h. After 1 h, the solution was frozen using a dry ice/acetone cooling bath, the headspace was evacuated on the Schlenk line, and the headspace was backfilled with *ca.* 1 atm CO. The mixture was stirred for an additional 15 h. The solution was then frozen using a dry ice/atone cooling bath, the headspace was evacuated on the Schlenk line, and the headspace was backfilled with *ca.* 1 atm CO. The mixture was stirred for an additional 2 d. The reaction vessel was then brought back in the glovebox. The C_6H_6 solution was filtered through Celite and volatiles were removed under reduced pressure. A yellow-orange powder was observed. Diffusion of

Et_2O into a saturated C_6H_6 solution of this yellow-orange powder afforded yellow crystals of **28a** (0.043 g, 0.058 mmol, 12.6%). ^1H NMR (400 MHz, C_6D_6) δ 7.25 (s, 2H, Ar-*H*$_3$), 7.20 (m, 4H, Ar-*H*$_6$ & Ar-*H*$_9$), 7.12 (m, 4H, Ar-*H*$_7$ & Ar-*H*$_8$), 2.42 (m, 2H, -C*H*$(CH_3)_2$), 2.31 (m, 2H, -C*H*$(CH_3)_2$), 1.41 (s, 9H, -C(C*H*$_3)_3$), 1.39 (m, 12H, -CH(C*H*$_3)_2$), 1.05 (dd, 6H, -CH(C*H*$_3)_2$), 0.74 (dd, 6H, -CH(C*H*$_3)_2$). $^{13}C\{^1H\}$ NMR (101 MHz, C_6D_6) δ 176.97 (t Ir-*C*O, J_{PC} = 11.1 Hz), 149.29 (app t, Ar-*C*$_5$, J_{PC} = 6.6 Hz), 141.89 (t, Ar-*C*$_1$, J_{PC} = 1.0 Hz), 139.50 (s, Ar-*C*$_4$), 134.44 (s, Ar-*C*$_2$), 133.61 (app t, Ar-*C*$_6$, J_{PC} = 4.0 Hz), 132.24 (app t, Ar-*C*$_9$, J_{PC} = 2.0 Hz), 130.58 (app t, Ar-*C*$_7$ or Ar-*C*$_8$, J_{PC} = 1.0 Hz), 129.30 (s, Ar-*C*$_3$), 125.77 (app t, Ar-*C*$_7$ or Ar-*C*$_8$, J_{PC} = 3.0 Hz), 123.81 (app t, Ar-*C*$_{10}$, J_{PC} = 22.7 Hz), 34.48 (s, -*C*$(CH_3)_3$), 31.88 (s, -C(*C*$H_3)_3$), 28.06 (app t, -*C*$H(CH_3)_2$, J_{PC} = 16.2 Hz), 25.29 (app t, -*C*$H(CH_3)_2$, J_{PC} = 15.2 Hz), 19.71 (app t, -CH(*C*$H_3)_2$, J_{PC} = 1.5 Hz), 19.36 (app t, -CH(*C*$H_3)_2$, J_{PC} = 2.0 Hz), 18.93 (app t, -CH(*C*$H_3)_2$, J_{PC} = 2.0 Hz), 16.41 (app t, -CH(*C*$H_3)_2$, J_{PC} = 3.0 Hz). $^{31}P\{^1H\}$ NMR (121 MHz, C_6D_6) δ 38.57 (s). ν_{CO} = 1929 cm^{-1} (solid, powder). Anal. calcd. for $C_{35}H_{47}IrO_2P_2$ (%): C, 55.76; H, 6.28. Found: C, 55.63; H, 5.99.

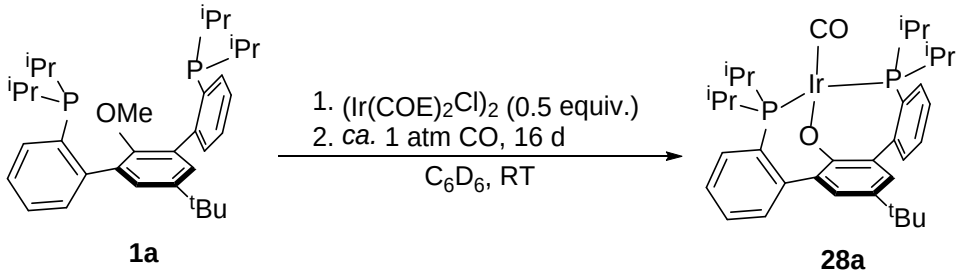

1a **28a**

Method B: In the glovebox, a 20 mL scintillation vial was charged with diphosphine **1a** (0.020 g, 0.036 mmol, 1.00 equiv.) and $(Ir(COE)_2Cl)_2$ (0.016 g, 0.018 mmol, 0.50 equiv.). C_6D_6 (ca. 0.6 mL) was added to afford a homogenous orange solution. This solution was transferred to a J. Young tube. The J. Young tube was capped and

removed from the glovebox. On the Schlenk line, the J. Young Tube was degassed via three freeze-pump-thaw cycles using a dry ice/acetone bath and *ca.* 1 atm CO was added. The tube was inverted ten times and left standing for 16 d. A mixture of species (NMR yield: **28a**, 91%) was observed by NMR.

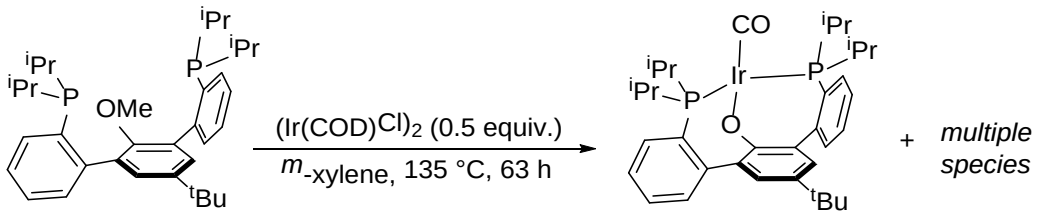

1a **28a**

Method C: In the glovebox, a 20 mL scintillation vial was charged with diphosphine **1a** (0.020 g, 0.036 mmol, 1.00 equiv) and $(Ir(COD)Cl)_2$ (0.012 g, 0.018 mmol, 0.50 equiv.). *m*-Xylene (*ca.* 0.6 mL) was added to afford a homogenous orange solution. This solution was transferred to a J. Young tube. The J. Young tube was capped, removed from the glovebox, and placed in an oil bath pre-heated to 135 °C. After 63 h of heating, the tube was removed from the oil bath and a mixture of species (NMR Yield: **28a**, 48%) was observed by NMR.

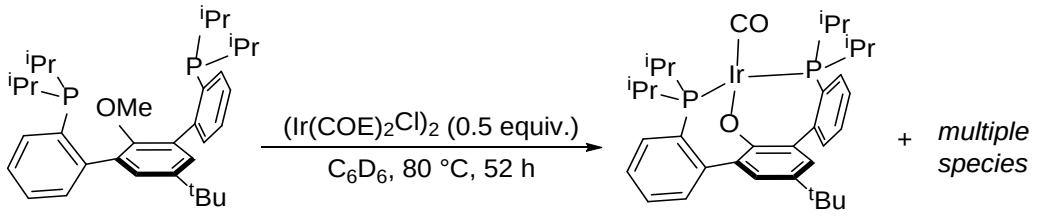

1a **28a**

Method D: In the glovebox, a 20 mL scintillation vial was charged with diphosphine **1a** (0.020 g, 0.036 mmol, 1.00 equiv) and $(Ir(COE)_2Cl)_2$ (0.016 g, 0.018 mmol, 0.50 equiv.). C_6D_6 (*ca.* 0.6 mL) was added to afford a homogenous orange solution. This solution was transferred to a J. Young tube. The J. Young tube was capped, removed

from the glovebox, and placed in an oil bath pre-heated to 80 °C. After 52 h of heating, the tube was removed from the oil bath and a mixture of species (NMR Yield: **28a**, 17%) was observed by NMR.

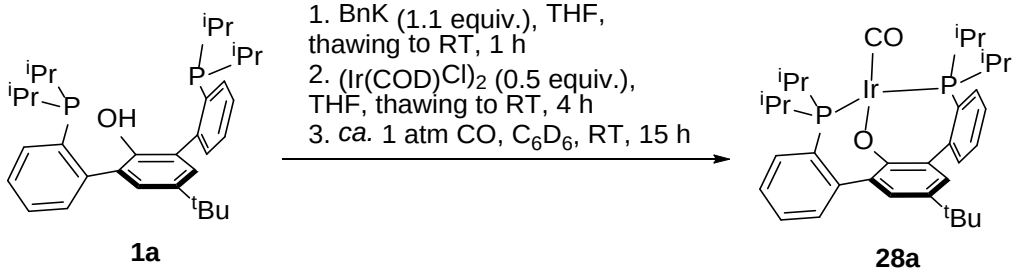

Method E: In the glovebox, a 20 mL scintillation vial was charged with a magnetic stir bar, diphosphine **1c** (0.060 g, 0.112 mmol, 1.00 equiv.). and THF (2 mL). A pale yellow solution was observed. A separate vial was charged with BnK[43] (0.015 g, 0.112 mmol, 1.10 equiv.) and THF (1 mL). A red-orange solution was observed. Both vials were frozen in a liquid N_2-chilled cold well. The just-thawed solution of BnK was then added dropwise to a thawing solution of **1c** while stirring. At the start of addition, a red-orange color was observed with the addition of each drop but dissipated quickly. Towards the end of the addition, the red-orange color persisted. A red-orange color was observed upon completion of the addition and the mixture was allowed to warm to room temperature while stirring over the course of 1 h. Volatiles were removed under reduced pressure to afford an orange residue. Hexanes (1 mL) was added, the residue was triturated, and volatiles were removed to afford an orange solid. This orange solid was extracted with three portions of C_6H_6 (1 mL), the portions of C_6H_6 were combined, and the C_6H_6 solution was filtered through Celite. Volatiles were removed under reduced pressure and an orange solid was observed. Again using a liquid N_2-chilled cold well, a just-thawed solution of this orange solid (0.056 g, 0.098) in THF (1 mL)

was added to a thawing slurry of $(Ir(COD)_2Cl)_2$ (0.036 g, 0.054 mmol, 0.50 equiv.) in THF (1 mL) in a 20 mL scintillation vial charged with a magnetic stir bar. The mixture was allowed to warm to room temperature while stirring over the course of 4 h. Volatiles were removed under reduced pressure to afford an orange residue. Hexanes (1 mL) was added, the residue was triturated, and volatiles were removed to afford an orange solid. A portion of this orange solid (0.008 g) was extracted with C_6D_6 (1 mL). The C_6D_6 solution was filtered through Celite and transferred to a J. Young tube. The J. Young Tube was sealed and removed from the glovebox. On the Schlenk line, the solution was degassed via three freeze-pump-thaw cycles using a dry ice/acetone cooling bath and ca. 1 atm CO was added. The tube was inverted 10 times and left standing at room temperature. After 15 h, **28a** (NMR yield: quantitative) was observed by NMR.

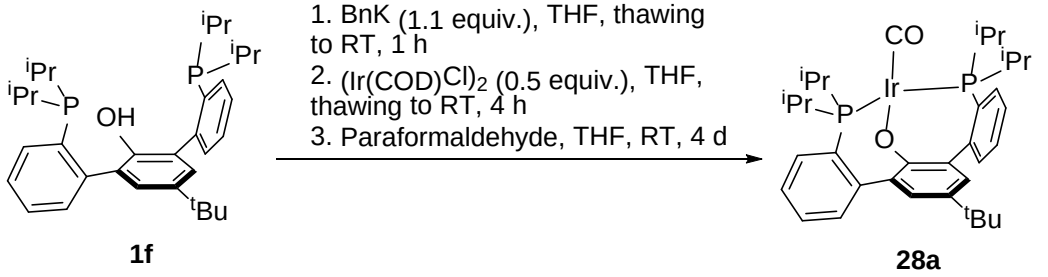

1f **28a**

Method F: The above procedure (*Method E* for preparation of **28a**) was followed until the addition of the product of diphosphine **1c** and BnK[43] to a solution of $(Ir(COD)Cl)_2$. Volatiles were removed to afford an orange residue. Hexanes (1 mL) was added, the residue was triturated, and volatiles were removed to afford an orange solid. The orange solid was extracted with three portions of C_6H_6 (1 mL), the portions of C_6H_6 were combined, and the C_6H_6 solution was filtered through Celite. Volatiles were removed under reduced pressure and an orange solid was observed. A portion of

this orange solid (0.034 g) was dissolved in THF (2 mL) and transferred to a 20 mL scintillation vial charged with a stir bar and a slurry of paraformaldehyde (0.001 g, 0.044 mmol, 1.10 equiv.) in THF (1 mL). The mixture was stirred at ambient temperature. After 4 d, a yellow solution was observed and **28a** (NMR yield: quantitative) was observed by NMR.

Synthesis of [1,3-bis(2'-diisopropylphosphinophenyl)-5-tert-butyl-2-methoxybenzene]-iridium(I)(carbonyl)chloride (29a).

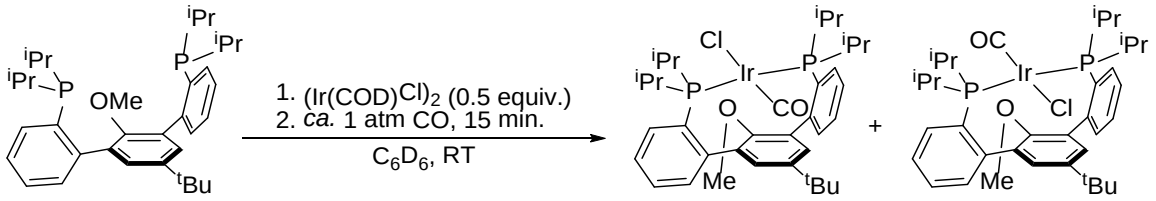

1a **29a**

In the glovebox, a 20 mL scintillation vial was charged with diphosphine **1a** (0.020 g, 0.036 mmol, 1.00 equiv.) and $(Ir(COD)Cl)_2$ (0.012 g, 0.018 mmol, 0.50 equiv.) as solids. To this vial was added C_6D_6 (ca. 0.6 mL). The solids were dissolved to afford an orange solution. This solution was transferred to a J. Young Tube. The tube was sealed and removed from the glovebox. On the Schlenk line, the solution was degassed via three freeze-pump-thaw cycles using an ice water bath then placed under *ca.* 1 atm CO. The J. Young Tube was inverted 5 times and a color change to a yellow solution was observed. The J. Young Tube was inverted a total of 10 times after addition of CO and left standing at 15 min. to afford a yellow solution of **29a** (mixture of species; NMR yield: **29a**, major isomer, 66%; **29a**, minor isomer, 33%; **28a**, 1%). ^{1}H NMR (300 MHz, C_6D_6) δ 7.45 (m, 2H, Ar-H_6, minor isomer), 7.36 (m, 2H, Ar-H_6, major isomer; m, 2H, Ar-H_6, minor isomer); 7.27 (m, 2H, Ar-H_5, major isomer), 7.22 (s, 2H, Ar-H_3, minor isomer), 7.16 (Ar-H_3, obscured by solvent residual, detected by

HSQC, major isomer), 7.15 – 7.04 (m, 4H, Ar-H_7 and Ar-H_8, major isomer; m, 4H, Ar-H_7 and Ar-H_8, minor isomer), 3.47 (m, 2H, -CH(CH$_3$)$_2$, minor isomer), 3.05 (s, 3H, -OCH_3, major isomer), 3.01 (m, 2H, -CH(CH$_3$)$_2$, major isomer), 2.97 (s, 3H, -OCH_3, minor isomer), 2.54 (m, 2H, -CH(CH$_3$)$_2$, major isomer), 2.42 (m, 2H, -CH(CH$_3$)$_2$, minor isomer), 1.59 (dd, 6H, -CH(CH_3)$_2$, minor isomer), 1.48 – 1.32 (m, 12H, -CH(CH_3)$_2$, major isomer; m, 12H, -CH(CH_3)$_2$, minor isomer), 1.35 (s, 9H, -C(CH_3)$_3$, major isomer), 1.27 (s, 9H, -C(CH_3)$_3$, minor isomer), 1.20 (dd, 6H, -CH(CH_3)$_2$, major isomer), 1.14 – 1.03 (dd, 6H, -CH(CH_3)$_2$, major isomer; dd, 6H, -CH(CH_3)$_2$, minor isomer). ^{13}C{^{1}H} (101 MHz, C$_6$D$_6$) δ 171.88 (t, Ir-CO, J_{PC} = 12.6 Hz, major isomer), 171.63 (t, Ir-CO J_{PC} = 11.1 Hz, minor isomer), 153.12 (s, Ar-C_1, minor isomer), 152.22 (s, Ar-C_1, major isomer), 146.72 (app t, Ar-C_{10}, major isomer, J_{PC} = 11.6 Hz), 145.65 (m, Ar-C_{10}, minor isomer), 144.31 (s, Ar-C_4, major isomer), 143.82 (s, Ar-C_4, minor isomer), 136.20 (app t, Ar-C_2, minor isomer, J_{PC} = 1.5 Hz), 135.40 (app t, Ar-C_2, major isomer, J_{PC} = 2.0 Hz), 134.45 (m, Ar-H_5, minor isomer), 133.72 (app t, Ar-H_5, major isomer, J_{PC} = 20.2 Hz), 132.35 (app t, Ar-H_6, minor isomer, J_{PC} = 1.5 Hz), 132.25 (app t, Ar-H_6, major isomer, J_{PC} = 1.5 Hz), 132.15 – 131.89 (m, Ar-H$_9$, major and minor isomers), 129.13 (s, Ar-H_8, major isomer), 129.09 (s, Ar-H_8, minor isomer), 128.96 (s, Ar-H_3, major isomer), 128.09 (Ar-H_3, obscured by solvent residual, detected by HSQC, minor isomer), 126.96 (app t, Ar-H_7, minor isomer, J_{PC} = 3.0 Hz), 126.59 (app t, Ar-H_7, major isomer, J_{PC} = 3.0 Hz), 60.32 (s, -OCH$_3$, major isomer), 60.09 (s, -OCH$_3$, minor isomer), 34.46 (s, -C(CH$_3$)$_3$, major isomer), 34.34 (s, -C(CH$_3$)$_3$, minor isomer), 31.76 (s, -C(CH$_3$)$_3$, major isomer), 31.39 (s, -C(CH$_3$)$_3$, minor isomer), 29.90 (app t, -CH(CH$_3$)$_2$, minor isomer), J_{PC} = 14.1 Hz), 27.83 (app t, -CH(CH$_3$)$_2$, major isomer, J_{PC} = 27.83 Hz), 25.73 (app t, -CH(CH$_3$)$_2$, minor isomer, J_{PC} = 13.6 Hz), 25.31 (app t, -

*C*H(CH$_3$)$_2$, major isomer, J_{PC} = 13.6 Hz), 22.62 (s, br, -CH(*C*H$_3$)$_2$, minor isomer), 21.34 (app t, -CH(*C*H$_3$)$_2$, J_{PC} = 1.5 Hz), 21.27 (s, -CH(*C*H$_3$)$_2$), 21.00 (app t, -CH(*C*H$_3$)$_2$, J_{PC} = 3.0 Hz), 20.55 (app t, -CH(*C*H$_3$)$_2$, J_{PC} = 1.5 Hz), 20.26 (s, -CH(*C*H$_3$)$_2$, major isomer), 20.14 (s, -CH(*C*H$_3$)$_2$), 19.25 -CH(*C*H$_3$)$_2$. ^{31}P{^{1}H} NMR (121 MHz, C$_6$D$_6$) δ 31.82 (s, minor isomer), 26.43 (s, major isomer). ν_{CO} = 1937 cm^{-1} (solid, film).

Synthesis of [2,6-bis(2'-diisopropylphosphinophenyl)-4-tert-butyl-phenoxide]nickel(II)-chloride (32a).

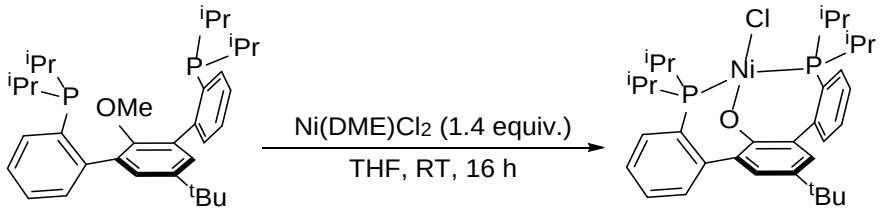

1a **32a**

In the glovebox, a colorless solution of diphosphine **1a** (0.04 g, 0.07 mmol, 1.00 equiv.) in THF (3 mL) was added dropwise to a slurry of Ni(DME)Cl$_2$ (0.02 g, 0.10, 1.40 equiv.), a yellow powder, in THF (1.5 mL) in a 20 mL scintillation vial charged with a magnetic stir bar. Upon addition, a pale purple color was observed. The mixture was stirred at room temperature. After 2 h, a dark purple color was observed. After 16 h, volatiles were removed under reduced pressure. The resulting purple-gray residue was triturated with 2 mL hexanes and solvent removed under reduced pressure to afford a purple-gray powder. This purple-gray powder was washed with three portions of hexanes (1.5 mL). The washed precipitate was extracted with three portions of toluene (1.5 mL). This solution was filtered through Celite and solvent removed under reduced pressure to afford **32a** as a purple powder (0.03 g, 0.04 mmol, 61% yield). ^{1}H NMR (300 MHz, C$_6$D$_6$) δ 7.53 (s, 2H, Ar-*H*$_3$), 7.20 (m, 2H, Ar-*H*$_9$), 7.12 (m, 4H, Ar- *H*$_7$ and Ar-*H*$_8$), 6.97 (m, 2H, Ar- *H*$_6$), 2.59 (m, 2H, -C*H*(CH$_3$)$_2$), 2.11

(m, 2H, -C*H*(CH_3)$_2$), 1.88 (dd, 6H, -CH(C*H*)$_3$), 1.80 (dd, 6H, -CH(C*H*)$_3$), 1.53 (s, 9H, C(C*H*$_3$)$_3$), 1.21 (dd, 6H, -CH(C*H*)$_3$), 0.63 (dd, 6H, -CH(C*H*)$_3$). ^{13}C{^{1}H} NMR (101 MHz, C_6D_6) δ 148.21 (app t, Ar-*C*$_2$, J_{PC} = 2.0 Hz), 148.00 (app t, Ar-*C*$_9$, J_{PC} = 7.1 Hz), 142.73 (s, Ar-*C*$_4$), 133.90 (t, Ar-*C*$_1$, J_{PC} = 1.0 Hz), 133.27 (app t, Ar-*C*$_7$ or Ar-*C*$_8$, J_{PC} = 4.0 Hz), 131.00 (app t, Ar-*C*$_9$, J_{PC} = 1.5 Hz), 130.54 (app t, Ar-*C*$_7$ or Ar-*C*$_8$, J_{PC} = 1.0 Hz), 129.77 (s, Ar-*C*$_3$), 125.09 (app t, Ar-*C*$_6$, J_{PC} = 3.0 Hz), 122.80 (app t, Ar-*C*$_{10}$, J_{PC} = 19.7 Hz), 34.57 (s, -*C*(CH_3)$_3$), 31.95 (s, -C(*C*H$_3$)$_3$), 23.16 (app t, -*C*H(CH_3)$_2$, J_{PC} = 9.6 Hz), 21.34 (app t, -*C*H(CH_3)$_2$, J_{PC} = 11.1 Hz), 19.69 (app t, -CH(*C*H$_3$)$_2$, J_{PC} = 2.5 Hz), 19.43 (app t, -CH(*C*H$_3$)$_2$, J_{PC} = 3.0 Hz), 18.73 (app t, -CH(*C*H$_3$)$_2$, J_{PC} = 2.5 Hz), 15.28 (app t, -CH(*C*H$_3$)$_2$, J_{PC} = 2.5 Hz). ^{31}P{^{1}H} NMR (121 MHz, CD_2Cl_2). δ 13.74 (s). ^{1}H NMR (300 MHz, CD_2Cl_2) δ 7.53 (m, 2H, Ar-*H*$_9$), 7.48 (t, 2H, Ar-*H*$_8$), 7.37 (s, 2H, Ar-*H*$_3$), 7.29 (t, 2H, Ar-*H*$_7$), 7.16 (d, 2H, Ar-*H*$_6$), 2.62 (m, 2H, -C*H*(CH_3)$_2$), 2.34 (m, 2H, -C*H*(CH_3)$_2$), 1.96 (s, 9H, -C(C*H*$_3$)$_3$), 1.80 (dd, 6H, -CH(C*H*$_3$)$_2$), 1.48 (dd, 6H, -CH(C*H*$_3$)$_2$), 0.98 (dd, 6H, -CH(C*H*$_3$)$_2$), 0.86 (dd, 6H, -CH(C*H*$_3$)$_2$). ^{13}C{^{1}H} NMR (126 MHz, CD_2Cl_2) δ 147.43 (app t, Ar-*C*$_{10}$), 146.96 (t, Ar-*C*$_4$), 143.36 (s, Ar-*C*$_1$), 133.36 (app t. Ar-*C*$_2$), 133.05 (Ar-*C*$_6$), 131.26 (s, Ar-*C*$_9$), 130.69 (s, Ar-*C*$_8$), 129.72 (s, Ar-*C*$_3$), 125.40 (t, Ar-*C*$_7$), 122.47 (t, Ar-*C*$_5$), 34.68 (s, -*C*(CH_3)$_3$), 31.78 (s, -*C*(CH_3)$_3$), 23.20 (t, -C*H*(CH_3)$_2$), 21.31 (t, -C*H*(CH_3)$_2$), 19.55 (t, -CH(*C*H$_3$)$_2$), 19.29 (t, -CH(*C*H$_3$)$_2$), 18.49 (t, -CH(*C*H$_3$)$_2$), 15.37 (t, -CH(*C*H$_3$)$_2$). ^{31}P{^{1}H} NMR (121 MHz, CD_2Cl_2) δ 13.71 (s). Anal. calcd. for $C_{34}H_{47}ClOP_2Ni$ (%): C, 65.04; H, 7.55. Found: C, 65.15; H, 7.43.

Synthesis of [2,6-bis(2'-diisopropylphosphinophenyl)-4-dimethylamino-phenoxide] nickel(II)chloride (32b).

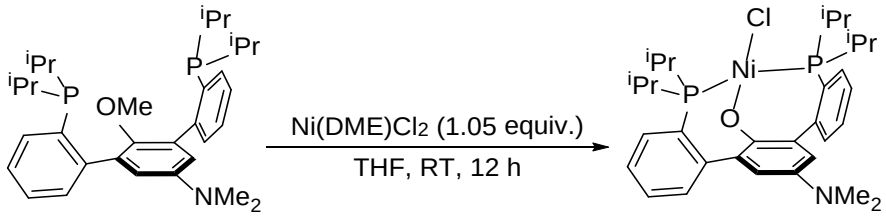

1b **32b**

In the glovebox, a 20 mL scintillation vial was charged with a stir bar, $Ni(DME)Cl_2$ (0.043 g, 0.196 mmol, 1.05 equiv.), and THF (2 mL). To this yellow slurry was added diphosphine **1b** (0.100 g, 0.187 mmol, 1.00 equiv.) as a solution in THF (2 mL) and the reaction mixture was stirred vigorously. After 1 h, a dark green solution was observed. After 12 h, volatiles were removed under reduced pressure to afford a dark green oil. Hexanes (1 mL) was added, the crude reaction mixture was titurated, and volatiles were removed under reduced pressure. The resulting green solid was washed with three times with Et_2O (1 mL) then dissolved in C_6H_6 (5 mL) and filtered through Celite. Volatiles were removed under reduced pressure. The resulting green solid was dissolved in 8 mL Et_2O, filtered again through Celite, and left to stand at room temperature. Dark green crystals were observed, the mother liquor was decanted, the crystals were washed once with Et_2O (1 mL), and volatiles were removed under reduced pressure to afford **32b** (0.023 g, 0.037 mmol, 32.2%) as a dark green crystalline solid. Crystals suitable for X-ray diffraction were grown from a saturated solution of Et_2O. ^1H NMR (300 MHz, C_6D_6) δ 7.23 (m, 4H, Ar-H_6 & Ar-H_9), 7.13 (m, 2H, Ar-H_7 or Ar-H_8), 6.99 (s, 2H, Ar-H_3), 6.98 (m, 2H, Ar-H_7 or Ar-H_8), 2.78 (s, 6H, -$N(CH_3)_2$), 2.62 (m, 2H, -$CH(CH_3)_2$), 2.14 (m, 2H, -$CH(CH_3)_2$), 1.85 (m, 12H, -$CH(CH_3)_2$), 1.25 (dd, 6H, -$CH(CH_3)_2$), 0.67 (dd, 6H, -$CH(CH_3)_2$). $^{13}C\{^1H\}$ NMR (101

MHz, C_6D_6) δ 148.14 (app t, Ar-*C*$_5$, J_{PC} = 7.1 Hz), 146.14 (s, Ar-*C*$_4$), 141.28 (app t, Ar-*C*$_{10}$, J_{PC} = 12.1 Hz), 134.90 (s, Ar-*C*$_2$), 133.21 (app t, Ar-*C*$_6$ or Ar-*C*$_9$, J_{PC} = 4.0 Hz), 131.17 (app t, Ar-*C*$_6$ or Ar-*C*$_9$, J_{PC} = 1.0 Hz), 130.39 (s, br, Ar-*C*$_7$ or Ar-*C*$_8$), 124.99 (app t, br, Ar-*C*$_7$ or Ar-*C*$_8$, J_{PC} = 2.5 Hz), 123.23 (t, Ar-*C*$_1$, J_{PC} = 19.2 Hz), 118.73 (s, Ar-*C*$_3$), 41.78 (s, -N(*C*H$_3$)$_2$), 23.30 (app t, -*C*H(CH$_3$)$_2$, J_{PC} = 8.6 Hz), 21.20 (app t, -*C*H(CH$_3$)$_2$, J_{PC} = 10.6 Hz), 19.62 (app t, -CH(*C*H$_3$)$_2$, J_{PC} = 2.5 Hz), 19.50 (app t, -CH(*C*H$_3$)$_2$, J_{PC} = 3.5 Hz), 19.04 (app t, -CH(*C*H$_3$)$_2$, J_{PC} = 2.5 Hz), 15.32 (app t, -CH(*C*H$_3$)$_2$, J_{PC} = 2.5 Hz). $^{31}P\{^1H\}$ NMR (121 MHz, C_6D_6) δ 14.04 (s). Anal. calcd. for $C_{32}H_{44}ClNNiOP_2$ (%):C, 62.52; H, 7.21; N, 2.28. Found: C, 62.38; H, 6.99; N, 2.28.

Synthesis of [1,3-bis(2'-diisopropylphosphinophenyl)-5-tert-butyl-2-methoxybenzene]-palladium(II)chloride (33a).

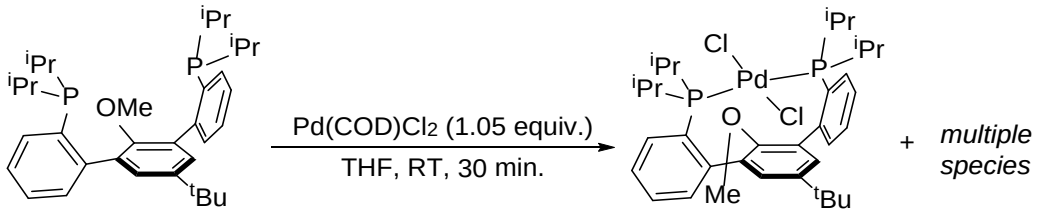

1a **33a**

In the glovebox, a 20 mL scintillation vial was charged with a magnetic stir bar, Pd(COD)Cl_2 (0.012 g, 0.048 mmol, 1.05 equiv.), and THF (1 mL). A yellow solution was observed. A pale yellow solution of diphosphine **1a** (0.025 g, 0.046 mmol, 1.00 equiv.) in THF (2 mL) was added dropwise to the solution of Pd(COD)Cl_2. After 15 min., an orange homogenous solution was observed. After 30 min., volatiles were removed under reduced pressure. An orange oil was observed. C_6H_6 (1 mL) was added. A homogenous orange solution was observed. Volatiles were removed under reduced pressure. A gummy orange solid was observed. This solid was dissolved in benzene (2 mL), filtered through Celite, and volatiles were removed under reduced

pressure to afford a gummy orange solid. Tituration with hexanes (1 mL) followed by pentane (1 mL) afforded a light orange powder (0.025 g, mixture of species; NMR yield: 79% **33a** 4% phenoxide **35a**). ^{1}H NMR (400 MHz, C_6D_6) δ 7.44 (m, 2H, Ar-*H*$_9$), 7.38 (m, 2H, Ar-*H*$_6$), 7.33 (s, 2H, Ar-*H*$_3$), 7.21 (t, 2H, Ar-*H*$_8$), 7.09 (t, 2H, Ar-*H*$_7$), 3.14 (s, br, 2H, -C*H*$(CH_3)_2$), 3.07 (s, 3H, -OC*H*$_3$), 2.66 (s, br, 2H, -C*H*$(CH_3)_2$), 1.64 (dd, 6H, -CH(C*H*$_3)_2$), 1.43 (m, 12H, -CH(C*H*$_3)_2$), 1.36 (s, 9H, -C(C*H*$_3)_3$), 1.22 (dd, 6H, -CH(C*H*$_3)_2$). ^{13}C{^{1}H} NMR (101 MHz, C_6D_6) δ 152.52 (s, Ar-*C*$_1$), 145.39 (s, br, Ar-*C*$_4$), 144.60 (s, Ar-*C*$_2$), 136.07 (s, br, Ar-*C*$_{10}$), 134.80 (m, Ar-*C*$_5$), 132.39 (app t, Ar-*C*$_6$), 132.06 (app t, Ar-*C*$_9$), 130.13 (s, br, Ar-*C*$_3$), 129.42 (s, Ar-*C*$_8$), 126.70 (app t, Ar-*C*$_7$, J_{PC} = 3.0 Hz), 60.75 (s, -O*C*H_3), 34.48 (s, -*C*$(CH_3)_3$), 31.41 (s, -C(*C*$H_3)_3$), 27.50 (s, br, -*C*$H(CH_3)_2$), 26.97 (s, br, -*C*$H(CH_3)_2$), 21.52 (s, br, -CH(*C*$H_3)_2$), 20.92 (s, -CH(*C*$H_3)_2$), 20.25 (app t, -CH(*C*$H_3)_2$, J_{PC} = 1.0 Hz), 19.72 (s, -CH(*C*$H_3)_2$). ^{31}P{^{1}H} NMR (121 MHz, C_6D_6) δ 26.28 (s).

Synthesis of [(1,3-bis(2'-diisopropylphosphinophenyl)-5-tert-butyl-2-methoxybenzene)-palladium(II)bisacetontrile][tetrafluoroborate] (34a).

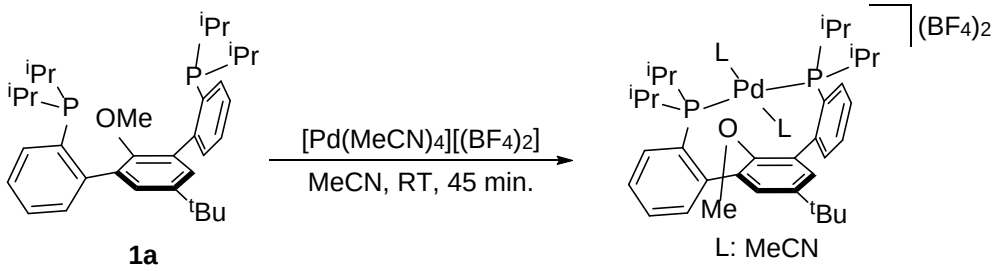

1a **34a**

In the glovebox, a 20 mL scintillation vial was charged with a magnetic stir bar, $[Pd(MeCN)_2][(BF_4)_2]$ (0.405 g, 0.911 mmol, 1.00 equiv.), and MeCN (1 mL). A yellow solution was observed. A yellow slurry of diphosphine **1a** (0.500 g, 0.911 mmol, 1.00 equiv.) in MeCN (2 mL) was added to the solution of $[Pd(MeCN)_2][(BF_4)_2]$. After 30

min., a dark red solution was observed. After 45 min., volatiles were removed under reduced pressure. A red oil was observed. This solid was dissolved in a minimum of MeCN and filtered through Celite. A precipitate was observed after this MeCN solution was left standing at room temperature. The solution was filtered through Celite and volatiles removed from the filtrate to afford **34a** (0.429 g, 0.471 mmol, 51.7%) as a light brown solid. ^{1}H NMR (300 MHz, CD_3CN) δ 7.77 (m, 4H, Ar-*H*), 7.70-7.61 (m, 4H Ar-*H*), 7.48 (s, 2H, Ar-H_3), 3.09 (s, 3H, -OCH_3), 3.04 (m, 2H, -C*H*$(CH_3)_2$), 2.37 (m, 2H, -C*H*$(CH_3)_2$), 1.57 (dd, 6H, -CH(CH_3)$_2$), 1.47 (dd, 6H, -CH(CH_3)$_2$), 1.36 (s, 9H, -C(CH_3)$_3$), 1.25 (dd, 6H, -CH(CH_3)$_2$), 1.12 (dd, 6H, -CH(CH_3)$_2$). ^{13}C{^{1}H} NMR (101 MHz, CD_3CN) δ 151.68 (s, Ar-C_1), 148.13 (s, Ar-C_4), 143.81 (app t, Ar-*C*, J_{PC} = 6.6 Hz), 137.01 (app t, Ar-*C*, J_{PC} = 2.5 Hz), 133.53 (app t, Ar-*C*H, J_{PC} = 4.0 Hz), 133.42 (app t, Ar-*C*H, J_{PC} = 3.0 Hz), 133.07 (s, Ar-*C*H), 130.73 (s, Ar-C_3), 129.34 (app t, Ar-*C*H, J_{PC} = 4.0 Hz), 129.21 (s, Ar-*C*H), 62.26 (s, -O*C*H_3), 35.36 (s, -*C*$(CH_3)_3$), 31.55 (s, -C(*C*H_3)$_3$), 27.93 (app t, -*C*H$(CH_3)_3$, J_{PC} = 11.6 Hz), 26.73 (app t, -*C*H$(CH_3)_3$, J_{PC} = 11.6 Hz), 21.23 (app t, -CH(*C*H_3)$_2$, J_{PC} = 1.5 Hz), 20.03 (s, -CH(*C*H_3)$_2$), 19.67 (s, -CH(*C*H_3)$_2$), 18.88 (s, -CH(*C*H_3)$_2$). ^{19}F NMR (282 MHz, CD_3CN) δ -149.28 (s). ^{31}P{^{1}H} (121 MHz, CD_3CN) δ 38.38 (s). Anal. calcd. for $C_{39}H_{56}B_2F_8N_2OP_2Pd$ (%): C, 51.43; H, 6.20; N, 3.08. Found: C, 49.71; H, 6.06; N, 3.55. Low in nitrogen despite multiple analyses.

Synthesis of [2,6-bis(2'-diisopropylphosphinophenyl)-4-tert-butyl-phenoxide]-palladium(II)chloride (35a).

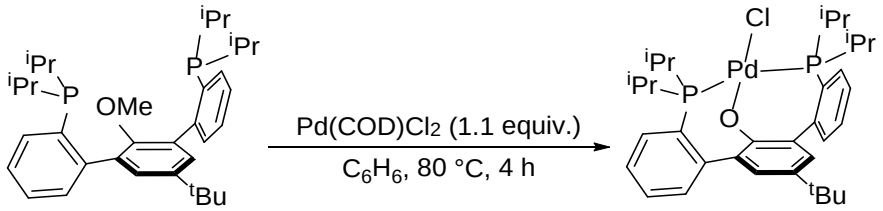

1a **35a**

In the glovebox, a 100 mL Schlenk tube fitted with a Teflon screw cap was charged with diphosphine **1a** (0.200 g, 0.365 mmol, 1.00 equiv.) as a solution in C_6H_6 (2 mL), $Pd(COD)Cl_2$ (0.115 g, 0.401 mmol, 1.10 equiv.) as a solution in C_6H_6 (2 mL), and a stir bar. An orange solution was observed. The Schlenk tube was placed in an oil bath preheated to 80 ºC and heated while stirring. After 4 h, the Schlenk tube was removed from the oil bath and brought into the glovebox. A red solution was observed. This C_6H_6 solution was filtered through Celite and volatiles removed under reduced pressure to afford **35a** (0.233 g, 0.352 mmol, 96.7%) as a red solid. ^{1}H NMR (400 MHz, C_6D_6) δ 7.31 (s, 2H, Ar-*H*$_3$), 7.23 (m, 2H, Ar-*H*$_9$), 7.15 (obscured to solvent residual, detected by HSQC, 2H, Ar-*H*$_6$), 7.13 (m, 2H, Ar-*H*$_7$), 7.00 (m, 2H, Ar-*H*$_8$), 2.96 (m, 2H, -C*H*$(CH_3)_2$), 2.19 (m, 2H, -C*H*$(CH_3)_2$), 1.60 (dd, 6H, -CH(C*H*$_3)_2)_2$), 1.50 (dd, 6H, -CH(C*H*$_3)_2)_2$), 1.44 (s, 9H, -C(C*H*$_3)_3$), 1.10 (dd, 6H, -CH(C*H*$_3)_2)_2$), 0.68 (dd, 6H, -CH(C*H*$_3)_2)_2$). ^{13}C{^{1}H} NMR (126 MHz, C_6D_6) δ 152.48 (t, Ar-*C*$_1$, J_{PC} = 3.2 Hz), 149.09 (app t, Ar-*C*$_5$, 6.9 Hz), 142.04 (s, C_2), 134.01 (app t, Ar-*C*$_7$, J_{PC} = 3.8 Hz), 131.57 (t, Ar-*C*$_1$, J_{PC} = 2.52 Hz), 131.41 (app t, Ar-*C*$_9$, J_{PC} = 1.3 Hz), 130.84 (s, Ar-*C*$_6$), 129.81 (s, Ar-*C*$_3$), 125.40 (app t, Ar-*C*$_8$, J_{PC} = 3.2 Hz), 122.53 (app t, Ar-*C*$_{10}$, J_{PC} = 22.1 Hz), 34.35 (s, -*C*$(CH_3)_3$), 31.97 (s, -C(*C*$H_3)_3$), 23.96 (app t, -*C*$H(CH_3)_2$, J_{PC} = 11.3 Hz), 22.17 (app t, -*C*$H(CH_3)_2$, J_{PC} = 12.0 Hz), 19.59 (app t, -CH(*C*$H_3)_2$, J_{PC} = 3.2 Hz), 19.40 (app t, -

$CH(CH_3)_2$, J_{PC} = 3.2 Hz), 18.69 (app t, -$CH(CH_3)_2$, J_{PC} = 2.5 Hz), 15.40 (app t, -$CH(CH_3)_2$, J_{PC} = 1.9 Hz). $^{31}P\{^1H\}$ NMR (121 MHz, C_6D_6) δ 27.08 (s). Anal. calcd. for $C_{34}H_{47}ClOP_2Pd$ (%): C, 60.45; H, 7.01. Found: C, 60.12; H, 6.80.

Synthesis of [1,3-bis(2'-diisopropylphosphinophenyl)-5-tert-butyl-2-methoxy-benzene]platinum(II)chloride (36a).

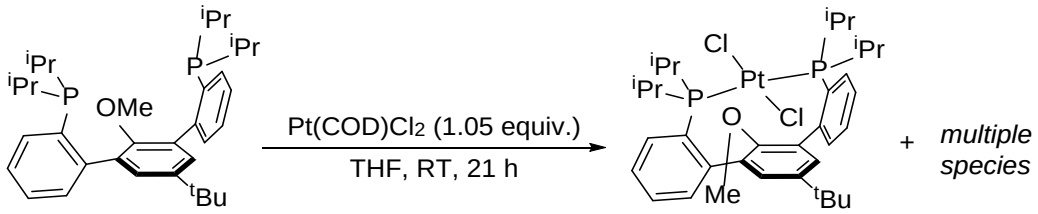

1a **36a**

In the glovebox, a 20 mL scintillation vial was charged with $Pt(COD)Cl_2$ (0.036 g, 0.096 mmol, 1.05 equiv.), and THF (1 mL). To this slurry was added diphosphine **1a** (0.050 g, 0.091 mmol, 1.00 equiv.) as a solution in THF (2 mL). After 4 h, a yellow solution was observed. After 21 h, volatiles were removed under reduced pressure. Hexanes (1 mL) was added, the crude yellow oil was titurated, and volatiles were removed under reduced pressure. The resulting light yellow solid was washed three times with hexanes (1 mL) and then extracted with three portions of Et_2O (1 mL). Volatiles were removed under reduced pressure to afford an off-white powder (0.028 g, mixture of species; NMR yield: **36a**, 84%). ^1H NMR (300 MHz, C_6D_6) δ 7.45 (m, 2H, Ar-H_9), 7.38 (m, 2H, Ar-H_6), 7.29 (s, 2H, Ar-H_3), 7.21 (m, 2H, Ar-H_7), 7.10 (m, 2H, Ar-H_8), 3.24 (m, 2H, -C$H(CH_3)_2$), 3.08 (s, 3H, -OCH_3), 2.78 (m, 2H, -C$H(CH_3)_2$, 1.63 (dd, 6H, -CH(C$H_3)_2$), 1.42 (m, 12H, -CH(C$H_3)_2$), 1.35 (s, 9H, -C(C$H_3)_3$), 1.22 (dd, 6H, -CH(C$H_3)_2$). $^{13}C\{^1H\}$ NMR (101 MHz, C_6D_6) δ 153.23 (s, Ar-C_1), 145.46 (s, br, Ar-C_{10}), 144.18 (s, Ar-C_4), 135.87 (s, br, Ar-C_2), 133.61 (app t, Ar-C_5, J_{PC} = 22.2 Hz), 132.81 (s, br, Ar-C_9), 132.12 (app t, Ar-C_6, J_{PC} = 4.0 Hz), 129.60 (s, br, Ar-C_7), 129.35

(s, Ar-*C*$_3$), 126.65 (app t, Ar-*C*$_8$, J_{PC} = 3.5 Hz), 60.53 (s, -O*C*H$_3$), 34.41 (s, -*C*(CH$_3$)$_3$, 31.45 (s, -C(*C*H$_3$)$_3$), 26.30 (s, br, -*C*H(CH$_3$)$_2$), 25.59 (s, br, -*C*H(CH$_3$)$_2$), 21.45 (s, br, -CH(*C*H$_3$)$_2$), 20.75 (s, -CH(*C*H$_3$)$_2$), 20.09 (app t, -CH(*C*H$_3$)$_2$, J_{PC} = 1.0 Hz), 19.54 (s, -CH(*C*H$_3$)$_2$). $^{31}P\{^1H\}$ NMR (121 MHz, C_6D_6) δ 17.96 (J_{PtP} = 2608.8 Hz).

Synthesis of [2,6-bis(2'-diisopropylphosphinophenyl)-4-tert-butyl-phenoxide]-platinum(II)chloride (37a).

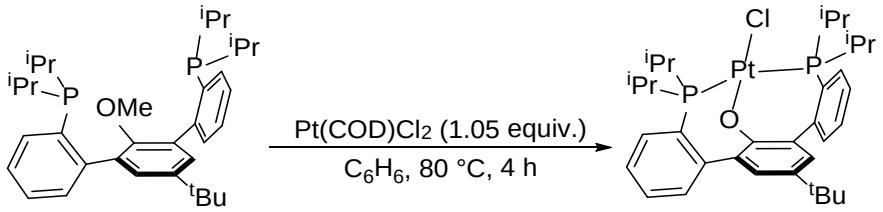

1a **37a**

In the glovebox, a 100 mL Schlenk tube fitted with a Teflon screw cap was charged with diphosphine **1a** (0.500 g, 0.911 mmol, 1.00 equiv.) as a solution in C_6H_6 (2 mL), Pt(COD)Cl_2 (0.358 g, 0.957 mmol, 1.05 equiv.) as a slurry in C_6H_6 (6 mL), and a stir bar. The Schlenk tube was sealed, removed from the glovebox, and placed in an oil bath preheated to 80 ºC and heated while stirring. After 4 h, the Schlenk tube was removed from the oil bath and brought into the glovebox. A yellow solution was observed. This C_6H_6 solution was filtered through Celite and volatiles removed under reduced pressure to afford a yellow solid. This yellow solid was washed three times with Et_2O (4 mL) then dissolved in a minimum of C_6H_6. Diffusion of Et_2O into this concentrated C_6H_6 afforded **37a** (crude yield: 85%, determined by NMR; isolated yield: 0.106 g, 0.139 mmol, 15.2 %) as a yellow crystalline solid. ^1H NMR (300 MHz, C_6D_6) δ 7.33 (s, 2H, Ar-*H*$_5$), 7.23 (m, 2H, Ar-*H*$_6$), 7.13 (detected by HSQC, obscured by solvent residual, Ar-*H*$_9$), 7.14 (m, 2H, Ar-*H*$_8$), 7.04 (m, 2H, Ar-*H*$_7$), 3.04 (m, 2H, -C*H*(CH$_3$)$_2$), 2.35 (m, 2H, -C*H*(CH$_3$)$_2$), 1.60 (dd, 6H, -CH(C*H*$_3$)$_2$), 1.50 (dd, 6H, -

CH(C*H*$_3$)$_2$), 1.44 (s, 9H, -C(C*H*$_3$)$_3$), 1.04 (dd, 6H, -CH(C*H*$_3$)$_2$), 0.70 (dd, 6H, -CH(C*H*$_3$)$_2$). ^{13}C{^{1}H} NMR (101 MHz, C_6D_6) δ 151.36 (app t, Ar-*C*$_{10}$, J_{PC} = 1.0 Hz), 148.23 (app t, Ar-*C*$_1$, J_{PC} = 6.1 Hz), 141.78 (s, Ar-*C*$_4$), 134.39 (app t, Ar-*C*$_9$, J_{PC} = 4.0 Hz), 131.89 (s, Ar-*C*$_2$), 131.77 (app t, Ar-*C*$_6$, J_{PC} = 3.0 Hz), 130.68 (s, br, Ar-*C*$_8$), 129.54 (s, br, Ar-*C*$_3$), 125.69 (app t, Ar-*C*$_7$, J_{PC} = 3.5 Hz), 120.51 (t, Ar-*C*$_5$, J_{PC} = 24.2 Hz), 34.33 (s, -*C*(CH$_3$)$_3$), 32.00 (s, -C(*C*H$_3$)$_3$), 24.58 (app t, -*C*H(CH$_3$)$_2$, J_{PC} = 15.2 Hz), 21.09 (app t, -*C*H(CH$_3$)$_2$, J_{PC} = 15.2 Hz), 19.20 (app t, -CH(*C*H$_3$)$_2$, J_{PC} = 2.5 Hz), 18.83 (app t, -CH(*C*H$_3$)$_2$, J_{PC} = 2.5 Hz), 18.20 (app t, -CH(*C*H$_3$)$_2$, J_{PC} = 2.0 Hz), 15.38 (app t, -CH(*C*H$_3$)$_2$, J_{PC} = 1.5 Hz). ^{31}P{^{1}H} NMR (121 MHz, C_6D_6) δ 25.27 (J_{PtP} = 2836.2 Hz). ^{1}H NMR (300 MHz, CD_2Cl_2) δ 7.58 (m, 2H Ar-*H*$_6$), 7.51 (m, 2H, Ar-*H*$_8$), 7.39 (m, 2H, Ar-*H*$_7$), 7.18 (m, 2H, Ar-*H*$_9$), 7.13 (s, 2H, Ar-*H*$_3$), 2.78 (m, 4H, -C*H*(CH$_3$)$_2$), 1.50 (dd, 6H, -CH(C*H*$_3$)$_2$), 1.42 (dd, 6H, -CH(C*H*$_3$)$_2$), 1.34 (s, 9H, -C(C*H*$_3$)$_3$), 0.94 (dd, 6H, -CH(C*H*$_3$)$_2$), 0.84 (dd, 6H, -CH(C*H*$_3$)$_2$). ^{13}C{^{1}H} NMR (101 MHz) δ 150.22 (s, Ar-*H*$_3$), 147.66 (app t, Ar-*C*$_2$, J_{PC} = 6.1 Hz), 142.42 (s, Ar-*C*$_4$), 134.23 (app t, Ar-*C*$_6$, J_{PC} = 2.5 Hz), 131.29 (app t, Ar-*C*$_{10}$, J_{PC} = 1.0 Hz), 130.88 (app t, Ar-*C*$_8$, J_{PC} = 1.0 Hz), 129.50 (s, Ar-*C*$_3$), 126.08 (app t, Ar-*C*$_7$, J_{PC} = 3.5 Hz), 120.24 (app t, Ar-*C*$_5$, J_{PC} = 24.7 Hz), 34.42 (s, -*C*(CH$_3$)$_3$), 31.79 (s, -C(*C*H$_3$)$_3$), 24.63 (app t, -C*H*(CH$_3$)$_2$, J_{PC} = 15.2 Hz), 21.09 (app t, -C*H*(CH$_3$)$_2$, J_{PC} = 14.6 Hz), 19.03 (app t, -CH(*C*H$_3$)$_3$, J_{PC} = 2.0 Hz), 18.69 (app t, -CH(*C*H$_3$)$_3$, J_{PC} = 2.5 Hz), 18.00 (app t, -CH(*C*H$_3$)$_3$, J_{PC} = 2.0 Hz), 15.53 (app t, -CH(*C*H$_3$)$_3$, J_{PC} = 1.5 Hz). ^{31}P{^{1}H} NMR (121 MHz, CD_2Cl_2) δ 25.12 (J_{PtP} = 2812.0 Hz). Anal. calcd. for $C_{34}H_{47}ClOP_2Pt$ (%): C, 53.44; H, 6.20. Found: C, 53.16; H, 6.19.

Synthesis of [1,3-bis(2'-diisopropylphosphinophenyl)-5-tert-butyl-2-methoxybenzene]-cobalt(I)bromide (37a).

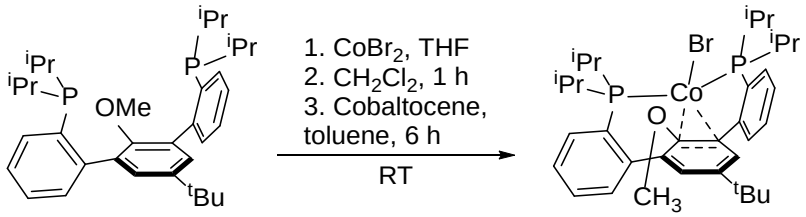

1a **38a**

In the glovebox, a 20 mL scintillation vial was charged with a magnetic stir bar, $CoBr_2$ (0.156 g, 0.711 mmol, 1.30 equiv.), and THF (2 mL). A blue solution was observed. Diphopshine **1a** (0.300 g, 0.547 mmol, 1.00 equiv.) was added as a solution in THF (2 mL). Volatiles were removed under reduced pressure to afford a gummy light blue solid. CH_2Cl_2 (4 mL) was added, the solid was triturated, and stirred for 1 h. A green solution was observed. Volatiles were removed under reduced pressure to afford a gummy green solid. Toluene (4 mL) was added and the solid was triturated. Cobaltocene (0.103 g, 0.547 mmol, 1.00 equiv.) was added dropwise as a solution in toluene (2 mL). The mixture was stirred for 6 h. A yellow solution was observed. The solution was filtered through Celite and volatiles were removed under reduced pressure. Hexanes was added to the resulting dark red oil and triturated. The volatiles were removed under reduced pressure and the resulting solid was extracted three times with hexanes (5 mL). The hexanes extract was filtered through Celite and volatiles removed under reduced pressure. The resulting red oil was dissolved in a minimum of Et_2O, filtered once more through Celite, and placed in a -35 °C freezer. Dark red crystals were observed. The mother liquor was decanted and the crystals were washed twice with Et_2O (1 mL) to afford compound **38a** (0.053 g, 0.077 mmol, 14.0%) as a dark red crystalline solid. Crystals suitable for x-ray diffraction were grown

from a saturated solution on Et_2O. ^1H NMR (300 MHz, C_6D_6) δ 51.27 (s, br), 24.23 (s, br), 21.43 (s, br), 17.70 (s), 9.88 (s), 8.13 (s), 5.80 (s, br), 1.01 (s), -0.63 (s), -4.16 (s, br), -7.45 (s, br), -9.68 (s, br). μ_{eff} calcdd. for Co^I, S = 1: 2.83 μ_B. μ_{eff} found: 2.72 μ_B (Evans'method, C_6D_6/THF). Anal. calcd. for $C_{35}H_{50}BrCoOP_2$ (%): C, 61.14; H, 7.33. Found: C, 61.14; H, 7.44.

Crystallographic Data

CCDC deposition numbers (1411633, **38a**; 1411634, **19a**; 1411635, **28a**; 1411636, **8a**; 1411637, **32b**; 1411638, **26a**; 1441639, **5a**; 1411640, **34a**) contain the supplementary crystallographic data for this paper. These data can be obtained free of charge from The Cambridge Crystallographic Data Centre via www.ccdc.cam.ac.uk/data_request/cif.

Refinement Details. In each case, crystals were mounted on a glass fiber or MiTeGen loop using Paratone oil, then placed on the diffractometer under a nitrogen stream. For compounds **5a**, **8a**, **19a**, **28a**, **32b**, **34a**, and **38a**, low temperature (100 k) X-ray data was obtained on a Bruker KAPPA APEXII CCD based diffractometer (Mo fine-focus sealed X-ray tube, Kα = 0.71073 Å). For compound **26a**, low temperature (100 K) X-ray data was obtained Bruker D8 VENTURE Kappa Duo PHOTON 100 CMOS based diffractometer (Mo IμS HB micro-focus sealed X-ray tube, Kα = 0.71073 Å). All diffractometer manipulations, including data collection, integration, and scaling were carried out using the Bruker APEXII software.[51] Absorption corrections were applied using SADABS.[52] Space groups were determined on the basis of systematic absences and intensity statistics and the structures were solved in the Olex 2 software interface[53] by intrinsic phasing using XS[54] (incorporated into SHELXTL) and refined by full-matrix least

squares on F2. All non-hydrogen atoms were refined using anisotropic displacement parameters. Hydrogen atoms were placed in the idealized positions and refined using a riding model. The structure was refined (weighed least squares refinement on F2) to convergence. Graphical representation of structures with 50% probability thermal ellipsoids were generated using Diamond 3 visualization software.[55]

Table 2.1. Crystal and Refinement Data for 5a, 8a, 19a, 26a.

	Complex **5a**	Complex **8a**	Complex **19a**	Complex **26a**
Empirical formula	$C_{35}H_{50}OP_2Pd_{0.69}$	$C_{35}H_{50}OP_2Pt$	$C_{34}H_{48}ClP_2Rh$	$C_{37.5}H_{54}ClOP_2Rh$
Formula weight (g/mol)	622.11	743.78	657.02	721.10
T (K)	100	100(2)	100(2)	100
Radiation	MoKα (λ = 0.71073)	MoKα (λ = 0.71073)	MoKα (λ = 0.71073)	MoKα (λ = 0.71073)
a (Å)	11.2133(4)	15.5042(7)	21.062(8)	26.5795(9)
b (Å)	15.3800(6)	15.5042(7)	10.977(4)	23.0419(8)
c (Å)	19.1855(8)	11.8599(8)	29.071(11)	24.1024(8)
α (deg)	90	90	90	90
β (deg)	92.738(2)	90	105.84(2)	103.6640(10)
γ (deg)	90	120	90	90
V (Å^3)	3305.0(2)	2468.9(2)	6466(4)	14343.5(8)
Z	4	3	8	16
Cryst. syst.	monoclinic	hexagonal	monoclinic	Monoclinic
Space group	$P2_1/n$	$P3_1$	$P2_1/c$	Cc
ρ_{calcd}g (cm^3)	1.250	1.501	1.350	1.336
2 σ range (deg)	3.4 to 77.54	4.458 to 87.8	3.986 to 57.058	4.506 to 79.662
Crystal size/mm	0.28 x 0.25 x 0.07	0.28 × 0.26 × 0.14	0.28 × 0.13 × 0.05	0.24 x 0.19 x 0.06
μ (mm^{-1})	0.520	4.385	0.731	0.668
GOF	1.211	0.980	1.816	1.009
R1, wR2 (I> 2σ (I))	0.0674, 0.1917	0.0234, 0.0400	0.0699, 0.0808	0.0639, 0.0915

Table 2.2. Crystal and Refinement Data for 28a, 32b, 34a, 38a.

	Complex **28a**	Complex **32b**	Complex **34a**	Complex **38a**
Empirical formula	$C_{35}H_{47}IrO_2P_2$	$C_{32}H_{44}ClNNiOP_2$	$C_{41}H_{59}B_2F_8N_3OP_2Pd$	$C_{38}H_{56}BrCoOP_2$
Formula weight (g/mol)	753.87	614.78	951.87	729.60
T (K)	100(2)	100(2)	100(2)	100.0(2)
Radiation	MoKα (λ = 0.71073)	MoKα (λ = 0.71073)	MoKα (λ = 0.71073)	MoKα (λ = 0.71073)
a (Å)	15.4739(5)	17.0566(7)	12.3085(5)	18.7532(9)
b (Å)	15.4739(5)	10.9300(4)	17.2927(7)	12.5873(6)
c (Å)	11.8879(5)	33.5079(14)	21.7237(9)	15.6898(7)
α (deg)	90	90	82.133(2)	90
β (deg)	90	97.838(2)	86.587(2)	96.330(3)
γ (deg)	120	90	86.032(2)	90
V ($Å^3$)	2465.10(15)	6188.5(4)	4563.5(3)	3681.0(3)
Z	3	8	4	4
Cryst. syst.	hexagonal	monoclinic	triclinic	monoclinic
Space group	$P3_1$	$P2_1/n$	P-1	$P2_1/1$
ρ_{calcd}g (cm^3)	1.523	1.320	1.385	1.317
2 σ range (deg)	4.58 to 106.76	3.92 to 60.3	1.894 to 77.678	3.904 to 74.614
Crystal size/mm	0.40 × 0.27 × 0.23	0.18 × 0.16 × 0.08	0.42 × 0.34 × 0.15	0.44 × 0.28 × 0.05
μ (mm^{-1})	4.188	0.842	0.544	1.666
GOF	0.907	1.050	1.044	0.980
R1, wR2 (I> 2σ (I))	0.0249, 0.0404	0.0570, 0.1043	0.0548, 0.1289	0.0392, 0.0892

REFERENCES

(1) (a) Rosen, B. M.; Quasdorf, K. W.; Wilson, D. A.; Zhang, N.; Resmerita, A.-M.; Garg, N. K.; Percec, V. *Chem. Rev.* **2011**, *111*, 1346-1416; (b) Li, B.-J.; Yu, D.-G.; Sun, C.-L.; Shi, Z.-J. *Chem. Eur. J.* **2011**, *17*, 1728-1759; (c) Cornella, J.; Zarate, C.; Martin, R. *Chem. Soc. Rev.* **2014**, *43*, 8081-8097; (d) Tobisu, M.; Chatani, N. *Acc. Chem. Res.* **2015**, *48*, 1717-1726.
(2) Zakzeski, J.; Bruijnincx, P. C. A.; Jongerius, A. L.; Weckhuysen, B. M. *Chem. Rev.* **2010**, *110*, 3552-3599.
(3) (a) Álvarez-Bercedo, P.; Martin, R. *J. Am. Chem. Soc.* **2010**, *132*, 17352-17353; (b) Cornella, J.; Gómez-Bengoa, E.; Martin, R. *J. Am. Chem. Soc.* **2013**, *135*, 1997-2009.
(4) Boerjan, W.; Ralph, J.; Baucher, M. *Annu. Rev. Plant. Biol.* **2003**, *54*, 519-546.
(5) (a) Komiya, S.; Srivastava, R. S.; Yamamoto, A.; Yamamoto, T. *Organometallics* **1985**, *4*, 1504-1508; (b) Iqbal, J.; Srivastava, R. *Tetrahedron* **1991**, *47*, 3155-3170; (c) Wang, B.; Yin, Z.; Li, Y.; Yang, T.-X.; Meng, X.-B.; Li, Z.-J. *J. Org. Chem.* **2011**, *76*, 9531-9535; (d) Yu, D.-G.; Wang, X.; Zhu, R.-Y.; Luo, S.; Zhang, X.-B.; Wang, B.-Q.; Wang, L.; Shi, Z.-J. *J. Am. Chem. Soc.* **2012**, *134*, 14638-14641; (e) Song, W.; Ackermann, L. *Angew. Int. Ed. Chem.* **2012**, *51*, 8251-8254.
(6) (a) Empsall, H. D.; Hyde, E. M.; Jones, C. E.; Shaw, B. L. *J. Chem. Soc., Dalton Trans.* **1974**, 1980-1985; (b) van der Boom, M. E.; Liou, S.-Y.; Ben-David, Y.; Vigalok, A.; Milstein, D. *Angew. Chem. Int. Ed. Engl.* **1997**, *36*, 625-626; (c) Han, X.-H.; Yamamoto, Y. *J. Organomet. Chem.* **1998**, *561*, 157-165; (d) Murakami, M.; Itahashi, T.; Amii, H.; Takahashi, K.; Ito, Y. *J. Am. Chem. Soc.* **1998**, *120*, 9949-9950; (e) van der Boom, M. E.; Liou, S.-Y.; Ben-David, Y.; Shimon, L. J. W.; Milstein, D. *J. Am. Chem. Soc.* **1998**, *120*, 6531-6541; (f) Rao, H.; Li, C.-J. *Angew. Int. Ed. Chem.* **2011**, *50*, 8936-8939; (g) Arisawa, M.; Nihei, Y.; Suzuki, T.; Yamaguchi, M. *Org. Lett.* **2012**, *14*, 855-857; (h) Zhu, Y.; Smith, D.; Herbert, D.; Gatard, S.; Ozerov, O. *Chem. Commun.* **2012**, *48*, 218-220; (i) Kinuta, H.; Tobisu, M.; Chatani, N. *J. Am. Chem. Soc.* **2015**, *137*, 1593-1600.
(7) (a) Amouri, H.; Vaissermann, J.; Rager, M. N.; Besace, Y. *Inorg. Chem.* **1999**, *38*, 1211-1215; (b) Choi, J.; Choliy, Y.; Zhang, X.; Emge, T. J.; Krogh-Jespersen, K.; Goldman, A. S. *J. Am. Chem. Soc.* **2009**, *131*, 15627-15629; (c) Lao, D. B.; Owens, A. C. E.; Heinekey, D. M.; Goldberg, K. I. *ACS Catal.* **2013**, *3*, 2391-2396; (d) Miller, A. J. M.; Kaminsky, W.; Goldberg, K. I. *Organometallics* **2014**, *33*, 1245-1252; (e) Haibach, M. C.; Lease, N.; Goldman, A. S. *Angew. Int. Ed. Chem.* **2014**, *53*, 10160-10163.
(8) (a) Wenkert, E.; Michelotti, E. L.; Swindell, C. S.; Tingoli, M. *J. Org. Chem.* **1984**, *49*, 4894-4899; (b) Zim, D.; Lando, V. R.; Dupont, J.; Monteiro, A. L. *Org. Lett.* **2001**, *3*, 3049-3051; (c) Dankwardt, J. W. *Angew. Chem. Int. Ed.* **2004**, *43*, 2428-2432; (d) Sergeev, A. G.; Hartwig, J. F. *Science* **2011**, *332*, 439-443; (e) Sergeev, A. G.; Webb, J. D.; Hartwig, J. F. *J. Am. Chem. Soc.* **2012**, *134*, 20226-20229; (f) Zarate, C.; Manzano, R.; Martin, R. *J. Am. Chem. Soc.* **2015**, *137*, 6754-6757; (g) van der Boom, M. E.; Liou, S.-Y.; Shimon, L. J. W.; Ben-David, Y.; Milstein, D. *Inorg. Chim. Acta.* **2004**, *357*, 4015-4023.
(9) (a) Sun, J.-S.; Uzelmeier, C. E.; Ward, D. L.; Dunbar, K. R. *Polyhedron* **1998**, *17*, 2049-2063; (b) Weissman, H.; Shimon, L. J. W.; Milstein, D. *Organometallics* **2004**, *23*, 3931-3940; (c) Shmidt, A. F.; Smirnov, V. V. *Kinet. Catal.* **2005**, *46*, 495-501; (d) Zhou, C.; Liu, Q.; Li, Y.; Zhang, R.; Fu, X.; Duan, C. *J. Org. Chem.* **2012**, *77*, 10468-10472.
(10) (a) Jones, C. E.; Shaw, B. L.; Turtle, B. L. *J. Chem. Soc., Dalton Trans.* **1974**, 992-999; (b) Zhang, X.; Watson, E. J.; Dullaghan, C. A.; Gorun, S. M.; Sweigart, D. A. *Angew. Int. Ed. Chem.* **1999**, *38*, 2206-2208; (c) Kataoka, Y.; Nakamura, T.; Tani, K. *Chem. Lett.* **2003**,

32, 66-67; (d) Manbeck, K. A.; Kundu, S.; Walsh, A. P.; Brennessel, W. W.; Jones, W. D. *Organometallics* **2012**, *31*, 5018-5024.
(11) Kelley, P.; Lin, S.; Edouard, G.; Day, M. W.; Agapie, T. *J. Am. Chem. Soc.* **2012**, *134*, 5480-5483.
(12) (a) Li, Z.; Zhang, S.-L.; Fu, Y.; Guo, Q.-X.; Liu, L. *J. Am. Chem. Soc.* **2009**, *131*, 8815-8823; (b) Quasdorf, K. W.; Antoft-Finch, A.; Liu, P.; Silberstein, A. L.; Komaromi, A.; Blackburn, T.; Ramgren, S. D.; Houk, K. N.; Snieckus, V.; Garg, N. K. *J. Am. Chem. Soc.* **2011**, *133*, 6352-6363.
(13) (a) Komiya, S.; Akai, Y.; Tanaka, K.; Yamamoto, T.; Yamamoto, A. *Organometallics* **1985**, *4*, 1130-1136; (b) Kim, Y. J.; Osakada, K.; Takenaka, A.; Yamamoto, A. *J. Am. Chem. Soc.* **1990**, *112*, 1096-1104; (c) Seligson, A. L.; Cowan, R. L.; Trogler, W. C. *Inorg. Chem.* **1991**, *30*, 3371-3381; (d) Kim, Y.-J.; Lee, J.-Y.; Osakada, K. *J. Organomet. Chem.* **1998**, *558*, 41-49.
(14) (a) Luo, Y.-R. *Comprehensive Handbook of Chemical Bond Energies*; CRC Press: Boca Raton, 2007; (b) Yu, D.-G.; Li, B.-J.; Shi, Z.-J. *Acc. Chem. Res.* **2010**, *43*, 1486-1495.
(15) (a) Bertsch, S.; Braunschweig, H.; Forster, M.; Gruss, K.; Radacki, K. *Inorg. Chem.* **2011**, *50*, 1816-1819; (b) Bauer, J.; Braunschweig, H.; Dewhurst, R. D.; Radacki, K. *Chem. Eur. J.* **2013**, *19*, 8797-8805.
(16) Herberich, G. *Zeitschrift für Naturforschung. Teil b, Anorganische Chemie, organische Chemie* **1979**, *34B*, 638-639.
(17) (a) Bryndza, H. E.; Calabrese, J. C.; Marsi, M.; Roe, D. C.; Tam, W.; Bercaw, J. E. *J. Am. Chem. Soc.* **1986**, *108*, 4805-4813; (b) Romeo, R.; Alibrandi, G. *Inorg. Chem.* **1997**, *36*, 4822-4830.
(18) Park, S.; Pontier-Johnson, M.; Roundhill, D. M. *J. Am. Chem. Soc.* **1989**, *111*, 3101-3103.
(19) Herbert, D. E.; Lara, N. C.; Agapie, T. *Chem. Eur. J.* **2013**, *19*, 16453-16460.
(20) Grotjahn, D. B.; Zeng, X.; Cooksy, A. L.; Kassel, W. S.; DiPasquale, A. G.; Zakharov, L. N.; Rheingold, A. L. *Organometallics* **2007**, *26*, 3385-3402.
(21) (a) Aullon, G.; Bellamy, D.; Guy Orpen, A.; Brammer, L.; Eric, A. B. *Chem. Commun.* **1998**, 653-654; (b) Krumper, J. R.; Gerisch, M.; Magistrato, A.; Rothlisberger, U.; Bergman, R. G.; Tilley, T. D. *J. Am. Chem. Soc.* **2004**, *126*, 12492-12502.
(22) (a) Ceriotti, A.; Ciani, G.; Sironi, A. *J. Organomet. Chem.* **1983**, *247*, 345-350; (b) Morgan, B. P.; Smith, R. C. *J. Organomet. Chem.* **2008**, *693*, 11-16.
(23) (a) Rees, W. M.; Churchill, M. R.; Fettinger, J. C.; Atwood, J. D. *Organometallics* **1985**, *4*, 2179-2185; (b) Bernard, K. A.; Churchill, M. R.; Janik, T. S.; Atwood, J. D. *Organometallics* **1990**, *9*, 12-16; (c) Canepa, G.; Brandt, C. D.; Ilg, K.; Wolf, J.; Werner, H. *Chem. Eur. J.* **2003**, *9*, 2502-2515; (d) Kuznetsov, V. F.; Lough, A. J.; Gusev, D. G. *Inorg. Chim. Acta.* **2006**, *359*, 2806-2811; (e) Salem, H.; Shimon, L. J. W.; Leitus, G.; Weiner, L.; Milstein, D. *Organometallics* **2008**, *27*, 2293-2299; (f) Frech, C. M.; Shimon, L. J. W.; Milstein, D. *Organometallics* **2009**, *28*, 1900-1908.
(24) (a) Wang, K.; Emge, T. J.; Goldman, A. S.; Li, C.; Nolan, S. P. *Organometallics* **1995**, *14*, 4929-4936; (b) Canepa, G.; Brandt, C. D.; Werner, H. *Organometallics* **2001**, *20*, 604-606.
(25) Merola, J. S. In *Encyclopedia of Inorganic and Bioinorganic Chemistry*; John Wiley & Sons, Ltd: 2011.
(26) Adams, J. J.; Lau, A.; Arulsamy, N.; Roddick, D. M. *Organometallics* **2011**, *30*, 689-696.
(27) Punji, B.; Emge, T. J.; Goldman, A. S. *Organometallics* **2010**, *29*, 2702-2709.

(28) (a) Vigalok, A.; Rybtchinski, B.; Gozin, Y.; Koblenz, T. S.; Ben-David, Y.; Rozenberg, H.; Milstein, D. *J. Am. Chem. Soc.* **2003**, *125*, 15692-15693; (b) van der Boom, M. E.; Zubkov, T.; Shukla, A. D.; Rybtchinski, B.; Shimon, L. J. W.; Rozenberg, H.; Ben-David, Y.; Milstein, D. *Angew. Int. Ed. Chem.* **2004**, *43*, 5961-5963.
(29) (a) Rowen Churchill, M.; Fettinger, J. C.; Rees, W. M.; Atwood, J. D. *J. Organomet. Chem.* **1986**, *308*, 361-371; (b) Miller, C. A.; Janik, T. S.; Lake, C. H.; Toomey, L. M.; Churchill, M. R.; Atwood, J. D. *Organometallics* **1994**, *13*, 5080-5087; (c) Dahlenburg, L.; Herbst, K.; Kühnlein, M. *Z. Anorg. Allg. Chem.* **1997**, *623*, 250-258.
(30) (a) Sutherland, B. R.; Cowie, M. *Inorg. Chem.* **1984**, *23*, 2324-2331; (b) Shin, J. H.; Bridgewater, B. M.; Churchill, D. G.; Parkin, G. *Inorg. Chem.* **2001**, *40*, 5626-5635.
(31) Bradley, D. C. *Alkoxo and Aryloxo Derivatives of Metals*; Academic Press: San Diego, 2001.
(32) Poignant, G.; Nlate, S.; Guerchais, V.; Edwards, A. J.; Raithby, P. R. *Organometallics* **1997**, *16*, 124-132.
(33) (a) Yamamoto, Y.; Sato, R.; Ohshima, M.; Matsuo, F.; Sudoh, C. *J. Organomet. Chem.* **1995**, *489*, C68-C70; (b) Yamamoto, Y.; Sato, R.; Matsuo, F.; Sudoh, C.; Igoshi, T. *Inorg. Chem.* **1996**, *35*, 2329-2336.
(34) Rogers, C. W.; Patrick, B. O.; Rettig, S. J.; Wolf, M. O. *J. Chem. Soc., Dalton Trans.* **2001**, 1278-1283.
(35) Dunbar, K. R.; Haefner, S. C.; Uzelmeier, C. E.; Howard, A. *Inorg. Chim. Acta.* **1995**, *240*, 527-534.
(36) Zheng, F.; Hutton, A. T.; van Sittert, C. G. C. E.; Moss, J. R.; Mapolie, S. F. *Dalton Trans.* **2013**, *42*, 11163-11179.
(37) Suess, D. L. M.; Peters, J. C. *J. Am. Chem. Soc.* **2013**, *135*, 4938-4941.
(38) Cordero, B.; Gomez, V.; Platero-Prats, A. E.; Reves, M.; Echeverria, J.; Cremades, E.; Barragan, F.; Alvarez, S. *Dalton Trans.* **2008**, 2832-2838.
(39) Pangborn, A. B.; Giardello, M. A.; Grubbs, R. H.; Rosen, R. K.; Timmers, F. J. *Organometallics* **1996**, *15*, 1518-1520.
(40) Elan Pharmaceuticals, I. *U. S. Patent* **2005**, *087215 A1*.
(41) Burger, A.; Wilson, E. L.; Brindley, C. O.; Bernheim, F. *J. Am. Chem. Soc.* **1945**, *67*, 1416-1419.
(42) Berliner, M. A.; Belecki, K. *J. Org. Chem.* **2005**, *70*, 9618-9621.
(43) Maaranen, J.; Hoikka, J.; Rauotio, S. *U. S. Patent* **2007**, *37939 A1*.
(44) Bielawski, M.; Zhu, M.; Olofsson, B. *Adv. Synth. Catal.* **2007**, *349*, 2610-2618.
(45) Hossain, M. D.; Kitamura, T. *Tetrahedron* **2006**, *62*, 6955-6960.
(46) Fulmer, G. R.; Miller, A. J. M.; Sherden, N. H.; Gottlieb, H. E.; Nudelman, A.; Stoltz, B. M.; Bercaw, J. E.; Goldberg, K. I. *Organometallics* **2010**, *29*, 2176-2179.
(47) Oh, C. H.; Kim, J. S.; Jung, H. H. *J. Org. Chem.* **1999**, *64*, 1338-1340.
(48) Albrecht, M.; Schneider, M. *Synthesis* **2000**, *2000*, 1557-1560.
(49) Xiao, Z.-P.; Wang, Y.-C.; Du, G.-Y.; Wu, J.; Luo, T.; Yi, S.-F. *Synth. Commun.* **2010**, *40*, 661-665.
(50) Hodges, J. A.; Raines, R. T. *Org. Lett.* **2006**, *8*, 4695-4697.
(51) Woodward, L. A.; Glover, A. T. *Trans. Faraday Soc.* **1948**, *44*, 608-616.
(52) Sheldrick, G. M., "SADABS (version 2008/2001): Program for Absorption Correction for Data from Area Detector Frames", University of Göttingen, 2008.
(53) Dolomanov, O. V.; Bourhis, L. J.; Gildea, R. J.; Howard, J. A. K.; Puschmann, H. *J. Appl. Crystallogr.* **2009**, *42*, 339-341.
(54) Sheldrick, G. M. *Acta. Crys.* **2008**, *A64*, 112-122.

(55) Brandenburg, K. **1999**, DIAMOND. Crystal Impact GbR, Bonn, Germany.

CHAPTER 3

Selectivity for Hydrogenolysis vs. Hydrogenation with Rhodium and Iridium Catalysts in the Cleavage of Aryl Ethers as Models of Lignin

Abstract

Hydrogenolysis and hydrogenation reactions of ethers and phenols relevant to the degradation of lignin were studied with a precatalyst consisting of biscycloocteneiridium(I)chloride in neat substrate at 180 °C. Rh/C was tested for comparison. With limiting H_2, arene-rich cleaved products were isolated. At higher H_2 pressure, hydrocarbon products were major. More hydrogenolysis was observed with Ir than with Rh. The relative rates of hydrogenolysis followed the trend: diaryl ether > phenol > aryl-alkyl ether ≈ alcohol ≈ dialkyl ether. Addition of mesoporous silica facilitated acid-catalyzed dehydration of alcohols and alkyl ethers, leading to exhaustive deoxygenation and hydrogenation when coupled with H_2/Ir catalysis.

INTRODUCTION

Cleavage of the aryl C–O bond of aryl ethers represents a key transformation in the conversion of lignin to aromatic compounds useful as precursors in chemical synthesis or as fuel additives.[1] This transformation has been employed with homogeneous Ni catalysts for cross-coupling chemistry and for removal of oxygen-based directing groups with silanes.[2] Hydrogenolysis of aryl ethers was reported with Ni-N-heterocyclic carbene catalysts.[3] Mechanistic studies of intramolecular cleavage of aryl ether bonds has been studied with Rh(I)[4] and Ni(0).[4b,5] In the presence of micelles, hydrogenolysis/hydrogenation of aryl ethers was observed with Ni precursors.[6] A variety of heterogeneous catalysts have been investigated for the cleavage of aryl ethers. Systems based on Raney Ni,[7] $Ni(cod)_2$ (cod = 1,5-cyclooctadiene) and NaO^tBu,[8] Rh/C in supercritical CO_2,[9] Ni/SiO_2[10] have been reported. Additionally, hydrodeoxygenation of phenols was reported with Pd/C/acid[11] and $Ni/Nafion/SiO_2$ catalysts.[10,12] Although recent experiments have focused on less stringent conditions, aryl C–O bond cleavage often requires high temperatures or pressures.[1c,7b,13] Hydrogenolysis effects deoxygenation without consumption of additional hydrogen for conversion of arenes to saturated hydrocarbons.[14] An important selectivity consideration is the extent of hydrogenolysis vs hydrodeoxygenation leading to products with different applications. Herein we report Ir catalysts for the cleavage of aryl ethers and comparative studies of hydrogenolysis vs. hydrodeoxygenation with Ir and Rh.

We have previously reported on the mechanism of intra- and intermolecular aryl C–O bond cleavage facilitated by Ni.[5] Phosphine ligands were screened with Rh and Ir precursors for potential intermolecular C–O bond cleavage reactivity in neat

aryl ether substrate. $(Ir(COE)_2Cl)_2$ (coe = cyclooctene) was found to generate a catalyst that displays the desired reactivity in the presence of H_2 at 180 °C and in the absence of additional Lewis basic additives. Sulfided Ir/Al_2O_3 and $IrMo/Al_2O_3$ catalysts were reported to perform hydrogenolysis of diphenyl ether, albeit at much higher temperatures and pressures (350 °C, 137 atm H_2).[13b] Given the growing interest in the cleavage of aryl ethers relevant to biomass conversion, we investigated the behavior of the present Ir catalyst under a variety of conditions. For comparison, we also studied Rh/C, which has been studied previously. While in supercritical CO_2, C–O bond cleavage and hydrogenation of diphenyl ether to form cyclohexane and cyclohexanol has been observed,[9] with wood meal, in dioxane-water, phenolic products were obtained.[15] Since the products of cleavage of aryl ethers with Rh/C depend on reaction conditions and (or) nature of substrate, the Ir and Rh catalysts were studied under similar conditions.

Results and Discussion

Reactions were performed in batch mode in Schlenk tubes with Teflon stoppers. The catalyst was generated *in situ* from $(Ir(COE)_2Cl)_2$ upon heating in neat substrate. Generally, increased temperature favored hydrogenolysis (arene) products vs. hydrogenation (alkane) products. At 180 °C, with 3 mol % catalyst loading and moderate H_2 pressure, substantial amounts of arenes were generated; therefore, these conditions were further investigated for various catalysts and substrates. Under the conditions studied, a limiting amount (3.3 equiv., 1 atm; 13.3 equiv., 4 atm) of H_2 was present.

Arenes were the major cleavage products (60%, 1:5 PhOH:PhH) using $(Ir(COE)_2Cl)_2$ as a precatalyst.[16] (Entry 1, Table 3.1) Rh/C afforded lower arene generation (40%) with benzene (36%) as major product overall and cyclohexanol (34%) major among the hydrogenated products (Entry 2). Increasing H_2 pressure to 4 atm resulted in full hydrogenation of the ether cleavage products with both Ir and Rh catalysts (Entries 5, 6). Only 16% Cy_2O was observed with the Ir catalyst, whereas the yield of Cy_2O was 46% using Rh/C.

Further studies were focused on limiting H_2 amounts, allowing for interrogation of the relative levels of hydro-genolysis and hydrogenation/deoxygenation. The products of the hydrogenolysis/hydrogenation of Ph_2O were submitted to the same reaction conditions to better understand the observed selectivities (Table 3.1, Entries 9-23). For both the Rh- and Ir-catalyzed reactions, low conversions were observed with PhOCy and Cy_2O (Entries 9, 10, 12, 13).

Table 3.1. Hydrogenolysis/Hydrogenation of Diphenyl Ether (A) and Its Derivatives (B-F).

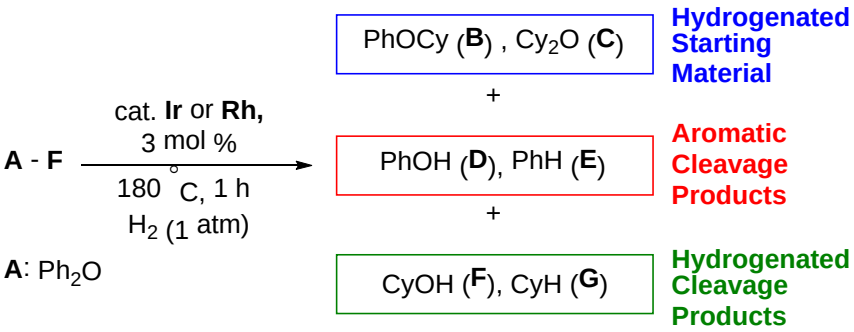

Entry	Catalyst	Substrate	B, %	C, %	D, %	E, %	F, %	G, %
1	**Ir**	**A**	2	3	9	50	16	12
2	**Rh**	**A**	17	6	4	36	34	5
3	**Ir'**	**A**	3	1	10	46	4	24
4	**Ir***	**A**	0	2	10	40	0	27
5[a]	**Ir**	**A**	0	16	0	0	23	59
6[a]	**Rh**	**A**	0	46	0	0	26	25
7[a]	**Ir'**	**A**	0	6	0	2	3	85
8[a]	**Ir***	**A**	0	0	0	0	0	102
9	**Ir**	**B**	92	2	0	3	0	1
10	**Rh**	**B**	65	15	0	3	11	1
11	**Ir***	**B**	0	6	5	15	0	56
12	**Ir**	**C**	0	72	0	0	9	10
13	**Rh**	**C**	0	75	0	0	11	14
14	**Ir***	**C**	0	0	0	0	0	99
15	**Ir**	**D**	0	1	4	44	24	20
16	**Rh**	**D**	0	17	0	2	70	15
17	**Ir***	**D**	0	6	0	31	0	54
18	**Ir**	**E**	0	0	0	53	0	44
19	**Rh**	**E**	0	0	0	8	0	95
20	**Ir***	**E**	0	0	0	20	0	84
21	**Ir**	**F**	0	26	0	0	70	4
22	**Rh**	**F**	0	16	0	0	38	37
23	**Ir***	**F**	0	0	0	0	0	97

[a] 4 atm H_2 used. **Ir**: $(Ir(COE)_2Cl)_2$. **Rh**: Rh/C, 5 wt%. **Ir'**: $[(coe)_2IrCl]_2$ and MCM-41 (silica, mesostructured). **Ir***: $(Ir(COE)_2Cl)_2$ and Al-MCM-41 (aluminosilicate, mesostructured). Conversions: entry 1 – 95%; 3 – 94%, 4 – 92%, 2, 5-8 - 100%; for all other entries, recovered starting material shaded. Reactions neat in 1.000 mmol substrate. Quantification of yields by GC after extraction with 0.025 M solution of *n*-tridecane in Et_2O using *n*-tridecane as an external standard. Reactions run in

duplicate; std. dev. < 5%. 1 atm H_2 = 3.3 equiv., 4 atm H_2 = 13.3 equiv. H_2 relative to substrate. See Experimental Section for further details.

A substantial portion of PhOH was converted to PhH (44%) with the Ir catalyst, while Rh/C led almost exclusively to hydrogenation (Entries 15, 16). High conversion of PhH to CyH (95%) was observed with Rh/C compared to moderate conversion using Ir (44%, Entries 18-19). Some etherification was observed from CyOH to afford Cy_2O for both Ir and Rh/C (26% and 16%, respectively; Entries 21, 22).

Figure 3.1. Proposed Mechanism for Hydrogenolysis/Hydrogenation Pathways for Ir and Rh Catalysts.

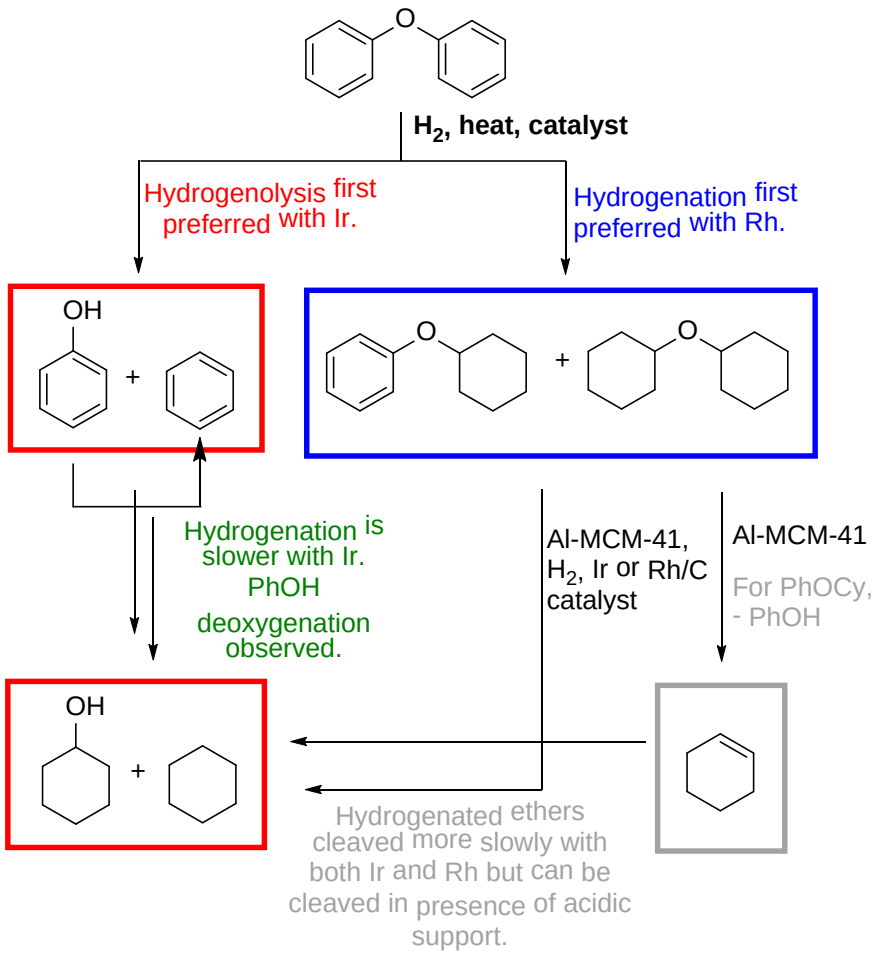

Trials with PhH as substrate indicate that Ir performs hydrogenation more slowly compared to Rh/C, allowing for longer residence times for benzene. With PhOH, Rh/C again performs primarily hydrogenation. Ir leads to cleavage of the aryl C–O bond of phenol to give benzene, a process that is competitive with hydrogenation. This phenol hydrogenolysis accounts for the higher yield of PhH relative to that of PhOH in reactions with Ph_2O and represents a relatively mild method for total deoxygenation of aryl ethers with a preference for arene products. Hydrogenolysis of phenol has been previously reported for heterogenous Mo[17], Pd[11,18], and Pt/H_2SO_4[19] catalysts.

Given that alkyl ethers are cleaved slowly under these conditions, the mechanism of ether cleavage is proposed to first involve initial hydrogenolysis of the an aryl C–O bond as the major pathway. (Figure 3.1) If hydrogenation occurs first, the resulting alkyl ethers are significantly less reactive toward reductive cleavage. Since Rh is a better hydrogenation catalyst, the products funnel toward hydrogenated ether with lower yields of the cleaved products. The arenes formed upon aryl ether cleavage are further hydrogenated with Rh/C, while with Ir, hydrogenolysis of phenol to give benzene is a significant reaction pathway. Overall, the Ir catalyst leads to more cleavage as well as higher yields of arene products.

Mesoporous silica (MCM-41) and aluminosilicate (Al-MCM-41) were added to reaction mixtures to act as support for the *in situ* generated Ir catalyst. The CyOH:CyH ratio changed significantly: without additive, a 4:3 ratio was observed; with MCM-41, 1:6; with Al-MCM-41, only CyH was observed. These data suggest conversion of CyOH to CyH in the presence of mesoporous silica. In control experiments, both CyOH and Cy_2O were converted to cyclohexene in the presence of Al-MCM-41 under N_2 at 180 °C

in the absence of Ir. Under these conditions, 20% conversion of PhOCy to PhOH and cyclohexene was observed.

Table 3.2. Hydrogenolysis/Hydrogenation of *o*-Methyl Phenol.

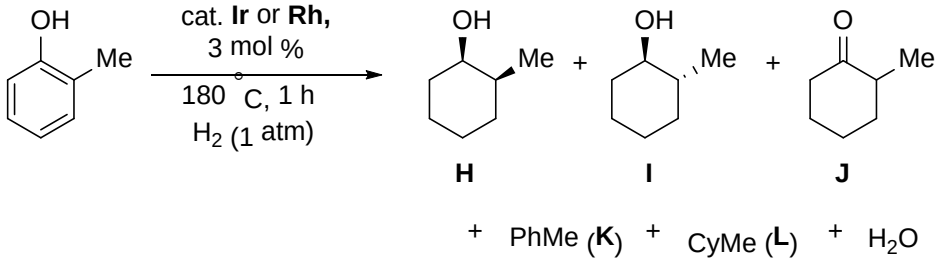

Entry	Catalyst	Conversion, %	**H**, %	**I**, %	**J**, %	**K**, %	**L**, %
1	**Ir**	85	4	4	9	40	9
2	**Rh**	100	14	23	42	1	14

Ir: $(Ir(COE)_2Cl)_2$. **Rh**: Rh/C, 5 wt%. Reactions neat in 1.0 mmol substrate. Quantification of yields by GC after extraction with 0.025 M solution of *n*-tridecane in Et_2O using *n*-tridecane as an external standard. Reactions run in duplicate; std. dev. < 5%. 1 atm H_2 =3.3 equiv. See ***SI*** for further details.

Solid acids are known to mediate alkyl C–O bond cleavage of ethers and alcohols.[11b,20] In the presence of Ir/Al-MCM-41 and H_2, substrates CyOH or PhOH lead to CyH (Table 3.1; Entries 17 and 23); for PhOH, CyOH is not observed. These data indicate that subsequent to alkyl ether cleavage and alcohol dehydration facilitated by the acidic support, the resulted olefin is hydrogenated. Increasing H_2 pressure to 4 atm resulting in full conversion of Ph_2O to CyH in the Ir/Al-MCM-41 system (Table 3.1, Entry 8). Consistent with our control reactions, good conversion of otherwise recalcitrant PhOCy and Cy_2O to cleavage products was observed with Ir and Al-MCM-41 (Table 3.1, Entries 11 and 14). Thus, mesoporous silica complements hydrogenolysis by converting hydrogenated but not cleaved products that react slowly with Rh and Ir catalysts (alkyl ethers, alcohols) to alkenes and aromatics.

Table 3.3. Hydrogenolysis/Hydrogenation of Anisole, Ethoxybenzene, and Isopropoxybenzene.

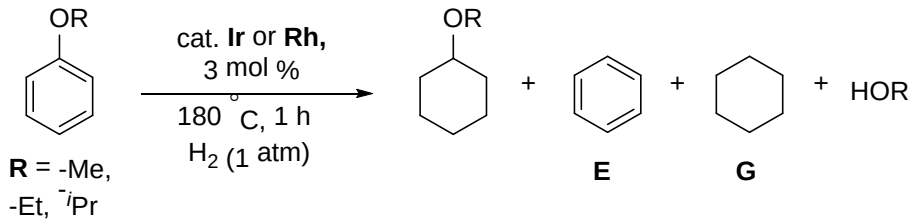

Entry	Ru	Catalyst	Conversion (%)	E, %	Gm %
1	-Me	**Ir**	31	14	5
2	-Me	**Rh**	26	3	0
3	-Et	**Ir**	59	27	9
4	-Et	**Rh**	88	9	14
5	-iPr	**Ir**	65	21	23
6	-iPr	**Rh**	92	5	17

Ir: $(Ir(COE)_2Cl)_2$. **Rh**: Rh/C, 5 wt%. Reactions neat in 1.0 mmol substrate. Quantification of yields by GC after extraction with 0.025 M solution of *n*-tridecane in Et_2O using *n*-tridecane as an external standard. Reactions run in duplicate; std. dev. < 5%. 1 atm H_2 = 3.3 equiv. See **Experimental Details** for further details.

Reactions with *o*-methyl phenol and phenyl alkyl ethers (Tables 3.2 and 3.3) were pursued to determine the effect of increasing steric bulk on the product distribution. Products corresponding to C–O bond cleavage were major with the Ir catalyst (40% PhMe, 9% CyMe). Conversion to deoxygenation products was low in the case of Rh (15% for PhMe and CyMe combined). Phenyl alkyl ethers with larger alkyl groups showed increased conversion for both Ir and Rh catalysts. This could be a consequence of the increased boiling points of the substrates within the series, with the lighter substrates being heated to above their boiling temperature and likely partitioning substantially in the gas phase. For each substrate, the Ir catalyst shows more conversion to the deoxygenated arene product (PhH) than the Rh catalyst (19 vs.

3% for methyl, 36 vs. 23% for ethyl, and 44 vs. 22% *i*-propyl substituents, respectively). These data further highlight the difference in selectivity between the two systems, with preference for hydrogenolysis vs. hydrogenation for Ir compared to the Rh catalyst. A labeling study to determine if aryl-alkyl ether cleavage proceeded by a mechanism of oxidative addition, β-hydride abstraction, and reductive elimination as previously reported by our group[5] was complicated by deuterium scrambling. (see *Experimental Details*, "Additional Experiments")

Conclusions

In summary, catalytic hydrogenolysis and hydrogenation of aryl-aryl ethers and aryl-alkyl ethers were studied using commercially available precursors. Rh- and Ir-catalyzed systems were both shown to hydrogenolyze aryl-aryl ethers. Investigations into the mechanism of these reactions show that alcohols, aryl alkyl ethers, and dialkyl ethers are more difficult to cleave than their diaryl ether counterparts. Thus, an effective catalyst for aryl ether cleavage carries out hydrogenolysis more rapidly than hydrogenation. Moderate amounts of arene products were observed in the case of limiting H_2 pressure and could be isolated prior to hydrogenation; hydrocarbon products could be obtained using higher H_2 pressures (4 atm). Cleavage of the aryl C–O bond of phenol by iridium was observed, demonstrating full deoxygenation of aryl ethers. In the presence of mesoporous silica, acid-catalyzed cleavage of alkyl-ethers occurred complementing the reactivity of the Ir-only catalyst and leading to exhaustive deoxygenation and hydrogenation of diaryl ethers.

EXPERIMENTAL SECTION

General considerations

Substrates diphenyl ether, phenyl cyclohexyl ether, phenol, benzene, cyclohexanol, *o*-cresol, anisole, and *tert*-butylbenzene were purchased commercially. Dicyclohexyl ether[21] was synthesized according to literature. Alkyl-aryl ethers ethoxybenzene and isopropoxybenzene were synthesized from phenol through substitution with alkyl iodides (ethyl iodide and isopropyl iodide) following an adapted literature procedure[22] and matched previously reported spectra (PhOEt,[23] PhO^{i}Pr[24]). *tert*-butylbenzene-d_1 was prepared from 1-bromo-4-(*tert*-butyl)benzene from treatment with *n*-BuLi followed by quenching with excess D_2O and matched previously reported spectra.[25] Commercially available cyclohexane, *cis*-2-methylcyclohexanol, *trans*-2-methylcyclohexanol, 2-methylcyclohexanone, toluene, methylcyclohexane were used as received as standards for GC calibration. Manipulations were conducted in a N_2-filled glovebox or using standard Schlenk technique under N_2 unless otherwise specified. Alumina and 3 Å molecular sieves were activated by heating under vacuum at 200 °C for at least 12 h prior to use. Silica, mesostructured, MCM-41 type (hexagonal) was purchased from Sigma-Aldrich: unit cell size = 4.5 - 4.8 nm; pore size = 0.98 cm^3/g pore volume, 2.1 – 2.7 nm pore size; spec. surface area ca. 1000 m^2/g. Aluminosilicate, mesostructured, MCM-41 (hexagonal): aluminum, ca. 3%; unit cell size = 4.6 – 4.8 nm; pore size = 1.0 cm^3/g pore volume, 2.5 – 3 nm pore size; spec. surface area ca. 940 – 1000 m^2/g. Mesostructured silica ("MCM-41") and mesostructured aluminosilica ("Al-MCM-41") were heated in an oil bath under vacuum. This oil bath was and held at 150 °C for 16 h before use. Celite® was purchased commercially and used as received. Et_2O used in catalyst loading and

benzene used as substrate were dried by Grubbs' method[26] and placed over 3 Å molecular sieves prior to use. Diphenyl ether, phenyl cyclohexyl ether, anisole, dicyclohexyl ether, ethoxybenzene, and isopropoxybenzene were stirred over CaH_2 overnight, filtered through alumina, and stored over 3 Å molecular sieves in a nitrogen-filled glovebox prior to use.

Analysis of reactions with substrates *tert*-butylbenzene and *o*-cresol by gas chromatograph was performed on an Agilent 6850 FID gas chromatograph equipped with a flame ionization detector and DB-Wax polyethylene glycol capillary column. Runs were performed using the following program: hold at 40 °C for 4 minutes, ramp temperature at 50 °C min^{-1} to 90 °C, hold at 90 °C for 4 minutes, ramp temperature at 75 °C min^{-1} to 300 °C, hold at 300 °C for 4 minutes.

Analysis of reactions with all other substrates by gas chromatography was performed on an Agilent 6890N instrument using a flame ionization detector and DB-1 capillary column (10 m length, 0.10 mm diameter, 0.40 μm). Runs used the following program: hold at 40 °C for 3 minutes, ramp temperature at 50 °C min^{-1} to 290 °C, hold at 290 °C for 5 minutes.

Analysis of reactions with all substrates by gas chromatograph mass spectrometry (GC-MS) was performed on an Agilent 6890 instrument equipped with an HP-5MS 30 m x 0.25 mm x 0.50 μm capillary column (Agilent). The GC was interfaced to an Agilent 5973N mass selective detector.

Procedures for Hydrogenolysis/Hydrogenation Studies. Procedure B was used for protic substrates phenol, cyclohexanol, and *o*-cresol; Procedure A was used for all other substrates.

Hydrogenolysis/Hydrogenation Procedure A. In a N_2-filled glovebox, an 80 mL Schlenk tube (ca. 5 mm x 16 mm) fitted with a Teflon screw cap was charged with a stir bar (3 x 12.7 mm). 5 wt % Rh/C (61.7 mg, 0.030 mmol, 0.03 equiv.) or $((coe)_2IrCl)_2$ (13.4 mg, 0.015 mmol, 0.015 equiv.) was transferred to the reaction vessel as a suspension in a minimum of Et_2O. Addition of a minimum of Et_2O and transfer of the resulting suspension was completed once more to ensure near-quantitative transfer of catalyst. For reactions with MCM-41 or Al-MCM-41, a 20 mL scintillation vial was charged with a stir bar, mesoporous silica (100 mg), $(Ir(COE)_2Cl)_2$ (13.4 mg, 0.015 mmol, 0.015 equiv.), and 5 mL Et_2O to afford an orange solution with white precipitate. This solution was stirred for a minimum of 3 h. The suspension and stir bar were transferred to the reaction vessel. Addition of a minimum of Et_2O to the scintillation vial and transfer of the resulting suspension was completed to ensure near-quantitative transfer of catalyst. Solvent was removed from the reaction vessel under reduced pressure. For reactions with $(Ir(COE)_2Cl)_2$, an orange powder was observed. For reactions with $(Ir(COE)_2Cl)_2$ and mesoporous silica, a light orange powder was observed. For reactions with Rh/C, a black powder was observed. Substrate (1.00 mmol) was then added using a 250 µL syringe. The reaction vessel was sealed and removed from the glovebox. On a Schlenk line, the reaction vessel was cooled to 77 K with liquid nitrogen and the headspace was evacuated. For the addition of *ca.* 4 atm H_2, *ca.* 3.3 equiv., the evacuated reaction vessel was pressurized at 77 K, then sealed and warmed to room temperature. For the addition of *ca.* 1 atm H_2, *ca.* 13.3 equiv., the reaction vessel was sealed, allowed to warm to room temperature, then pressurized with *ca.* 1 atm H_2 and sealed again. The reaction vessel was subsequently placed in a silicone oil bath pre-heated to 180 °C such that only a small amount of the Schlenk

tube below the level of the Teflon screw cap was not submerged in oil. The reaction was left stirring vigorously in the oil bath for 1 h. After 1 h, the vessel was removed from the oil bath and allowed to cool for 10 min. A suspension of black precipitate in a colorless solution was observed. The reaction vessel was then chilled for 15 min. by submerging in an ice water bath such that only a small amount of the Schlenk tube below the level of the Teflon screw cap was not submerged in ice water. The reaction vessel was then opened and 9 mL of a 0.025 M solution of *n*-tridecane in Et_2O was added. The reaction vessel was resealed, shaken vigorously for 15 s, then the reaction mixture was pushed through a plug of Celite. 0.4 mL of this solution was further diluted with 0.8 mL of a 0.025 M solution of *n*-tridecane in Et_2O. Yields were then determined by GC. Reported yields are the average of duplicate runs. On average, standard deviations between runs were below 5%.

Hydrogenolysis/Hydrogenation Procedure B. Procedure B is similar to Procedure A, but the addition of substrate differs. For Procedure B, substrates were added to the reaction vessel charged with rhodium or iridium catalyst on a Schlenk line under a counter flow of N_2 at room temperature. The rest of Procedure A was then followed as described above.

Additional Experiments: Hydrogenolysis/Hydrogenation of *tert*-Butylbenzene-d_1

Table 3.4. Hydrogenolysis/Hydrogenation of *tert*-Butylbenzene.

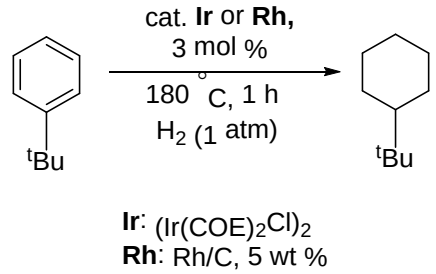

		GC Yields		
Entry	Catalyst	Conversion, %	Hydrogenated Product	Mass Balance
1	**Ir**	73	67	94
2	**Rh**	96	96	100

Figure 3.2. Proposed Mechanisms for Hydrogenolysis of Aryl-Alkyl Ethers with and without H_2.

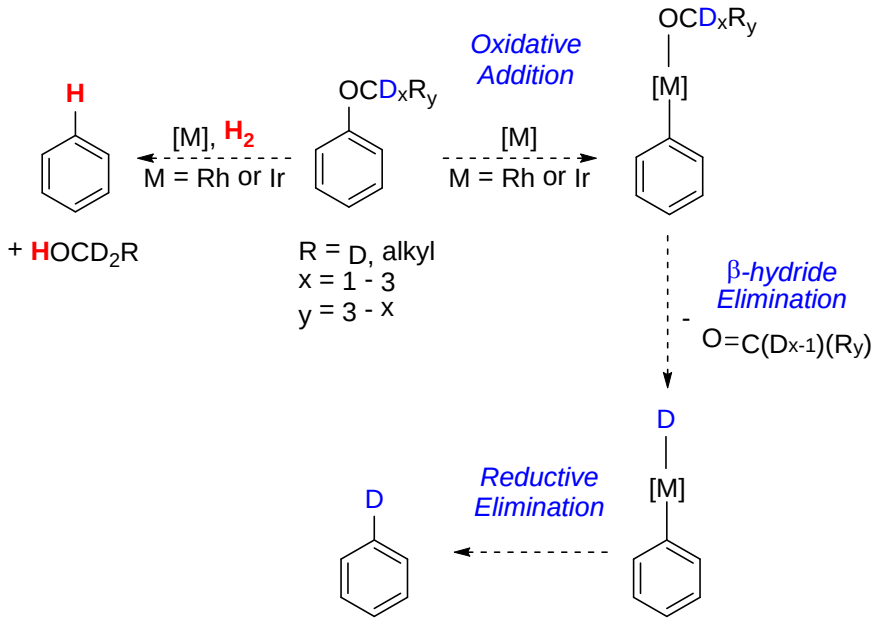

A deuterium labeling study was designed to determine if hydrogenolysis of aryl-alkyl ethers proceeds through addition of H_2 across the aryl C-O bond or through

oxidative addition, β-hydride elimination, and reductive elimination (without H_2) as previously reported by our group for nickel species.[5]

As a control, a d_1-labeled aromatic (*tert*-butylbenzene-d_1) was subjected to standard reaction conditions (180 °C, 1 atm H_2) for 30 min. to determine if scrambling would preclude identification of d_1-labeled aromatic products of hydrogenolysis/hydrogenation of labeled aryl-alkyl ethers. This reaction was performed according to *Hydrogenolysis/Hydrogenation Procedure B*. The product extracted in Et_2O/*n*-tridecane was diluted to a concentration of *ca.* 3 μmol and analyzed by GC-MS. Under hydrogenolysis/hydrogenation reaction conditions for 30 min., *tert*-butylbenzene-d_1 (m/z = 135) incorporates H atoms to afford *tert*-butylbenzene-d_0 (m/z = 134) and incorporates D atoms (up to m/z = 138). Scrambling of the deuterium labels thus prevented exclusion of a mechanistic pathway through labeling of aryl-alkyl ethers.

Figure 3.3. Hydrogenation of *tert*-Butylbenzene-d_1.

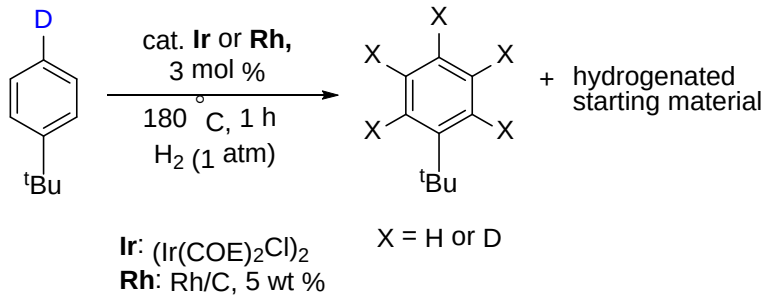

Additional Experiments: Hydrogenolysis/Hydrogenation of Diphenyl Ether: Mercury Drop Test

Table 3.5. Hydrogenolysis/Hydrogenation of Diphenyl Ether: Hg^0 Drop Test.[16b]

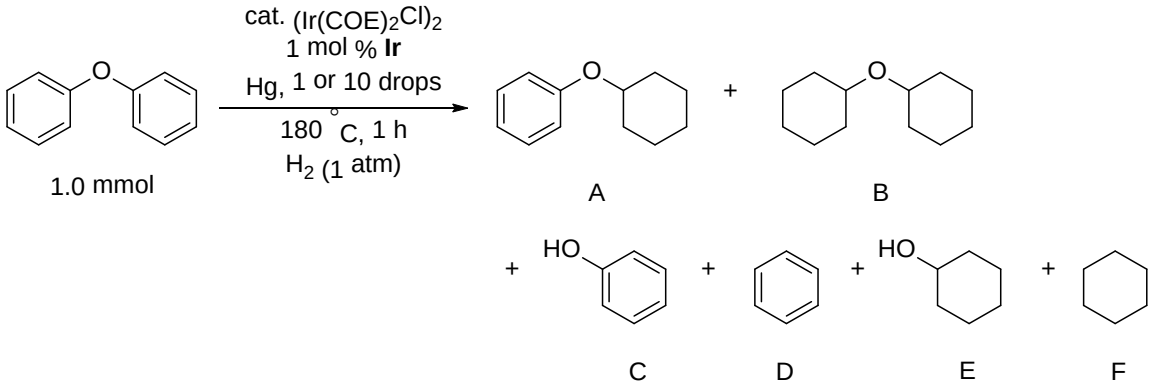

			GC Yields (%)						
			Hydrogenated Ether		Arene Cleavage Products		Hydrogenated Cleavage Products		Mass Balance
Entry	Hg	Conversion	A	B	C	D	E	F	
1	1 drop	21	2	0	0	1	0	2	85
2	10 drops	0	0	0	0	0	0	0	90

Hg added on Schlenk line using a glass pipet under counterflow of N_2 before pressurizing with H_2.

References

(1) (a) Rinaldi, R.; Schuth, F. *Energy Environ. Sci.* **2009**, *2*, 610-626; (b) Zakzeski, J.; Bruijnincx, P. C. A.; Jongerius, A. L.; Weckhuysen, B. M. *Chem. Rev.* **2010**, *110*, 3552-3599; (c) Pandey, M. P.; Kim, C. S. *Chem. Eng. Technol.* **2011**, *34*, 29-41.
(2) (a) Wenkert, E.; Michelotti, E. L.; Swindell, C. S. *J. Am. Chem. Soc.* **1979**, *101*, 2246-2247; (b) Wenkert, E.; Michelotti, E. L.; Swindell, C. S.; Tingoli, M. *J. Org. Chem.* **1984**, *49*, 4894-4899; (c) Dankwardt, J. W. *Angew. Chem. Int. Ed.* **2004**, *43*, 2428-2432; (d) Tobisu, M.; Shimasaki, T.; Chatani, N. *Angew. Chem. Int. Ed.* **2008**, *47*, 4866-4869; (e) Rosen, B. M.; Quasdorf, K. W.; Wilson, D. A.; Zhang, N.; Resmerita, A.-M.; Garg, N. K.; Percec, V. *Chem. Rev.* **2010**, *111*, 1346-1416; (f) Tobisu, M.; Yamakawa, K.; Shimasaki, T.; Chatani, N. *Chem. Commun.* **2011**, *47*, 2946-2948; (g) Cornella, J.; Gómez-Bengoa, E.; Martin, R. *J. Am. Chem. Soc.* **2013**, *135*, 1997-2009.
(3) Sergeev, A. G.; Hartwig, J. F. *Science* **2011**, *332*, 439-443.
(4) (a) van der Boom, M. E.; Liou, S.-Y.; Ben-David, Y.; Vigalok, A.; Milstein, D. *Angew. Chem. Int. Ed. Engl.* **1997**, *36*, 625-626; (b) van der Boom, M. E.; Liou, S.-Y.; Ben-David, Y.; Shimon, L. J. W.; Milstein, D. *J. Am. Chem. Soc.* **1998**, *120*, 6531-6541.
(5) Kelley, P.; Lin, S.; Edouard, G.; Day, M. W.; Agapie, T. *J. Am. Chem. Soc.* **2012**, *134*, 5480-5483.
(6) Samant, B. S.; Kabalka, G. W. *Chem. Commun.* **2012**, *48*, 8658-8660.
(7) (a) Chandler, G. S.; Sasse, W. H. F. *Aust. J. Chem.* **1963**, *16*, 20-30; (b) Wang, X.; Rinaldi, R. *ChemSusChem* **2012**, *5*, 1455-1466.
(8) Sergeev, A. G.; Webb, J. D.; Hartwig, J. F. *J. Am. Chem. Soc.* **2012**, *134*, 20226-20229.
(9) Chatterjee, M.; Ishizaka, T.; Suzuki, A.; Kawanami, H. *Chem. Commun.* **2013**, *49*, 4567-4569.
(10) He, J.; Zhao, C.; Lercher, J. A. *J. Am. Chem. Soc.* **2012**, *134*, 20768-20775.
(11) (a) Zhao, C.; He, J.; Lemonidou, A. A.; Li, X.; Lercher, J. A. *J. Catal.* **2011**, *280*, 8-16; (b) Zhao, C.; Lercher, J. A. *ChemCatChem* **2012**, *4*, 64-68.
(12) (a) Zhao, C.; Kou, Y.; Lemonidou, A. A.; Li, X.; Lercher, J. A. *Chem. Commun.* **2010**, *46*, 412-414; (b) Zhao, C.; Kasakov, S.; He, J.; Lercher, J. A. *J. Catal.* **2012**, *296*, 12-23.
(13) (a) Petrocelli, F. P.; Klein, M. T. *Ind. Eng. Chem. Res.* **1985**, *24*, 635-641; (b) Shabtai, J.; Nag, N. K.; Massoth, F. E. *J. Catal.* **1987**, *104*, 413-423.
(14) Elliott, D. C. *Energy Fuels* **2007**, *21*, 1792-1815.
(15) (a) Pepper, J. M.; Fleming, R. W. *Can. J. Chem.* **1978**, *56*, 896-898; (b) Sudo, K.; Mullord, D. J.; Pepper, J. M. *Can. J. Chem.* **1981**, *59*, 1028-1031.
(16) (a) A Hg drop test was conducted to determine if a homogenous Ir complex or heterogenous Ir particulate was responsible for the observed reactivity. In the presence of a single drop of mercury, 20% conversion of Ph_2O to CyH, CyOH, and Cy2O was observed under 1 atm H_2 with Ir at 180 °C, compared to 95% conversion under identical conditions in the absence of Hg. With 10 drops of Hg, no conversion of Ph_2O was detected. This significant decrease in activity with added Hg suggests a heterogenous species is catalytically operative, but does not completely rule out homogenous catalysis; (b) Whitesides, G. M.; Hackett, M.; Brainard, R. L.; Lavalleye, J. P. P. M.; Sowinski, A. F.; Izumi, A. N.; Moore, S. S.; Brown, D. W.; Staudt, E. M. *Organometallics* **1985**, *4*, 1819-1830.
(17) (a) Woodward, L. A.; Glover, A. T. *Trans. Faraday Soc.* **1948**, *44*, 608-616; (b) Kallury, R. K. M. R.; Tidwell, T. T.; Boocock, D. G. B.; Chow, D. H. L. *Can. J. Chem.*

1984, *62*, 2540-2545; (c) Jongerius, A. L.; Jastrzebski, R.; Bruijnincx, P. C. A.; Weckhuysen, B. M. *J. Catal.* **2012**, *285*, 315-323.
(18) Zhao, C.; Camaioni, D. M.; Lercher, J. A. *J. Catal.* **2012**, *288*, 92-103.
(19) (a) Bagnell, L. J.; Jeffery, E. A. *Aust. J. Chem.* **1980**, *33*, 2565-2569; (b) Bagnell, L.; Jeffery, E. *Aust. J. Chem.* **1981**, *34*, 697-698.
(20) Ploypradith, P.; Cheryklin, P.; Niyomtham, N.; Bertoni, D. R.; Ruchirawat, S. *Org. Lett.* **2007**, *9*, 2637-2640.
(21) Zhang, Y.-J.; Dayoub, W.; Chen, G.-R.; Lemaire, M. *Tetrahedron* **2012**, *68*, 7400-7407.
(22) Schmittel, M.; Ammon, H. *Synlett* **1999**, *6*, 750-752.
(23) Song, L. X.; Wang, H. M.; Guo, X. Q.; Bai, L. *J. Org. Chem.* **2008**, *73*, 8305-8316.
(24) Quach, T. D.; Batey, R. A. *Org. Lett.* **2003**, *5*, 1381-1384.
(25) Miura, Y.; Oka, H.; Yamano, E.; Morita, M. *J. Org. Chem.* **1997**, *62*, 1188-1190.
(26) Pangborn, A. B.; Giardello, M. A.; Grubbs, R. H.; Rosen, R. K.; Timmers, F. J. *Organometallics* **1996**, *15*, 1518-1520.

APPENDIX A

Homobimetallic Chromium Complexes for Olefin Oligomerization and Polymerization

Abstract

Towards improved selective oligomerization technologies for the preparation of α-olefins, the reactivity of mono- and bisphenoxyiminoquinolines in the presence of chromium, ethylene, and methylaluminoxane activators was explored. A series of Cr complexes supported by phenoxyiminoquinoline ligands was prepared. In oligomerization/polymerization trials, insoluble polyethylene as well as a distribution of oligomers was observed. Higher activity was observed with the bisphenoxyiminoquinoline scaffold versus the monometallic control. Synthesis of a triptycenyl-substituted phenoxyiminoquinoline, reported in the literature to display higher activity and selectivity for α-olefin in ethylene oligomerization is proposed to aid in optimization of reaction conditions for the newly synthesized compounds. Substitution of aryl linker and of the quinoline ring is proposed for engendering selectivity in the oligomers distribution observed in catalytic trials.

INTRODUCTION

Linear α-olefins (LAOs) are key building blocks in the large-scale synthesis of plastics, detergents, lubricants and related petrochemical products.[1] LAOs are produced industrially the oligomerization of ethylene or by the Fischer-Tropsch[2] process. High costs are incurred in the separation of mixtures of LAOs. Current industrial technology for the production of LAOs include full range, on-purpose, and upgrading strategies, which generate mixtures of LAOs, selectively generate one LAO, or convert a hydrocarbon feed to a desired LAO product, respectively.[3] Production of insoluble higher molecular weight polymers necessitates halting an industrial process to remove the generated polymer and wastes hydrocarbon feedstocks. Distillation can be effective in the separation of olefins of different length but mixtures of internal olefins are difficult to separate from one another.[1] Thus, the development of methods for production of single α-olefins in high purity is an important area of research.

The Shell Higher Olefin Process (SHOP) is used to produce ca. 1,000,000 tons/yr. of α-olefins in a Schulz-Flory distribution using Ni and diarylphosphinoacetic acids.[4] The Phillips trimerization system (Cr, 2,5-dimethyl-pyrrole, and alkylating agent) is used to produce ca. 50,000 tons/yr. of 1-hexene from ethylene.[1b,5] Dimerization of 1,3-butadiene has been employed by Dow Chemical to produce 1-octene selectively.[6] Ethylene tetramerization has also been reported and a commercial process using Cr and PNP donor ligands has been developed by Sasol.[7] Improved and complimentary processes for the selective oligomerization of LAOs from ethylene with little to no polymer production are highly desirable.

Gibson and co-workers have reported phenoxyiminoquinoline Cr compounds produce a near Schulz-Flury distribution of LAOs (the distribution is perturbed

Figure A.1a. Cossee Mechanism for Ethylene Oligomerization/Polmerization.

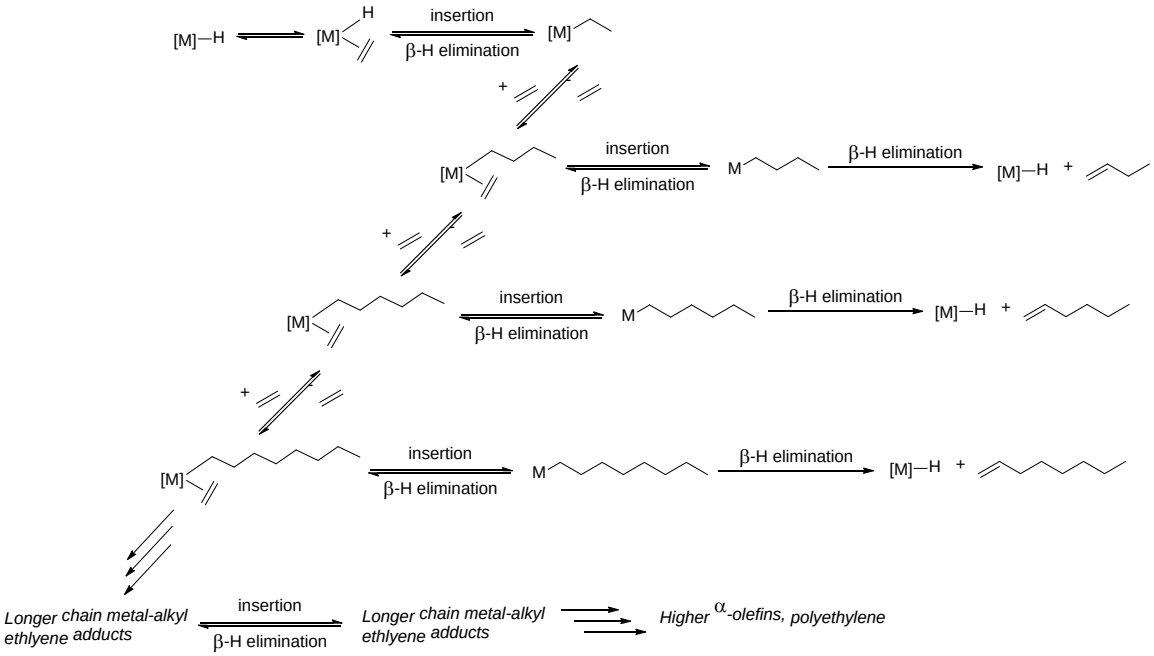

Figure A.1b. Metallocyclic Mechanism for Ethylene Oligomerization/Polmerization.

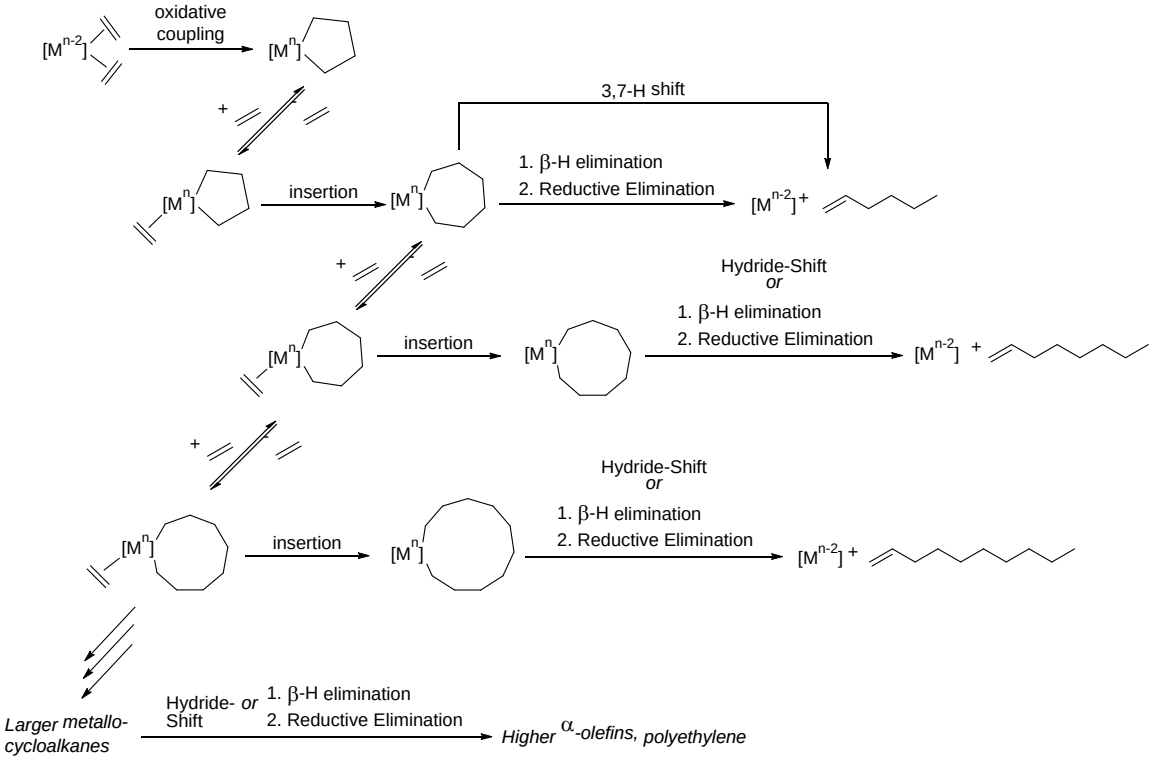

slightly by chain transfer to Al).[8] Deuterium-labeling experiments performed with a 1:1 C_2H_4:C_2D_4 mixture provided evidence for a metallocyclic versus Cossee mechanism (see Figure A.1a and A.1b).[8c,8d] In a high-throughput screen, oligomerization and/or polymerization activity was demonstrated to vary depending on phenoxyiminoquinoline substitution, with *ortho*-triptycenyl substitution affording a precatalyst (**39,** see Table A.1) with an activity of 7450 g·mmol^{-1}·h^{-1}·bar^{-1} with 98.9% LAO selectivity.[8a,8b] Our group has reported that a bimetallic effect inhibits the deactivation of dinickel bisphenoxyiminato compounds for ethylene polymerization by Lewis bases,[9] facilitates the insertion polymerization of polar monomers by dinickel bisphenoxyiminato without masking of the heteroatom group,[10] and increases the isotacticity of polypropylene and polyhexene generated by dizirconium amine bis(phenolate) versus previously reported monometallic analogues.[11] In a similar strategy, a bimetallic effect was envisioned to possibly encourage elimination of metallocycles of a specific size to result in production selective production of LAOs through ethylene oligomerization.

Figure A.2. Effect of Tethered Cr on Metallocycle Growth in Hypothetical Intermediate in Ethylene Oligomerization.

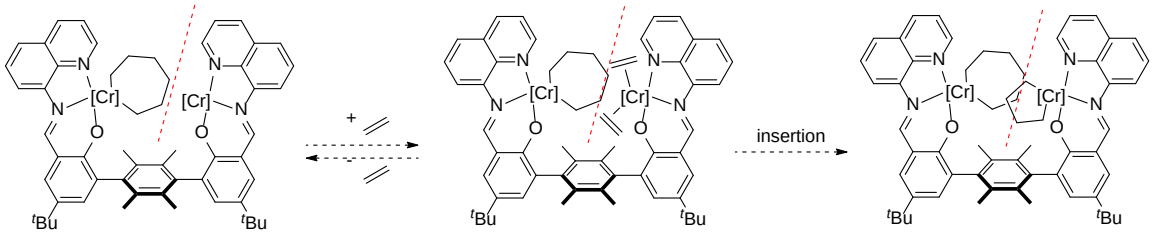

In this hypothesized mechanism, a growing Cr metallocycle would be influenced by the presence of a tethered Cr center (Figure A.2) bound to ethylene or a second

metallocycle. Elimination is envisioned to afford α-olefin as a single product or a smaller distribution than the pseudo Shulz-Flory distribution afford by the example reported by Gibson *et al.*

RESULTS & DISCUSSION

Salicylaldehyde **40**[9b] (Scheme A.1) and bissalicylaldehyde **41**[10] (Scheme A.2) were synthesized accorded to literature procedures. Neigishi coupling of bromo-4-(*tert*-butyl)-1-(methoxymethoxy)benzene and bromo-pentamethylbenzene or 1,4-dibromo-tetramethylbenzene afforded the desired biphenyl compound **42** and terphenyl compound **43**. *ortho*-Formylation installs the aldehyde moieties in both cases.

Scheme A.1. Synthesis of Salicylaldehyde 40.

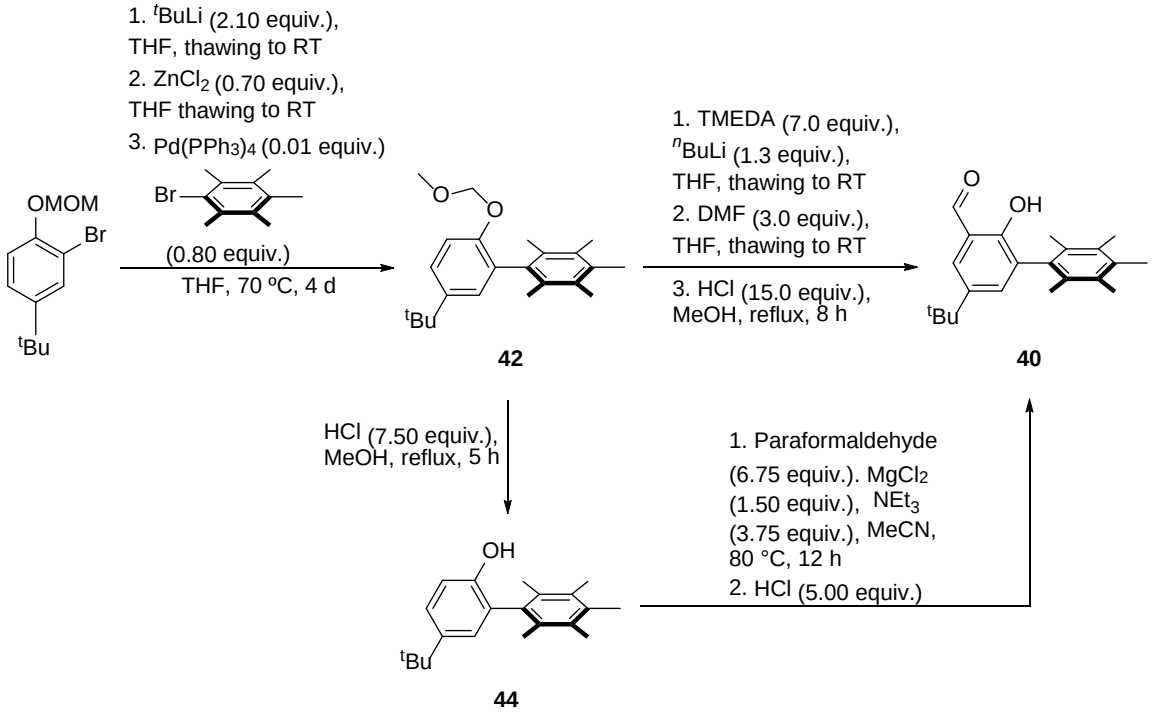

Scheme A.2. Synthesis of Bissalicylaldehyde 41.

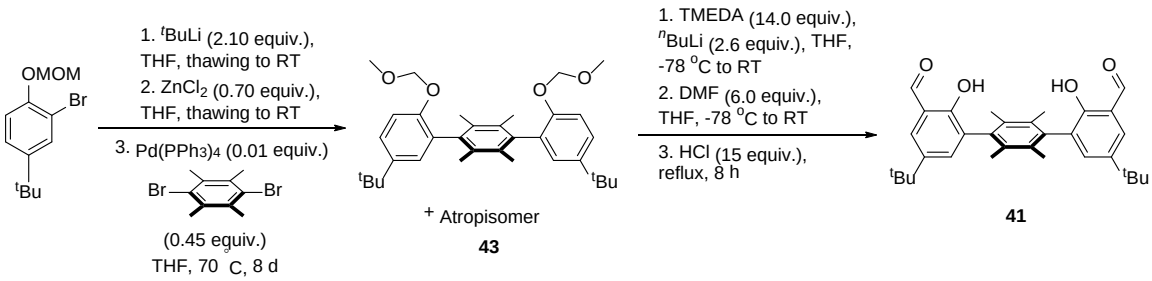

An alternative strategy was explored for the preparation of **40** through treatment of alcohol **44** with paraformaldehyde, $MgCl_2$, and NEt_3 in CH_3CN and provided the desired salicylaldehyde in good yield. This strategy is anticipated to be relevant for the preparation of bissalicyladehyde **41**.

Condensation of **40** and **41** with 8-aminoquinoline afforded desired iminophenoxyquinoline compounds **45** and **46**. Both heating in toluene in the presence of molecular sieves and refluxing in EtOH were effective in generating the desired proligands. A color change from orange to dark red was observed upon treatment of these iminophenoxyquinolines with $CrMeCl_2(THF)_3$[12] in THF. The putative Cr compounds were subsequently tested for oligomerization and polymerization activity in the presence of Al activator and pressure of C_2H_4 with Dr. Gyeongshin Choi (Table A.1). The triphenylsilyl-substituted compound **49**, prepared in our group by Dr. Choi, was tested due to similiarity to the reported triptycenyl compound **39**.

Scheme A.3. Synthesis of Phenoxyiminoquinoline Cr Complexes 47 and 48.

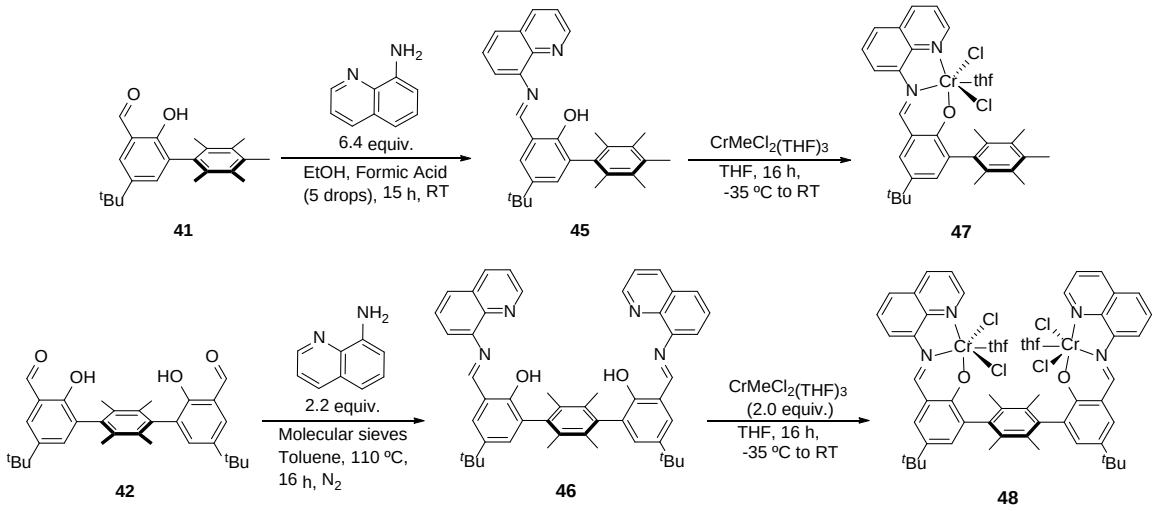

Stirring a solution of **49** in a Fischer-Porter vessel with a total volume of 10 mL of toluene and modified methylaluminoxane (MMAO, 100 equiv.) in heptane in the presence of C_2H_4 (60 PSI) at 25 °C for 1 h afforded only 23 mg of insoluble polyethylene (Table A.1, Entry 1). No α-olefins were detected by gas chromatography or mass spectrometry (GC or GC-MS) In contrast, compound **39** is reported in the literature to afford 98.9% α-olefin with an activity of 7450 $mg \cdot \mu mol^{-1} \cdot h^{-1} \cdot bar^{-1}$ (Table A.1). Activation of pre-catalyst **39** was accomplished through treatment with 2200 equiv. of a 10% solution of methylaluminoxane (MAO) in toluene.[8c] To test if the activity of **49** could be increased by changing the activation protocol, the experiment was repeated with pressurization with C_2H_4 followed by injection of MMAO solution in heptane via needle and syringe (Entry 2). In this experiment, only 12 mg of polymer was observed.

MAO was then tested under the catalytic conditions, given the literature precedent. MAO composition is known to vary with age and method of preparation.[13] Volatiles were removed from a 30% MAO solution in toluene under reduced pressure and the resulting powder was dried under reduced pressure at 110 °C. This powder was added to a solution of **49** in toluene in a Fischer-Porter vessel which was allowed to stir for *ca.* 15 min. before being pressurized with C_2H_4 (Entry 3). Gratifyingly, an order of magnitude increase in activity was observed – 627 mg of insoluble polyethylene was observed and trace amounts of a distribution (C_{10} – C_{24}) of α-olefin was observed. The activity of **49** in this reaction is still an order of magnitude less than that reported for compound **39**. It is worth noting that use of MAO in toluene solution may result in oligomerization with activity comparable to that reported for **39**. In

addition, synthesis of **39** and testing under identical reaction conditions is envisioned to aid in optimization of reaction conditions to provide higher activities.

Reaction condition were explored with **49** and solid MAO activator to screen for conditions which increase activity. The amount of MAO was doubled (600 equiv., Entry 4) given the literature precedent (2000 equiv.). The temperature was doubled (50 °C) to possibly encourage elimination of growing alkyl chains or metallocycles, depending on the operative mechanism (Entry 5). Decreasing the C_2H_4 pressure by a quarter was envisioned to slow the rate of alkyl chain or metallocycle growth, possible allowing for increased elimination, although activity was anticipated to suffer (Entry 6). No significant increase in activity was observed. A distribution of α-olefins (C_{10} – C_{24}) was observed with increased MAO loading and temperature. Low activity comparable to experiments with MMAO were observed with decreased ethylene pressure, and no α-olefins could be observed at the decreased pressure.

Given that a significant activity increase was not observed after changing MAO loading, temperature, or pressure, initial reaction conditions for oligomerization/polymerization reacts were pursued with compounds **47** and **48** (Entries 7 & 8) to provide evidence for a bimetallic effect on product distribution. With compound **47**, activity was on the same order of magnitude as for **49** (Entry 7). However, α-olefins were not observed by GC-MS with the less bulky pentamethyl phenyl group. With compound **48**, an activity increase was observed and oligomers could be detected by GC-MS. In this reaction, signals consistent with C_{10} - C_{32} products were detected. These data provide initial evidence of an effect of the tethered second phenoxyiminoquinoline moiety on oligomerization and polymerization activity.

Comparison of activity of **39** under the same reaction conditions is necessary to determine if the relatively lower activity is due to experimental conditions or inherent to the structure of compounds **47 - 49**. If activities can be increased, a 1:1 C_2H_4:C_2D_4 mixture can be used to determine if a metallocyclic mechanism is operative.

Table A.1. Oligomerization/Polymerization of Phenoxyiminoquinoline Cr compounds 47-49.

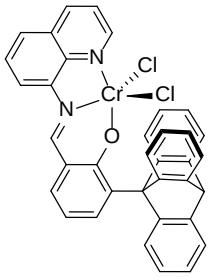

39[a]

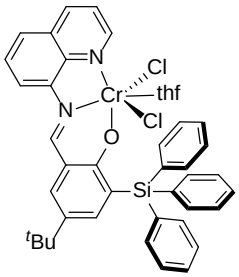

49

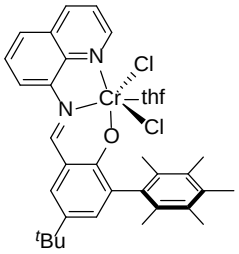

47

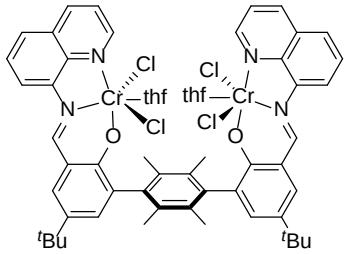

48

run	cat	p (psi)	T (ºC)	activator	equiv. of activator[b]	insoluble polymer (mg)	α-olefin[c]	acitivity (mg/μmol Cr•h•bar)
n/a	**39**[a]	58	50	MAO	2200		98.9%	7450
1	**49**	60	25	**MMAO**	100	23	–	*ca.* 1
2[d]	**49**	60	25	**MMAO**	100	12	–	*ca.* 1
3	**49**	60	25	**MAO**	300	627	C_{10} ~ C_{24}	*ca.* 50[f]
4	**49**	60	25	MAO	**600**	354	C_{10} ~ C_{24}	*ca.* 30[f]
5	**49**	60	**50**	MAO	300	431	C_{10} ~ C_{24}	*ca.* 40[f]
6	**49**	**15**	25	MAO	300	34	–	*ca.* 10
7	**47**	60	25	MAO	300	357	–	*ca.* 30
8[e]	**48**	60	25	MAO	200	1652	C_{10} ~ C_{32}	*ca.* 150[f]

Reaction conditions: toluene (10 mL), 3 μmol catalyst, 1 h, Fischer-Porter vessel. Catalyst was treated by MAO or MMAO before pressurization of Fischer-Porter vessel with ethylene. [a] Reported by Gibson *et al.* Organometallics **2009**, *28*, p. 7033.[8d] [b] Based on Cr. [c] Detected by GC and GC-MS. [d] MMAO was added under ethylene pressure. [e] 1.5 μmol catalyst was used. [f] Estimated by comparison of GC-MS peak height of adamantane peaks to oligomer peaks. Calibration curves were not calculated; oligomer yield is approximate.

If a metallocycle mechanism is operative, extension of the tether from a tetraphenyl linker to an anthracenyl linker may prevent expansion of these metallocycle to afford a wide distribution of oligomers (e. g., C_{10} – C_{32}). Substitution[14] at the 2-position of 8-aminoquinoline has been reported and may also inhibit metallocycle expansion. Increasing steric bulk may be effective in the generation of a smaller distribution of oligomers regardless of whether or not a metallocyclic mechanism is operative.

CONCLUSIONS:

Phenoxyiminoquinoline proligands were prepared for use in Cr-catalyzed olefin oligomerization. Metallation with $CrMeCl_2(THF)_3$ afforded several new compounds. Ethylene oligomerization and polymerization activity (*ca.* 500 $mg \cdot \mu mol^{-1} \cdot h^{-1} \cdot bar^{-1}$) was detected using solid MAO as activator. An order of magnitude decrease in oligomerization and polymerization activity was observed by changing activator (MAO to MMAO) or reducing pressure (60 to 15 PSI). Activities are an order of magnitude lower than those reported for a reported triptycenyl-substituted phenoxyiminoquinoline system reported to be 98.9% selective for generation of a pseudo Schulz-Flory distribution of α-olefins. Preparation of a novel dichromium compound supported by a rigid terpenyl linker was envisioned to afford a precatalyst that would limit metallocycle growth in ethylene oligomerization and afford α-olefins with high selectivity. Use of a putative bimetallic phenoxyiminoquinoline Cr compound resulted in higher activity but a distribution of oligomers (C_{10} – C_{32}) was observed. Changing of activator (MAO in toluene is reported) and testing the experimental setup with the related triptycenyl-substituted phenoxyiminoquinoline Cr compound is anticipated to allow for optimization of oligomerization activity for the newly synthesized compounds. If activity of compounds compares with reported examples under optimized conditions, introduction of increased steric bulk through substitution of the 2-position of the quinoline ring or use of an extended linker between phenoxyiminoquinoline donors (e.g., napthyl or anthracenyl) may facilitate elimination of oligomers of specific carbon length, engendering selectivity desired in the oligomerization reaction.

EXPERIMENTAL SECTION:

General considerations

Unless otherwise indicated, reactions performed under inert atmosphere were carried out in oven-dried glassware in a glovebox under a N_2 atmosphere purified by circulation through RCI-DRI 13X-0408 Molecular Sieves 13X, 4x8 Mesh Beads and BASF PuriStar® Catalyst R3-11G, 5x3 mm (Research Catalysts, Inc.). Manipulations were conducted in a N_2-filled glovebox or using standard Schlenk technique under N_2 unless otherwise specified. 2-bromo-4-(*tert*-butyl)phenol[15], 1,4-bis(2'-hydroxyl-3'-formyl-5'-*tert*-butyl)-tetramethylbenzene (**42**),[10] 3-pentamethylphenyl-5-*tert*-butyl-2-hydroxyl-benzaldehyde (**41**),[9b] 1-bromo-2,3,4,5,6-pentamethylbenzene[16] and $CrCl_2Me(THF)_3$[12] were synthesized according to literature procedure. 2-bromo-4-(*tert*-butyl)-1-(methoxymethoxy)benzene was synthesized from 2-bromo-4-(*tert*-butyl)phenol through protection with chloromethyl methyl ether[17] and matched previously reported spectra.[9b] (CAUTION: Chloromethyl methyl ether is highly toxic and a known carcinogen.) 1-Iminoquinolyl-3-tert-butyl-5-triphenylsilyl-phenol was synthesized by Dr. Gyeongshin Choi from 2,6-dibromo-4-(*tert*-butyl)phenoxy)triphenylsilane, which has been previously reported.[18] Retro-Brook rearrangement affords a phenol which can be elaborated to the desired salicylaldehyde and phenoxyiminoquinoline in a similar fashion to the procedures outlined below. Alumina and 3 Å molecular sieves were activated by heating under vacuum at 200 °C for at least 12 h prior to use. Polymer-grade C_2H_4 was purchased from Gas Innovations. Modified methaluminoxane (MMAO: 7 wt. % in heptane) was purchased from Akzo Nobel. Methylaluminoxane (MAO: 30% in toluene) was purchased from Albemarle Corp. ^1H and ^{13}C NMR spectra were recorded on Varian or Bruker spectrometers at ambient temperature unless

denoted otherwise. Chemical shifts are reported with respect to internal solvent for ^{1}H and ^{13}C NMR data, respectively: 7.26 ppm and 77.16 ppm ($CDCl_3$).[19] Analysis of reactions by gas chromatography (GC) was performed on an Agilent 6890N instrument using a flame ionization detector and DB-1 capillary column (10 m length, 0.10 mm diameter, 0.40 μm). Analysis of reactions by gas chromatograph mass spectrometry (GC-MS) was performed on an Agilent 6890 instrument equipped with an HP-5MS 30 m x 0.25 mm x 0.50 μm capillary column (Agilent). The GC was interfaced to an Agilent 5973N mass selective detector.

Synthesis of 1,4-bis(3'-iminoquinolyl-2'-hydroxyl--5'-tert-butyl)-tetramethylbenzene (46).

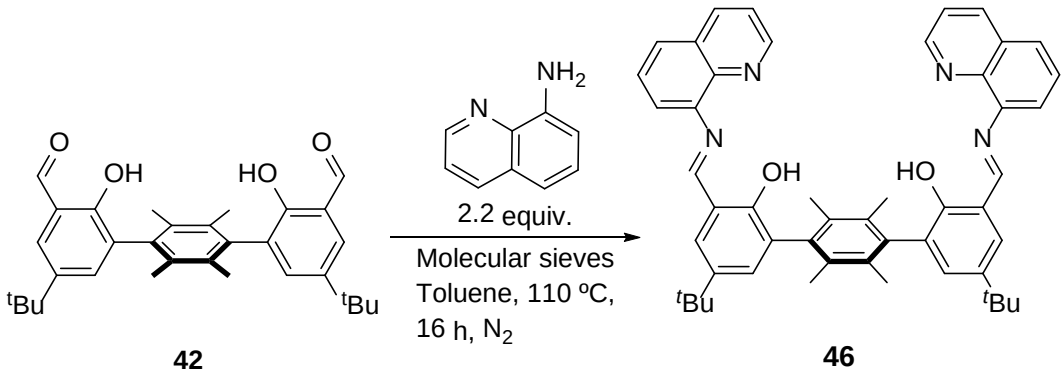

42 **46**

A 100 mL Schlenk tube fitted with a Teflon screw cap was charged with a stir bar, heated in an oven for 1 h, and evacuated on a Schlenk line and allowed to cool to room temperature. The vessel was charged with 1,4-bis(2'-hydroxyl-3'-formyl-5'-*tert*-butyl)-tetramethylbenzene (**42**: 0.130 g, 0.267 mmol, 1.0 equiv.) and 8-aminoquinoline (0.085, 0.588 mmol, 2.2 equiv.) using Schlenk technique and the reaction vessel was place under vacuum for 1 h. The Schlenk tube was sealed and brought into a N_2-filled dry box. In the glovebox, 10 mL toluene and a number of molecular sieves sufficient to cover the bottom of the Schlenk tube. The Schlenk

tube was removed from the glovebox and placed in an oil bath preheated to 110 °C. The reaction vessel was heated for 16 h. After 16 h, the reaction vessel was cooled to room temperature. Volatiles were removed under reduced pressure to afford an orange residue. The Schlenk tube was brought into the glovebox and the residue was washed thrice with 2 mL portions of pentane, then hexanes, then Et_2O. The resulting orange powder was extracted with toluene and filtered through Celite to afford the desired bisphenoxyiminoquinoline **46** (0.055 g, 0.074 mmol, 27.9%) as an orange powder. ^{1}H NMR (300 MHz, $CDCl_3$) δ 9.09 (s, 1H, imine-*H*), 8.98 (m, 2H, quinoline-*H*), 8.18 (m, 2H, quinoline-*H*), 7.70 (m, 2H, quinoline-*H*), 7.59 – 7.50 (m, 4H, quinoline-*H*), 7.47 (d, 2H, Ar-*H*), 7.44 (m, 2H, quinoline-*H*), 7.38 (d, 2H, Ar-*H*), 2.11 (s, 12H, Ar-C-CH_3), 1.38 (s, 18H, Ar-C-C(CH_3)$_3$). ^{13}C{^{1}H} NMR (101 MHz, $CDCl_3$) δ 166.19 (s, imine-*C*H), 157.19 (s, quinoline-*C*H), 150.46 (s, quinoline-*C*), 145.91 (s, Ar-*C*), 142.38 (s, quinoline-*C*), 141.14 (Ar-*C*-C(CH$_3$)$_3$), 137.28 (s, Ar-*C*), 136.09 (s, quinoline-*C*H), 133.13 (s, Ar-*C*H), 132.62 (s, Ar-*C*-CH$_3$), 130.79 (s, Ar-*C*), 129.36 (s, quinoline-*C*), 127.67 (s, Ar-*C*H), 126.70 (s, quinoline-*C*H), 125.88 (s, quinoline-*C*H), 121.68 (s, quinoline-*C*H), 119.91 (s, quinoline-*C*H), 118.92 (Ar-*C*), 34.31 (s, Ar-C-*C*(CH$_3$)$_3$, 31.67 (s, Ar-C-C(*C*H$_3$)$_3$), 18.17 (s, Ar-C-*C*H$_3$). ^{1}H NMR (400 MHz, C_6D_6) δ 14.56 (s, 2H, -O*H*), 8.80 (s, 2H, imine-C*H*), 8.78 (m, 2H, quinoline-*H*), 7.57 (m, 2H, quinoline-*H*), 7.48 (d, 2H, Ar-*H*), 7.35 (d, 2H, Ar-*H*), 7.29 (m, 2H, quinoline-*H*), 7.16 (m, 4H, quinoline-*H*), 6.77 (m, 2H, quinoline-*H*), 2.30 (s, 12H, Ar-C(CH_3)), 1.31 (s, 18H, Ar-C(CH_3)$_3$). ^{13}C{^{1}H} NMR (101 MHz, C_6D_6) δ 165.90 (s, Ar-*C*), 158.27 (s, imine-*C*H), 150.65 (s, quinoline-*C*), 146.15 (s, quinoline-*C*), 143.11 (s, quinoline-*C*), 141.04 (s, -*C*(CH$_3$)$_3$), 138.15 (s, Ar-*C*), 135.59

(s, quinoline-*C*H), 133.04 (s, Ar-*C*), 132.96 (s, Ar-*C*H), 132.06 (s, quinoline-*C*H), 129.48 (s, quinoline-*C*H), 128.04 (obscured by solvent residual, detected by HSQC, Ar-*C*H), 126.58 (s, quinoline-*C*H), 125.99 (s, quinoline-*C*H), 121.76 (s, quinoline-*C*H), 119.61 (s, Ar-*C*), 119.33 (s, Ar-*C*), 34.18 (s, -*C*(CH_3)$_3$), 31.66 (s, -C(*C*H_3)$_3$), 18.50 (s, Ar-C(*C*H_3)). Mass calcd. for $C_{50}H_{50}N_4O_2$: 739.4012. Found: 739.4019, M + H.

Synthesis of 1-pentamethylphenyl-2-methoxymethoxy-5-tert-butyl-benzene (42).

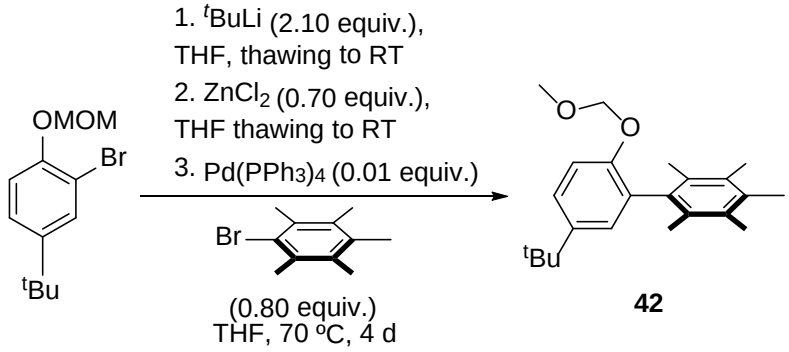

The procedure[10] reported for the preparation of 1,4-bis(2'-hydroxyl-3'-formyl-5'-*tert*-butyl)-tetramethylbenzene was modified to prepare 1-pentamethylphenyl-2-methoxymethoxy-5-tert-butyl-benzene (**42**). In the glovebox, a 500 L Schlenk flask fitted with a Teflon screw cap was charged with a stir bar, 200 mL THF, and 2-bromo-4-(*tert*-butyl)-1-(methoxymethoxy)benzene (18.76 g, 68.7 mmol, 1.00 equiv.). The reaction mixture was frozen in a liquid N_2-chilled cold well. BuLi (9.24 g, 144.2 mmol, 2.10 equiv.) was added portion-wise (*ca.* 1 g/portion) to the stirring, thawing reaction mixture such that frozen solvent was observed at all times during addition. The reaction mixture was chilled in the cold well to maintain the thawing conditions. Upon the completion of addition, the reaction mixture was allowed to warm to room temperature. A light red solution is observed. $ZnCl_2$ (6.56 g, 48.1 mmol, 0.70 equiv.)

was then added as a solid at room temperature. The reaction mixture was allowed to stir for 30 min. A heterogeneous solution was observed. $Pd(Ph_3)_4$ (0.80 g, 0.7 mmol, 0.01 equiv.) and bromo-pentamethylbenzene (12.48 g, 54.9 mmol, 0.80 equiv.) were then added as solids at room temperature. A pale yellow heterogeneous solution was observed. The reaction was stirred in an oil bath pre-heated to 70 °C for 3 d. After 3 d, the Schlenk tube was removed from the oil bath and allow to cool to room temperature. A brown heterogeneous mixture was observed. The reaction mixture was filtered through a coarse fitted funnel packed with Celite. The reaction vessel was washed with 3 portions of CH_2Cl_2 (50 mL) and this organic layer was filtered through Celite and combined with the THF filtrate. Volatiles were removed under reduced pressure using rotary evaporation. The resulting brown residue was extracted with 3 portions of CH_2Cl_2 (100 mL) the combined organics were again filtered through a fritted funnel packed with Celite. This organic layer was washed twice with H_2O (100 mL) and once with brine (100 mL). The organic layer was then dried with $Mg(SO_4)_2$, filtered, and volatiles were removed from the filtrate under reduced pressure using rotary evaportation to afford a brown residue. MeOH was added to the brown residue and the mixture was triturated and sonicated to afford 1-pentamethylphenyl-2-methoxymethoxy-5-tert-butyl-benzene (**42**) in good purity as a white solid with an impurity of bromo-pentamethylbenzene. Sublimation of bromo-pentamethylbenzene from the crude mixture allows for isolation of pure compound **42**. ^{1}H NMR (300 MHz, $CDCl_3$) δ 7.33 (dd, 1H, Ar-*H*), 7.19 (d, 1H, Ar-*H*), 7.07 (d, 1H, Ar-*H*), 5.08 (s, 2H, $ArOCH_2OCH_3$), 3.37 (s, 3H, $ArOCH_2OCH_3$), 2.34 (s, 3H, $Ar\text{-}C_6(CH_3)_5$), 2.30 (s, 6H, $Ar\text{-}C_6(CH_3)_5$), 2.00 (s, 6H, $Ar\text{-}C_6(CH_3)_5$), 1.33 (s, 9H, $-C(CH_3)_3$). $^{13}C\{^1H\}$ NMR (101 MHz, $CDCl_3$) δ 152.31 (s, Ar-*C*), 144.72 (s, Ar-*C*), 136.72 (s, Ar-*C*), 134.03 (s, Ar-

*C*7), 132.23 (s, Ar-*C*8-10), 132.22 (s, Ar-*C*8-10), 131.70 (s, Ar-*C*8-10), 128.88 (Ar-*C*2 or Ar-*C*3), 124.54 (Ar-*C*5), 114.21 (Ar-*C*2 or Ar-*C*3), 94.44 (s, ArO*C*H2OCH3), 55.78 (s, ArOCH2O*C*H3), 34.32 (s, -*C*(CH3)3), 31.67 (s, -C(*C*H3)3), 18.26 (s, Ar-C6(*C*H3)5), 17.06 (s, Ar-C6(*C*H3)5), 16.80 (s, Ar-C6(*C*H3)5). MS (m/z) calcd. for $C_{23}H_{32}O_2$: 339.2324 (M+H). Found: 339.2319 (FAB+, (M+H)-H2).

Synthesis of 1-pentamethylphenyl-3-tert-butyl-5-formyl-phenol. (40).

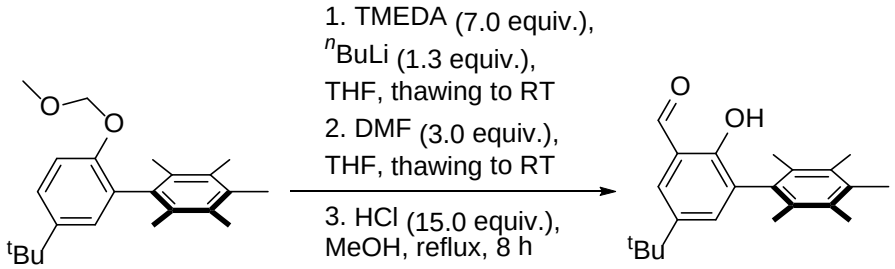

42 **40**

Method A: A 100 mL Schlenk tube fitted with a Teflon screw cap was charged with a stir bar and placed in an oven for 1 h. After 1 h, the Schlenk tube was evacuated on the Schlenk line while cooling to room temperature. Using Schlenk technique, 1-pentamethylphenyl-2-methoxymethoxy-5-tert-butyl-benzene (**42**: 4.290 g, 12.60 mmol, 1.0 equiv.) was added as a solid and placed under vacuum for 3 h. After 3 h, the Schlenk flask was sealed and brought into a N2-filled drybox. THF (40 mL) and tetramethylethylenediamine (10.248 g, 13.1 mL, 88.18 mmol, 7.0 equiv.) were added to the reaction vessel. The mixture was frozen in a liquid N2-chilled cold well. A just-thawed solution of *n*BuLi (6.55 mL of 2.5 M solution in hexanes, 16.38 mmol, 1.3 equiv.) was added dropwise to the thawing reaction mixture. An orange solution was observed with an off-white precipitate. The reaction mixture was allowed to come to room temperature and stir for 2 h. The mixture was again frozen in the cold well. A just-thawed solution of dimethylformamide (2.76 g, 2.91 mL, 37.80 mmol, 3.0 equiv.)

was added to the thawing reaction mixture. The mixture was allowed to come to room temperature and stirred for 12 h. A pale yellow solution was observed. The reaction mixture was transferred to a round bottom flask and volatiles were removed under reduced pressure via rotary evaporation to afford a pale yellow resiude. MeOH (100 mL), HCl (conc. HCl, nominally 12 M, 15.7 mL, 188.98 mmol, 15.0 equiv.), and a stir bar were added to the residue. A reflux condenser was affixed and the mixture was refluxed for 5 h. The reaction was concentrated to afford a precipitate. Filtrate and washing with MeOH afforded the desired salicylaldehyde 1-pentamethylphenyl-3-tert-butyl-5-formyl-phenol (**40**: 1.150 g, 3.54, 28.1%) as a white solid. NMR data matched previously spectra.[9b]

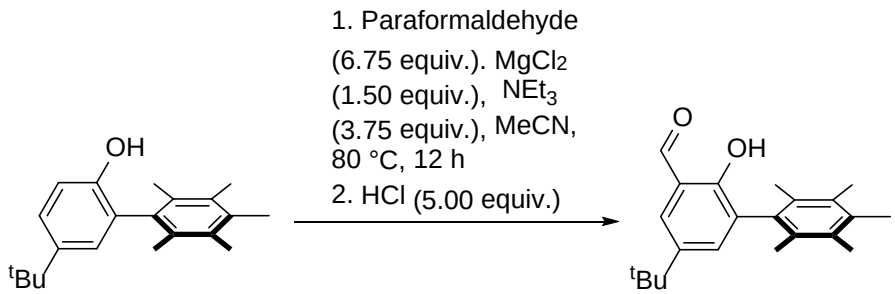

44 **40**

Method B: A procedure reported by Skattebøl and co-workers[20] for the *ortho*-formylation of phenols was used for preparation of salicylaldehyde **40**. A 100 mL Schlenk tube fitted with a Teflon screw cap was charged with a stir bar and placed in an oven for 1 h. After 1 h, the Schlenk tube was evacuated on the Schlenk line while cooling to room temperature. Using Schlenk technique, 1-pentamethylphenyl-3-tert-butyl-phenol (**44**: 1.379 g, 4.65 mmol, 1.00 equiv.; for preparation, see below) was added as a solid and the reaction vessel was evacuated for 3 h. The Schlenk flask was sealed and brought into the glovebox. Paraformaldehyde (0.943 g, 31.40 mmol, 6.75

equiv.), $MgCl_2$ (0.455 g, 6.98 mmol, 1.50 equiv.) NEt_3 (1.765 g, 2.4 mL, 17.45 mmol, 3.75 equiv.), and MeCN (10 mL) were added. The Schlenk tube was removed from the glovebox and placed in an oil bath pre-heated to 80 °C for 12 h. After 12 h, the mixture was removed from heating and allow to cool to remove temperature. The reaction mixture was quenched with HCl (1.94 mL, conc. HCl, nominally 12 M, 23.25 mmol, 5.00 equiv.). Volatiles were removed under reduced pressure via rotary evaporation. Column chromatography using 95:5 hexanes:EtOAc ($R_f \approx 0.3$) affords 1-pentamethylphenyl-3-tert-butyl-5-formyl-phenol (**40**, 1.123 g, 3.46 mmol, 74.4%) as a white solid.

Synthesis of 1-pentamethylphenyl-3-tert-butyl-phenol (44).

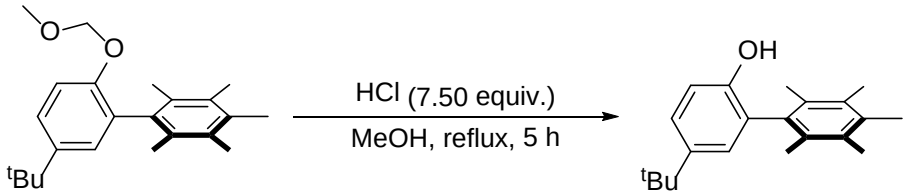

42 **44**

A 100 mL round bottom flask was charged with 1-pentamethylphenyl-2-methoxymethoxy-5-tert-butyl-benzene (**42**: 5.000 g, 16.86 mmol, 1.00 equiv.; MeOH precipitate with impurity of bromopentaphenylbenzene), HCl (10.5 mL, conc. HCl, nominally 12 M, 252.97 mmol, 7.50 equiv.), MeOH (100 mL) and a stir bar. The mixture was refluxed for 5 h. Volatiles were removed under reduced pressure via rotary evaporation. Column chromatography using 4:1 hexanes:CH_2Cl_2 as eluent afforded 1-pentamethylphenyl-3-tert-butyl-phenol (**44**) as a white solid. ^{1}H NMR (300 MHz, $CDCl_3$) δ 7.27 (dd, 1H, Ar-*H*), 7.01 (d, 1H, Ar-*H*), 6.91 (d, 1H, Ar-*H*), 4.49 (s, 1H, Ph-O*H*), 2.31 (s, 3H, Ar-C-C*H*$_3$), 2.27 (s, 6H, Ar-C-C*H*$_3$), 1.97 (s, 6H, Ar-C-C*H*$_3$), 1.29 (s, 9H, -C(C*H*$_3$)$_3$).

Synthesis of 1-iminoquinoline-3-tert-butyl-5-pentamethylphenyl--phenol (45).

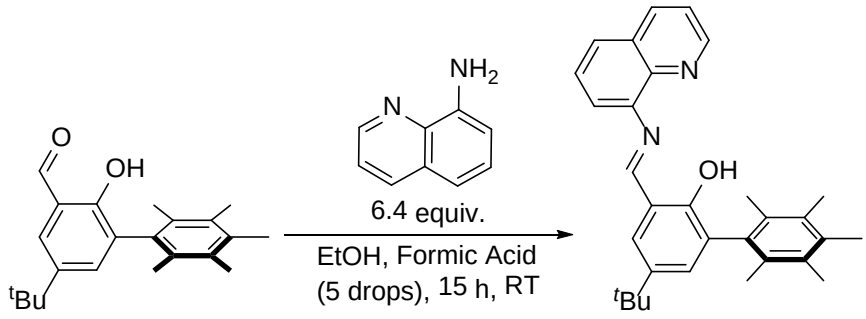

41 **45**

A 100 mL round bottom flask was charged with 1-pentamethylphenyl-3-tert-butyl-5-formyl-phenol (**41**: 0.350 g, 1.080 mmol, 1.0 equiv.), 8-aminoquinoline (1.000 g, 6.936 mmol, 6.4 equiv.), and EtOH (10 mL). Formic acid (5 drops) was added and the resulting mixture was stirred at room temperature for 15 h. An orange precipitate was observed. The precipitate was isolated on a fritted glass funnel washed with a large volume of EtOH to afford 1-iminoquinoline-3-tert-butyl-5-pentamethylphenyl--phenol (**45**: 0.308 g, 0.684 mmol, 63.4%) as an orange solid. ^{1}H NMR (400 MHz, $CDCl_3$) δ 13.64 (s, 1H, -O*H*), 9.10 (s, 1H, imine-*H*), 8.93 (m, 1H, quinoline-*H*), 8.18 (m, 1H, quinoline -*H*), 7.70 (m, 1H, quinoline -*H*), 7.56 (m, 1H, quinoline -*H*), 7.51 (m, 1H, quinoline -*H*), 7.45 (d, 1H, Ar-*H*), 7.44 (m, 1H, quinoline -*H*), 7.27 (d, 1H, Ar-*H*), 2.30 (s, 3H, Ar-C(C*H*$_3$)), 2.28 (s, 6H, Ar-C(C*H*$_3$)), 2.05 (s, 6H, Ar-C(C*H*$_3$)), 1.35 (s, 9H, Ar-C(C*H*$_3$)$_3$). ^{13}C{^{1}H} NMR (400 MHz, $CDCl_3$) δ 166.04 (s, imine-*C*H), 156.92 (s, Ar-*C*), 150.37 (s, quinoline-*C*H), 145.76 (s, quinoline-*C*), 142.41 (s, quinoline-*C*), 141.44 (s, Ar-*C*-C(CH$_3$)$_3$), 136.14 (s, quinoline-*C*H), 135.41 (s, Ar-*C*), 134.49 (s, Ar-*C*-CH$_3$), 132.94 (s, Ar-*C*H), 132.48 (s, Ar-*C*-CH$_3$), 132.37 (s, Ar-*C*-CH$_3$), 130.89 (s, Ar-*C*), 129.36 (s, quinoline-*C*), 127.60 (Ar-*C*H), 126.73 (s, quinoline-*C*H), 126.02 (s, quinoline-*C*H), 121.72 (s, quinoline-*C*H), 119.81 (s, quinoline-*C*H), 118.89 (s, Ar-*C*),

34.26 (s, Ar-*C*(CH$_3$)$_3$), 31.61 (s, Ar-C(*C*H$_3$)$_3$), 18.28 (s, Ar-C(*C*H$_3$), 17.03 (s, Ar-C(*C*H$_3$), 16.90 (s, Ar-C(*C*H$_3$). MS (m/z) calcd. for $C_{31}H_{34}N_2O$: 451.2749 (M+H). Found: 451.2758 (FAB+, (M+H)).

Metallation of 1-iminoquinoline-3-tert-butyl-5-pentamethylphenyl—phenol (45) with CrMeCl$_2$(THF)$_3$ to afford 47.

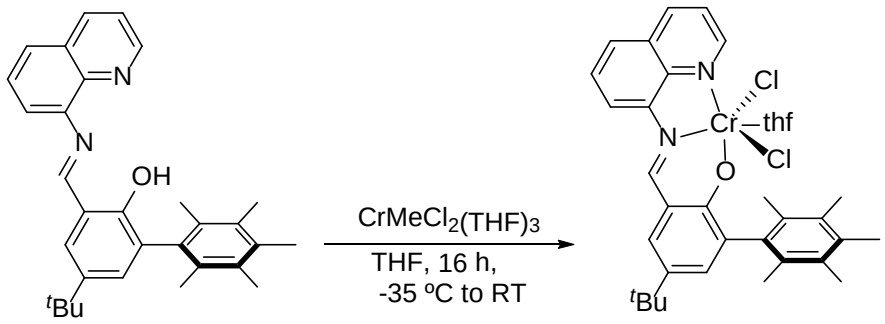

45 **47**

A 20 mL scintillation vial was charged with a stir bar, THF (3 mL), and phenoxyiminoquinoline (**45**: 0.308 g, 0.68 mmol). An orange homogenous solution was observed. A separate vial was charged with CrMeCl$_2$(THF)$_3$[12] (0.242 g, 0.68 mmol) and THF (2 mL). A light green solution was observed. Both solutions were chilled in a -35 °C freezer. The chilled solution of **45** was added to the chilled solution of CrMeCl$_2$(THF)$_3$ and the reaction mixture was allowed to warm to room temperature. After 1 h, a dark red solution was observed. After 16 h, a red precipitate was observed. Volatiles were removed under reduced pressure to afford a red-brown powder which was used without further purification for C_2H_4 oligomerization/polymerization reactions.

Metallation of 1,4-bis(3'-iminoquinolyl-2'-hydroxyl--5'-tert-butyl)-tetramethylbenzene (46) with $CrMeCl_2(THF)_3$ to afford 48.

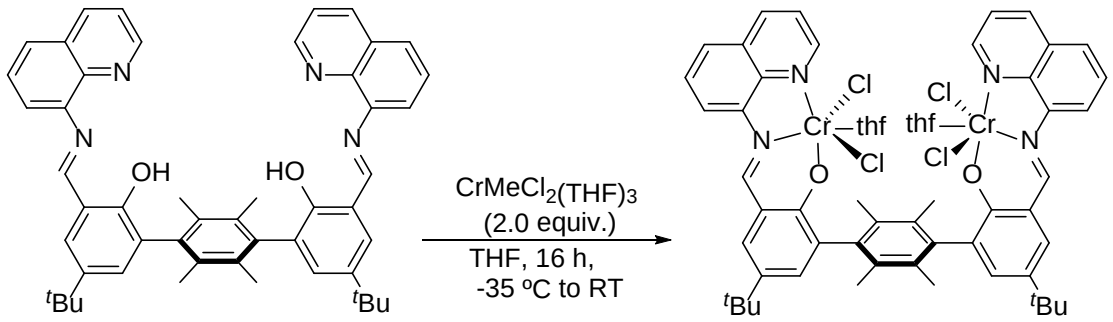

46 **48**

A 20 mL scintillation vial was charged with a stir bar, THF (3 mL), and bisphenoxyiminoquinoline (**46**: 0.055 g, 0.07 mmol, 1.0 equiv.). An orange homogenous solution was observed. A separate vial was charged with $CrMeCl_2(THF)_3$[12] (0.053 g, 0.15 mmol, 2.0 equiv.) and THF (2 mL). A light green solution was observed. Both solutions were chilled in a -35 °C freezer. The chilled solution of **46** was added to the chilled solution of $CrMeCl_2(THF)_3$ and the reaction mixture was allowed to warm to room temperature. After 1 h, a dark red solution was observed. After 16 h, a red precipitate was observed. Volatiles were removed under reduced pressure to afford a red-brown powder which was used without further purification for C_2H_4 oligomerization/polymerization reactions.

Metallation of 1-iminoquinoline-3-tert-butyl-5-triphenylsilyl-phenol with $CrMeCl_2(THF)_3$ to afford 49.

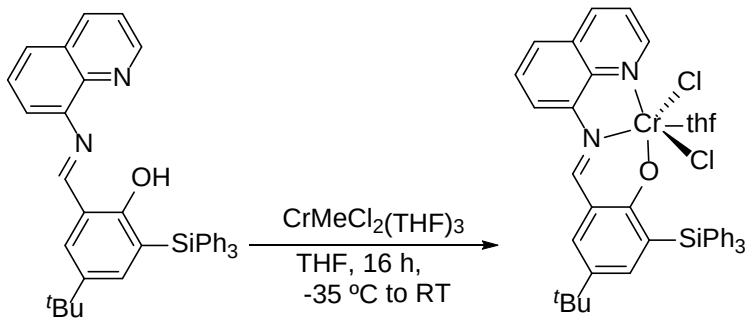

49

A 20 mL scintillation vial was charged with a stir bar, THF (3 mL), and 1-Iminoquinolyl-3-tert-butyl-5-triphenylsilyl-phenol (0.093 g, 0.17 mmol). An orange homogenous solution was observed. A separate vial was charged with $CrMeCl_2(THF)_3$[12] (0.059 g, 0.17 mmol) and THF (2 mL). A light green solution was observed. Both solutions were chilled in a -35 °C freezer. The chilled solution of phenoxyiminoquinoline was added to the chilled solution of $CrMeCl_2(THF)_3$ and the reaction mixture was allowed to warm to room temperature. After 1 h, a dark red solution was observed. After 16 h, a red precipitate was observed. Volatiles were removed under reduced pressure to afford a yellow-brown powder which was used without further purification for C_2H_4 oligomerization/polymerization reactions.

Oligomerization/Polymerization Procedure A: MMAO Activator.

A Fischer-Porter vessel was charged with a stir bar heated in an oven for 8 h and introduced into the glovebox. A Fischer-Porter reactor top/regulator was introduced into the glovebox after being placed under dynamic vacuum for a minimum of 8 h. In the glovebox, the Fischer-Porter vessel was charged with a solution of phenoxyiminoquinoline Cr compound (3.0 μmol, 1.0 equiv.) and a solution of

MMAO (0.15 mL, 7 wt% Al in heptane, 0.3 mmol, 100.0 equiv.). The reactor was sealed, removed from the glovebox, and place in an oil bath pre-heated to the specified temperature. The Fischer-Porter apparatus was then charged with the desired pressure of C_2H_4 and allowed to stir vigorously for the specific period of time. Typically, *ca.* 15 min. elapsed between addition of activator and pressurization with C_2H_4. After the specified period of time, the reactor was removed from the oil bath, vented to release C_2H_4, and 10 mL of 1 M HCl was added to afford a biphasic mixture. A known mass of adamantane (*ca.* 0.008 g, 0.059 mmol to 0.015 g, 0.110 mmol) was added as a solution in 2 mL toluene. An aliquot was then taken from the organic (top) layer of the biphasic mixture for quantification of 1-hexene or 1-octene production by GC and identification of higher oligomers by GC-MS.

Oligomerization/Polymerization Procedure B: Solid MAO Activator.

"Oligomerization/Polymerization Procedure A" (above) was followed except for choice of activator. Solid MAO (0.052 g, 0.3 mmol, 300 equiv.) was added to a 10 mL solution of phenoxyiminoquinoline Cr compound (0.002 g, 3.0 μmol, 1.0 equiv.) in the glovebox (no MMAO was used). The rest of "Procedure A" was then followed.

REFERENCES

(1) (a) Skupinska, J. *Chem. Rev.* **1991**, *91*, 613-648; (b) McGuinness, D. S. *Chem. Rev.* **2011**, *111*, 2321-2341; (c) Agapie, T. *Coord. Chem. Rev.* **2011**, *255*, 861-880.
(2) (a) Rofer-DePoorter, C. K. *Chem. Rev.* **1981**, *81*, 447-474; (b) Jahangiri, H.; Bennett, J.; Mahjoubi, P.; Wilson, K.; Gu, S. *Catal. Sci. Tech.* **2014**, *4*, 2210-2229.
(3) *Process Evaluation/Research Planning: Linear Alpha Olefins, Oct. 2015 Report*; Nexant Chemical, Oct. 2015.
(4) Keim, W. *Angew. Chem. Int. Ed.* **2013**, *52*, 12492-12496.
(5) (a) Manyik, R. M.; Walker, W. E.; Wilson, T. P. *J. Catal.* **1977**, *47*, 197-209; (b) Dixon, J. T.; Green, M. J.; Hess, F. M.; Morgan, D. H. *J. Organomet. Chem.* **2004**, *689*, 3641-3668.
(6) (a) Takahashi, S.; Shibano, T.; Hagihara, N. *Tetrahedron Lett.* **1967**, *8*, 2451-2453; (b) Smutny, E. J. *J. Am. Chem. Soc.* **1967**, *89*, 6793-6794.
(7) Bollmann, A.; Blann, K.; Dixon, J. T.; Hess, F. M.; Killian, E.; Maumela, H.; McGuinness, D. S.; Morgan, D. H.; Neveling, A.; Otto, S.; Overett, M.; Slawin, A. M. Z.; Wasserscheid, P.; Kuhlmann, S. *J. Am. Chem. Soc.* **2004**, *126*, 14712-14713.
(8) (a) Jones, D. J.; Gibson, V. C.; Green, S. M.; Maddox, P. J. *Chem. Commun.* **2002**, 1038-1039; (b) Jones, D. J.; Gibson, V. C.; Green, S. M.; Maddox, P. J.; White, A. J. P.; Williams, D. J. *J. Am. Chem. Soc.* **2005**, *127*, 11037-11046; (c) Tomov, A. K.; Chirinos, J. J.; Jones, D. J.; Long, R. J.; Gibson, V. C. *J. Am. Chem. Soc.* **2005**, *127*, 10166-10167; (d) Tomov, A. K.; Gibson, V. C.; Britovsek, G. J. P.; Long, R. J.; van Meurs, M.; Jones, D. J.; Tellmann, K. P.; Chirinos, J. J. *Organometallics* **2009**, *28*, 7033-7040.
(9) (a) Radlauer, M. R.; Day, M. W.; Agapie, T. *J. Am. Chem. Soc.* **2012**, *134*, 1478-1481; (b) Radlauer, M. R.; Day, M. W.; Agapie, T. *Organometallics* **2012**, *31*, 2231-2243.
(10) Radlauer, M. R.; Buckley, A. K.; Henling, L. M.; Agapie, T. *J. Am. Chem. Soc.* **2013**, *135*, 3784-3787.
(11) Radlauer, M. R.; Agapie, T. *Organometallics* **2014**, *33*, 3247-3250.
(12) (a) Nishimura, K.; Kuribayashi, H.; Yamamoto, A.; Ikeda, S. *J. Organomet. Chem.* **1972**, *37*, 317-329; (b) Fernández, P.; Pritzkow, H.; Carbó, J. J.; Hofmann, P.; Enders, M. *Organometallics* **2007**, *26*, 4402-4412.
(13) Chen, E. Y.-X.; Marks, T. J. *Chem. Rev.* **2000**, *100*, 1391-1434.
(14) (a) Elderfield, R. C.; Gensler, W. J.; Bembry, T. H.; Williamson, T. A.; Weisl, H. *J. Am. Chem. Soc.* **1946**, *68*, 1589-1591; (b) Vangapandu, S.; Jain, M.; Jain, R.; Kaur, S.; Pal Singh, P. *Bioorgan. Med. Chem.* **2004**, *12*, 2501-2508; (c) Kochem, A.; Carrillo, A.; Philouze, C.; van Gastel, M.; du Moulinet d'Hardemare, A.; Thomas, F. *Eur. J. Inorg. Chem.* **2014**, *2014*, 4263-4267.
(15) Tietze, L. F.; Hungerland, T.; Düfert, A.; Objartel, I.; Stalke, D. *Chem. Eur. J.* **2012**, *18*, 3286-3291.
(16) Zysman-Colman, E.; Arias, K.; Siegel, J. S. *Can. J. Chem.* **2009**, *87*, 440-447.
(17) Berliner, M. A.; Belecki, K. *J. Org. Chem.* **2005**, *70*, 9618-9621.
(18) Muslin, D. V.; Lyapina, N. S. *Russ. Chem. Bull.* **1984**, *33*, 2141-2143.
(19) Fulmer, G. R.; Miller, A. J. M.; Sherden, N. H.; Gottlieb, H. E.; Nudelman, A.; Stoltz, B. M.; Bercaw, J. E.; Goldberg, K. I. *Organometallics* **2010**, *29*, 2176-2179.
(20) Hansen, T. V.; Skattebøl, L. *Org. Synth.* **2005**, *82*, 64-68.

APPENDIX B

Mid- to Late- Transition Metal Complexes Supported by Terphenyl and Biphenyl Phenols Bearing Pendant Phosphines

Published in part as:

Buss, J. A.; Edouard, G. A.; Cheng, C.; Shi, J.; Agapie, T. *J. Am. Chem. Soc.* **2014**, *136*, 11272-11275.

Abstract

A series of low-valent, low-coordinate terphenyl diphosphine, terphenyl bisphosphinophenol, and biphenyl phosphinophenol mid- to late-transition metal compounds were prepared. Such complexes are envisioned to be suitable for small molecule (C_2H_4, CO_2. H_2, N_2) activation chemistry. The ammonia borane dehydrogenation activity of a terphenyl diphosphine molybdenum complex is noted. Phosphine ligands bearing pendant phosphines are described. Hemilable metal-arene interactions are observed upon changing oxidations states, as well as coordinately accessible transition metal complexes.

INTRODUCTION

Earth-abundant first row transition metals typically catalyze reactions in one-electron steps, often undergoing deleterious side reactions that proceed via radical mechanisms. Redox non-innocent scaffolds were identified as early as the 1960s in work with metal dithiolenes.[1] Chirik,[2] Heyduk,[3] Wieghardt[4] and others have demonstrated that redox active scaffolds can confer noble character upon base metals.[5] Bisiminopyridine Fe[6] and Co[6b] have been demonstrated to be highly active olefin oligomerization catalysts with good selectivities for α-olefins; with Fe, reduction cyclization of enynes and diynes has been reported.[7] In nature, galactose oxidase features a Cu^{II} ion coordinated to a tyrosyl radical and catalyzes the oxidation of alcohols to aldehydes;[5] evidence of protein radicals has been reported in a variety of enzymatic reactions.[8] By incorporating a redox-active phenolic moiety into phosphine ligands previously demonstrated to be capable of stabilizing mid- to late-transition metals in a variety of geometries and oxidation states, chemistry typically reserved for precious metals (e.g., Ru, Rh, Ir, Pt) is proposed to be accessible using inexpensive base metals. (e. g., Mo, Fe, Co, Ni).

In the Agapie Group, P-arene-P diphosphine pincers and related triphosphine ligands have been used to support mid- to late-transition metals capable of a variety of organometallic transformations (Figure B.1).[9] Pincer-based metal complexes allow for precise control of stability and reactivity through systematic modification or variation of ligand donors, substituents, and transition metals. Previously, investigation of a P-arene-P pincer and ether-substituted variant demonstrated that a variety of coordination modes and oxidation states are accessible on the same ligand scaffold.[10]

Figure B.1. Terphenyl and Quaterphenyl Phosphine Mono-, Di-, and Tri-Nickel Complexes Synthesized by the Agapie Group.

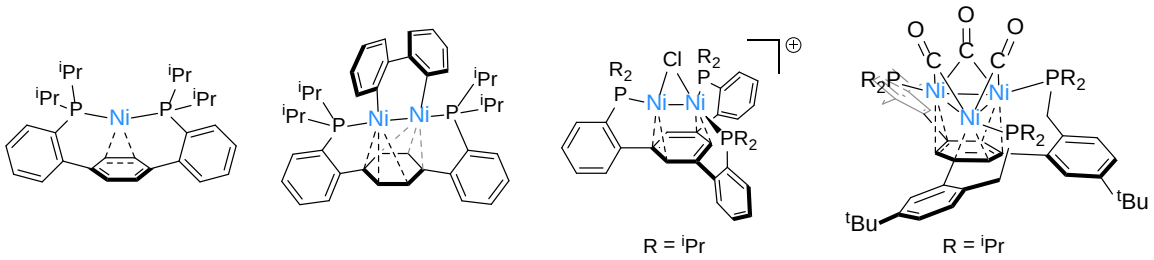

Appending a phenoxide donor to previously synthesized P-arene-P pincers is envisioned to afford a ligand with a redox non-innocent moiety (Figure B.2). On such a scaffold, a two electron transformation could occur either through loss of one electron from the metal center and a second from the aminophenol moiety or through loss of two electrons from the aminophenol with no formal oxidation state change at the metal center. Earth-abundant transition metals supported by the these ligands are envisioned to catalyze a diverse set of reactions, including olefin and alkene hydrogenation, hydrosilyation, selective olefin oligomerization, intra- and intermolecular cyclizations of unsaturated olefins, and cross-couplings (Figure B.3).

Figure B.2. Two-Electron Oxidation of Aminophenol Complex with One or No Electron Oxidation of the Metal Center.

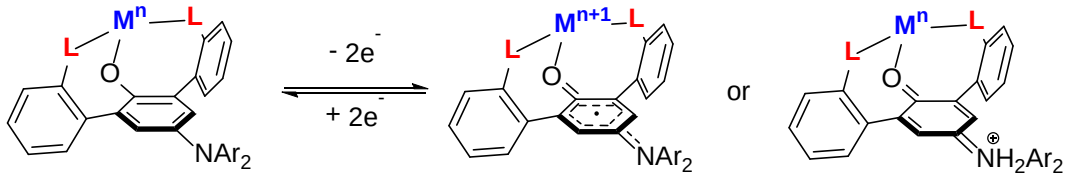

50

L = N, P, S
M = Mo, Fe, Co, Ni

Figure B.3. Proposed Mechanisms for Olefin Oligomerization, Hydrogenation, and Cross-Coupling at Base Metals Facilitated by Redox Non-Innocent Aminophenol Scaffold.

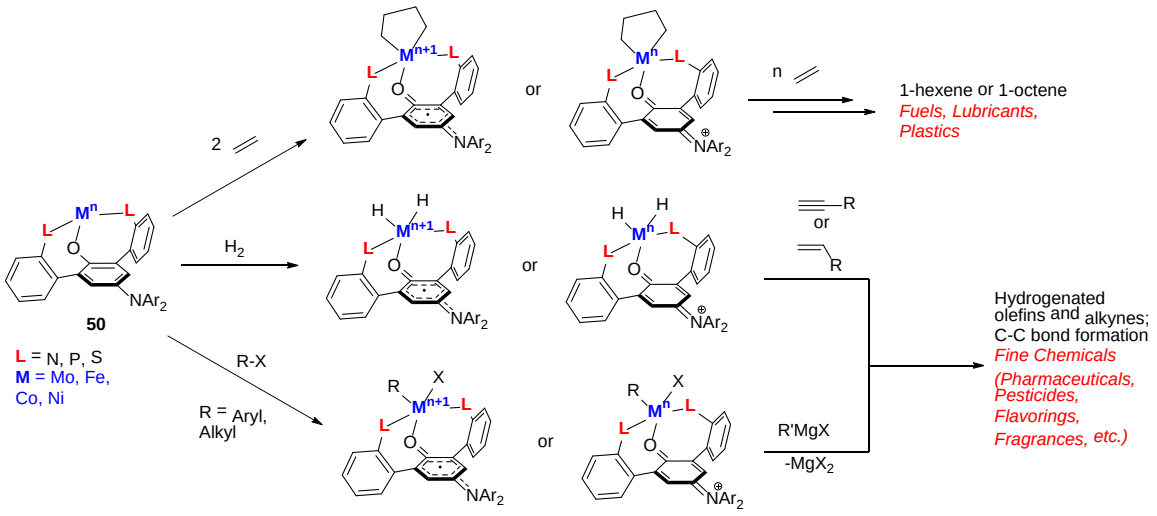

Species such as compound **50** are envisioned to be effective catalysts for selective olefin oligomerization, hydrogenation, and cross-couplings. Hydrocarbon upgrading of light olefins affords comonomers for production of linear low-density polyethylene (LLDPE) and higher olefins desirable for fuel blends or lubricants.[11] Selective olefin oligomerization proceeds through a two-electron redox cycle involving metallacyclic intermediates.[11] Similarly, hydrogenation and cross-coupling reactions catalyzed by homogenous species, important in the context of fine chemical synthesis, are proposed to involve oxidative addition of H_2 or aryl/alkyl halide coupling partner. The proposed aminophenol ligand bearing a pendant donor is anticipated to allow for these reactions to be catalyzed by earth-abundant transition metals (Figure B.3). Bisphenoxyamine ligands coordinated to Zr^{IV} compounds have been reported to reduce O_2 in a four-electron, two-proton transformation with no formal oxidation state change at Zr, providing evidence for the potential redox-noninnocence of

aminophenol ligands.[12] Such compounds have not been well studied and may provide improvements in activity and lifetimes compared to previously reported catalysts. Pendant donors and their substituents in the proposed system are modular. Phosphines, thioethers, carbenes, amides, and amines can be used as donors to tune the reduction potential of the metal center. Changing the substitution of the amine of the aminophenol moiety will also allow for tuning the redox potential of the ligand to optimize reactivity. Progress towards the synthesis of the family of compounds of this type is described herein.

Results & Discussion

m-Terphenyl diphosphine **51** and *p*-terphenyl diphosphine **52** were metallated with Mo, Fe, and Co precursors in efforts to access an entry into mid- to late-transition metal chemistry on these and related scaffolds. New compounds were isolated with Co and Mo.

Initial attempts to isolate a cobalt complex by metallating ligand **51** with $Co_2(CO)_8$, $Co(OTf)_2$, and $CoCl(P(Ph_3)_3)$ were unsuccessful. The ^{1}H and ^{31}P spectra of **51** was unchanged after treatment with $Co(OTf)_2$, and $CoCl(PPh_3)_3$ at room temperature and with heating. In the case of $Co_2(CO)_8$, a new species was observed by ^{31}P and ^{1}H NMR. However, attempts to crystallize this complex resulted in the formation of a species insoluble in common laboratory solvents, suggesting oligomerization. $Co_2(CO)_8$ itself is thermally unstable, decomposing to Co^0 and releasing CO at room temperature and forming the tetramer $Co_4(CO)_{12}$ with mild heating.[13] $Co(OTf)_2$ may be too hard or ionic to coordinate the soft or primarily covalent bonding environment of the terphenyl diphosphine. In the case of $CoCl(PPh_3)_3$, PPh_3 seems to be too strongly donating to be exchanged with another aryl phoshpine.

Metallation of **51** with $CoBr_2$ in CH_2Cl_2 afforded an emerald green solid (Figure B.4). This complex displayed no ^{31}P NMR resonances and a paramagnetic ^{1}H NMR spectrum. Single crystal XRD allowed for assignment of this complex as the tetrahedral dibromide **52**. Compound **52** displays no contacts to the central arene of the terphenyl diphosphine. In the presence of Zn^0, the same reaction gives rise to a diamagnetic complex (**53**) as the major product as observed by ^{1}H and ^{31}P NMR, consistent with reduction to an even electron species.

Scheme B.1. Metallation of Diphosphines *51* and *52* to afford Co^{I} and Co^{II} Compounds *53*-*56*.

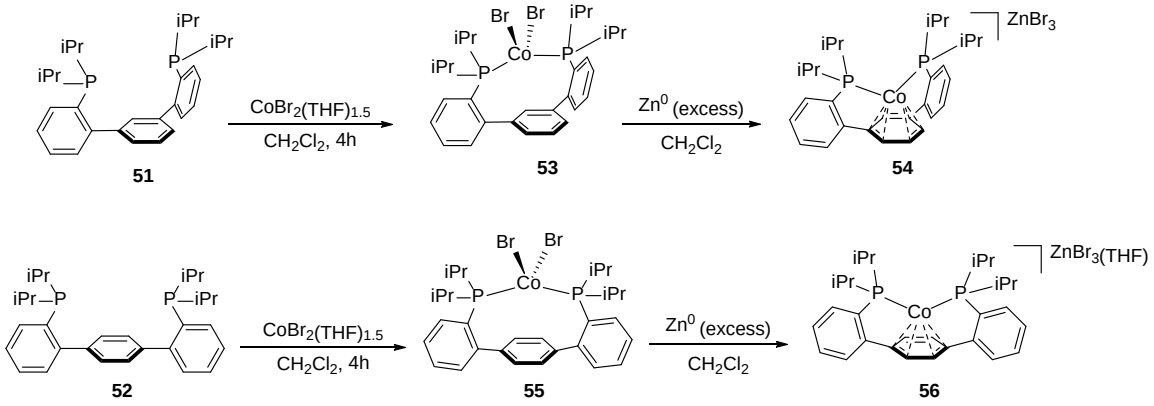

A compound with similar major features in its NMR spectra can be generated from the addition of a single equivalent of cobaltocene to *53*. The solid-state structure of the product of the reaction of *51*, $CoBr_2$, and Zn^0 has been determined to be the Co^{I} complex *54* (Figure B.4). In this species, the Co^{I} center is coordinated η^6 to the central aryl ring of the ligand.

Figure B.4. Solid-State Structures of (from left to right) *53*, *54*, and *56*. Shown for connectivity. Hydrogen atoms omitted for clarity. For compound *53*, disorder is observed at the ^{i}Pr substituent of atom "P2". For *54*, 0.5 Zn_2Br_6 counteranion omitted for clarity. For *55*, $ZnBr_3(THF)$ counteranion omitted for clarity.

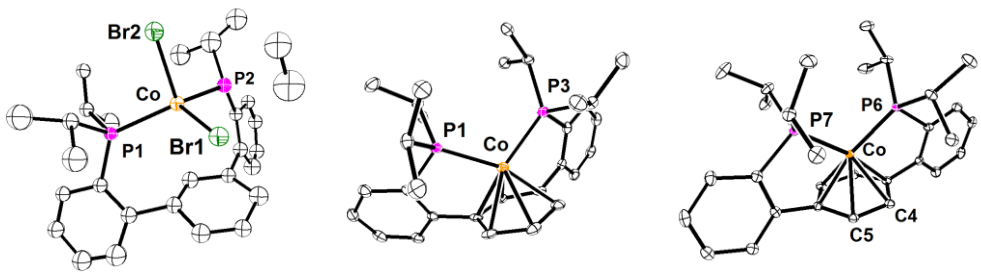

Using a similar strategy, a paramagnetic species putatively assigned as Co^{II} complex ***55*** was isolated by treating diphosphine ***52*** with $CoBr_2$ in CH_2Cl_2. Reduction affords Co^{I} complex ***56*** which displays η^6-coordination to the central aryl ring of the ligand. The structure of this new species was confirmed by determination of solid-state structure (Figure B.4) after single crystal X-ray diffraction (XRD). Compound ***55*** was generated in low yield (^{1}H NMR) and crystals suitable for single crystal x-ray diffraction have yet to be grown. This is consistent with the hypothesis that, relative to ligand ***52***, diphosphine ***51*** is a more effective ligand for first row transition metals whereas ***52***, which has a larger bite angle, may be better suited for coordination of second row transition metals and binuclear species.

This change in geometry from ***53*** to ***54*** and from ***55*** to ***56*** can be rationalized by electron count. In the absence of coordinating solvent (e.g. THF), the d^7 Co^{II} center cannot assume a geometry which results in an electron count of 18 and assumes a tetrahedral conformation which minimizes steric interactions. The d^8 Co^{I} center with its halide ligands abstracted gains an additional 10 electrons from the ligand to achieve the favored $18e^-$ total. The ability of diphosphines ***51*** and ***52*** to accommodate $1e^-$ changes in oxidation state is promising in the context to proposed transformations (see Figure B.3) which may require one electron from a transition metal and one electron from a redox non-innocent ligand scaffold to proceed.

Use of cobaltocene as a reductant and thalium triflate (TlOTf) as a halide abstractor as opposed to Zn^0 should allow for the isolation of a Co^{I} species with halide-free counteranions and facilitate further study of reactivity with small molecules. Treatment of ***53*** with lithium triethylborohydride ($LiEt_3BH$) and *p*-tolyl magnesium bromide (MgBrTol) gave rise to new paramagnetic species by ^{1}H NMR with

overlapping signals and a notably more complicated alkyl region in the case of MgBrTol. The reduction elimination of H_2 from a transient Co^{II}-dihydride complex or 4,4'-dimethyl-1,1'-biphenyl from a transient Co^{II}-ditolyl species would constitute an interesting transformation with implications for aryl cross-coupling chemistry. Further work is necessary to purify and characterize these compounds to determine the oxidation state and identity of the products of these reactions.

Studies with diphosphine ***52*** confirm that this ligand can support a monometallic mid-transition metal species in a range of oxidation states. Mr. Jade Shi, a then-undergraduate in the group, isolated the tricarbonyl species ***57*** as a bright orange solid by heating ***52*** in xylenes at 140 °C in the presence of $Mo(CO)_6$ (Scheme B.2). $MoCO_3(MeCN)_3$[14] has since been identified as a suitable Mo precursor for this transformation.[9f]

Scheme B.2. Synthesis of Molybdenum Species *57-59* Supported by Diphosphine *52*.

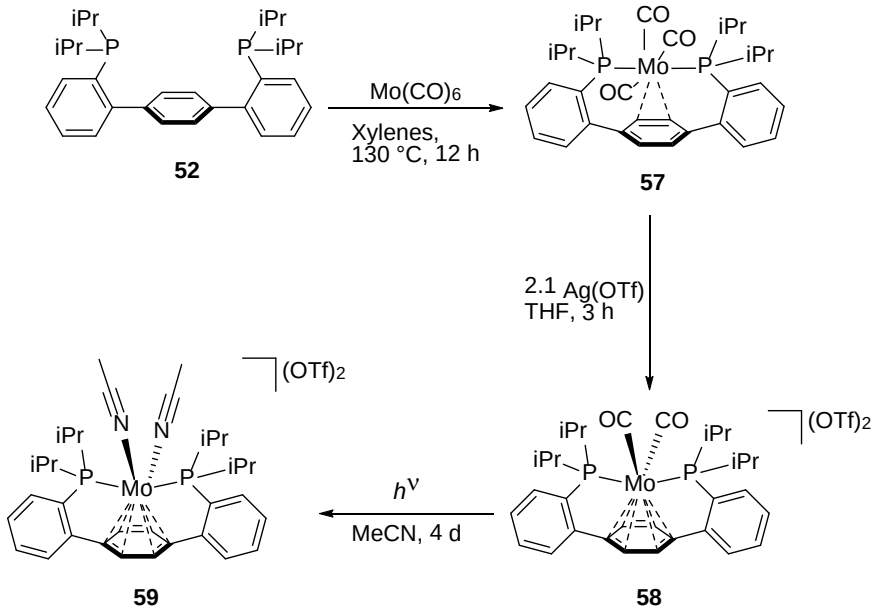

Compound **57** was characterized by ^{1}H and ^{31}P NMR, IR spectroscopy, and single crystal x-ray diffraction (XRD). Attempts were undertaken to replace the carbonyls with more labile ligands.

No change was observed in the ^{1}H or ^{31}P NMR spectrum of **57** after refluxing this species in MeCN. Oxidation of molybdenum carbonyl compounds has been reported to result in the release of CO, presumably by decreasing electron density at the molybdenum center and back-bonding into ligand CO π^* orbitals.[15] A similar strategy was employed here to displace the CO ligands of **57**. Compound **57** had been previously screened for reactivity with oxidants ferrocene and AgOTf (OTf: trifluoromethanesulfonate). Color changes were observed in both cases, and a mass consistent with a molybdenum dicarbonyl species was detected by mass spectrometry. Addition of two equivalents of AgOTf to **57** in THF afforded a single new diamagnetic species by ^{1}H and ^{31}P NMR. IR spectroscopy revealed a single strong CO stretch at 1937 cm^{-1}, consistent with the generation of a mono- or dicarbonyl species. (Compound **1** displays two CO stretches at 2030 cm^{-1} and 1976 cm^{-1}.) Single crystal XRD studies conducted on a suitable crystal of this complex revealed it to be dicarbonyl **58**. Compound **58** displays η^6-coordination to the central ring of the ligand. Comparison of solid-state structures of **57** and **58** show shorter metal-arene bond distances upon oxidation, from an average of 2.528(2) Å for **57** to 2.378(2) Å for **58**, consistent with more electron density being donated into the π^* orbitals of the central ring of the ligand with the loss of a π-accepting CO ligand.

As with **57**, compound **58** was refluxed in acetonitrile in an attempt to exchange the carbonyl ligands with more labile ligands. Again, no reaction was observed.

Figure B.5. Solid-State Structure of *57*-*59*. Hydrogen atoms omitted for clarity. Bond distances in Å.

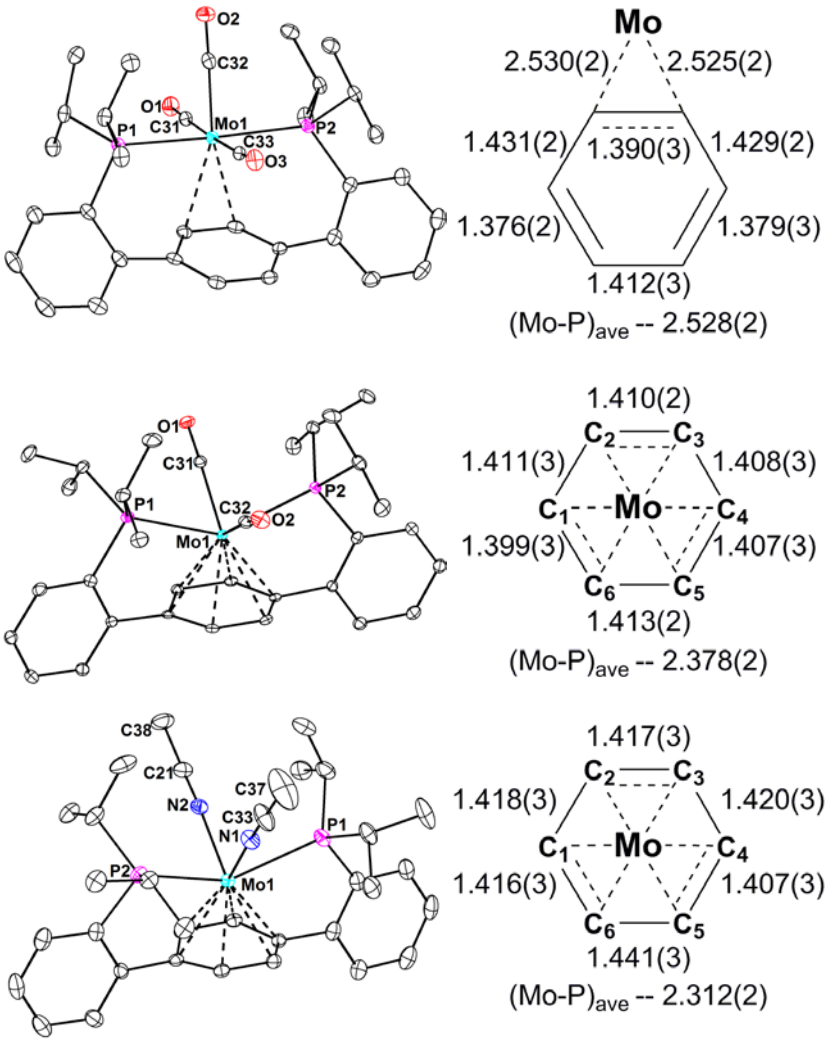

Irradiation of ***58*** in acetonitrile however, using a mercury lamp over the course of several days afforded a new diamagnetic species by ^{1}H and ^{13}C NMR. IR spectroscopy showed no stretches in the carbonyl region. A solid state structure confirmed assignment of this complex as the bisacetonitrile complex ***59*** (Figure B.5). This reaction most likely proceeds through photoexcitation of electrons from the molybdenum d-orbital manifold into the low lying π^* anti-bonding orbitals of the carbonyl ligands, facilitating ligand dissociation and coordination of acetonitrile.

Radicals have been observed through EPR studies of photoexcited single crystals of metal carbonyls.[16] Mo^{II} species **59** has been demonstrated by co-workers in our group to be a good catalyst for the dehydrogenation of ammonia borane, a molecule relevant for H_2 fuel storage.[9f] Mo species of this family display a rich and diverse chemistry with small molecules. They have been demonstrated in our group to bind N_2, reversibly bind CO_2, and form C–C bonds between the carbons of CO ligands in the presence of strong reductant.

Having demonstrated that Co and Mo compounds could be isolated and characterized in several geometries and oxidation states, chemistry with more rapidly accessible alkylphosphinophenols was explored before preparation of an aminophosphinophenol. Bisphosphinophenoxide Ni^{II}–Cl **32a** was isolated during the course of studies of intramolecular aryl and alkyl C–O bond cleavage chemistry.[10b] Reduction of compound **32a** with 2 equiv. of sodium naphthalenide affords a Ni^0 complex **60** coordinated to a soft arene ligand (Scheme B.3). This result again highlights the flexibility of the terphenyl phosphine scaffolds and their ability to provide hard or soft ligand environments depending on the oxidation state of a coordinated metal. A Ni^{II}-hydride **61** could be prepared by treating **32a** with either ^{t}BuLi or ^{t}BuMgBr, presumably through alkylation, loss of LiCl of MgBrCl, and β-hydride elimination. An alternative synthesis involves treatment of bisphosphinophenol **1f** with $Ni(COD)_2$ – oxidative addition across the O–H bond affords **61**. This chemistry has been extended by Mr. Choon Heng (Marcus) Low to afford Cr^{III} and Fe^{II} analogs to **61** (Scheme B.4) with an aminophenol moiety.

With compound **60**, treatment with excess acid afforded **1f**. Oligomerization trials with bisphosphenols, C_2H_4, and methylaluminoxane (MAO) have been undertaken by Mr. Low.

Scheme B.3. Synthesis of Bisphosphinophenol Nickel Compounds 60 and 61.

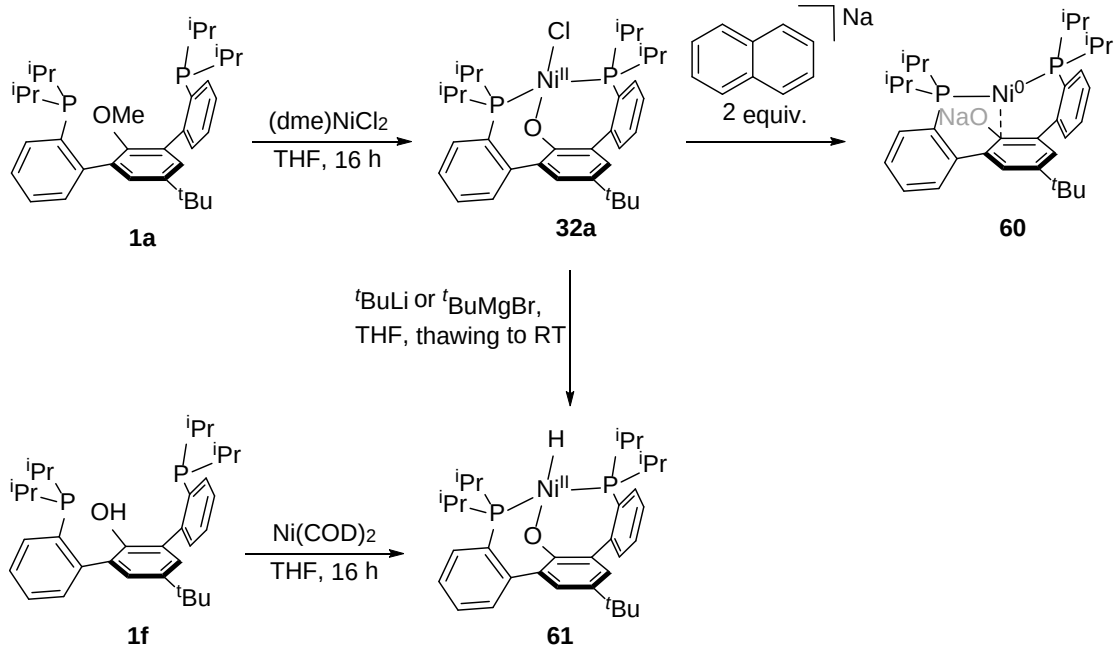

Scheme B.4. Synthesis of Bisphosphinophenoxide Cr and Fe Compounds (Marcus Low).

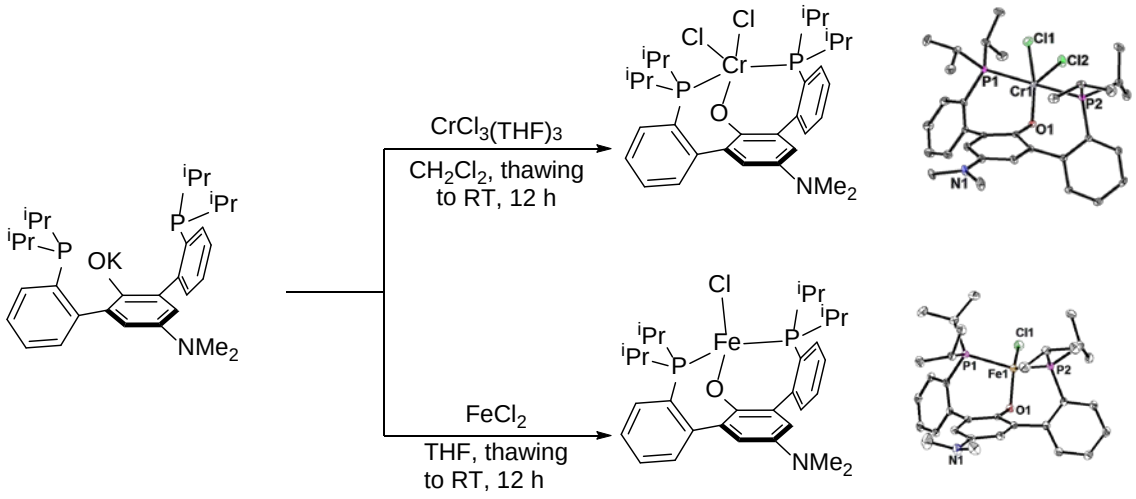

Removal of a pendant phosphine donor was envisioned to afford a Ni species with more accessible coordination sites. Thus, ligands bearing one pendant donor are envisioned. The flexibility and redox non-innocence of these ligands is anticipated stabilize intermediates during the rearrangements and electron transfers of a catalytic cycle.

Towards the preparation of phosphinophenol **64**, boronic ester **62** was prepared according to literature procedure (Scheme B.5). Elaboration to biphenyl bromide **63** was accomplished through Suzuki coupling of **62** with 1-bromo-2-iodobenzene. Installation of a phosphine substituent was accomplished through lithium halogen exchange and quenching with $^{i}Pr_2PCl$. Acidic work-up in MeOH results in deprotection of the methylmethoxy (-MOM) protecting group, affording the desired phosphinophenol **64**.

Scheme B.5. Synthesis of Phosphinophenol 64.

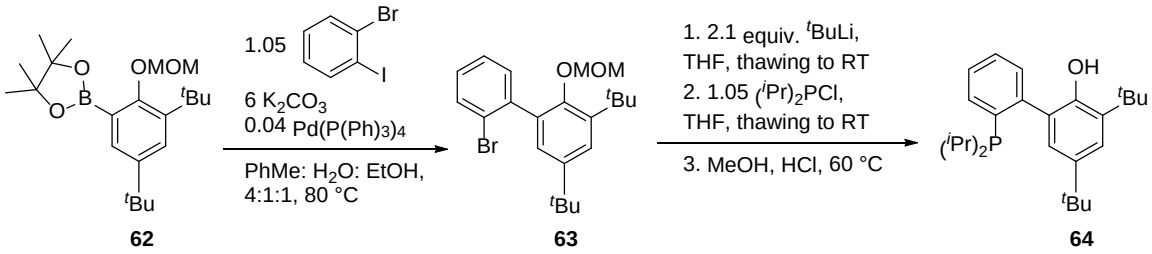

Treatment of **64** with $Ni(COD)_2$, deprotonation with base followed by treatment with $Ni(DME)Cl_2$ (DME: dimethoxyethane), and comproportionation of $Ni(COD)_2$ and $Ni(DME)Cl_2$ in the presence of **64** does not afford species consistent with coordination of Ni to the phosphinophenol (^{1}H and ^{31}P NMR). However, treatment of **64** with $Ni(TMEDA)Me_2$[17] (TMEDA: tetramethylethylenediamine) afforded Ni^{II}-Me compound **65** (Scheme B.6). A solid state structure confirmed the

initial assignment of **65** as a Ni^{II}-Me species based on NMR data and revealed η^5-coordination to the rearranged phenol moiety. The C–O bond distance of 1.253(2) Å is consistent with a double bond. Ni,[18] Pd,[18] and Ru[19] η^5-oxocyclohexadiene compounds have been previously reported. Given its similarity to the Shell Higher Olefin Process (SHOP)[20] catalyst for ethylene oligomerization, compound **65** is an attractive candidate for reactions under C_2H_4 pressure; such investigations have not yet been completed.

Scheme B.6. Synthesis of Ni^{II}-Me 65.

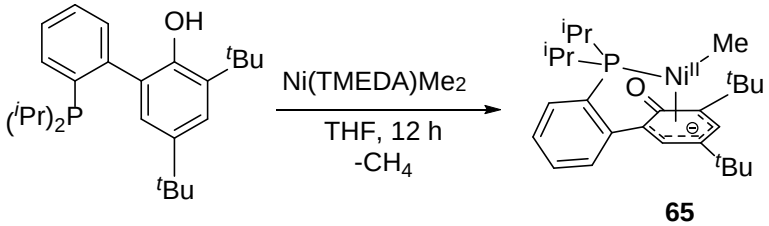

Figure B.6. Solid-State Structure of 65. Hydrogen atoms omitted for clarity. Bond distances in Å.

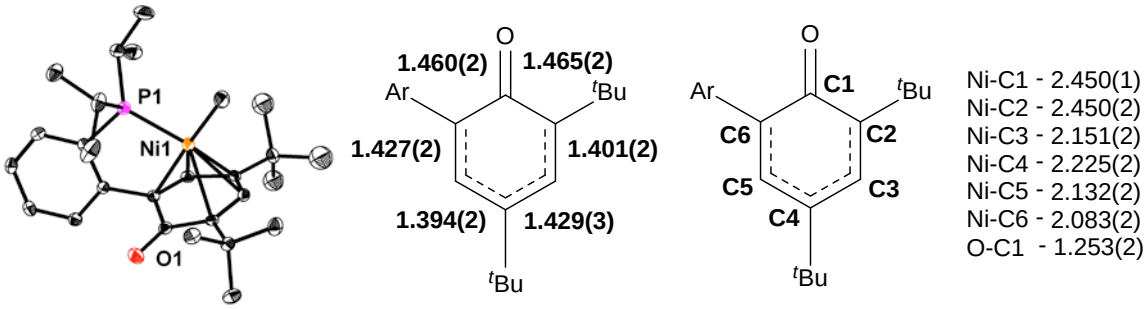

With structural evidence that phosphinophenol **64** could accommodate a first row transition metal with an sterically accessible face, C_2H_4 oligomerization and polymerization trials were attempted on conditions of C_2H_4 pressure (100 PSI) and MAO (360 equiv.) for 30 min. at 25 °C (Scheme B.7). Phosphinophenol **64** was

treated with benzyl potassium (BnK) and loss of the resonance assigned to phenol was observed by ^{1}H NMR to afford potassium phenoxide compound **66**.

Scheme B.7. Oligomerization/Polymerization Reactions with 66 and Fe, Co, and Cr Halide Precursors.

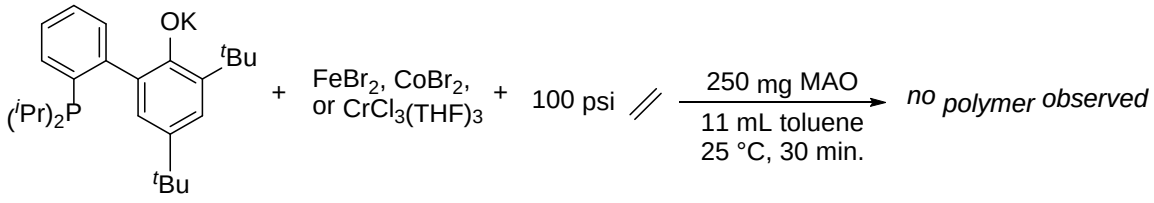

66
ca. 12 μmol

Scheme B.8. Oligomerization/Polymerization Reaction with 1a and $CrCl_3(THF)_3$.

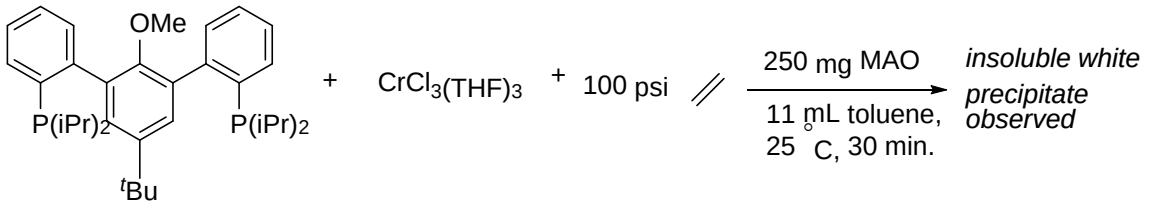

1a
ca. 12 μmol

In separate reactions, phenoxide **66** was treated with $FeBr_2$, $CoBr_2$, or $CrCl_3(THF)_3$ in toluene before being loaded in a Fischer-Porter apparatus and place under oligomerization/polymerization conditions. No insoluble polymer was observed and no C_2H_4 was observed in an aliquot of the reaction mixture analyzed by GC.

At this time, **1a** was tested under the above conditions for a possible effect on C_2H_4 oligomerization/polymerization activity (Scheme B.8). "PSP" and "PNP" ligands have been reported to selective afford α-olefins in the presence of Cr precursors, methylaluminoxane activator, and C_2H_4. In the absence of **1a**, *ca.* 0.5 g of insoluble

polymer was observed. In the presence of **1a**, a similar amount of insoluble polymer was observed. No oligomers were detected by GC in an aliquot from the reaction mixture.

Scheme B.9. Synthesis of Aminophosphinophenol 71.

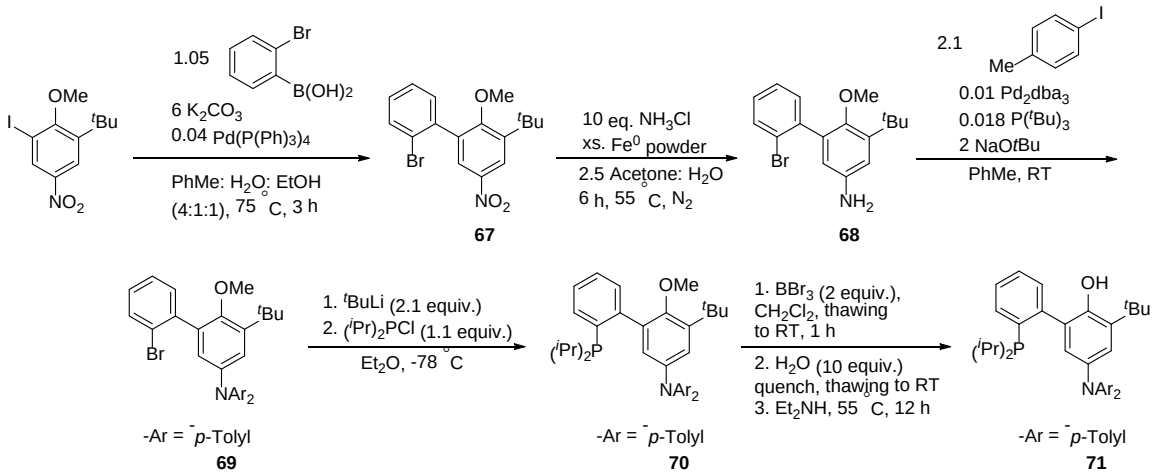

Given the lack of oligomer observed in reactions with C_2H_4 with **1a** or **66**, aminophosphinophenol **71** was prepared. The aminophenol moiety was envisioned to facilitate two electron processes, specifically transformations necessary for selective C_2H_4 oligomerization through a metallocyclic mechanism. 1-(tert-Butyl)-3-iodo-2-methoxy-5-nitrobenzene was prepared according to a reported literature procedure[21]. Suzuki coupling with (2-bromophenyl)boronic acid affords biphenyl bromide **67**. Reduction of compound **67** affords biphenyl amine **68**.[22] Use of Buchwald-Hartwig technology for amine arylation allows for preparation of di-*para*-tolyl amine **69** from **68**. Installation of phosphine is achieved by treatment of aryl amine bromide **69** with ^{t}BuLi followed by quenching with $(^i\text{Pr})_2\text{PCl}$ to afford **70**. Deprotection of methyl aryl ether **70** is achieved by treatment of the phosphine with BBr_3 followed by heating in Et_2NH to quench boron reagent affords the desired aminophosphinophenol **71**.

Scheme B.10. Oligomerization/Polymerization Reactions with 71 and $CrCl_3(THF)_3$.

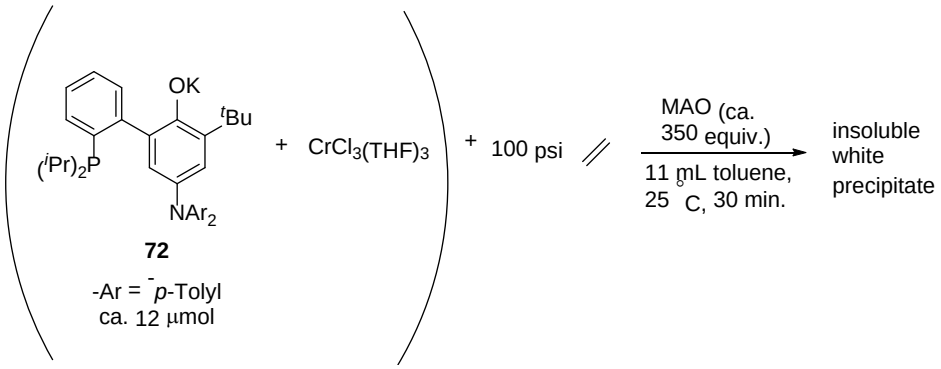

Compound **71** was treated with BnK to afford phenoxide **72**. Loss of the resonance assigned to the phenolic proton of **71** observed by ^{1}H NMR after treatment with BnK was consistent with the assignment. Compound **71** was treated with $CrCl_3(THF)_3$ in CH_2Cl_2, then used as a precatalyst under previously described oligomerization/polymerization conditions. An insoluble white precipitate was observed and no oligomers were detected from an aliquot of the reaction mixture analyzed by GC.

Scheme B.11. Metallation of 72 with $CrCl_3(THF)_3$, $FeBr_2$, and $CoBr_2$.

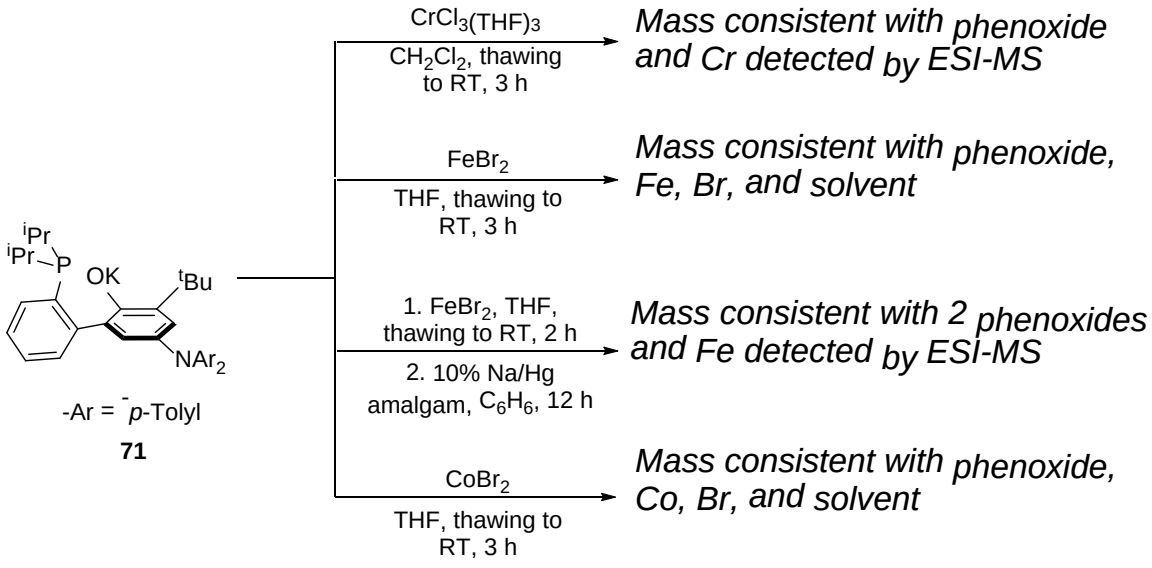

Metallations with Fe, Co, and Cr halides were attempted using **72** (Scheme B.11). Treatment of **72** with $CrCl_3(THF)_3$ allowed for observation of a mass consistent with phenoxide and Cr by ESI-MS. Treatment of **72** with $FeBr_2$ allowed for observation of a mass consistent with phenoxide and Fe by ESI-MS. Treatment of this material with Na/Hg resulted in observation of a new signal consistent with 2 phenoxide ligands and one Fe center. With $CoBr_2$ and **72** a mass which could be assigned to phenoxide, Co, Br, and THF solvent was observed. To date, a solid-state structure of a transition metal complex supported by phosphine **71** or its derivatives has not been obtained. Structural characterization of such compounds should facilitate screening for reactivity and design of new proligands to facilitate the desired $2e^-$ chemical transformations (Scheme B.3) proposed herein.

CONCLUSIONS:

Hemilabile ligands are ideal for stabilizing transition metals over a range of oxidation states. Low-valent mononuclear molybdenum, iron, cobalt and copper compounds supported by para- and meta- terphenyl diphosphine ligands were targeted. The metal-arene interactions were analyzed by single-crystal X-ray diffraction and solution-state nuclear magnetic resonance. Other investigators in our research group have demonstrated that, upon reduction of an isolated Mo^{II} precursor, a Mo^{0} complex is formed. This Mo^{0} complex can bind N_2 and CO_2 and oxidatively add H_2 to form a Mo^{II} dihydride. Compounds of this family are also effective ammonia borane dehydrogenation catalysts. This study was extended to the investigation of phenols bearing pendant phosphines, as A Ni^{II} compound supported by such a ligand has been demonstrated to be stabilized by the phenoxide donor whereas the corresponding reduced Ni^{0} complex is instead stabilized by a metal-arene interaction.

Experimental Section

General Considerations

Unless otherwise indicated, reactions performed under inert atmosphere were carried out in oven-dried glassware in a glovebox under a nitrogen atmosphere purified by circulation through RCI-DRI 13X-0408 Molecular Sieves 13X, 4x8 Mesh Beads and BASF PuriStar® Catalyst R3-11G, 5x3 mm (Research Catalysts, Inc.). Solvents for all reactions were dried by Grubbs' method.[23] Acetonitrile-d_3, benzene-d_6, chloroform-d_1, and dichloromethane-d_2 were purchased from Cambridge Isotope Laboratories. Benzene-d_6 was vacuum distilled from sodium benzophenone ketyl. Acetonitrile-d_3 and dichloromethane-d_2 were vacuum distilled from calcium hydride. Alumina and Celite were activated by heating under vacuum at 200 °C for 24 h. 1,3,-bis(2'-diisopropylphosphino)phenyl)benzene[9b] (**51**), 1,4,-bis(2'-diisopropylphosphino)phenyl)benzene[9c] (**52**), [2,6-bis(2'-diisopropylphosphinophenyl)-4-tert-butyl-phenoxide]nickel(II)-chloride[10b] (**32a**), $Mo(CO)_3(MeCN)_3$,[14] 2,6-bis(2'-diisopropylphosphinophenyl)-4-tert-butyl-phenol[10b] (**1f**), 1,3-bis(2'-diisopropylphosphinophenyl)-5-tert-butyl-2-methoxybenzene (**1a**),[10a] 2-(3,5-di-tert-butyl-2-(methoxymethoxy)phenyl)-4,4,5,5-tetramethyl-1,3,2-dioxaborolane,[24] benzyl potassium,[25] and 1-(tert-Butyl)-3-iodo-2-methoxy-5-nitrobenzene[21] were prepared according to previously reported literature procedures. $Ni(TMEDA)Me_2$[17] (TMEDA: tetramethylenediamine) was synthesized from $Ni(acac)_2(TMEDA)$[26] (acac: acetylacetone) and $Mg(TMEDA)Me_2$.[27] All other materials were used as received. ^1H, ^{13}C, ^{19}F, and ^{31}P NMR spectra were recorded on Varian or Bruker spectrometers at ambient temperature unless denoted otherwise. Chemical shifts are reported with respect to internal solvent for ^1H and ^{13}C NMR data, respectively: 1.94 ppm and 118.26 and 1.32 ppm (CD_3CN); 7.16 ppm and 128.06 ppm

(C_6D_6); 7.26 ppm and 77.16 ppm ($CDCl_3$); 5.32 ppm and 53.84 ppm (CD_2Cl_2).[28] ^{19}F and ^{31}P NMR chemical shifts are reported with respect to an external standard of C_6F_6 (-164.9 ppm) and 85% H_3PO_4 (0.0 ppm), respectively, unless denoted otherwise. IR measurements were obtained on a Bruker Alpha spectrometer equipped with a diamond ATR probe.

Experimental Details

Synthesis of [1,3,-bis(2'-diisopropylphosphino)phenyl)benzene]cobalt(II) bromide (53).

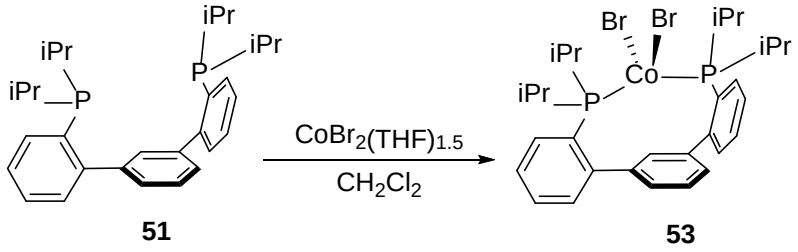

51 **53**

A 20 mL scintillation vial was charged with a magnetic stir bar, $CoBr_2$ (0.02 g, 0.09 mmol), and THF (3 mL). A colorless solution of **51** (0.04 g, 0.09 mmol) in THF (2 mL) was added and the reaction mixture stirred at room temperature. After 1 h, a color change from dark blue to emerald green was observed. After 2 h, solvent was removed *en vacuo*. DCM (3 mL) was added to the green residue and the reaction mixture was allowed to stir for 5 min. before the solvent was removed under reduced pressure. This process was repeated three times. The resulting powder was dissolved in DCM (3 mL) once more, filtered through Celite, and the solvent removed under reduced pressure to afford **53**. ^1H NMR (300 MHz, CD_2Cl_2). δ 26.41 (s, br), 23.12 (s, br), 21.23 (s, br), 17.15 (s, br), 13.93 (s, br), 8.17 (s, br), 3.63 (s, br), 0.15 (s), -1.67 (s, br), -5.06 (s, br), -13.16 (s, br). No ^{31}P NMR signal observed (121 MHz, CD_2Cl_2).

Synthesis of [1,4-bis(2'-diisopropylphosphino)phenyl)benzene]molybdenum(0)tricarbonyl (*57*).

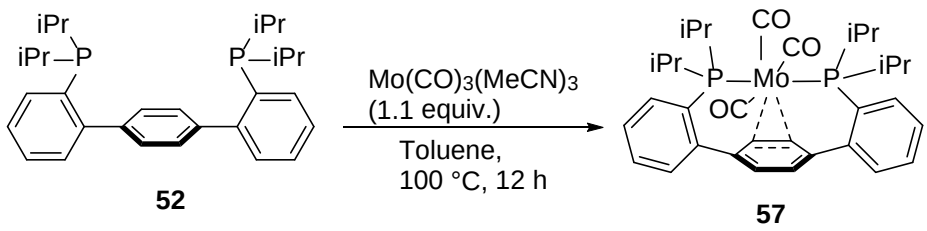

Addition of $Mo(CO)_3(MeCN)_3$[14] (1.43 g, 4.75 mmol, 1.1 equiv.) to a clear solution of ***52*** (2.05 g, 4.32 mmol, 1.0 equiv.) in toluene (50 mL) resulted in a yellow/green heterogeneous mixture. Following heating to 100 °C and stirring for 12 h, the mixture became a deep orange homogenous solution. The volatiles were removed under reduced pressure. The resulting orange solids were collected and washed with cold hexanes (2 x 15 mL). Residual volatiles were removed under reduced pressure to yield ***57*** (2.54 g, 3.81 mmol, 88 %). X-ray quality crystals were grown from vapor diffusion of pentane into a saturated THF solution of ***57***. ^{1}H NMR (500 MHz, CD_2Cl_2, 25 °C) δ 7.86 (m, 2H, aryl-*H*), 7.53 (m, 6H, aryl-*H*), 6.52 (br s, 4H, central arene-*H*), 2.75 (br s, 4H, C*H*$(CH_3)_2$), and 1.09-1.23 (br s, 24H, CH(C*H*$_3)_2$). ^{13}C{^{1}H} NMR (101 MHz, CD_2Cl_2, 25 °C) δ: 221.15 (t, *J* = 10.19 Hz, Mo-*C*O), 213.75 (t, *J* = 8.87 Hz, Mo-*C*O), 148.80 (t, *J* = 6.90 Hz, aryl-*C*), 139.99 (t, *J* = 2.74, central arene-*C*), 131.23 (s, aryl-*C*H), 131.02 (t, *J* = 9.41 Hz, aryl-*C*), 129.90 (s, aryl-*C*H), 129.35 (s, aryl-*C*H), 128.34 (s, aryl-*C*H), 33.83 (br s, *C*H$(CH_3)_2$), 19.88 (s, CH(*C*H$_3)_2$), and 19.43 (s, CH(*C*H$_3)_2$). ^{31}P{^{1}H} NMR (121 MHz, C_6D_6, 25 °C) δ: 51.01. IR (CaF_2 window, C_6H_6, cm^{-1}) ν_{CO}: 2298.5, 2192.8. Anal. Calcd. for ***57*** $C_{33}H_{40}MoO_3P_2$ (%): C, 61.68; H, 6.27. Found: C, 61.43; H, 5.99.

Synthesis of [(1,4-bis(2'-diisopropylphosphino)phenyl)benzene)molybdenum(II)dicarbonyl][bistrifluoromethylsulfonate] (58).

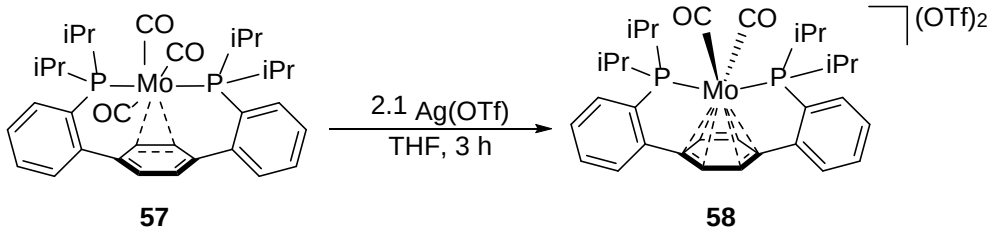

57 **58**

To a rapidly stirring solution of ***57*** (1.17 g, 1.82 mmol) in THF (50 mL), a solution of AgOTf (1.00 g, 3.83 mmol) in THF (35 mL) was added dropwise. With each drop, an darkening of the solution was observed. Complete addition of the silver solution led to a persistent purple/brown mixture, which was stirred at room temperature for 3 h. The volatiles were removed under reduced pressure to yield green/brown solids. These solids were collected on a fritted glass funnel and washed with THF (3 x 10 mL). The solid residue was extracted into MeCN (30 mL), filtered through Celite, and the resulting yellow solution was dried under reduced pressure. The yellow solids were dissolved in minimal MeCN and filtered through Celite once more. Et_2O was added to the filtrate which was then cooled to -35 °C. The precipitate was collected via vacuum filtration, providing ***58*** (1.16 g, 1.26 mmol, 69 %) as yellow microcrystals. X-ray quality crystals were obtained from vapor diffusion of diethyl ether into a saturated MeCN solution of ***58***. ^{1}H NMR (300 MHz, CD_3CN, 25 °C) δ: 7.93 (m, 2H, aryl-*H*), 7.83 (m, 6H, aryl-*H*), 7.15 (s, 4H, central arene-*H*), 3.35 (m, 4H, C*H*$(CH_3)_2$), and 1.29-1.44 (m, 24H, CH(C*H*$_3$)$_2$). ^{13}C{^{1}H} NMR (101 MHz, CD_3CN, 25 °C) δ: 219.03 (s, Mo-*C*O), 141.32 (dd, *J* = 7.58, 5.79, aryl-*C*), 137.69 (t, *J* = 3.93 Hz, central arene-*C*), 134.64 (s, aryl-*C*H), 133.93 (dd, *J* = 47.74, 8.22, aryl-*C*), 133.83 (s, aryl-*C*H), 132.12 (t, *J* = 3.07 Hz, aryl-*C*H), 128.58 (t, *J* = 5.70 Hz, aryl-*C*H), 122.07 (q, *J* = 320.73 Hz, $F_3CSO_3^-$),

104.72 (s, central arene-*C*H), 28.97 (q, *J* = 11.67 Hz, *C*H(CH$_3$)$_2$), 18.47 (s, CH(*C*H$_3$)$_2$), and 18.07 (s, CH(*C*H$_3$)$_2$). ^{31}P{^{1}H} NMR (121 MHz, CD$_3$CN, 25 °C) δ: 75.05. IR (CaF$_2$ window, C$_6$H$_6$, cm^{-1}) ν_{CO}: 2025.2, 1986.4. Anal. Calcd. for 3 $C_{34}H_{40}F_6MoO_8P_2S_2$ (%): C, 44.74; H, 4.42. Found: C, 44.65; H, 4.49.

Synthesis of [(1,4-bis(2'-diisopropylphosphino)phenyl)benzene)molybdenum(II)di-acetonitrile][bistrifluoromethylsulfonate] (59).

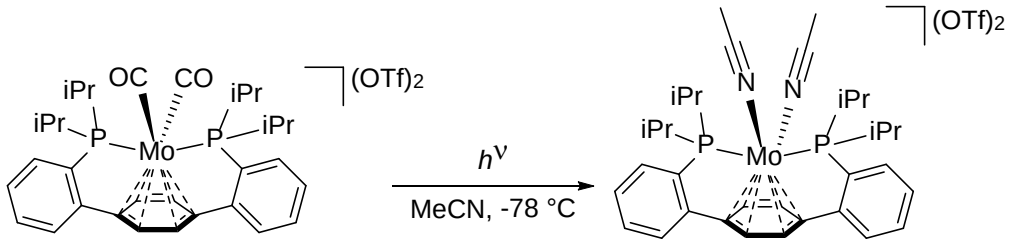

58 **59**

A bright yellow acetonitrile (20 mL) solution of **58** (533 mg, 0.583 mmol) was transferred to a quartz Schlenk tube, charged with a stir bar. The tube was degassed via three freeze-pump-thaw cycles and then, while stirring, irradiated with a 200 W Hg/Xe lamp at -78 °C for 2 h. The evolution of bubbles was observed and the solution steadily darkened to deep red. The flask was degassed as above and photolysis continued. With continued irradiation, the solution darkened to a deep purple color that glowed intensely under the UV light. This degas/irradiation process was continued until aliquots of the solution showed no presence of **58** or the putative monocarbonyl species by ^{31}P NMR (75.05 and 68.62 ppm, respectively). The total irradiation time was dependent on lamp age, frequency of degassing, and solution concentration, varying from 12 h to several days. Upon complete conversion, volatiles were removed under reduced pressure, providing deep purple solids. These solids were collected on a fritted funnel and washed with THF until the filtrate was colorless. The purple

microcrystalline product was collected (528 mg, 0.565 mmol, 97 %). Crystals suitable for X-ray diffraction were obtained from vapor diffusion of Et_2O into a saturated MeCN solution of **59**. ^{1}H NMR (300 MHz, CD_3CN, 25 °C) δ: 7.62-7.72 (m, 6H, aryl-*H*), 7.51-7.52 (m, 2H, aryl-*H*), 5.59 (t, 4H, *J* = 2.2 Hz, central arene-*H*), 2.86-2.93 (m, 4H, C*H*(CH_3)$_2$), 2.72 (m, 6H, NC(C*H*$_3$)), and 1.25-1.31 (m, 24H, CH(C*H*$_3$)$_2$). ^{13}C{^{1}H} NMR (126 MHz, CD_3CN, 25 °C) δ: 145.36 (t, *J* = 10.51 Hz, aryl-*C*), 143.35 (s, N*C*CH_3), 133.44 (s, aryl-*C*H), 132.35 (s, aryl-*C*H), 130.60 (dd, *J* = 62.25, 23.73, aryl-*C*), 130.57 (s, aryl-*C*H), 127.48 (s, aryl-*C*H), 123.39 (s, Mo- *C*NCH_3), 122.15 (q, *J* = 318.51, $F_3CSO_3^-$), 120.50 (s, central arene-*C*), 88.90 (s, central arene-*C*H), 25.74 (t, *J* = 9.77 Hz, *C*H(CH_3)$_2$), 18.67 (s, CH(*C*H_3)$_2$), 17.86 (s, CH(*C*H_3)$_2$), 7.03 (s, Mo-NC*C*H_3) and 6.52 (m, Mo-NC*C*H_3). ^{31}P{^{1}H} NMR (121 MHz, CD_3CN, 25 °C) δ: 63.35. Anal. Calcd. for **4**: $C_{36}H_{46}F_6MoN_2O_6P_2S_2$ (%): C, 46.06; H, 4.94; N, 2.98. Found: C, 45.09; H, 4.77; N, 3.25.

Synthesis of [sodium][(2,6-bis(2'-diisopropylphosphinophenyl)-4-tert-butyl-phenoxide)nickel(0)] (60).

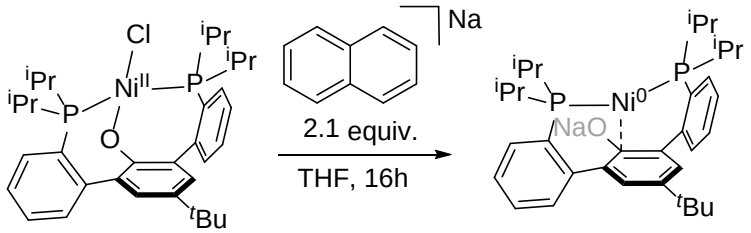

32a **60**

A 20 mL scintillation vial coating with a mirror of Na and charged with a stir bar was charged with naphthalene (0.021 g, 0.17 mmol, 2.1 equiv.) as a solution in THF (2 mL). The solution was stirred vigorously for 1 h. A dark green color, consistent with the formation of sodium naphthalenide[29] was observed. A separate 20 mL scintillation vial was charged with phenoxide Ni^{II}Cl compound **32** (0.050 g, 0.08 mmol, 1.0 equiv.),

THF (1 mL), and a stir bar. A dark purple solution was observed. The dark green solution was added and the vial of sodium napthalenide solution was rinsed with two portions of THF (1 mL) which was combined with the reaction mixture. A dark red solution was observed. After 1 h, volatiles were removed under reduced pressure. A dark red residue was observed. Pentane (1 mL) was added, the residue was triturated, and volatiles were removed under reduced pressure. The resulting residue was washed three times with pentane (1 mL) then extracted with three portions of C_6H_6 (1 mL). The combined C_6H_6 solution was filtered through Celite and volatiles were removed from the filtrate to afford **60**. Crystals suitable for X-ray diffraction were grown from a saturated solution of pentane. ^{1}H NMR (400 MHz, C_6D_6) δ 7.36 (m, 2H, Ar-*H*$_6$), 7.05 (m, 2H, Ar-*H*$_8$), 7.01 – 6.93 (m, 4H, Ar-*H*$_9$ & Ar-*H*$_7$), 6.40 (t, 2H, Ar-*H*$_3$, J_{PC} = 2.0 Hz), 2.15 (m, 2H, -C*H*(CH$_3$)$_2$), 1.88 (m, 2H, -C*H*(CH$_3$)$_2$), 1.39 (s, 9H, -C(C*H*$_3$)$_3$), 1.24 (dd, 6H, -CH(C*H*$_3$)$_2$), 1.04 (m, 12H, -CH(C*H*$_3$)$_2$), 0.68 (m, 6H, -CH(C*H*$_3$)$_2$). ^{13}C{^{1}H} NMR (101 MHz, C_6D_6) δ 152.24 (app t, Ar-*C*, J_{PC} = 14.7 Hz), 142.04 (app t, Ar-*C*, J_{PC} = 14.7 Hz), 132.71 (s, Ar-*C*$_1$), 130.29 (app t, Ar-*C*$_6$, J_{PC} = 2.5 Hz), 129.73 (s, Ar-*C*$_9$), 128.21 (obscured by solvent residual, detected by HSQC, Ar-*C*$_7$), 127.31 (s, Ar-*C*$_8$), 118.12 (s, Ar-*C*$_3$), 33.89 (s, -*C*(CH$_3$)$_3$, 32.18 (s, -C(*C*H$_3$)$_3$), 27.84 (app t, -*C*H(CH$_3$)$_2$, J_{PC} = 7.1 Hz), 20.55 (app t, -CH(*C*H$_3$)$_2$, J_{PC} = 6.1 Hz), 20.24 (s, br, -CH(*C*H$_3$)$_2$, 20.07 (app t, -*C*H(CH$_3$)$_2$, J_{PC} = 7.1 Hz), 19.77 (s, br, -CH(*C*H$_3$)$_2$), 19.16 (app t, -CH(*C*H$_3$)$_2$, J_{PC} = 6.1 Hz). Two Ar-*C* not detected. ^{31}P{^{1}H} NMR (121 MHz, C_6D_6) δ 38.31 (s).

Synthesis of [2,6-bis(2'-diisopropylphosphinophenyl)-4-tert-butyl-phenoxide]nickel(II)-hydride (61).

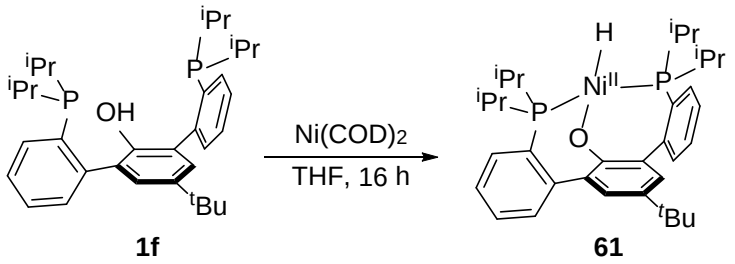

1f **61**

A 20 mL scintillation vial was charged with $Ni(COD)_2$ (0.052 g, 0.191 mmol), THF (2 mL), and a stir bar. A slurry of a yellow solid in THF was observed. Bisphosphinophenol **1f** (0.102 g, 0.19 mmol) was added as a colorless solution in THF (2 mL). After 16 h, a yellow solution was observed. Volatiles were removed under reduced pressure. Pentane (2 mL) was added and the mixture was triturated. The resulting yellow solid was washed with pentane (3 x 2 mL), hexanes (3 x 2 mL), and Et_2O (3 x 2 mL). The residue was then extracted with C_6H_6 (2 x 3 mL). The combined C_6H_6 solution was filtered through Celite and volatiles removed under reduced pressure to afford **61** (0.088 g, 0.15 mmol, 78.9%). ^{1}H NMR (300 MHz, C_6D_6) δ 7.38 (s, 2H, Ar-H_3), 7.34 - 7.30 (m, 2H, Ar-H_6), 7.22 – 7.15 (m, 4H, Ar-H_7 & Ar-H_9), 7.05 (m, 2H, Ar-H_8), 2.15 (m, 2H, -CH(CH_3)$_2$), 1.68 (m, 2H, -CH(CH_3)$_2$), 1.57 (dd, 6H, -CH(CH_3)$_2$), 1.50 (s, 9H, -C(CH_3)$_3$), 1.30 (dd, 6H, -CH(CH_3)$_2$), 1.04 (dd, 6H, -CH(CH_3)$_2$, 0.72 (dd, 6H, -CH(CH_3)$_2$), -25.62 (t, 1H, Ni-H, J_{PH} = 78.0 Hz). ^{13}C{^{1}H} NMR (101 MHz, C_6D_6) δ 150.75 (app t, Ar-C_5, J_{PC} = 8.6 Hz), 145.75 (s, Ar-C_1), 138.14 (s, Ar-C_4), 134.48 (s, Ar-C_2), 133.27 (app t, Ar-C_6, J_{PC} = 4.5 Hz), 130.75 (s, Ar-C_7 or Ar-C_9), 130.59 (s, Ar-C_7 or Ar-C_9), 129.98 (s, Ar-C_3), 125.92 (td, Ar-C_{10}, J_{PC} = 34.8 Hz, J_{HC} = 2.0 Hz), 125.13 (app t, Ar-C_8, J_{PC} = 4.5 Hz), 34.23 (s, -C(CH_3)$_3$), 32.19 (s, -C(CH$_3$)$_3$), 29.61 (td, -CH(CH_3)$_2$, J_{PC} = 14.6 Hz, J_{HC} = 3.7 Hz),

22.77 (t, -*C*H(CH$_3$)$_2$, J_{PC} = 12.1 Hz), 19.98 – 19.45 (m, -CH(*C*H$_3$)$_2$), 16.48 (s, -CH(*C*H$_3$)$_2$). ^{31}P NMR (121 MHz, C_6D_6) δ 39.37 (m).

Synthesis of 1-(2'-bromo)phenyl-2-methoxymethoxy-3,5-di-tert-butyl-benzene (63).

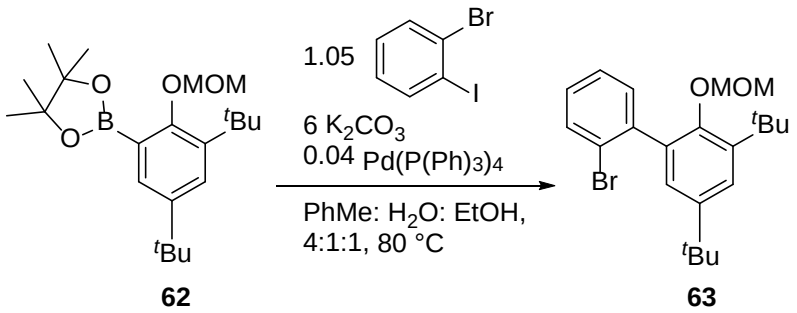

In the fume hood, a 500 mL Schlenk tube fitted with a Teflon screw cap was charged with 2-(methoxymethoxy)phenyl)-4,4,5,5-tetramethyl-1,3,2-dioxaborolane,[24] (1.950 g, 5.15 mmol, 1.1 equiv.), 1-bromo-2-iodobenzene (1.333 g, 4.71 mmol, 1.0 equiv.), K_2CO_3 (3.906 g, 28.26 mmol, 6.0 equiv.), toluene (100 mL), EtOH (30 mL), and H_2O (30 mL). On the Schlenk line, the reaction mixture was degassed via three freeze-pump-thaw cycles. With N_2 backflow, Pd(PPh$_3$)$_4$ (0.272 g, 0.24 mmol, 0.05 equiv.) was added, providing a yellow biphasic solution. The reaction was stirred at 80 °C for 23 h at which time the reaction mixture was transferred to a round bottom flask and concentrated under reduced pressure to a total volume of *ca.* 100 mL. This mixture was transferred to a separatory funnel and extracted with CH_2Cl_2 (*ca.* 75 mL) three times. The combined organics were washed with brine and dried over Mg(SO$_4$)$_2$. The volatiles were removed under reduced pressure, providing **63** as a brown oil. Material of this purity was heated under vacuum on the Schlenk line and used in a subsequent phosphination without further purification. ^{1}H NMR (300 MHz, CDCl$_3$) δ 7.70 (m, 1H, Ar-*H*), 7.52 – 7.43 (m, 2H, Ar-*H*), 7.24 – 7.16 (m, 2H, Ar-*H*), 7.09 (d, 1H, Ar-

H), 4.52 (d, 1H, -OC*H*$_2$OCH$_3$), 4.42 (d, 1H, -OC*H*$_2$OCH$_3$), 3.15 (s, 1H, -OCH$_2$OC*H*$_3$), 1.47 (s, 9H, -C(C*H*$_3$)$_3$, 1.33 (s, 9H, -C(C*H*$_3$)$_3$.

Synthesis of 1-(2'-diisopropylphosphino)phenyl-2-methoxymethoxy-3,5-di-tert-butyl-benzene.

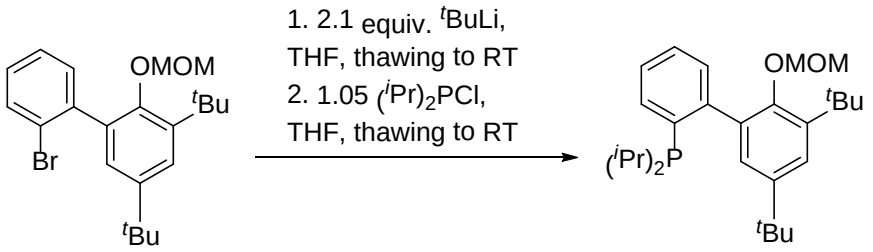

63

In the glovebox, a 250 mL round bottom flask charged with biphenyl bromide **63** (3.321 g, 6.59 mmol, 1.0 equiv.), THF (80 mL), and a stir bar. Separately, a 20 mL scintillation vial was charged with ^{t}BuLi (16.3 mL, 27.66 mmol, 1.7 M solution in heptane). The solutions were frozen in a liquid N_2-chilled cold well. The just-thawed solution of ^{t}BuLi was added to the thawing solution of **63**. The mixture was allowed to warm to room temperature. A separate 20 mL scintillation vial was charged with (^{i}Pr$_2$)PCl (2.111 g, 2.20 mL, 13.83 mmol, 2.1 equiv.). The reaction mixture and (^{i}Pr$_2$)PCl were frozen in a liquid N_2-chilled cold well. The just-thawed solution of (^{i}Pr$_2$)PCl was added to the thawing reaction mixture. The mixture was allowed to warm to room temperature and stir for 12 h. After 12 h, volatiles were removed under reduced pressure to afford a brown residue. Hexanes (10 mL) was added and the residue was triturated. Volatiles were removed under reduced pressure. The resulting powder was extracted with 3 portions of C_6H_6 (20 mL each). The combined organic layer was filtered through alumina. Volatiles were removed under reduced pressure. The resulting solid was precipitated from hexanes to afford the desired –MOM

protected phosphinophenol as a pale yellow solid which was used in a subsequent deprotection step without further purification. ^{1}H NMR (400 MHz, C_6D_6) δ 7.59 (d, 1H, Ar-*H*$_3$), 7.41 – 7.31 (m, 2H, Ar-*H*$_6$ & Ar-*H*$_9$), 7.14 – 7.12 (m, 2H, Ar-*H*$_{12}$ & Ar-*H*$_7$ or Ar-*H*$_8$), 7.04 (m, 1H, Ar-*H*$_7$ or Ar-*H*$_8$), 4.70 (d, 1H, -O*C*H$_2$OCH$_3$), 4.42 (d, 1H, -O*C*H$_2$OCH$_3$), 3.12 (s, 3H, -OCH$_2$OC*H*$_3$), 2.05 (m, 1H, -C*H*(CH$_3$)$_2$), 1.67 (s, 9H, -C(C*H*$_3$)$_3$; m, 1H, -C*H*(CH$_3$)$_2$), 1.35 (s, 9H, -C(C*H*$_3$)$_3$, 1.10 (m, 6H, -CH(C*H*$_3$)$_2$), 0.85 (m, 6H, -CH(C*H*$_3$)$_2$). ^{13}C{^{1}H} NMR (101 MHz, C_6D_6) δ 152.79 (d, Ar-*C*$_1$, J_{PC} = 1.0 Hz), 149.22 (d, Ar-*C*$_{10}$, J_{PC} = 31.3 Hz), 144.49 (s, -*C*(CH$_3$)$_3$), 141.53 (s, -*C*(CH$_3$)$_3$), 137.15 (d, Ar-*C*$_5$, J_{PC} = 23.2 Hz), 136.10 (d, Ar-*C*$_2$, J_{PC} = 6.1 Hz), 132.70 (d, Ar-*C*$_6$ or Ar-*C*$_9$, J_{PC} = 4.0 Hz), 131.21 (d, Ar-*C*$_6$ or Ar-*C*$_9$, J_{PC} = 6.1 Hz), 128.88 (d, Ar-*C*$_7$ or Ar-*C*$_8$, J_{PC} = 1.0 Hz), 128.80 (s, Ar-*C*$_7$ or Ar-*C*$_8$), 126.76 (s, Ar-*C*$_{12}$), 123.26 (s, Ar-*C*$_3$), 99.65 (s, -O*C*H$_2$OCH$_3$), 56.90 (s, -OCH$_2$O*C*H$_3$), 35.56 (s, -*C*(CH$_3$)$_3$), 34.64 (s, -*C*(CH$_3$)$_3$), 31.83 (s, -C(*C*H$_3$)$_3$), 31.11 (s, -C(*C*H$_3$)$_3$), 26.58 (d, -*C*H(CH$_3$)$_2$, J_{PC} = 18.1 Hz), 23.36 (d, -*C*H(CH$_3$)$_2$, J_{PC} = 15.2 Hz), 20.95 (d, -CH(*C*H$_3$)$_2$, J_{PC} = 16.2 Hz), 20.59 (d, -CH(*C*H$_3$)$_2$, J_{PC} = 11.1 Hz), 20.39 (d, -CH(*C*H$_3$)$_2$, J_{PC} = 19.2 Hz), 19.27 (d, -CH(*C*H$_3$)$_2$, J_{PC} = 8.1 Hz). ^{31}P{^{1}H} NMR (121 MHz, C_6D_6) δ -0.99 (s).

Synthesis of 2-(2'-diisopropylphosphino)phenyl-4,6-di-tert-butyl-phenol (64).

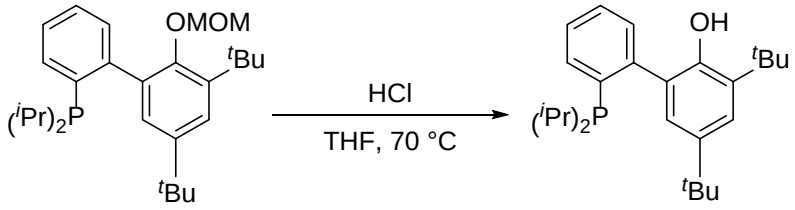

64

In a N_2-filled glovebox containing protic solvents, a 100 mL Schlenk tube fitted with a Teflon screw cap was charged with –MOM protected phosphinophenol (1.60 g, 3.61

mmol, 1.0 equiv.), aqueous HCl (9.0 mol, 10.83 mL, conc. HCl *ca.* 12 M, *ca.* 3.0 equiv.), THF (70 mL), a stir bar. The resulting mixture was place in an oil bath pre-heated to 70 °C for *ca.* 12 h, providing a homogenous orange solution. Volatiles were removed under reduced pressure. In a N_2-filled glovebox containing protic solvents, the resulting orange residue was taken up in CH_2Cl_2 (50 mL) and washed with saturated aqueous solutions of K_2CO_3 (50 mL x 2) and NH_4Cl (50 mL x 1). The volatiles were removed under reduced pressure, Et_2O was added, and the precipitate was isolated to afford phenol **64**. Material of this purity was used in a subsequent deprotonation with BnK without further purification. ^{1}H NMR (300 MHz, $CDCl_3$) δ 7.58 (m, 1H, Ar-*H*), 7.35 (m, 1H, Ar-*H*), 7.20 (m, 1H, Ar-*H*), 7.14 (m, 1H, Ar-*H*), 7.09 (m, 2H, Ar-*H*), 5.09 (d, 1H, -O*H*), 1.89 (m, 1H, -C*H*(CH_3)$_2$), 1.66 (s, 9H, -C(C*H*$_3$)$_3$), 1.54 (m, 1H, -C*H*(CH_3)$_2$), 1.37 (s, 9H, -C(C*H*$_3$)$_2$), 1.01 - 0.79 (m, 12, -CH(C*H*$_3$)$_2$). ^{31}P{^{1}H} NMR (121 MHz, C_6D_6) δ -0.45.

Synthesis of [2-(2'-diisopropylphosphino)phenyl-4,6-di-tert-butyl-oxocyclohexa-diene]nickel(II) methyl .(65)

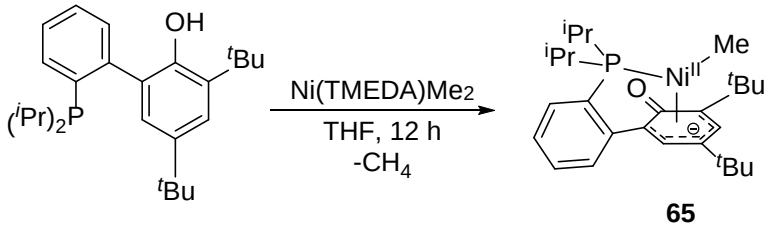

64 **65**

A 20 mL scintillation vial was charged with Ni(TMEDA)Me_2[17] (0.052 g, 0.25 mmol), THF (1 mL), and a stir bar. A yellow-brown solution was observed. A solution of phenol **64** (0.101 g, 0.25 mmol) in THF (1 mL) was added. A dark red solution was observed. After 4 h, the volatiles were removed under reduced pressure. Hexanes (1 mL) was added and the dark red residue was triturated. Volatiles were removed under

reduced pressure. The resulting residue was extracted with three portions of hexanes (*ca.* 2 mL each) and the combined hexanes solution was filtered through Celite. Volatiles were removed under reduced pressure to afford crude **65**. Crystals suitable for X-ray diffraction were grown from a concentrated hexanes solution. ^{1}H NMR (300 MHz, C_6D_6) δ 7.74 (m, 1H, Ar-*H*), 7.14 (m, 1H, Ar-*H*), 6.97 (m, 1H, Ar-*H*), 6.89 (m, 1H, Ar-*H*), 6.21 (m, 1H, oxocyclohexadienyl-*H*), 6.10 (d, 1H, oxocyclohexadienyl-*H*), 1.99 – 1.84 (m, 2H, -C*H*(CH_3)$_2$), 1.78 (s, 9H, -C(C*H*$_3$)$_3$), 1.24 (s, 9H, -C(C*H*$_3$)$_3$), 1.07 (dd, 3H, -CH(C*H*$_3$)$_2$), 0.99 – 0.78 (m, 9H, -CH(C*H*$_3$)$_2$), -0.37 (d, 3H, Ni-C*H*$_3$). ^{13}C{^{1}H} NMR (101 MHz, C_6D_6) δ 169.96 (s), 149.58 (d, Ar-*C*, J_{PC} =20.2 Hz), 140.46 (d, Ar-*C*, J_{PC} = 40.4 Hz), 130.99 (d, J_{PC} = 12.1 Hz), 130.55 (d, Ar-*C*H, J_{PC} = 2.0 Hz), 129.74 (s, Ar-*C*H), 128.16 (obscured by solvent residual, detected by HMBC, oxocyclohexadienyl-*C*-C(CH_3)$_3$), 126.73 (d, Ar-*C*H, J_{PC} = 6.1 Hz), 109.03 (d, oxocyclohexadienyl-*C*-C(CH_3)$_3$, J_{PC}= 5.1 Hz), 107.35 (s, Ar-*C*H, oxocyclohexadienyl-*C*H), 106.09 (d, Ar-*C*H, oxocyclohexadienyl-*C*H, J_{PC} = 6.1), 105.22 (d, J_{PC} = 5.1 Hz), 35.66 (s, -*C*(CH_3)$_3$), 34.05 (s, -*C*(CH_3)$_3$), 30.99 (s, -C(*C*H$_3$)$_3$), 30.12 (s, -C(*C*H$_3$)$_3$), 27.04 (d, -*C*H(CH_3)$_2$, J_{PC} = 24.2 Hz), 25.26 (d, -*C*H(CH_3)$_2$, J_{PC} = 26.3 Hz), 18.84 (d, -CH(C*H*$_3$)$_2$, J_{PC} = 3.0 Hz), 18.76 (d, -CH(C*H*$_3$)$_2$, J_{PC} = 3.0 Hz), 18.54 (s, -CH(C*H*$_3$)$_2$), 18.31 (s, -CH(C*H*$_3$)$_2$), -30.82 (d, Ni–*C*H$_3$, J_{PC} = 27.3 Hz). ^{31}P{^{1}H} NMR (121 MHz, C_6D_6) δ 64.33 (s).

Synthesis of [potassium][2-(2'-diisopropylphosphino)phenyl-4,6-di-tert-butyl-phenoxide] (66).

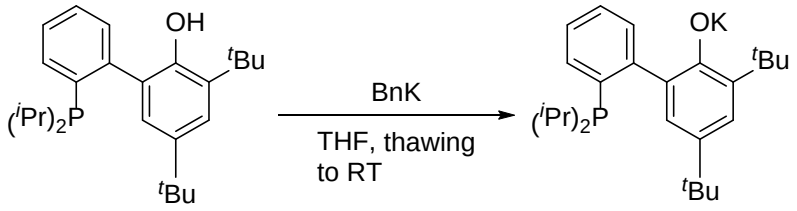

64 **66**

In the glovebox, a 20 mL scintillation vial was charged with phenol **64** (0.100 g, 0.25 mmol, 1.0 equiv.), THF (2 mL), and a stir bar. A separate 20 mL vial was charged with BnK (0.036 g, 0.28 mmol, 1.1 equiv.) and THF (2 mL). Both solution were frozen in a liquid N_2-chilled cold well. The just-thawed solution of BnK was added dropwise to a thawing solution of phenol **64**. A dark red color was observed upon completion of addition. Volatiles were removed under reduced pressure. Hexanes (2 mL) was added and the resulting dark red residue was titurated. Volatiles were removed under reduced pressure. The resulting residue was extracted with C_6H_6 (3 times, 2 mL). The combined C_6H_6 solution was filtered through Celite and volatiles were removed to afford an orange powder which was used for metallation with metal halides without further purification. ^{1}H NMR (300 MHz, C_6D_6) δ 7.52 (d, 1H, Ar-*H*), 7.24 (m, 1H, Ar-*H*), 7.11 (obscured by solvent residual), 7.05 (d, 1H, Ar-*H*), 6.99 (m, 2H, Ar-*H*), 1.95 (m, 2H, -C*H*(CH_3)$_2$), 1.54 (s, 9H, -C(C*H*$_3$)$_3$), 1.48 (s, 9H, -C(C*H*$_3$)$_3$), 0.99 – 0.78 (m, 12H, -CH(C*H*$_3$)$_2$). ^{31}P{^{1}H} NMR (121 MHz, C_6D_6) δ 2.92 (s, br), -0.03 (s).

Synthesis of 1-(2'-bromophenyl)-4-nitro-5-tert-butyl-6-methoxybenzene (67).

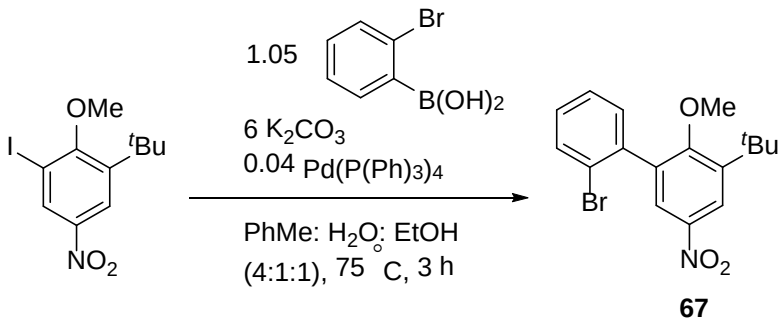

67

1-(2'-bromophenyl)-4-nitro-5-tert-butyl-6-methoxybenzene (**67**) was synthesized using a modification of the procedure reported by Albrecht and co-workers for the Suzuki coupling of aryl halides with boronic acids.[30] In the fume hood, a 500 mL Schlenk tube fitted with a Teflon screw cap was charged with 1-iodo-3-nitro-5-*tert*-butyl-6-methoxybenzene (4.000 g, 11.94 mmol, 1.00 equiv.), 2-bromophenylboronic acid (1.727 g, 12.53 mmol, 1.05 equiv.), K_2CO_3 (7.191 g, 35.81 mmol, 6.00 equiv.), toluene (160 mL), EtOH, (40 mL), deionized H_2O (40 mL), and a stir bar. On the Schlenk line, the reaction mixture was degassed via three freeze-pump-thaw cycles. With N_2 backflow, $Pd(PPh_3)_4$ (0.055 g, 0.48 mmol, 0.05 equiv.) was added, providing a yellow biphasic solution. The reaction was stirred at 75 °C for 3 h at which time the reaction mixture was transferred to a round bottom flask and concentrated under reduced pressure to a total volume of *ca.* 100 mL. This mixture was transferred to a separatory funnel and extracted with CH_2Cl_2 (*ca.* 75 mL) three times. The combined organics were washed with brine and dried over $Mg(SO_4)_2$. The volatiles were removed under reduced pressure, providing **67** as a yellow-brown oil. Material of this purity was used in a subsequent reduction without further purification.

Synthesis of 1-(2'-bromophenyl)-4-amino-5-tert-butyl-6-methoxybenzene (68).

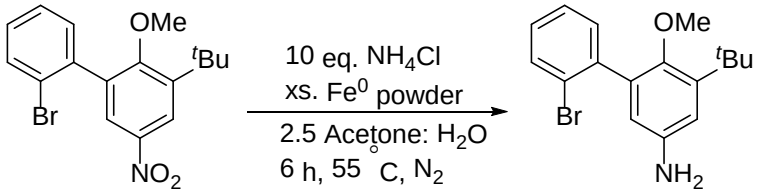

67 **68**

Biphenyl **67** was reduced according to a literature procedure.[31] A 500 mL round bottom was charged with **67** (4.170 g, 11.45 mmol, 1.0 equiv.), iron powder (2.557 g, 45.79 mmol, 4.0 equiv.), NH_4Cl (6.124 g, 114.49 mmol, 10.0 equiv.), acetone (100 mL), 50 mL (H_2O), and a stir bar. A reflux condenser was affixed to the round bottom and the reaction mixture was heated at 55 °C for 6 h under N_2. After 6 h, the reaction mixture was filtered through Celite and volatiles were evaporated from the filtrate. The dark residue was dissolved in 100 mL CH_2Cl_2. The organic layer was washed twice with H_2O (100 mL) and once with brine (100 mL). The organic layer was dried with $Mg(SO_4)_2$, filtered, and volatiles were removed from the filtrate. Column chromatography using 4:1 hexanes:EtOAc as eluent afforded biphenyl amine **68**. Amine of this purity was used in a subsequent Buchwald-Hartwing arylation without further purification. ^{1}H NMR (300 MHz, $CDCl_3$) δ 7.66 (m, 1H, Ar-*H*), 7.40 – 7.30 (m, 2H, Ar-*H*), 7.19 (m, 1H, Ar-*H*), 6.71 (d, 1H, Ar-*H*, J_{HH} = 3.0 Hz), 6.44 (d, 1H, Ar-*H*, J_{HH} = 3.0 Hz), 3.52 (s, br, 2H, -NH_2), 3.20 (s, 3H, -OCH_3), 1.39 (s, 9H, -C(CH_3)$_3$).

Synthesis of 1-(2'-bromophenyl)-4-ditolylamino-5-tert-butyl-6-methoxybenzene (68).

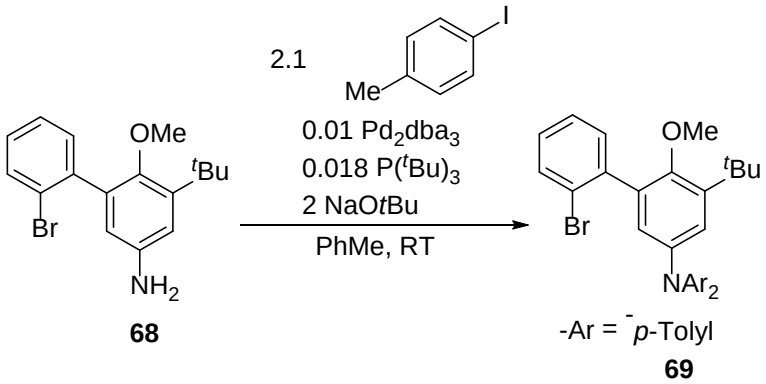

68 **69**

A 100 mL Schlenk tube fitted with a Teflon screw cap was charged with biphenyl amine **68** (2.420 g, 7.24 mmol, 1.0 equiv.) as a solution in a minimum in hexanes. Volatiles were removed under reduced pressure and the resulting residue was dried under vacuum for *ca.* 12 h. The Schlenk tube was sealed and brought into the glovebox. In the glovebox, the Schlenk tube was charged with *para*-tolyl-iodide (3.473 g, 0.016 mmol, 2.2 equiv.), NaO*t*Bu (2.087 g, 0.022 mmol, 3.0 equiv.), and toluene (20 mL). A toluene (5 mL) slurry of Pd_2dba_3 (dba: dibenzylideneacetone; 0.199 g, 0.217 mmol, 0.03 equiv.) and $P(^tBu)_3$ (0.141 g, 0.70 mmol, 0.10 equiv.) was added. The Schlenk flask was sealed, removed from the glovebox, and allowed to stir at room temperature. After *ca.* 16 h, an aliquot was removed from the reaction mixture under N_2 using Schlenk line technique and analyzed by GC-MS. Ditolyl amine product and *para*-tolyl-iodide was observed. The reaction mixture was poured into a round bottom flask and volatiles were removed under reduced pressure via rotary evaporation. The resulting dark oil was dissolved in a minimum of CH_2Cl_2 and filtered through silica. *para*-Tolyl-iodide was removed from the reaction crude by distillation using a Kugelrohr apparatus. The resulting dark oil was triturated with a minimum of MeOH to afford **69** as a light brown precipitate. ^{1}H NMR (300 MHz, $CDCl_3$) δ 7.59 (m, 1H,

Ar-*H*), 7.39 (m, 1H, Ar-*H*), 7.30 (m, 1H, Ar-*H*), 7.15 (m, 1H, Ar-*H*), 7.04 (d, 1H, Ar-*H*), 7.01 (m, 8H, tolyl Ar-*H*), 6.75 (d, 1H, Ar-*H*), 3.24 (s, 3H, -OCH_3), 2.29 (s, 6H, -N(Ph-*p*-CH_3)$_2$), 1.32 (s, 9H, -C(CH_3)$_3$). ^{1}H NMR (300 MHz, C_6D_6) δ 7.46 (d, 1H, Ar-*H*), 7.41 (m, 1H, Ar-*H*), 7.33 (m, 1H, Ar-*H*), 7.22 (m, 4H, tolyl Ar-*H*), 7.15 (d, 1H, Ar-*H*), 6.91 (m, 4H, tolyl Ar-*H*), 6.85 (m, 1H, Ar-*H*), 6.68 (m, 1H, Ar-*H*), 3.17 (s, 3H, -OCH_3), 2.06 (s, 6H, -N(Ph-*p*-CH_3)$_2$), 1.41 (s, 9H, -C(CH_3)$_3$).

Synthesis of 1-(2'-diisopropylphosphinophenyl)-4-ditolylamino-5-tert-butyl-6-methoxybenzene (70).

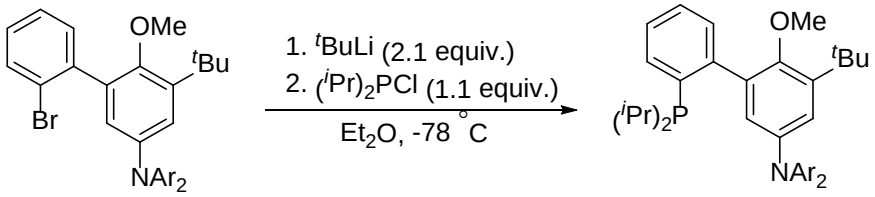

-Ar = -*p*-Tolyl
69

-Ar = -*p*-Tolyl
70

In a glovebox, a 100 mL Schlenk tube was charged with a colorless solution of biphenyl bromide **69** (0.163 g, 0.32 mmol, 1.0 equiv.) in Et_2O (20 mL). The Schlenk tube was removed from the glovebox and cooled to -78 °C in a dry ice/acetone bath. Under N_2, ^{t}BuLi (1.7 M in pentane, 0.66 mmol, 0.40 mL, 2.1 equiv.) was added via syringe to the solution. The resulting yellow-orange mixture was stirred for *ca.* 3 h at -78 °C. After *ca.* 3 h, chlorodiisopropylphosphine (0.053 g, 0.06 mL, 0.35 mmol, 1.1 equiv.) was added to the cold solution slowly via syringe. After addition, the reaction mixture was stirred 1 h at -78 °C. After 1 h, the reaction mixture was allowed to warm to room temperature and stirred at room temperature for 12 h. The volatile materials were removed under reduced pressure. In the glovebox, the pale yellow residue was extracted with three portions of pentane (20 mL each) and the combined organic layer

was filtered through Celite. The volatiles were removed from the filtrate under reduced pressure and a red oil was observed. Crude **70** was treated with BBr_3 without further purification in a subsequent deprotection step. ^1H NMR (300 MHz, C_6D_6) δ 7.45 (d, 1H, Ar-*H*), 7.36 (m, 1H, Ar-*H*), 7.30 (m, 1H, Ar-*H*), 7.22 (d, 4H, tolyl Ar-*H*), 7.08 – 7.02 (m, 3H, Ar-*H*), 6.88 (d, 4H, tolyl Ar-*H*), 3.03 (s, 3H, -OC*H*$_3$), 2.03 (s, 6H, -N(Ph-*p*-CH_3)$_2$), 1.78 – 1.56 (m, 2H, -C*H*(CH_3)$_2$), 1.15 – 0.78 (m, 9H, -CH(C*H*$_3$)$_2$, obscured by residual (^{i}Pr)$_2$PCl), 0.71 (m, 3H, -CH(C*H*$_3$)$_2$). $^{31}P\{^1H\}$ NMR (121 MHz, C_6D_6) δ -0.09.

Synthesis of 2-(2'-diisopropylphosphinophenyl)-4-ditolylamino-6-tert-butyl-phenol (71).

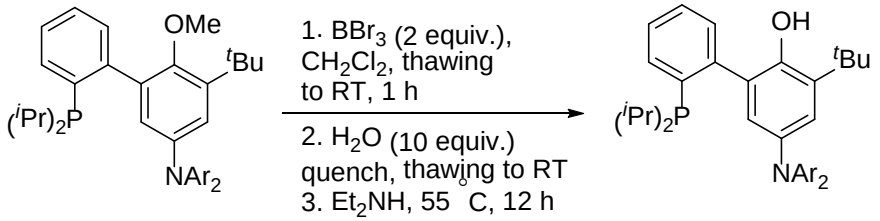

-Ar = -*p*-Tolyl **70**

-Ar = -*p*-Tolyl **71**

In the glovebox, a 20 mL scintillation vial was charged with anisole **70** (0.150 g, 0.27 mmol, 1.0 equiv.), CH_2Cl_2 (4 mL), a stir bar. An orange solution was observed. The solution was frozen in a liquid N_2-chilled cold well. BBr_3 (0.136 g, 0.05 mL, 2.0 BBr_3) was added via syringe to the thawing solution of **70**. The solution was allowed to thaw to room temperature. A dark red solution was observed. The reaction mixture was transferred to a 100 mL Schlenk tube fitted with a Teflon screw cap. The Schlenk tube was sealed and brought into a glovebox containing protic solvents under an N_2 atmosphere. H_2O (0.049 g, 0.05 mL, 2.72 mmol, 10.0 equiv.) was added to the reaction mixture. An exotherm was observed. An additional portion of H_2O (0.049 g,

0.05 mL, 2.72 mmol, 10.0 equiv.) was added. No exotherm was observed. Volatiles were removed under reduced pressure. Volatiles were removed under reduced pressure to afford an orange solvent. Et_2NH (4 mL) was added to the Schlenk tube. The Schlenk tube was sealed, removed from the glovebox, and placed in an oil bath pre-heated to *55* °C for 16 h. The reaction was removed from the oil bath and allowed to cool to room temperature. Volatiles were removed under reduced pressure on the Schlenk line. A yellow oil and white solid were observed. The Schlenk tube was returned to a glovebox containing protic solvents under an N_2 atmosphere. The yellow residue was extracted with 3 portions of pentane (2 mL each). The combined pentane solution was filtered through alumina. Volatiles were removed under reduced pressure to afford phenol **71** (0.099 g, 0.18 mmol, 67.7%). Material of this purity was placed under vacuum with heating on the Schlenk, brought into a drybox under inert atmosphere, and deprotonated without further purification. ^{1}H NMR (300 MHz, $CDCl_3$) δ 7.80 (m, 1H, Ar-*H*), 7.71 – 7.50 (m, 3H, Ar-*H*), 7.35 (m, 1H, Ar-*H*), 7.25 – 7.10 (m, 2H, Ar-*H*), 6.96 (m, 1H, Ar-*H*), 5.37 (s, 1H, -O*H*), 2.54 (s, 8H, -N(Ph-*p*-C*H*$_3$)$_2$), 2.43 (m, 1H, -C*H*(CH_3)$_2$), 2.16 (m, 1H, -C*H*(CH_3)$_2$), 1.64 (s, 9H, -C(C*H*$_3$)$_3$), 1.42 – 1.20 (m, 6H, -CH(C*H*$_3$)$_2$), 1.18 – 0.99 (m, 6H, -CH(C*H*$_3$)$_2$). ^{31}P{^{1}H} NMR (121 MHz, $CDCl_3$) δ 0.81. ^{1}H NMR (300 MHz, C_6D_6) δ 7.52 (d, 1H, Ar-*H*), 7.29 (d, 4H, tolyl Ar-*H*), 7.10 – 6.98 (m, 3H, Ar-*H*), 6.95 (d, 4H, tolyl Ar-*H*), 5.22 (s, 1H, -O*H*), 2.10 (s, 8H, -N(Ph-*p*-C*H*$_3$)$_2$), 1.90 (m, 1H, -C*H*(CH_3)$_2$), 1.75 (m, 1H, -C*H*(CH_3)$_2$), 1.53 (s, 9H, -C(C*H*$_3$)$_3$, 1.03 – 0.84 (m, 9H, -CH(C*H*$_3$)$_2$), 0.72 (m, 2H, -CH(C*H*$_3$)$_2$). ^{31}P{^{1}H} NMR (121 MHz, C_6D_6) δ 0.26.

Synthesis of [potassium][2-(2'-diisopropylphosphinophenyl)-4-ditolylamino-6-tert-butyl-phenoxide] (72).

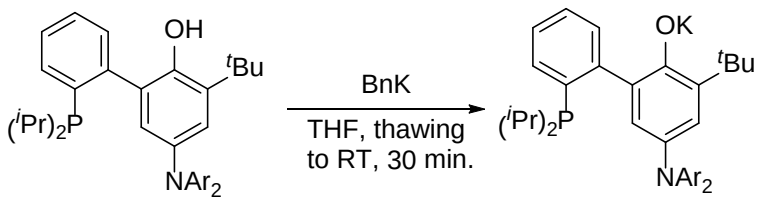

71 **72**

-Ar = -*p*-Tolyl

In the glovebox, a 20 mL scintillation vial was charged with phenol **71** (0.215 g, 0.40 mmol, 1.0 equiv.), THF (2 mL), and a stir bar. A light red solution was observed. A separate 20 mL vial was charged with BnK (0.063 g, 0.48 mmol, 1.2 equiv.) and THF (2 mL). Both solution were frozen in a liquid N_2-chilled cold well. The just-thawed solution of BnK was added dropwise to a thawing solution of phenol **71**. A dark red color was observed upon completion of addition. Volatiles were removed under reduced pressure. Hexanes (2 mL) was added and the resulting dark red residue was titurated. Volatiles were removed under reduced pressure. The resulting residue was extracted with C_6H_6 (3 times, 2 mL). The combined C_6H_6 solution was filtered through Celite and volatiles were removed to afford a red powder which was used for metallation with metal halides without further purification. ^{1}H NMR (300 MHz, C_6D_6) δ 7.46 – 7.36 (m, 4H, Ar-*H*), 7.06 – 6.85 (m, 8H, tolyl Ar-*H*), 1.94 (m, br, 2H, -C*H*$(CH_3)_2$), 1.39 (s, 9H, -C(C*H*$_3)_3$), 1.23 (s, 6H, -N(Ph-*p*-C*H*$_3)_2$), 0.99 – 0.81 (m, 12H, -CH(C*H*$_3)_2$). ^{31}P{^{1}H} NMR (121 MHz, C_6D_6) δ -4.29.

REFERENCES

(1) (a) Gray, H. B.; Williams, R.; Bernal, I.; Billig, E. *J. Am. Chem. Soc.* **1962**, *84*, 3596-3597; (b) Billig, E.; Williams, R.; Bernal, I.; Waters, J. H.; Gray, H. B. *Inorg. Chem.* **1964**, *3*, 663-666.
(2) Yu, R. P.; Darmon, J. M.; Milsmann, C.; Margulieux, G. W.; Stieber, S. C. E.; DeBeer, S.; Chirik, P. J. *J. Am. Chem. Soc.* **2013**, *135*, 13168-13184.
(3) Haneline, M. R.; Heyduk, A. F. *J. Am. Chem. Soc.* **2006**, *128*, 8410-8411.
(4) Lu, C. C.; Bill, E.; Weyhermüller, T.; Bothe, E.; Wieghardt, K. *J. Am. Chem. Soc.* **2008**, *130*, 3181-3197.
(5) Chirik, P. J.; Wieghardt, K. *Science* **2010**, *327*, 794-795.
(6) (a) Small, B. L.; Brookhart, M. *J. Am. Chem. Soc.* **1998**, *120*, 7143-7144; (b) J. P. Britovsek, G.; C. Gibson, V.; J. McTavish, S.; A. Solan, G.; J. P. White, A.; J. Williams, D.; J. P. Britovsek, G.; S. Kimberley, B.; J. Maddox, P. *Chem. Commun.* **1998**, 849-850.
(7) Sylvester, K. T.; Chirik, P. J. *J. Am. Chem. Soc.* **2009**, *131*, 8772-8774.
(8) Stubbe, J.; van der Donk, W. A. *Chem. Rev.* **1998**, *98*, 705-762.
(9) (a) Lin, S.; Herbert, D. E.; Velian, A.; Day, M. W.; Agapie, T. *J. Am. Chem. Soc.* **2013**, *135*, 15830-15840; (b) Chao, S. T.; Lara, N. C.; Lin, S.; Day, M. W.; Agapie, T. *Angew. Chem. Int. Ed.* **2011**, *50*, 7529-7532; (c) Velian, A.; Lin, S.; Miller, A. J. M.; Day, M. W.; Agapie, T. *J. Am. Chem. Soc.* **2010**, *132*, 6296-6297; (d) Lin, S.; Day, M. W.; Agapie, T. *J. Am. Chem. Soc.* **2011**, *133*, 3828-3831; (e) Suseno, S.; Horak, K. T.; Day, M. W.; Agapie, T. *Organometallics* **2013**; (f) Buss, J. A.; Edouard, G. A.; Cheng, C.; Shi, J.; Agapie, T. *J. Am. Chem. Soc.* **2014**, *136*, 11272-11275.
(10) (a) Kelley, P.; Lin, S.; Edouard, G.; Day, M. W.; Agapie, T. *J. Am. Chem. Soc.* **2012**, *134*, 5480-5483; (b) Edouard, G. A.; Kelley, P.; Herbert, D. E.; Agapie, T. *Organometallics* **2015**, *34*, 5254-5277.
(11) (a) McGuinness, D. S. *Chem. Rev.* **2011**, *111*, 2321-2341; (b) Agapie, T. *Coord. Chem. Rev.* **2011**, *255*, 861-880.
(12) Lu, F.; Zarkesh, R. A.; Heyduk, A. F. *Eur. J. Inorg. Chem.* **2012**, *2012*, 467-470.
(13) Mirbach, M. F.; Saus, A.; Krings, A. M.; Mirbach, M. J. *J Organomet Chem* **1981**, *205*, 229-237.
(14) Antonini, S.; Calderazzo, F.; Englert, U.; Grigiotti, E.; Pampaloni, G.; Zanello, P. *J. Organomet. Chem.* **2004**, *689*, 2158-2168.
(15) O'Donnell, T. A.; Phillips, K. A. *Inorg Chem* **1973**, *12*, 1437-1438.
(16) Hynes, R. C.; Preston, K. F.; Springs, J. J.; Tse, J. S.; Williams, A. J. *Journal of the Chemical Society, Faraday Transactions* **1991**, *87*, 3121.
(17) Connor, E. F.; Younkin, T. R.; Henderson, J. I.; Waltman, A. W.; Grubbs, R. H. *Chem. Commun.* **2003**, 2272-2273.
(18) Cámpora, J.; Reyes, M. L.; Hackl, T.; Monge, A.; Ruiz, C. *Organometallics* **2000**, *19*, 2950-2952.
(19) Loren, S. D.; Campion, B. K.; Heyn, R. H.; Tilley, T. D.; Bursten, B. E.; Luth, K. W. *J. Am. Chem. Soc.* **1989**, *111*, 4712-4718.
(20) Keim, W. *Angew. Chem. Int. Ed.* **2013**, *52*, 12492-12496.
(21) Abbott-Laboratories *U. S. Patent #39135* **2009**, 100.
(22) Xiao, Z.-P.; Wang, Y.-C.; Du, G.-Y.; Wu, J.; Luo, T.; Yi, S.-F. *Synth. Commun.* **2010**, *40*, 661-665.
(23) Pangborn, A. B.; Giardello, M. A.; Grubbs, R. H.; Rosen, R. K.; Timmers, F. J. *Organometallics* **1996**, *15*, 1518-1520.

(24) Klet, R. C.; VanderVelde, D. G.; Labinger, J. A.; Bercaw, J. E. *Chem. Commun.* **2012**, *48*, 6657-6659.
(25) Maaranen, J.; Hoikka, J.; Rauotio, S. *U. S. Patent* **2007**, *37939 A1*.
(26) Kaschube, W.; Pörschke, K. R.; Wilke, G. *J. Organomet. Chem.* **1988**, *355*, 525-532.
(27) Greiser, T.; Kopf, J.; Thoennes, D.; Weiss, E. *J. Organomet. Chem.* **1980**, *191*, 1-6.
(28) Fulmer, G. R.; Miller, A. J. M.; Sherden, N. H.; Gottlieb, H. E.; Nudelman, A.; Stoltz, B. M.; Bercaw, J. E.; Goldberg, K. I. *Organometallics* **2010**, *29*, 2176-2179.
(29) Connelly, N. G.; Geiger, W. E. *Chem. Rev.* **1996**, *96*, 877-910.
(30) Albrecht, M.; Schneider, M. *Synthesis* **2000**, *2000*, 1557-1560.
(31) Hodges, J. A.; Raines, R. T. *Org. Lett.* **2006**, *8*, 4695-4697.

APPENDIX C

Relevant Spectroscopic Data

Figure C.1. ^{1}H NMR spectrum of **5a** in C_6D_6.

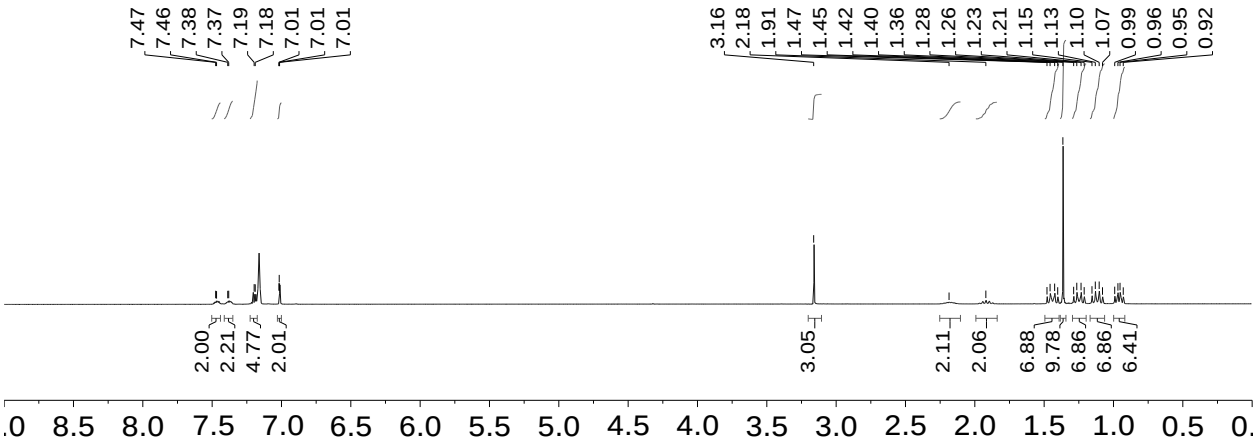

Figure C.2. $^{13}C\{^{1}H\}$ NMR spectrum of **5a** in C_6D_6.

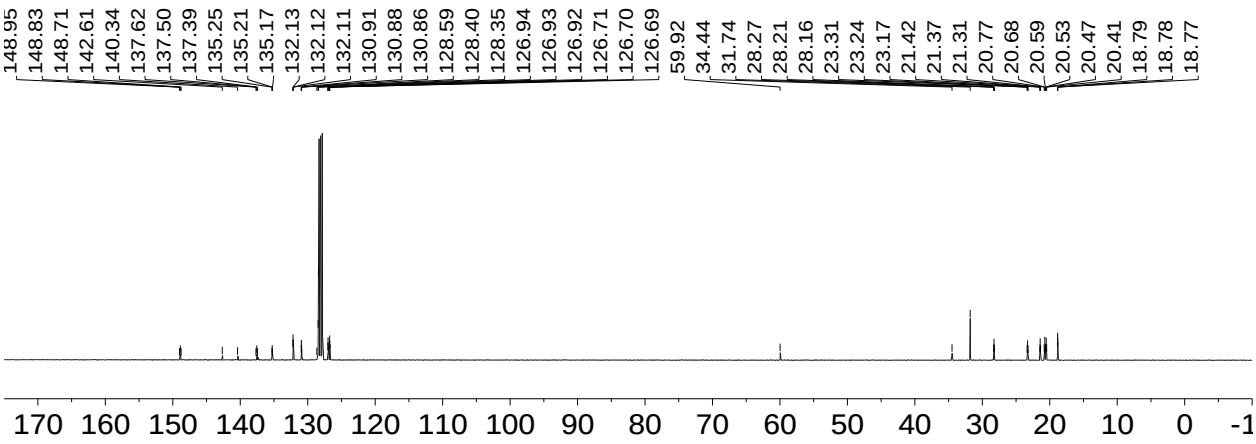

Figure C.3. $^{31}P\{^{1}H\}$ NMR spectrum of **5a** in C_6D_6.

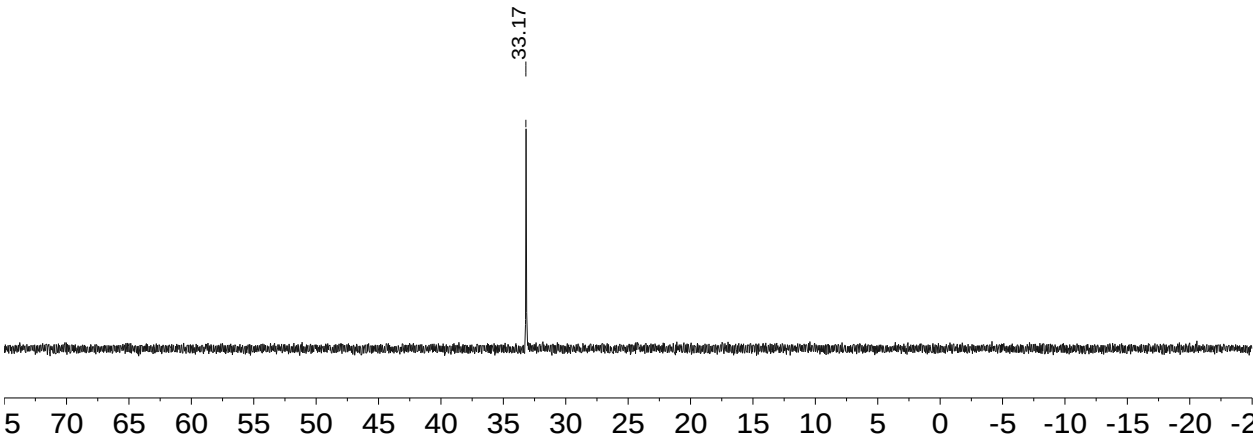

Figure C.4. ^{1}H NMR spectrum of **6a** in C_6D_6.

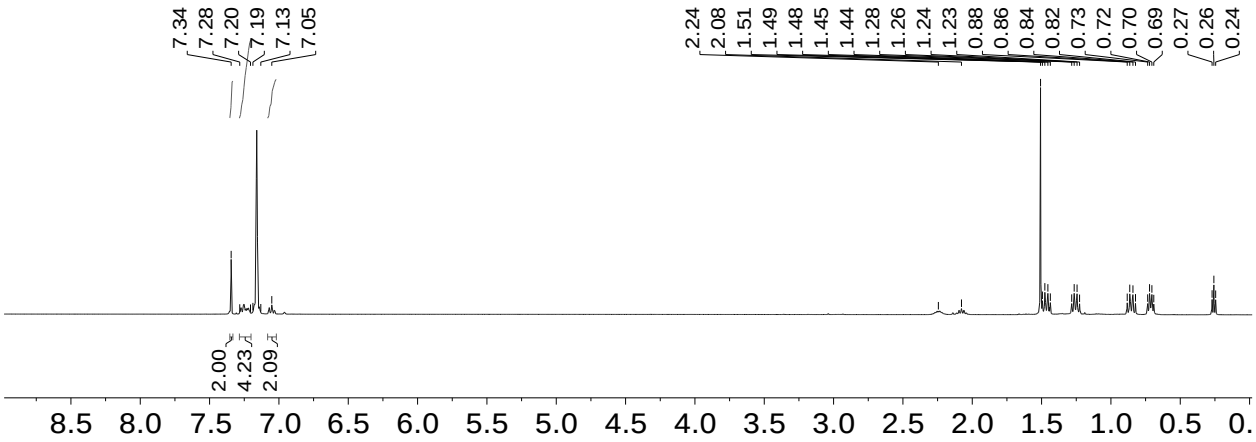

Figure C.5. $^{13}C\{^{1}H\}$ NMR spectrum of **6a** in C_6D_6.

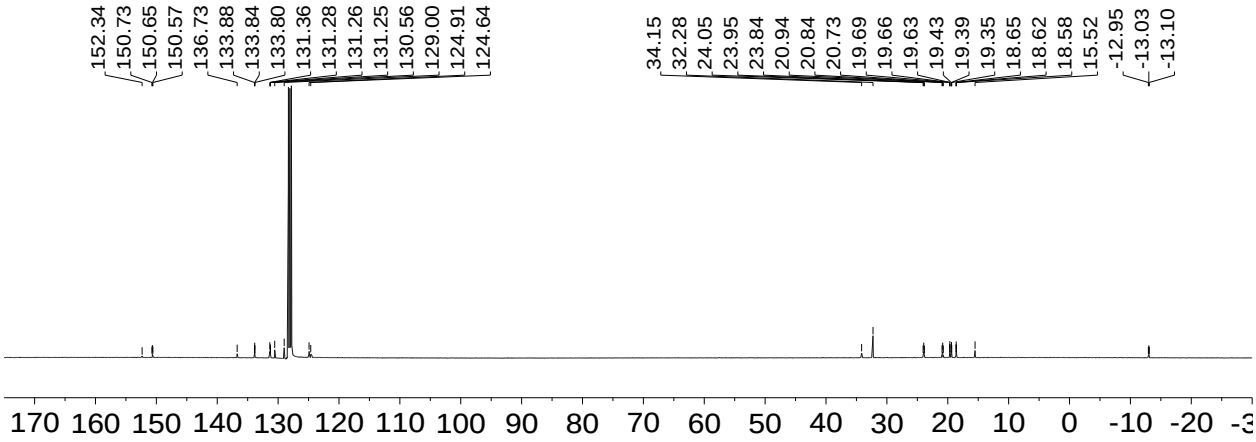

Figure C.6. $^{31}P\{^{1}H\}$ NMR spectrum of **6a** in C_6D_6.

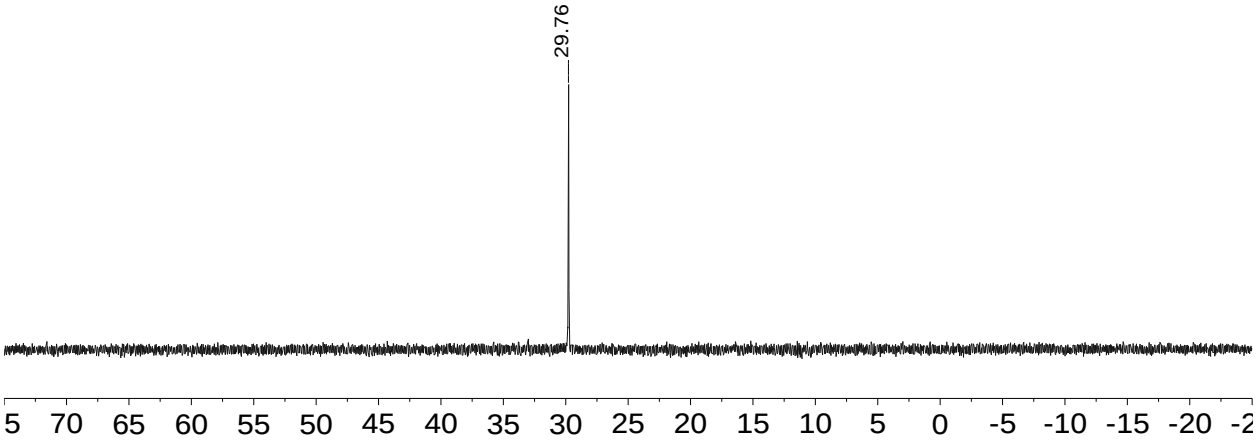

Figure C.7. ^{1}H NMR spectrum of **7a** in C_6D_6.

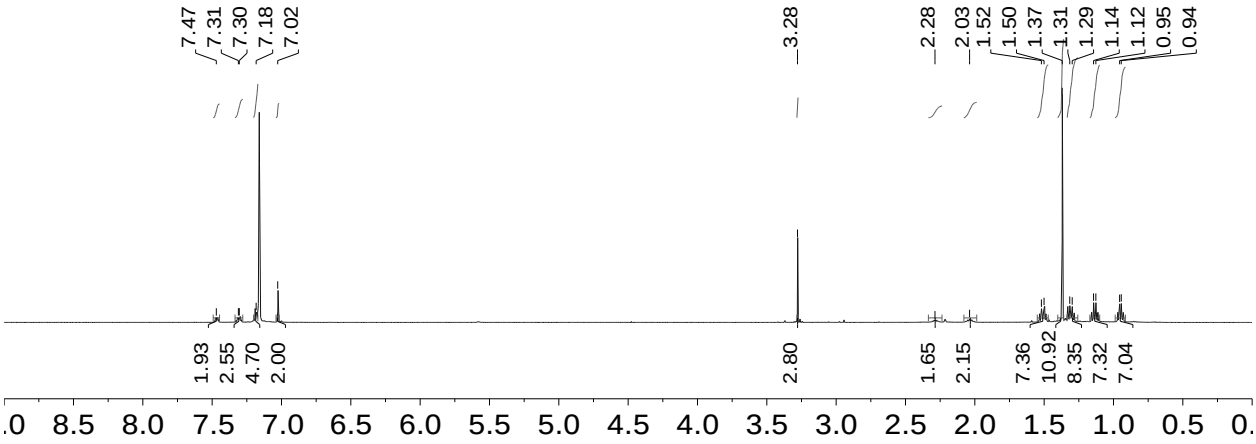

Figure C.8. $^{13}C\{^{1}H\}$ NMR spectrum of **7a** in C_6D_6.

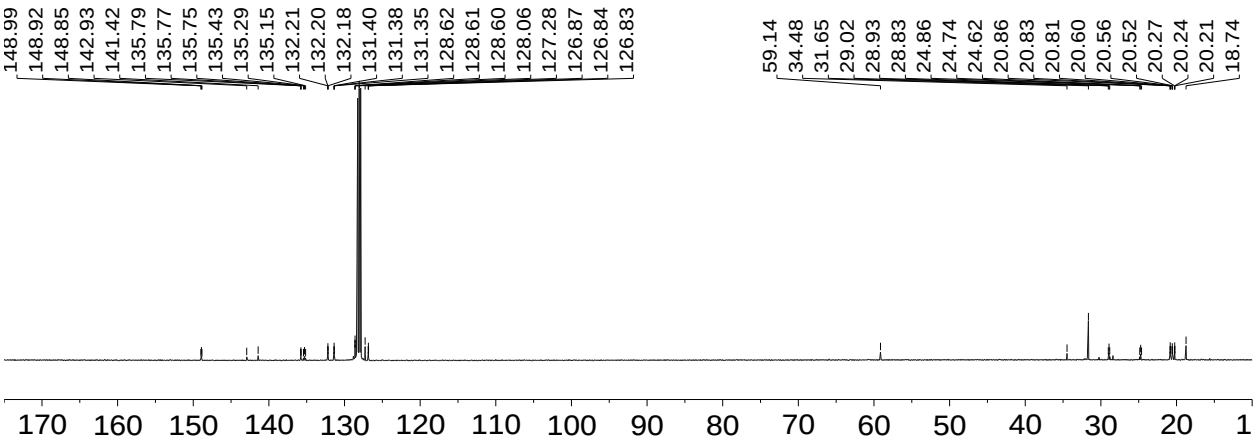

Figure C.9. $^{31}P\{^{1}H\}$ NMR spectrum of **7a** in C_6D_6.

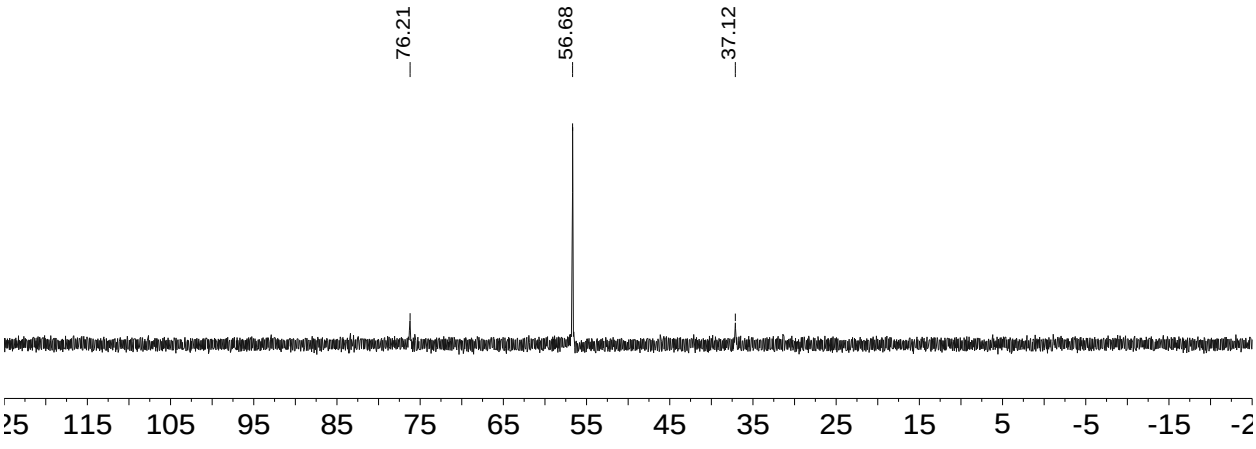

Figure C.10. ^{1}H NMR spectrum of **8a** in C_6D_6.

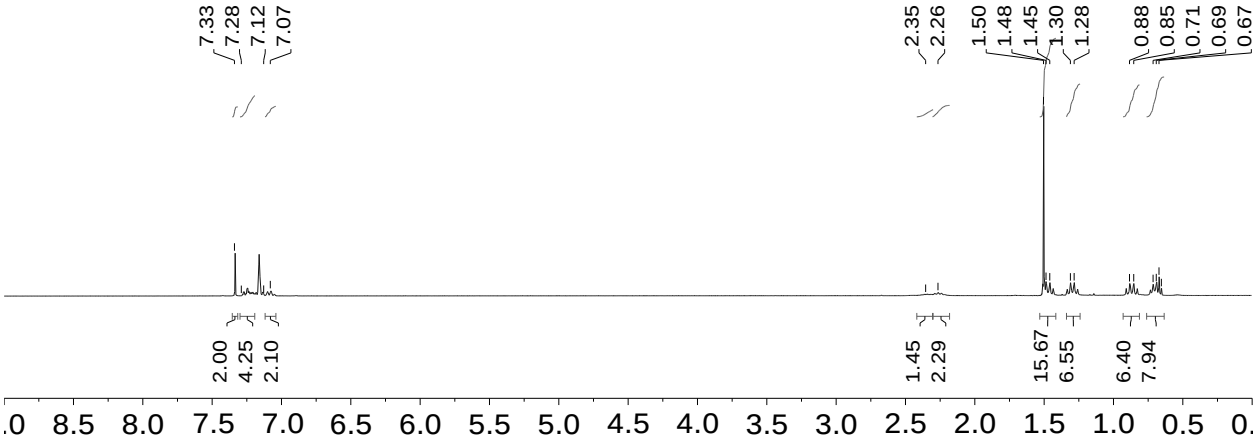

Figure C.11. $^{13}C\{^{1}H\}$ NMR spectrum of **8a** in C_6D_6.

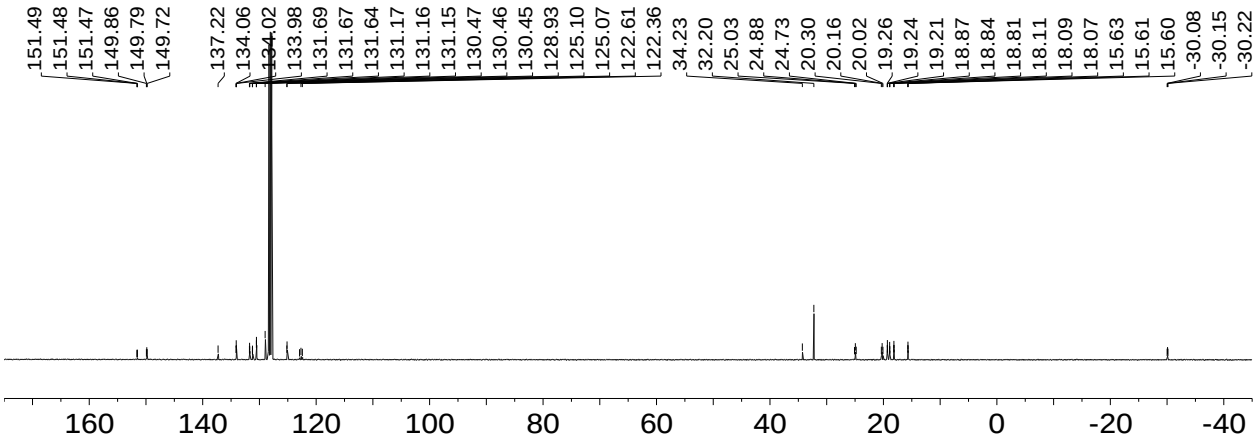

Figure C.12. $^{31}P\{^{1}H\}$ NMR spectrum of **8a** in C_6D_6.

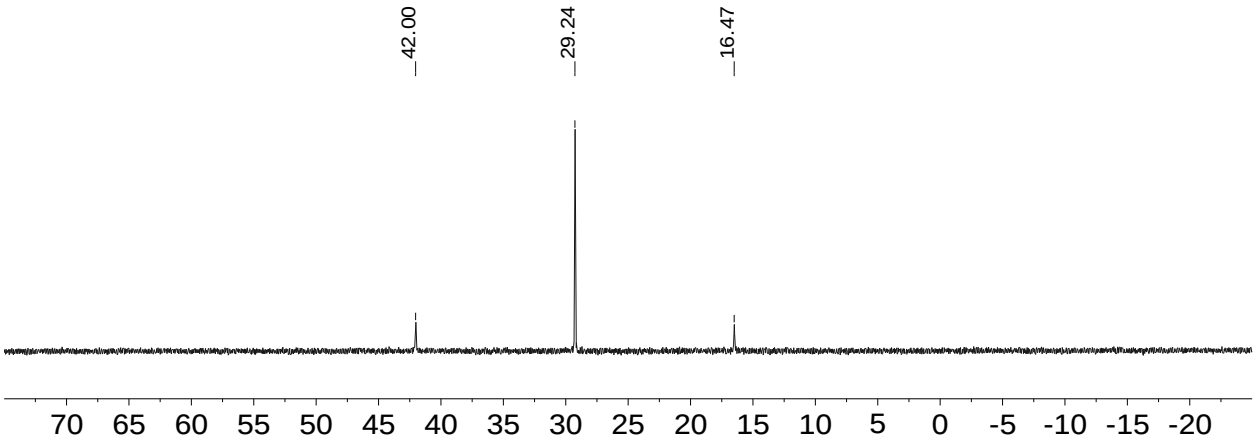

Figure C.13. ^{1}H NMR spectrum of 5-(tert-butyl)-1,3-diiodo-2-(4-nitrophenoxy)-benzene in $CDCl_3$.

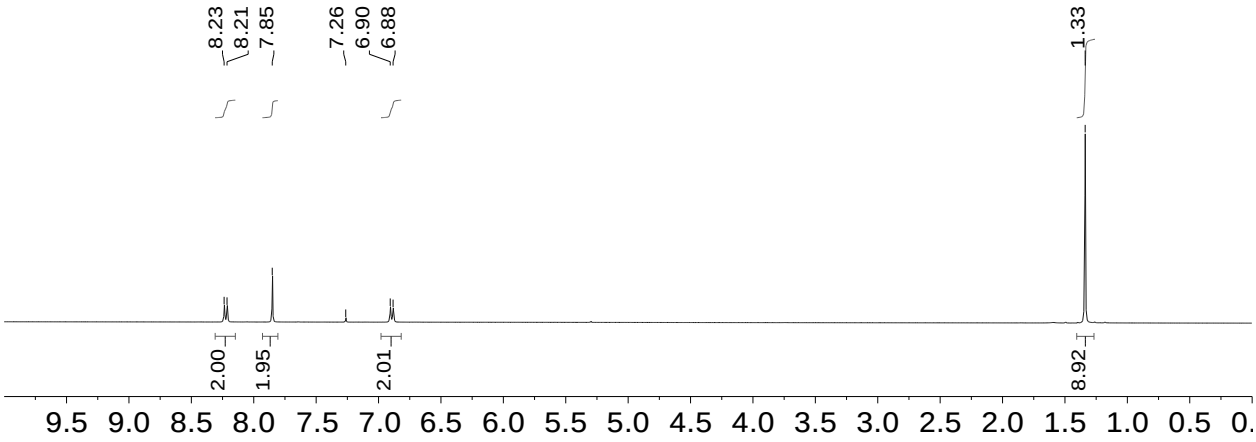

Figure C.14. $^{13}C\{^{1}H\}$ NMR spectrum of 5-(tert-butyl)-1,3-diiodo-2-(4-nitrophenoxy)benzene in $CDCl_3$.

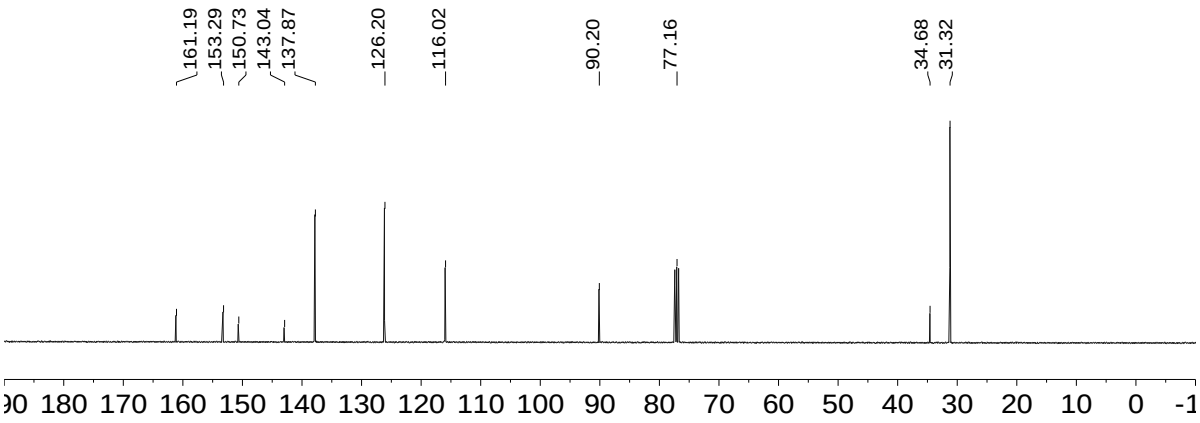

Figure C.15. ^{1}H NMR spectrum of 1,3-bis(2'-bromophenyl)-2-(4'-nitrophenoxy)-5-tert-butyl-benzene in $CDCl_3$. Note: Residual CH_2Cl_2 present.

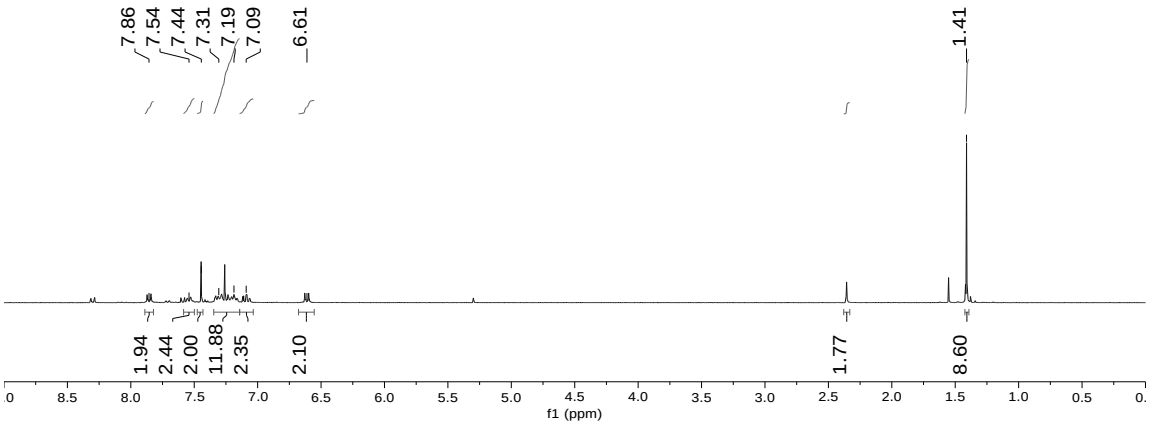

Figure C.16. ^{1}H NMR spectrum of 1,3-bis(2'-bromophenyl)-2-(4'-aminophenoxy)-5-tert-butyl-benzene in $CDCl_3$. Note: Residual CH_2Cl_2 and Et_2O present.

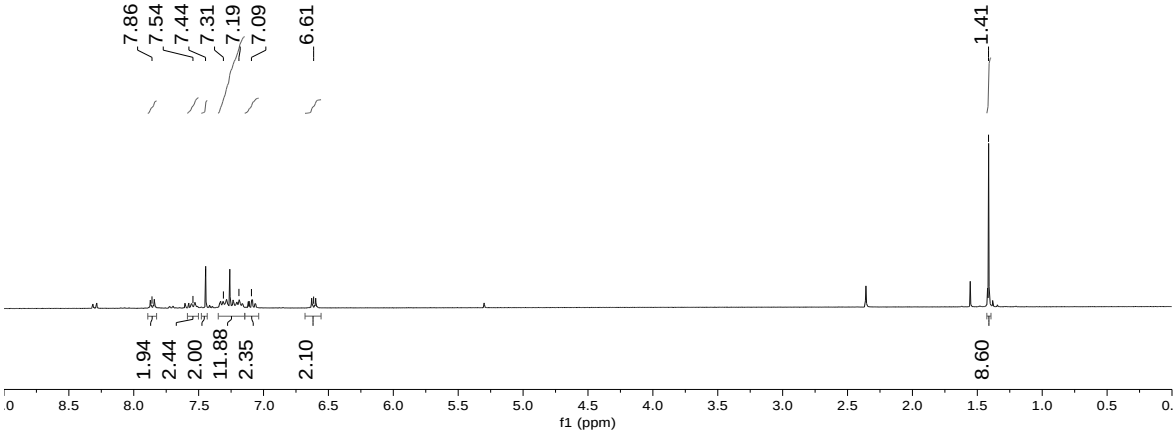

Figure C.17. ^{1}H NMR spectrum of 1,3-bis(2'-bromophenyl)-2-(4'-dimethylamino-phenoxy)-5-tert-butyl-benzene in C_6D_6. Note: Residual Et_2O present.

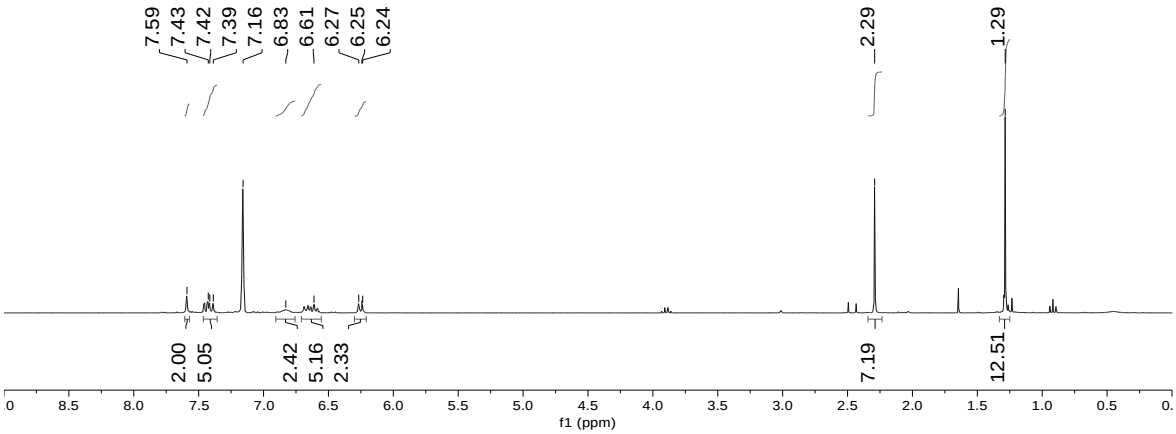

Figure C.18. ^{1}H NMR spectrum of **1c** at 25 °C in C_6D_6.

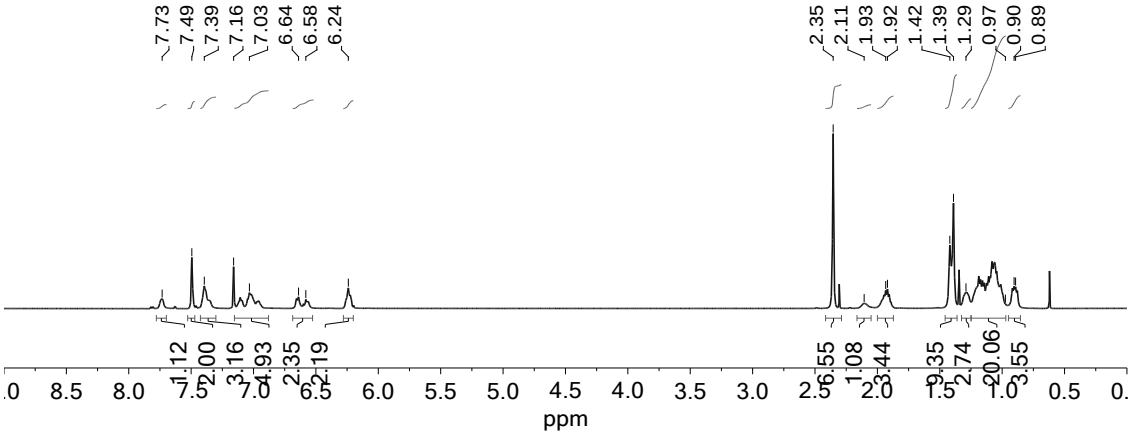

Figure C.19. $^{13}C\{^{1}H\}$ NMR spectrum of **1c** at 25 °C in C_6D_6.

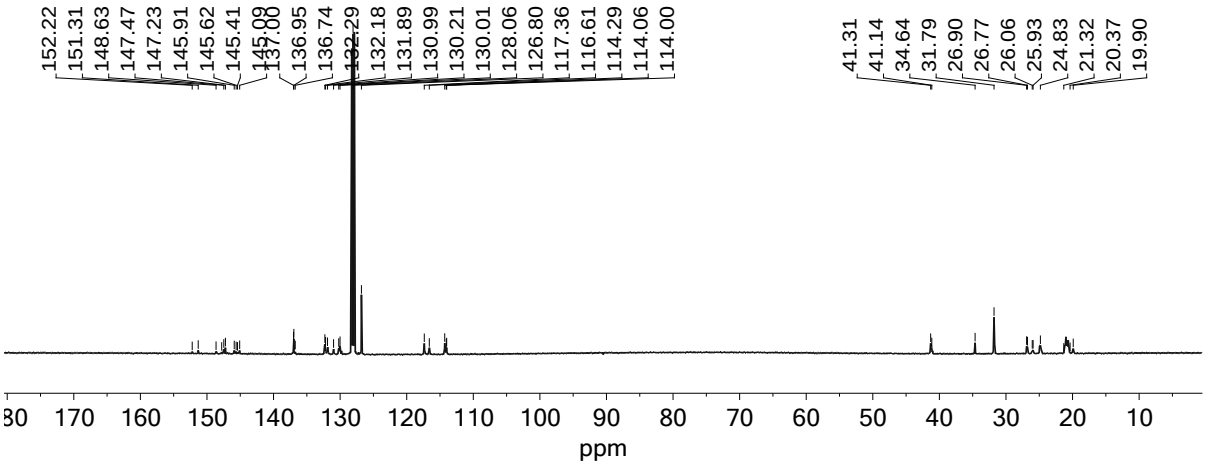

Figure C.20. $^{31}P\{^{1}H\}$ NMR spectrum of **1c** at 25 °C in C_6D_6.

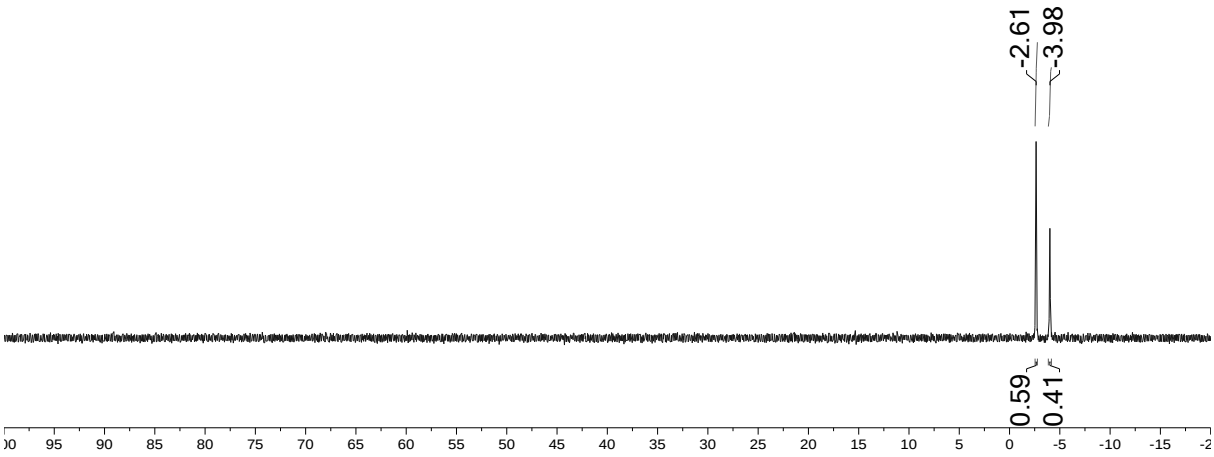

Figure C.21. ^{1}H NMR spectrum of **1c** at 70 °C in C_6D_6.

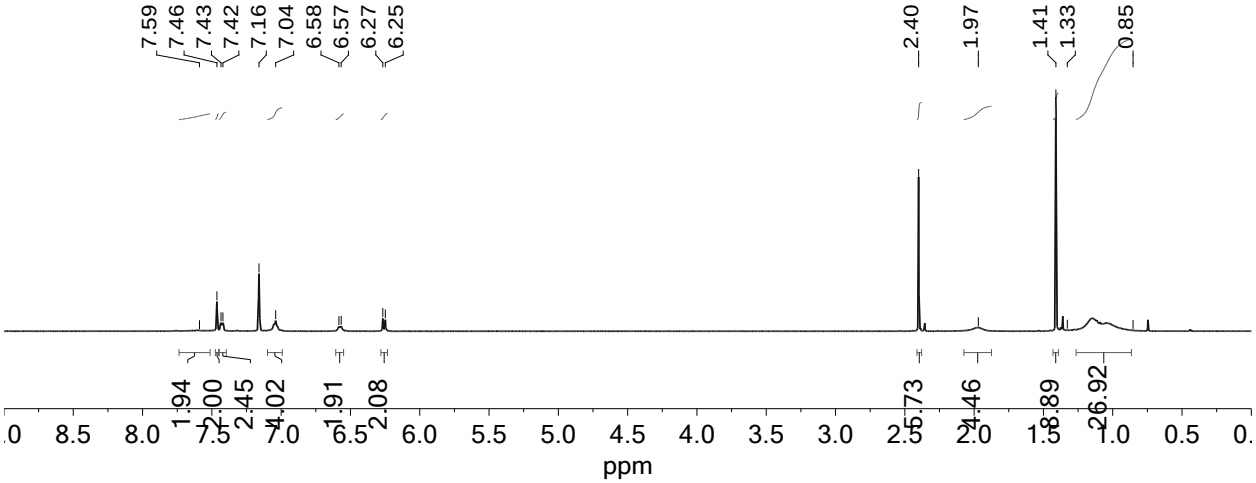

Figure C.22. ^{1}H NMR spectrum of 1,3-bis(2'-bromophenyl)-2-phenoxy-5-tert-butyl-benzene in $CDCl_3$.

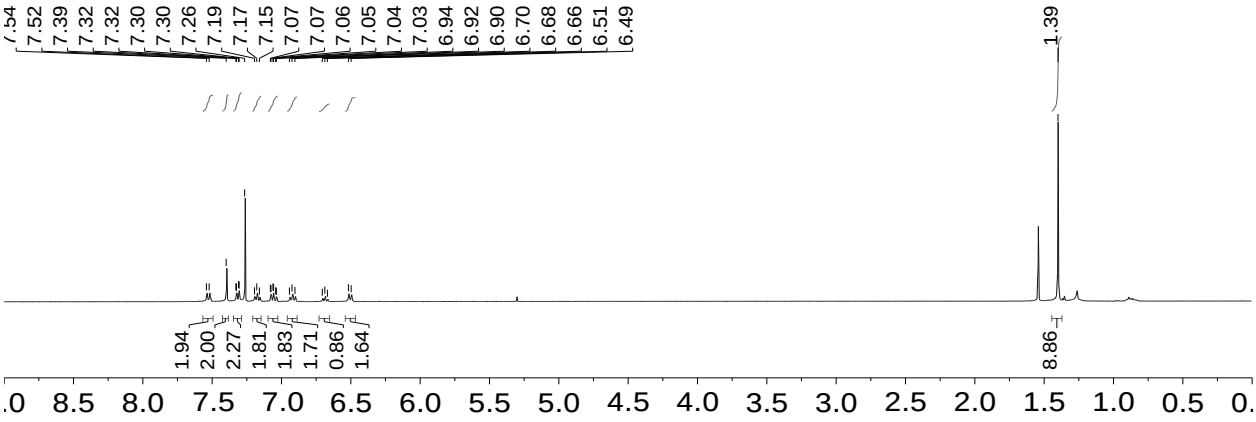

Figure C.23. $^{13}C\{^{1}H\}$ NMR spectrum of 1,3-bis(2'-bromophenyl)-2-phenoxy-5-tert-butyl-benzene in $CDCl_3$.

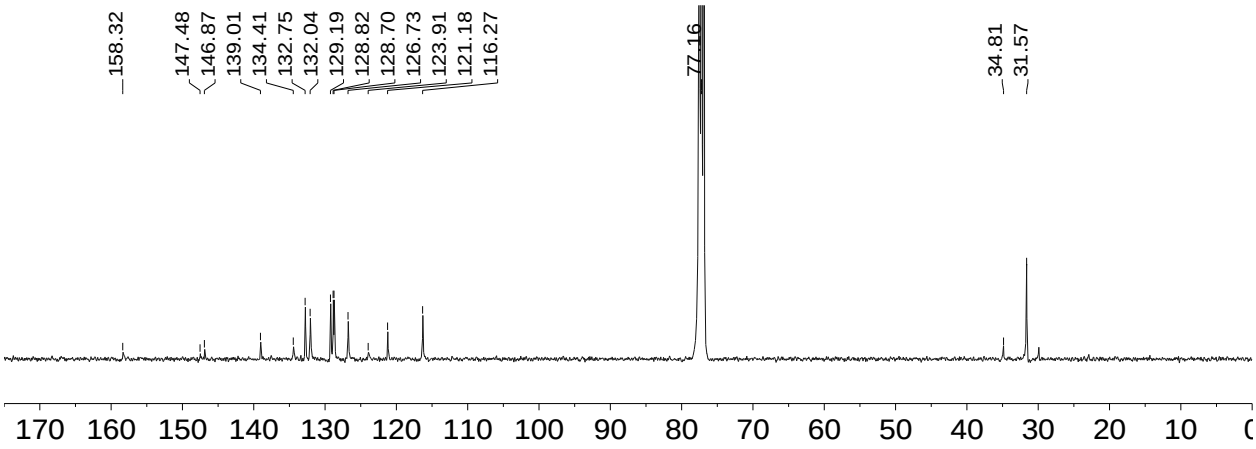

Figure C.24. ^{1}H NMR spectrum of **1d** at 25 °C in $CDCl_3$.

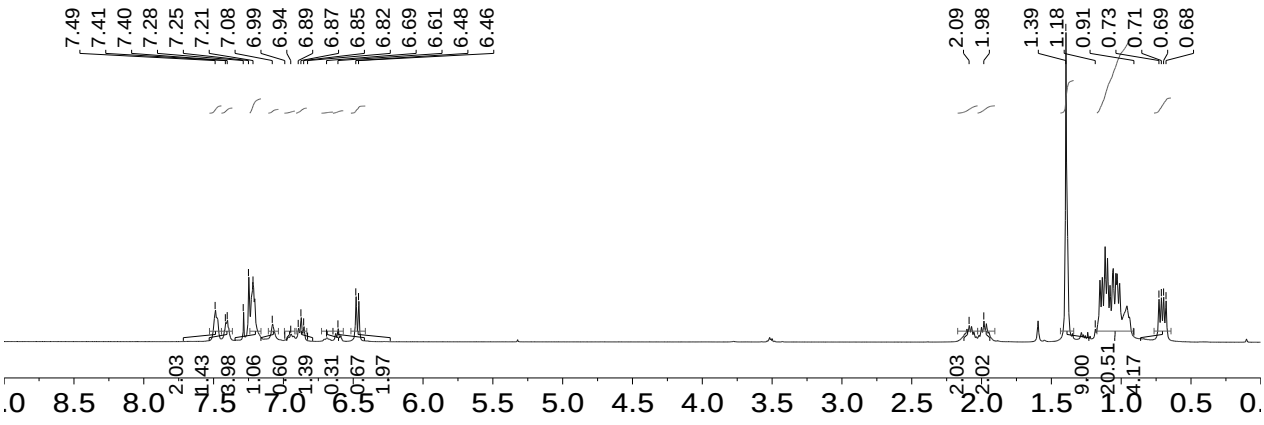

Figure C.25. ^{1}H NMR spectrum of **1d** at 25 °C in C_6D_6.

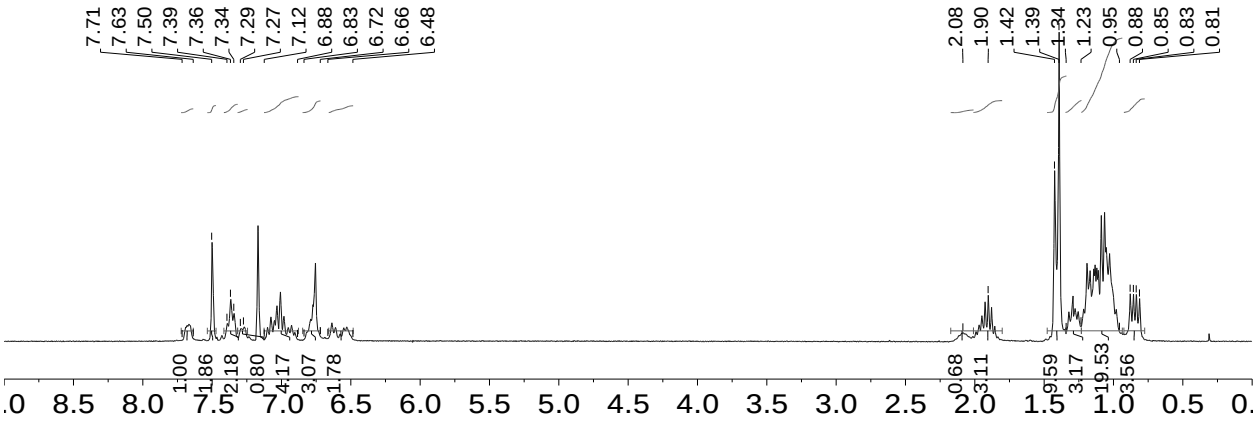

Figure C.26. $^{13}C\{^{1}H\}$ NMR spectrum of **1d** at 25 °C in $CDCl_3$.

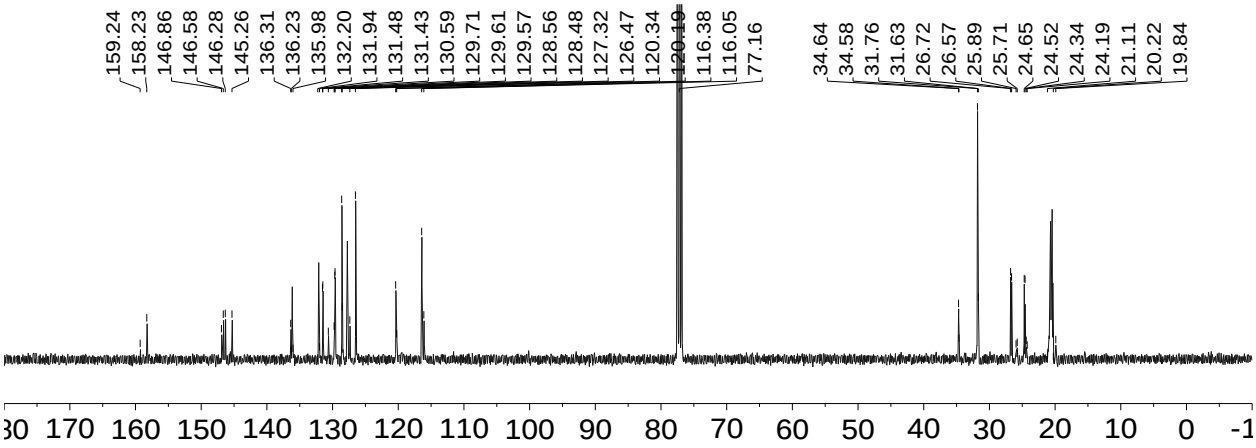

Figure C.27. $^{31}P\{^{1}H\}$ NMR spectrum of **1d** at 25 °C in $CDCl_3$.

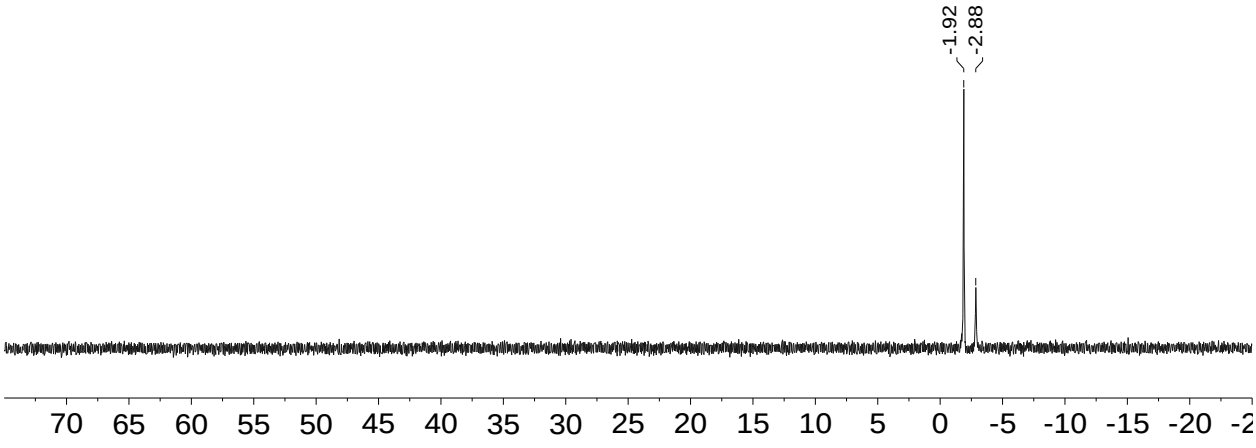

Figure C.28. $^{31}P\{^{1}H\}$ NMR spectrum of **1d** at 25 °C in C_6D_6.

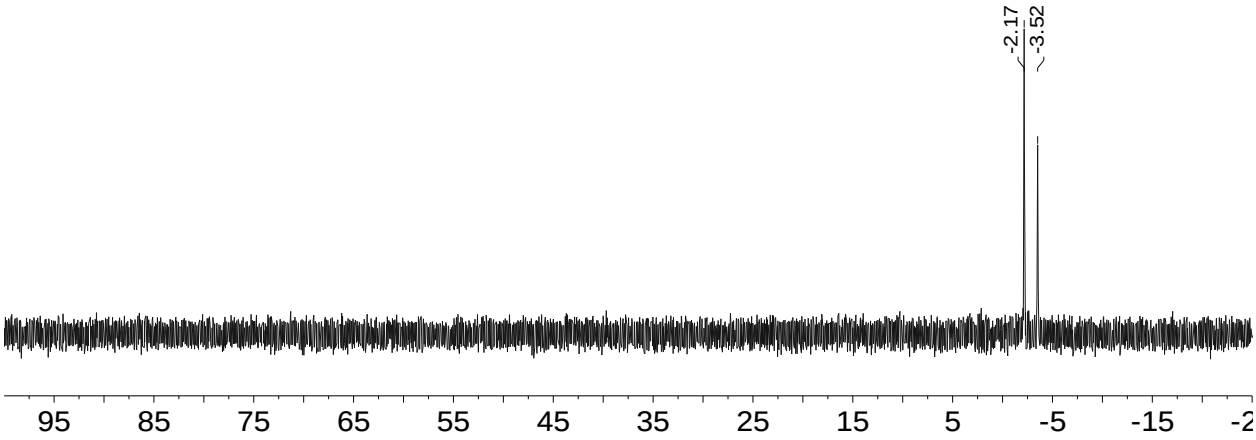

Figure C.29. ^{1}H NMR spectrum of **1d** at 70 °C in C_6D_6.

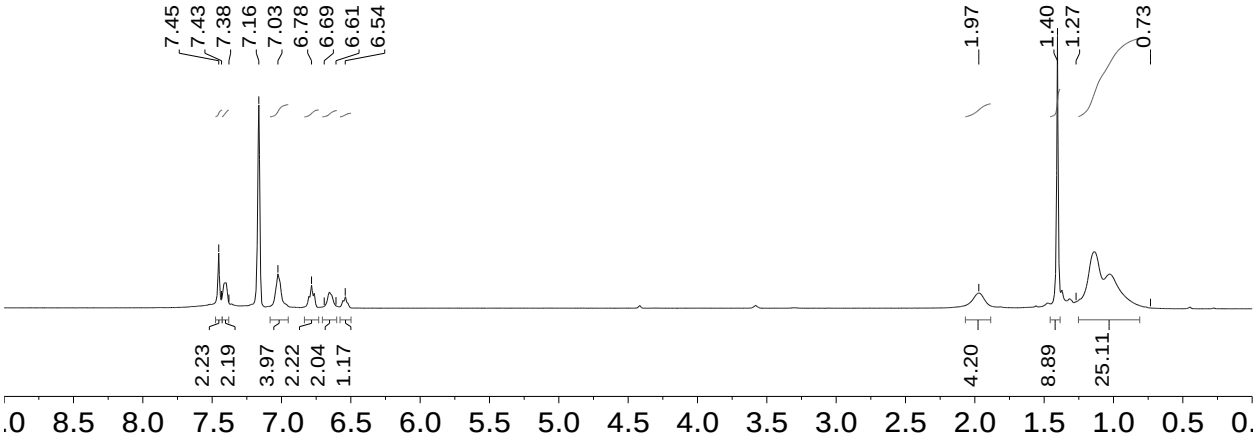

Figure C.30. $^{13}C\{^{1}H\}$ NMR spectrum of **1d** at 70 °C in C_6D_6.

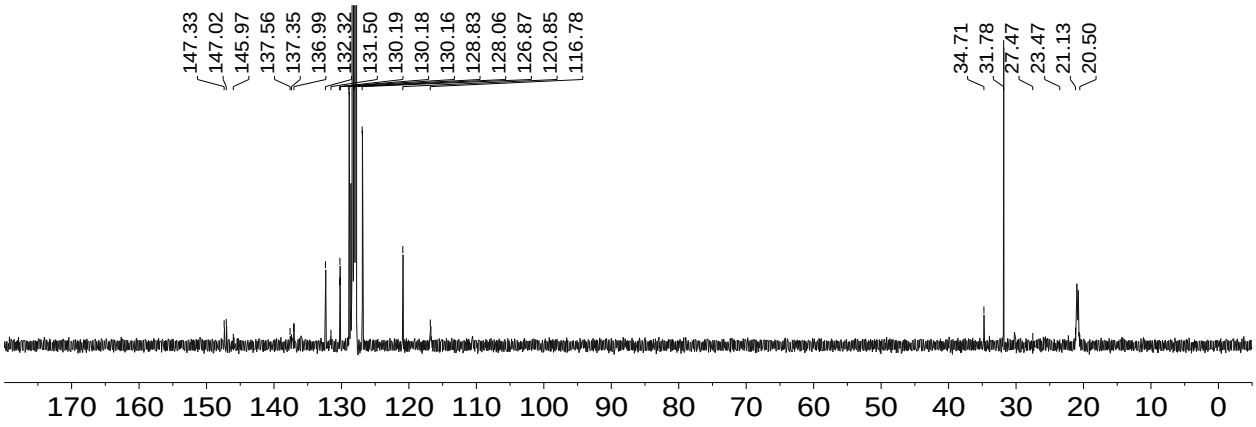

Figure C.31. $^{31}P\{^{1}H\}$ NMR spectrum of **1d** at 70 °C in C_6D_6. (Note: Referenced to solvent lock.)

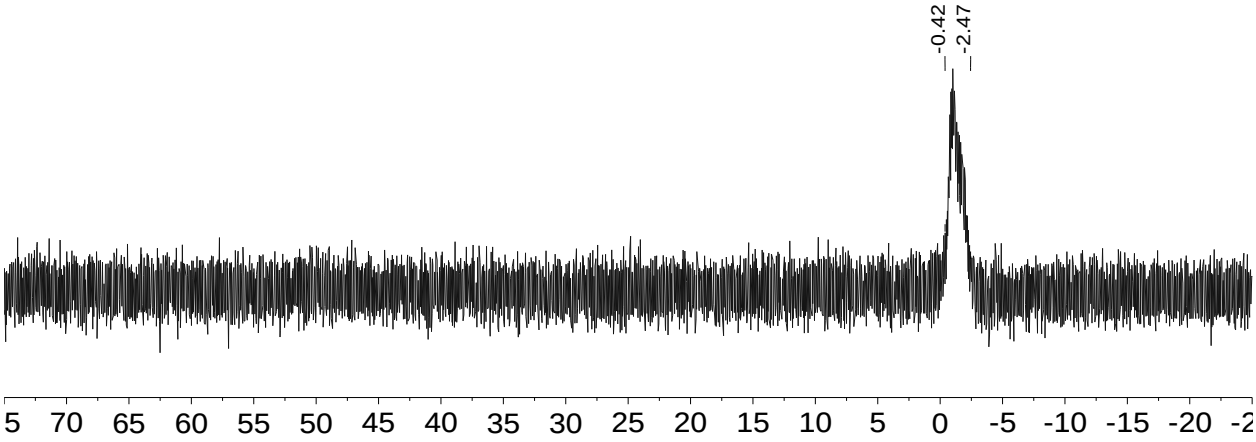

Figure C.32. ^{1}H NMR spectrum of **10d** in C_6D_6.

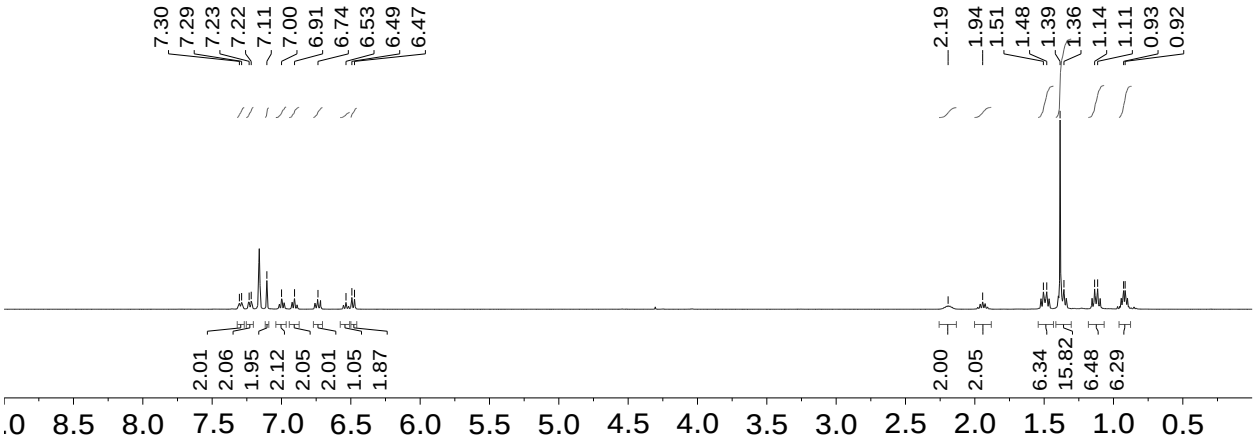

Figure C.33. $^{13}C\{^{1}H\}$ NMR spectrum of **10d** in C_6D_6.

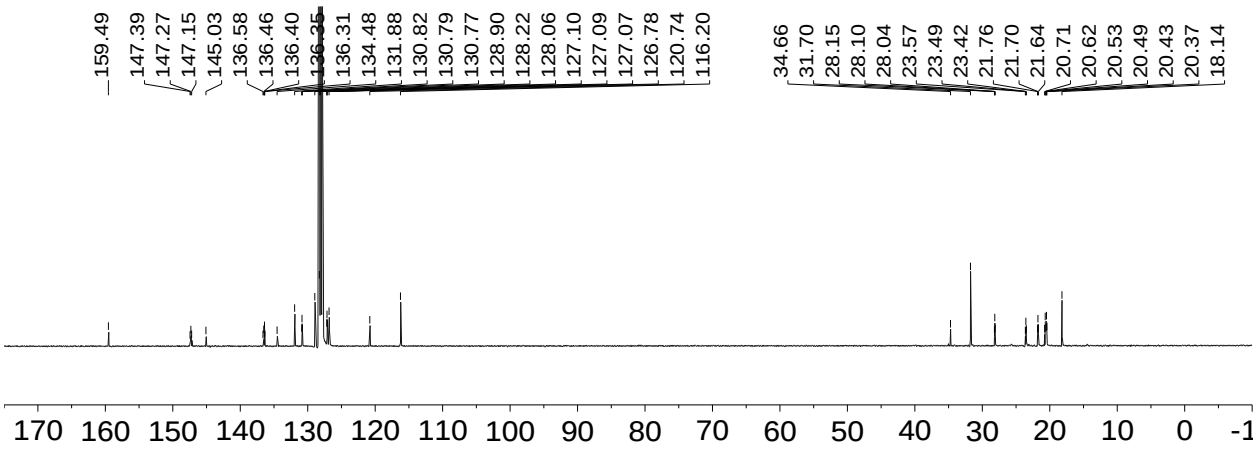

Figure C.34. $^{31}P\{^{1}H\}$ NMR spectrum of **10d** in C_6D_6.

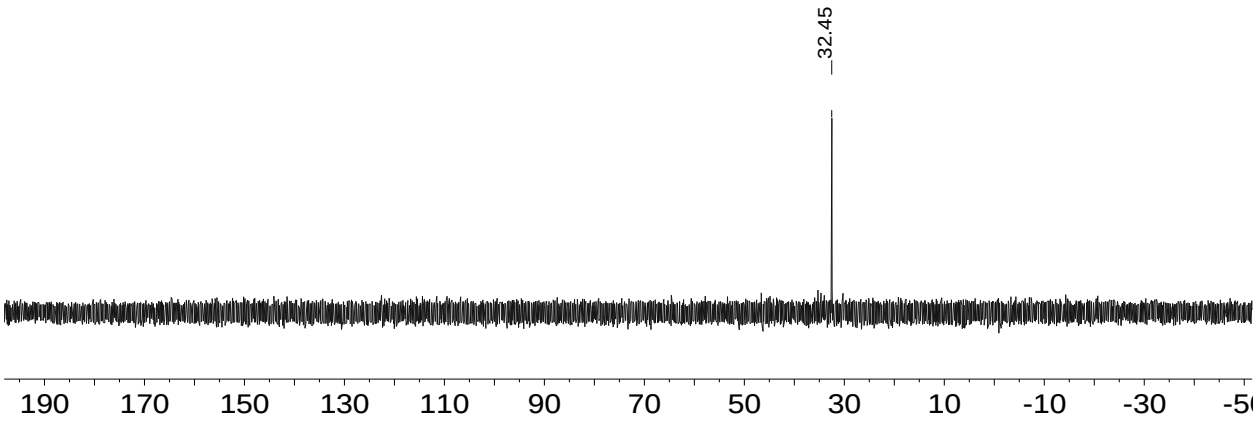

Figure C.35. ^{1}H NMR spectrum of **11d** in C_6D_6.

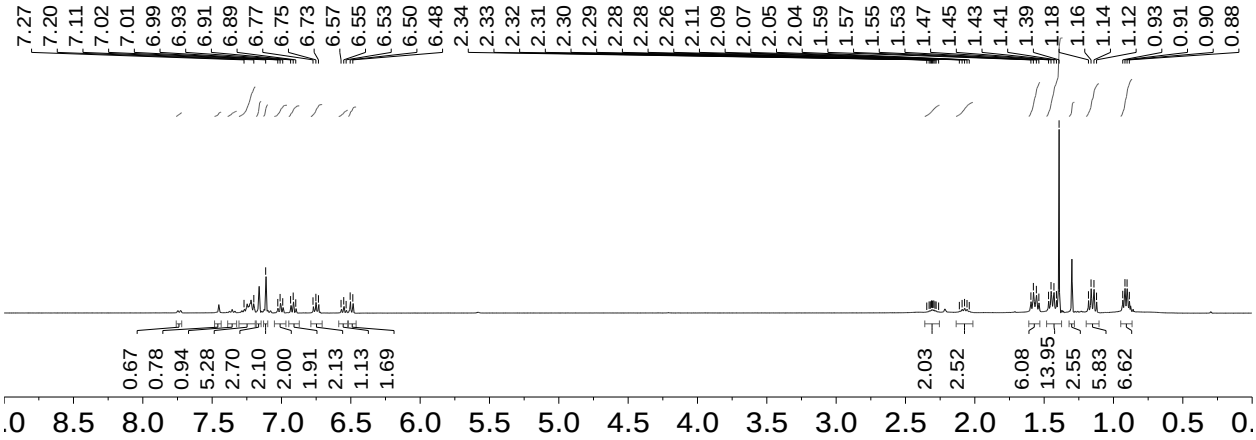

Figure C.36. $^{13}C\{^{1}H\}$ NMR spectrum of **11d** in C_6D_6.

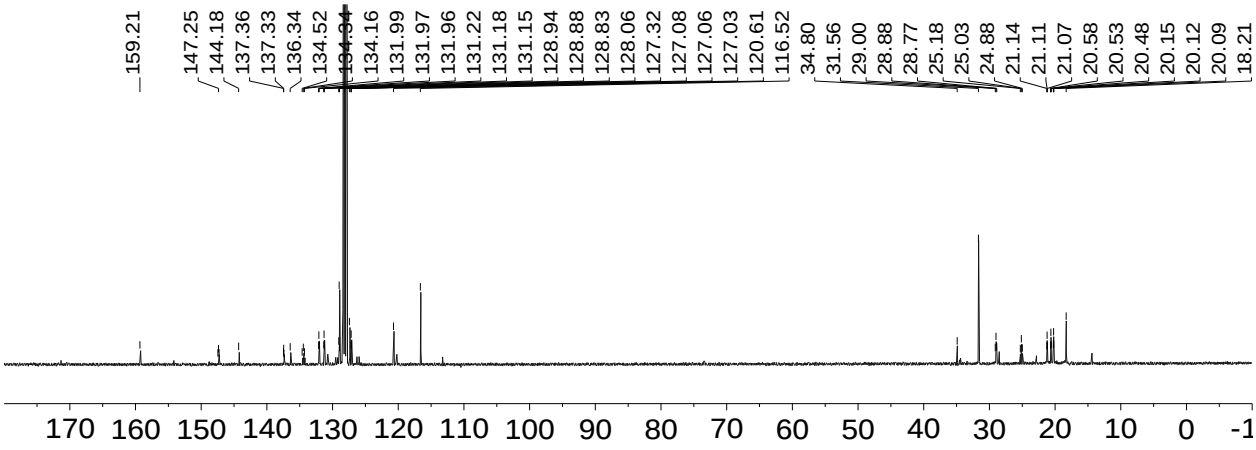

Figure C.37. $^{31}P\{^{1}H\}$ NMR spectrum of **11d** in C_6D_6.

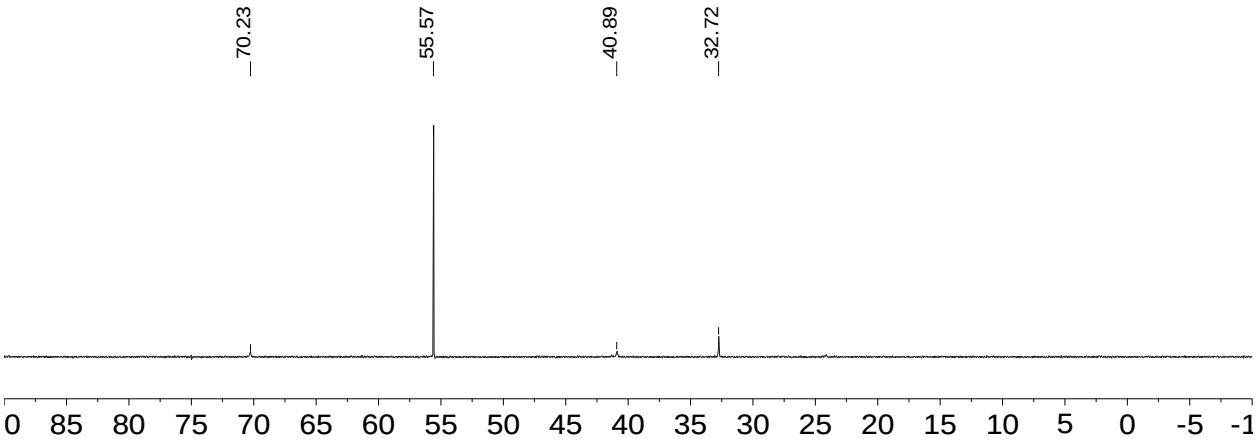

Figure C.38. ^{1}H NMR spectrum of **12c** in C_6D_6.

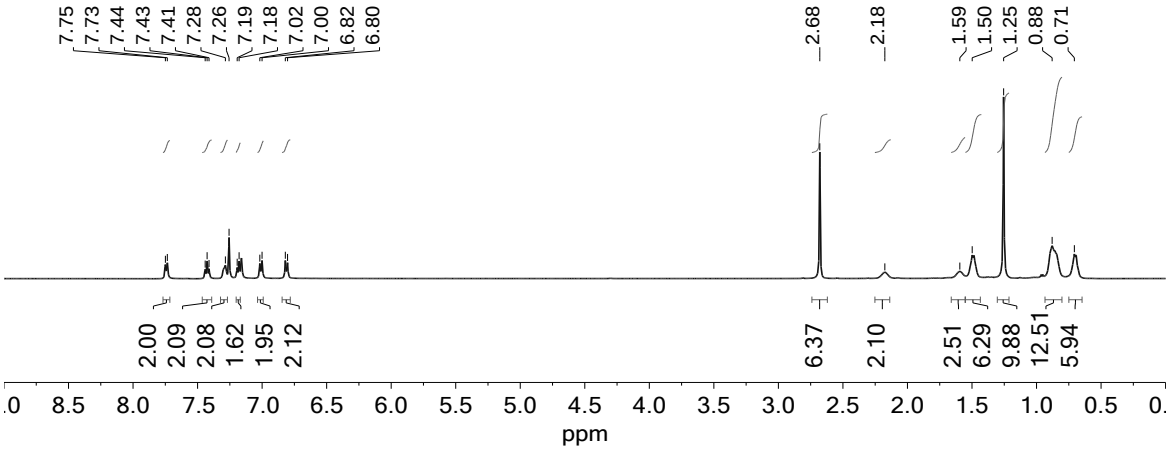

Figure C.39. $^{13}C\{^{1}H\}$ NMR spectrum of **12c** in C_6D_6.

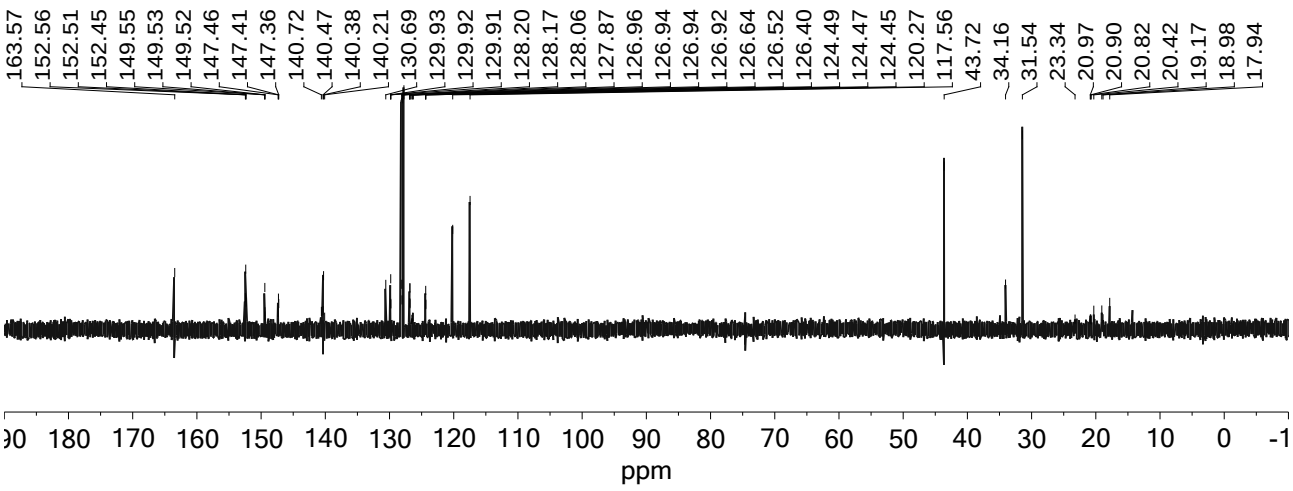

Figure C.40. $^{31}P\{^{1}H\}$ NMR spectrum of **12c** in C_6D_6.

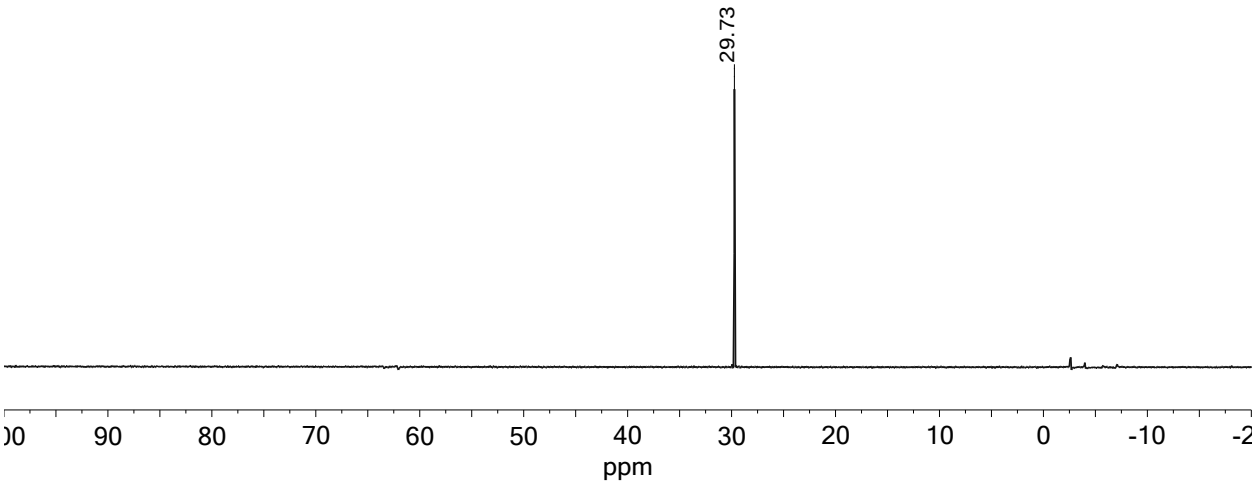

Figure C.41. ^{1}H NMR spectrum of **13d** in C_6D_6.

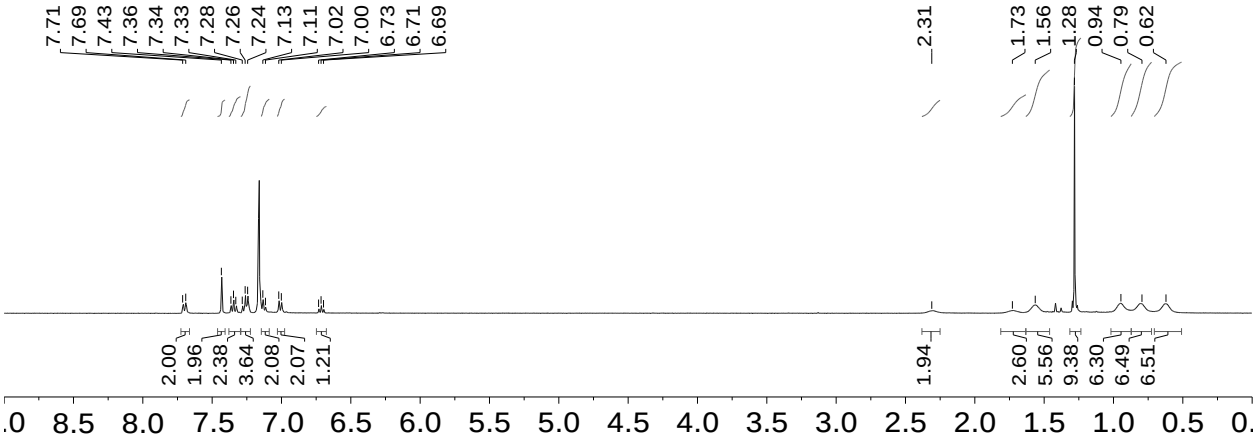

Figure C.42. $^{13}C\{^{1}H\}$ NMR spectrum of **13d** in C_6D_6.

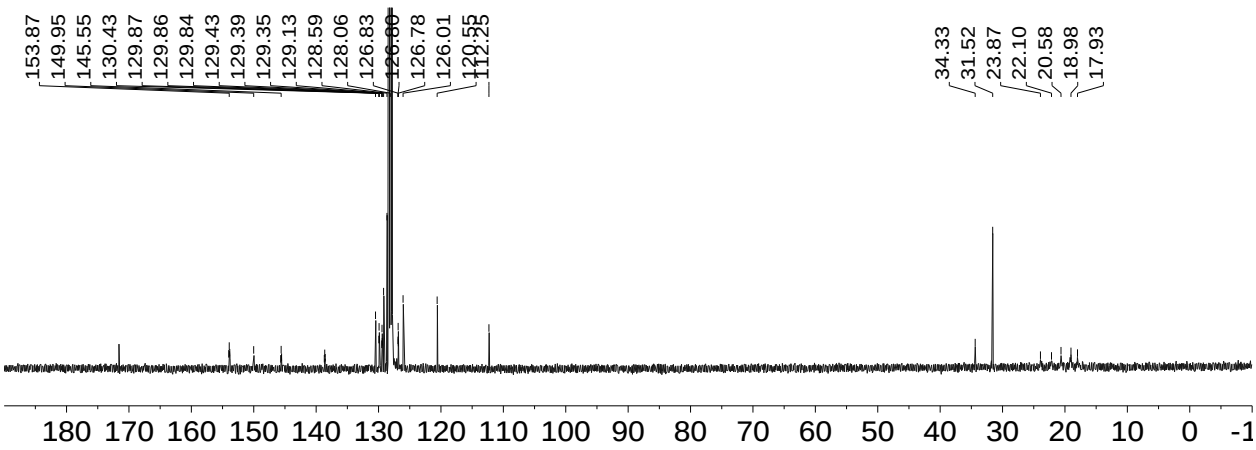

Figure C.43. $^{31}P\{^{1}H\}$ NMR spectrum of **13d** in C_6D_6.

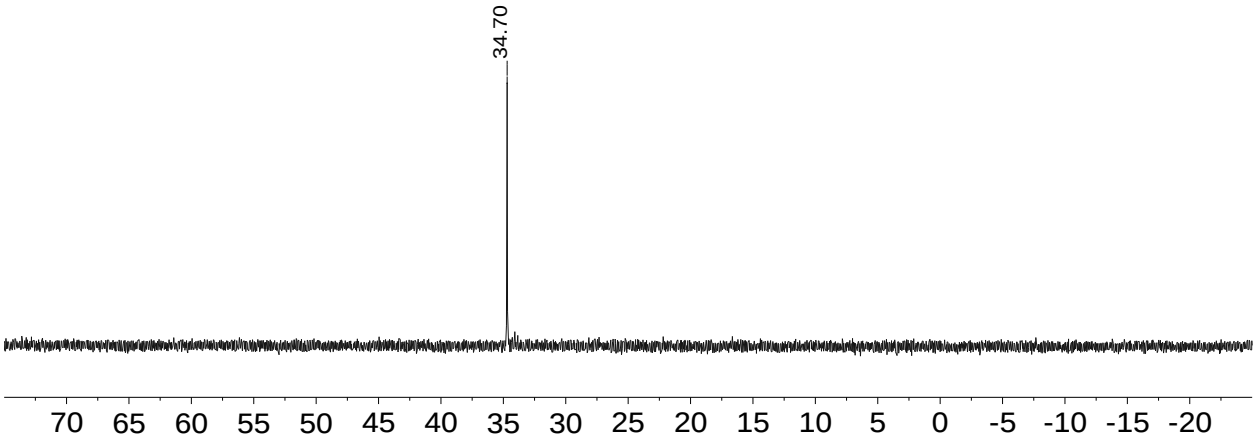

Figure C.44. ^{1}H NMR spectrum of **14d** in C_6D_6.

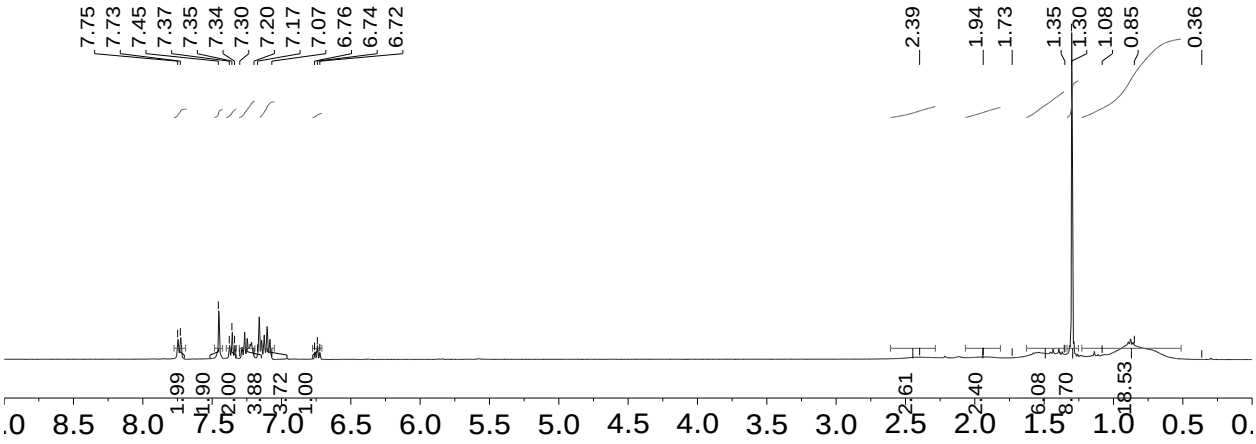

Figure C.45. $^{13}C\{^{1}H\}$ NMR spectrum of **14d** in C_6D_6.

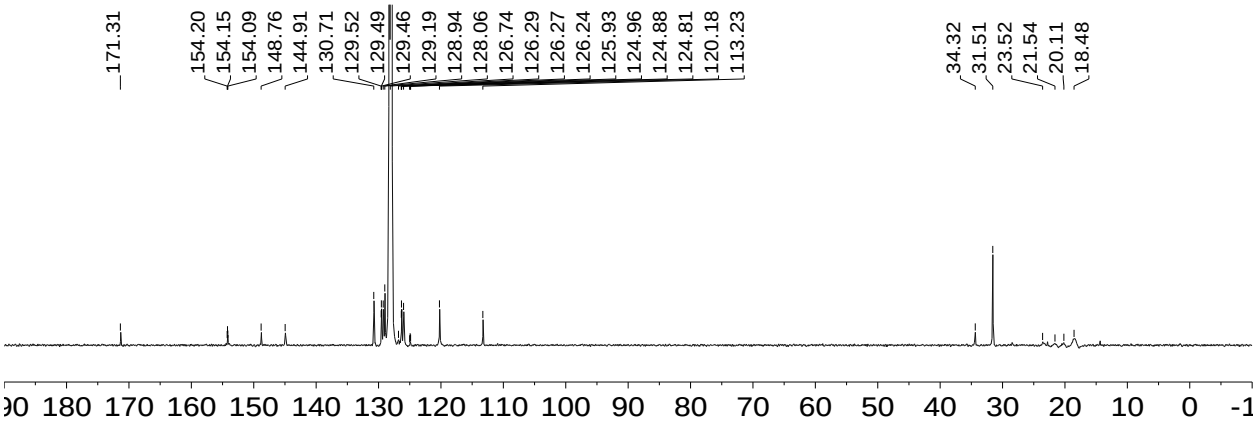

Figure C.46. $^{31}P\{^{1}H\}$ NMR spectrum of **14d** in C_6D_6.

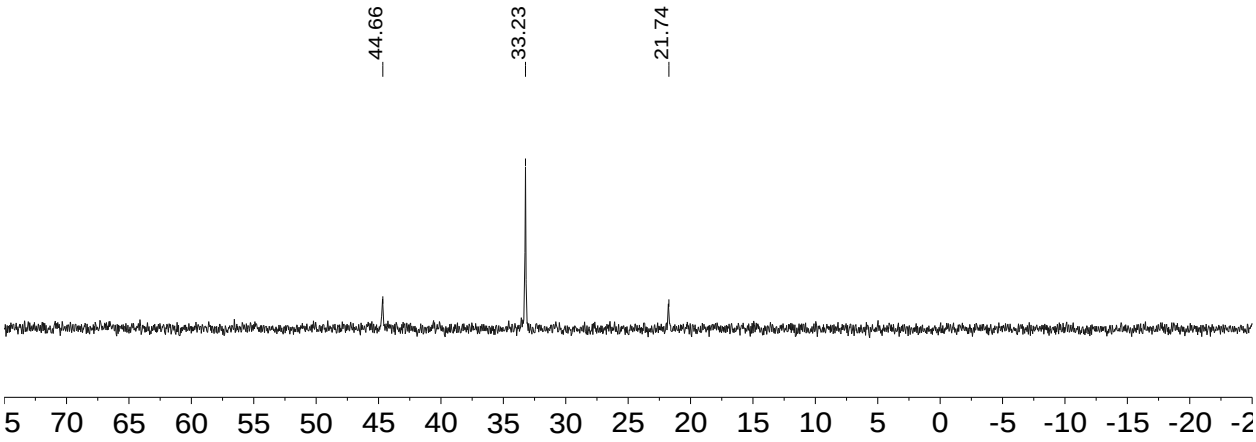

Figure C.47. ^{1}H NMR spectrum of **15a** in C_6D_6.

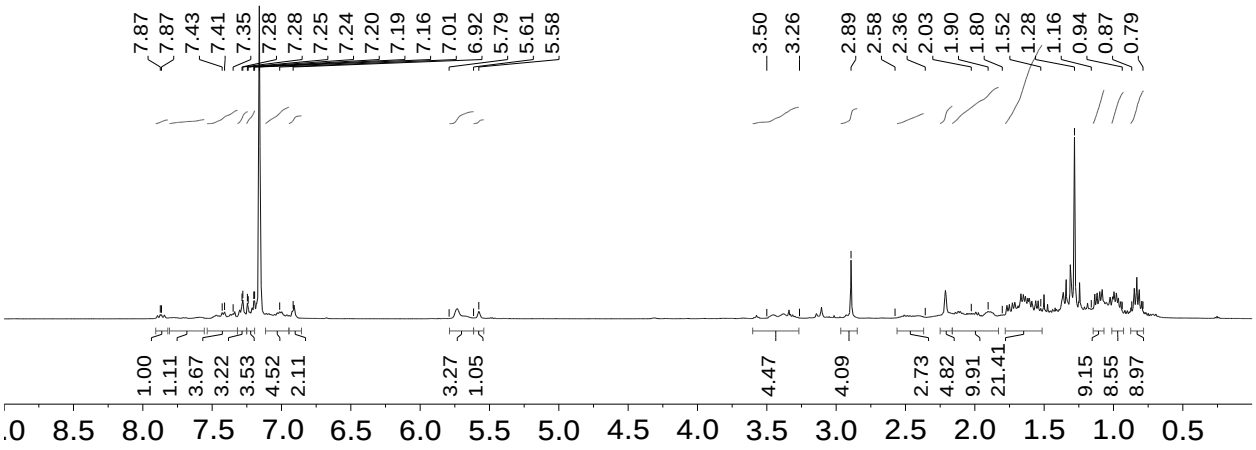

Figure C.48. $^{13}C\{^{1}H\}$ NMR spectrum of **15a** in C_6D_6.

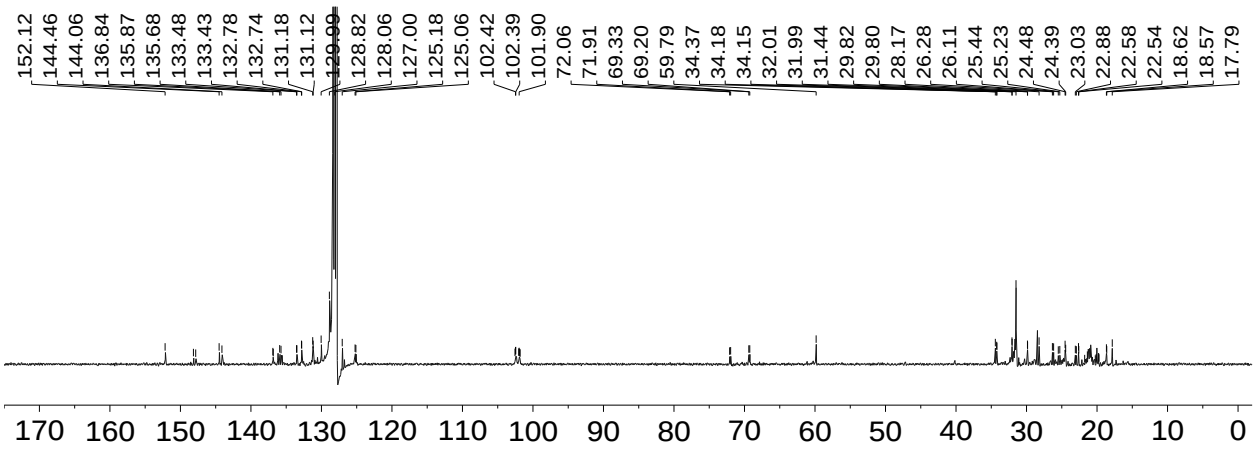

Figure C.49. $^{31}P\{^{1}H\}$ NMR spectrum of **15a** in C_6D_6.

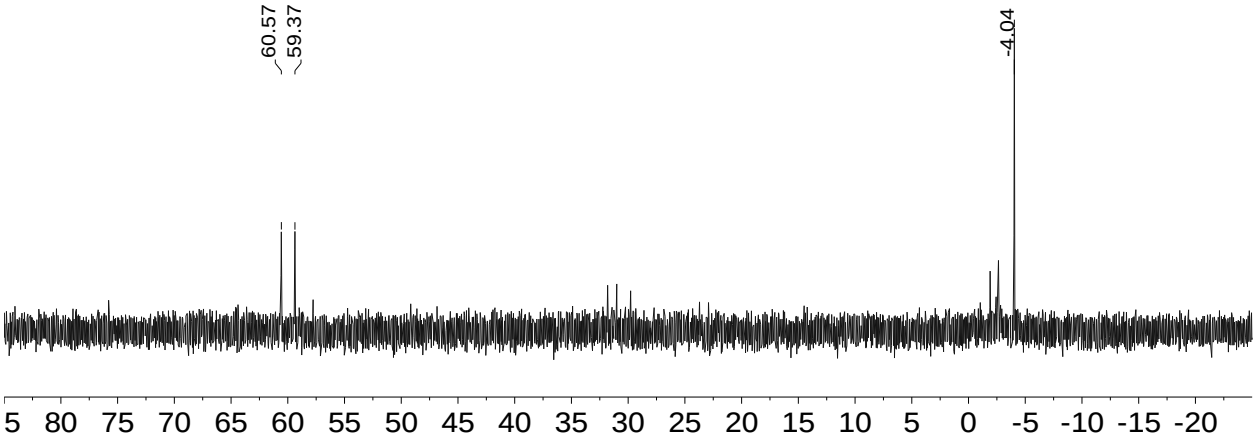

Figure C.50. ^{1}H NMR spectrum of **19a** at 25 °C in C_6D_6.

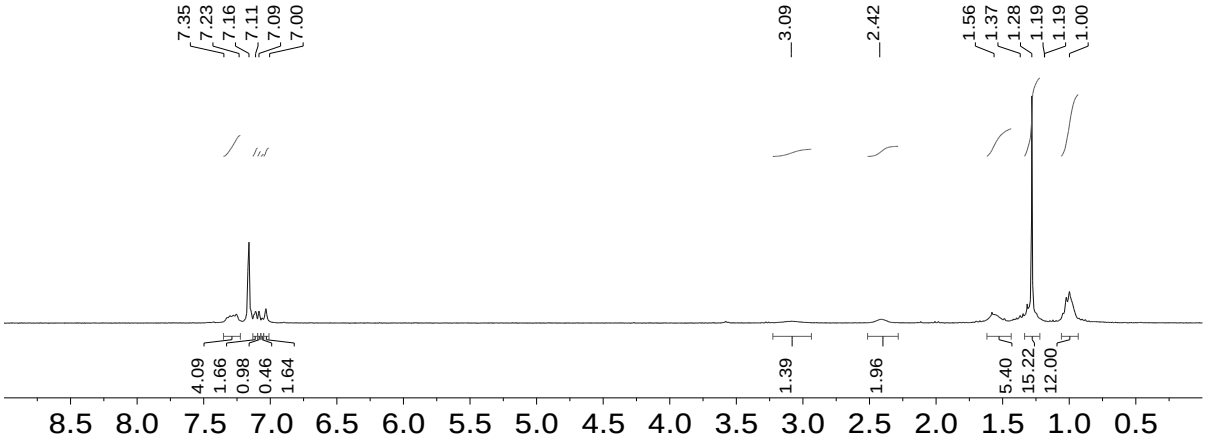

Figure C.51. $^{31}P\{^{1}H\}$ NMR spectrum of **19a** at 25 °C in C_6D_6.

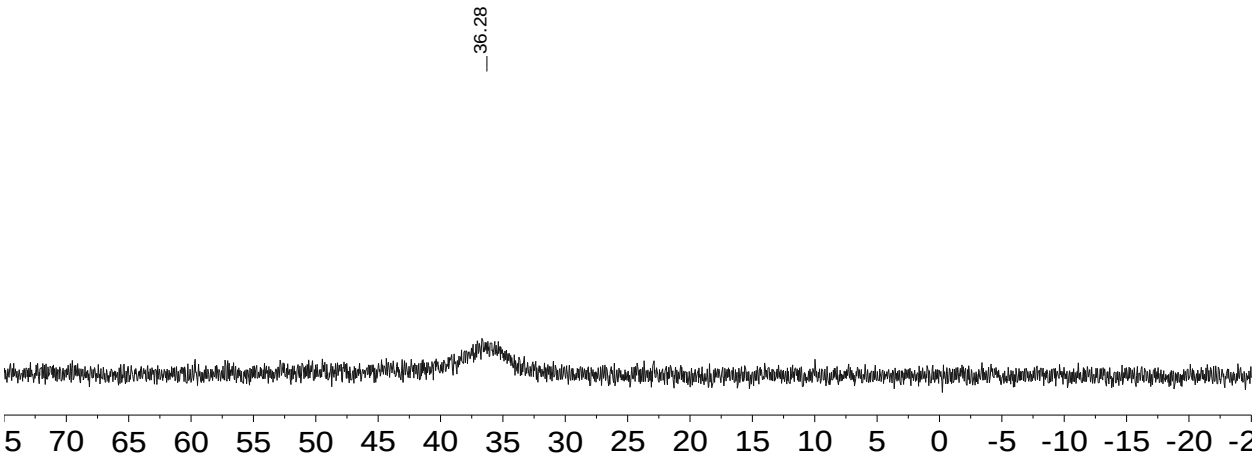

Figure C.52. $^{13}C\{^{1}H\}$ NMR spectrum of **19a** at 70 °C in C_6D_6.

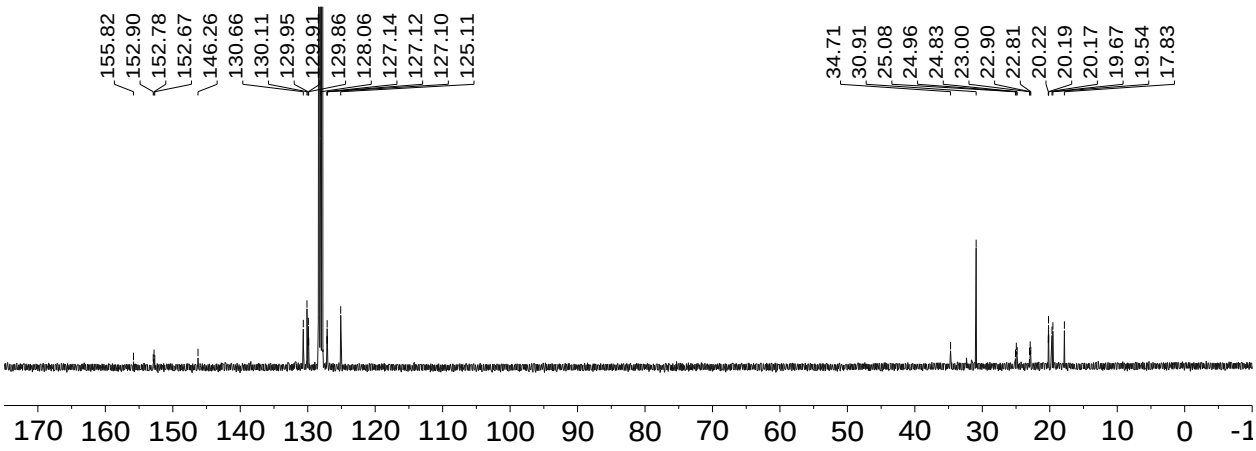

Figure C.53. $^{31}P\{^{1}H\}$ NMR spectrum of **19a** at 70 °C in C_6D_6.

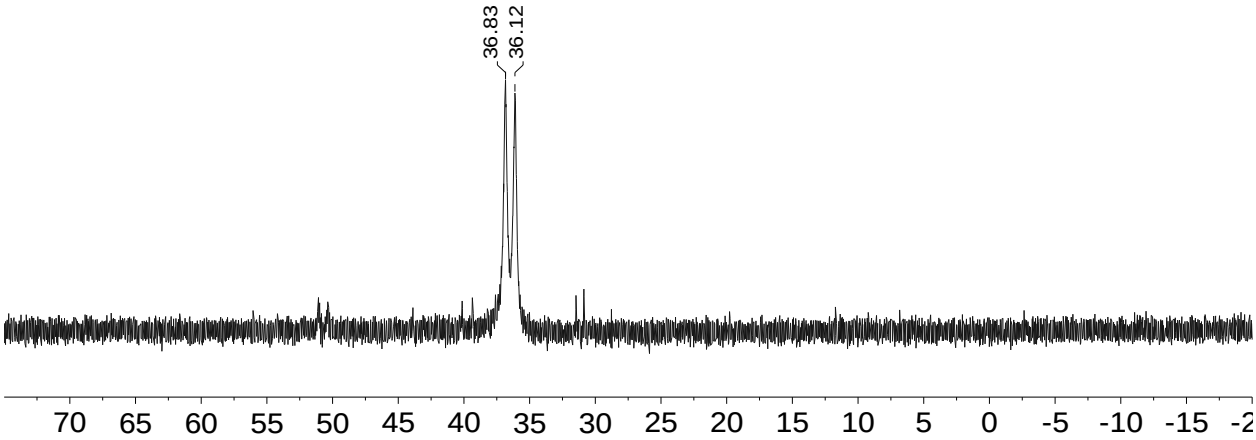

Figure C.54. ^{1}H NMR spectrum of 1,3-bis(2'bromophenyl)-5-tert-butyl-benzene in $CDCl_3$. Note: Residual CH_3OH present.

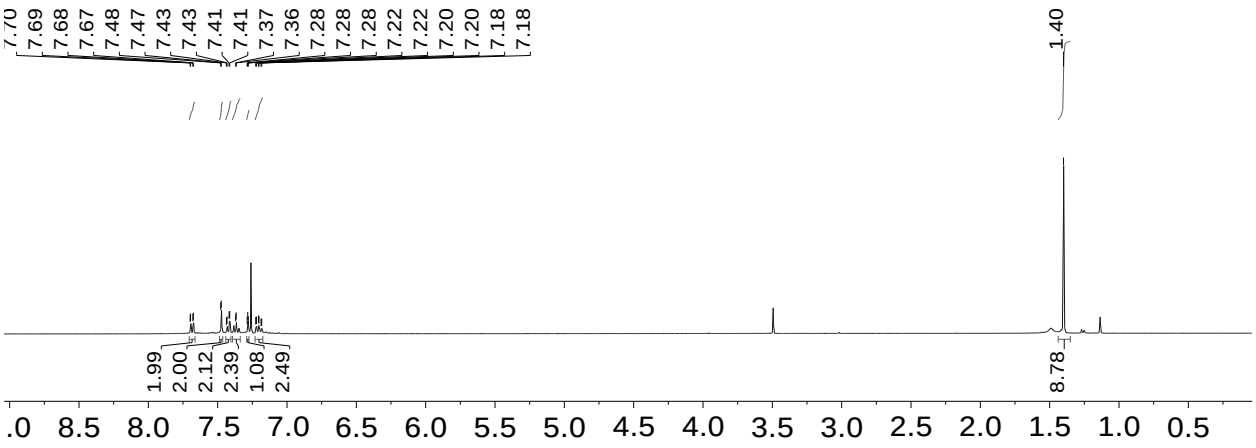

Figure C.55. ^{1}H NMR spectrum of **1e** in C_6D_6.

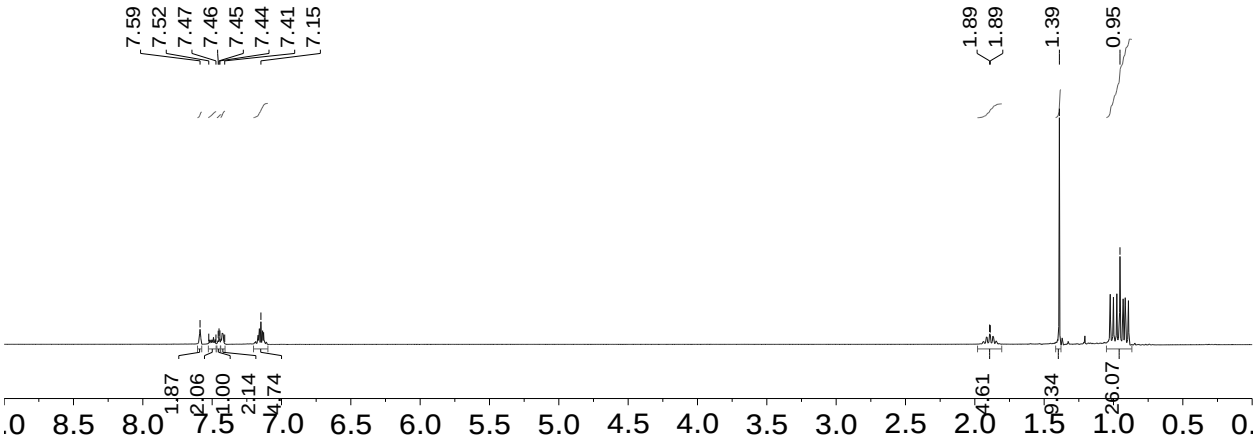

Figure C.56. $^{13}C\{^{1}H\}$ NMR spectrum of **1e** in $CDCl_3$.

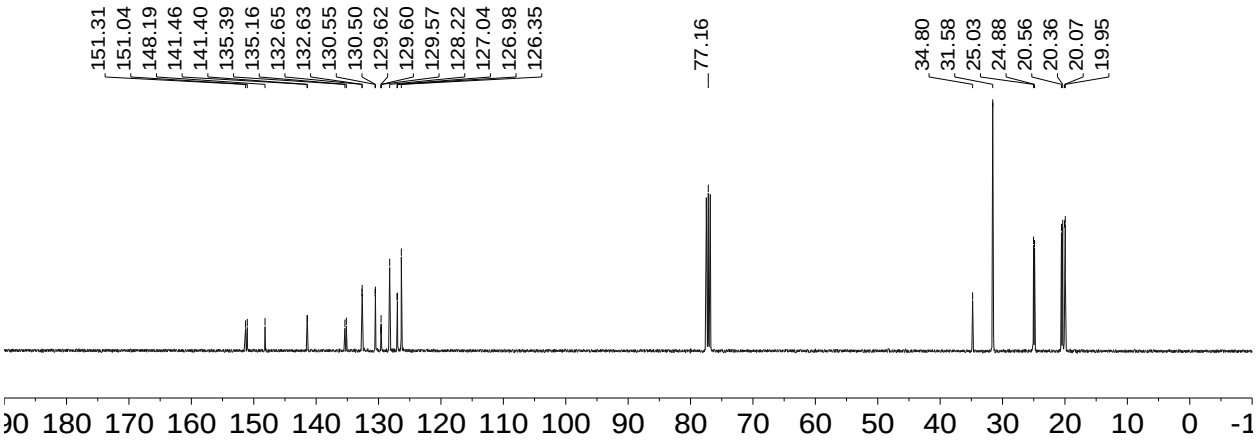

Figure C.57. $^{31}P\{^{1}H\}$ NMR spectrum of **1e** in C_6D_6.

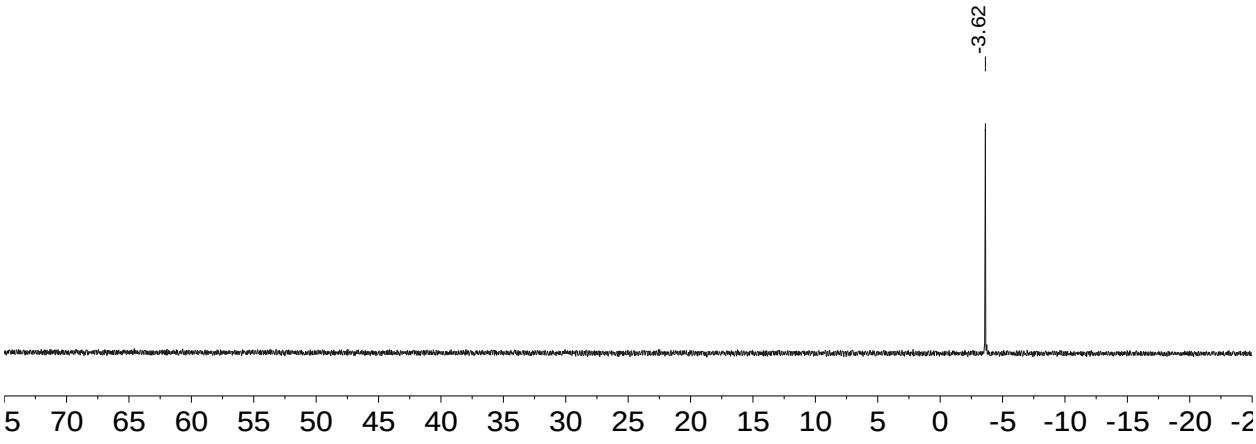

Figure C.58. ^{1}H NMR spectrum of **23a** in C_6D_6.

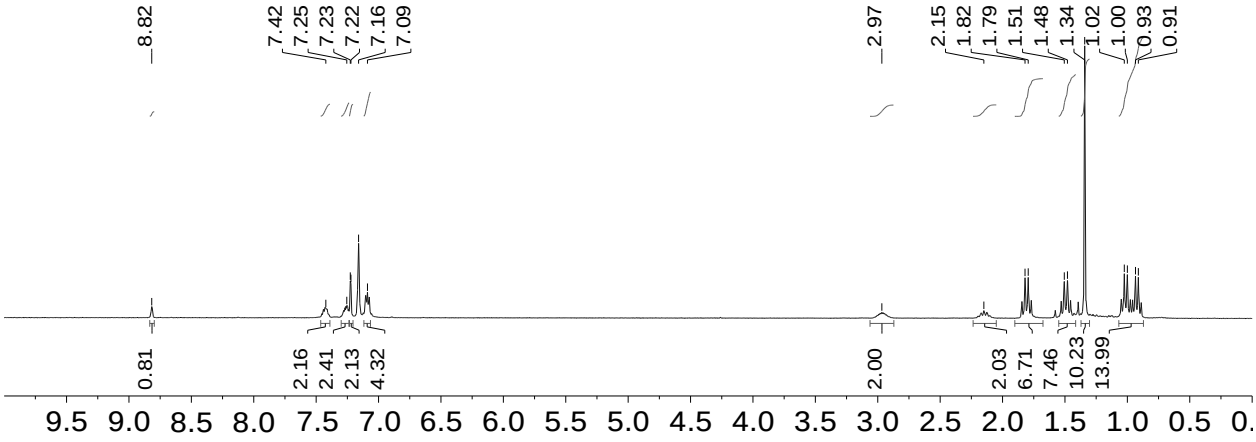

Figure C.59. $^{13}C\{^{1}H\}$ NMR spectrum of **23a** in C_6D_6.

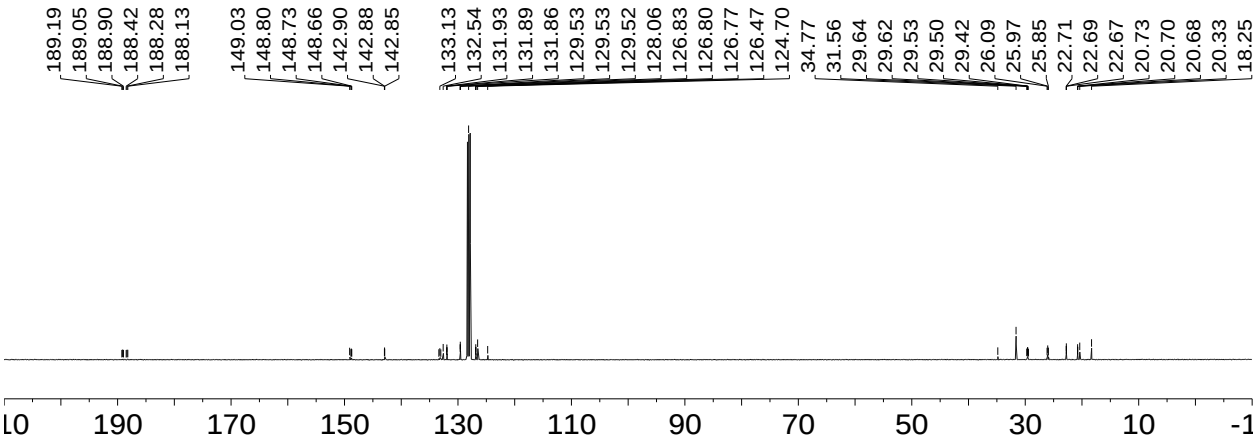

Figure C.60. $^{31}P\{^{1}H\}$ NMR spectrum of **23a** in C_6D_6.

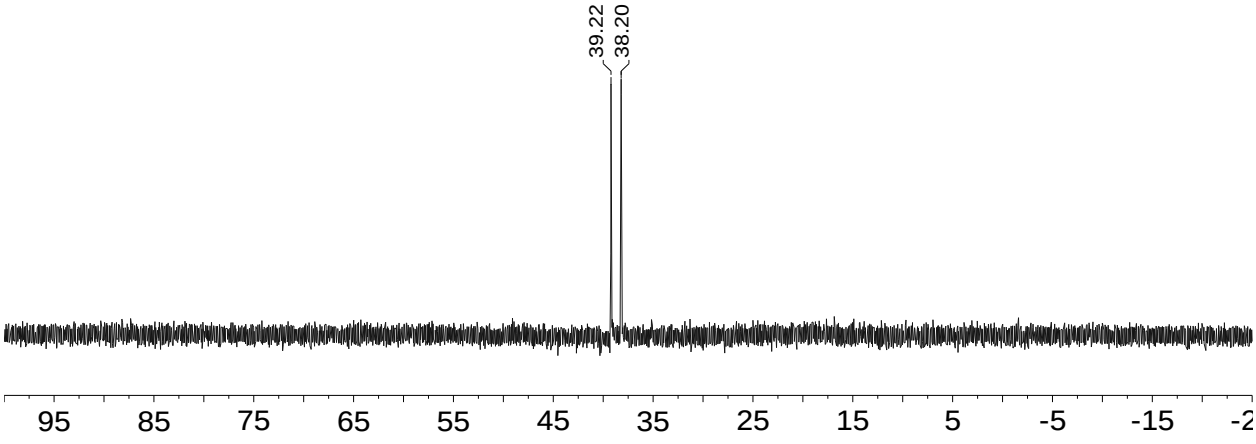

Figure C.61. ^{1}H NMR spectrum of **24a** in C_6D_6.

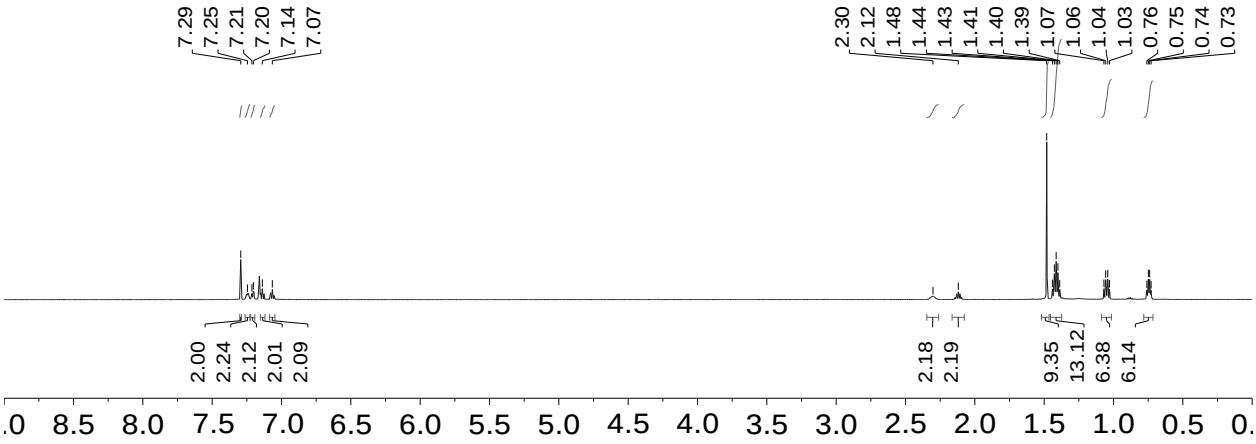

Figure C.62. $^{13}C\{^{1}H\}$ NMR spectrum of **24a** in C_6D_6.

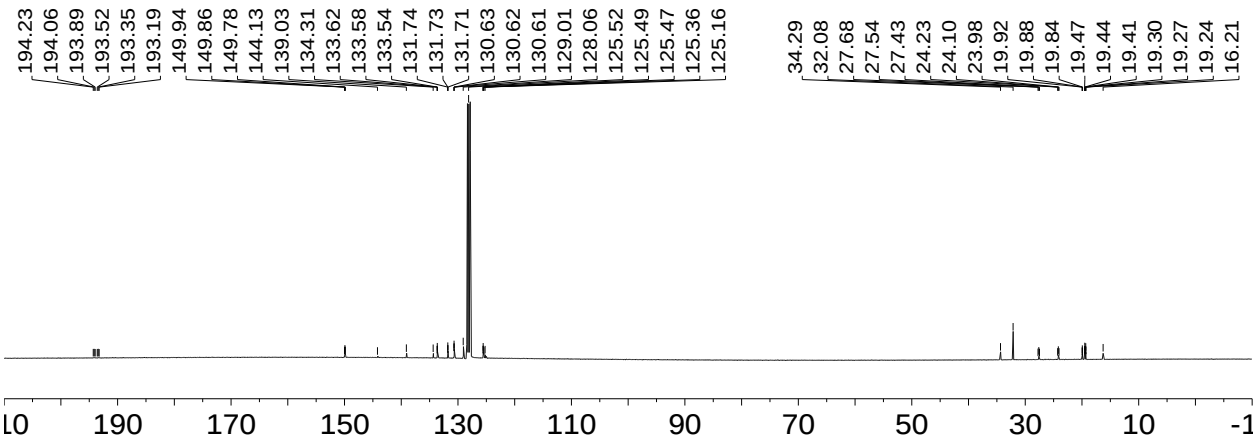

Figure C.63. $^{31}P\{^{1}H\}$ NMR spectrum of **24a** in C_6D_6.

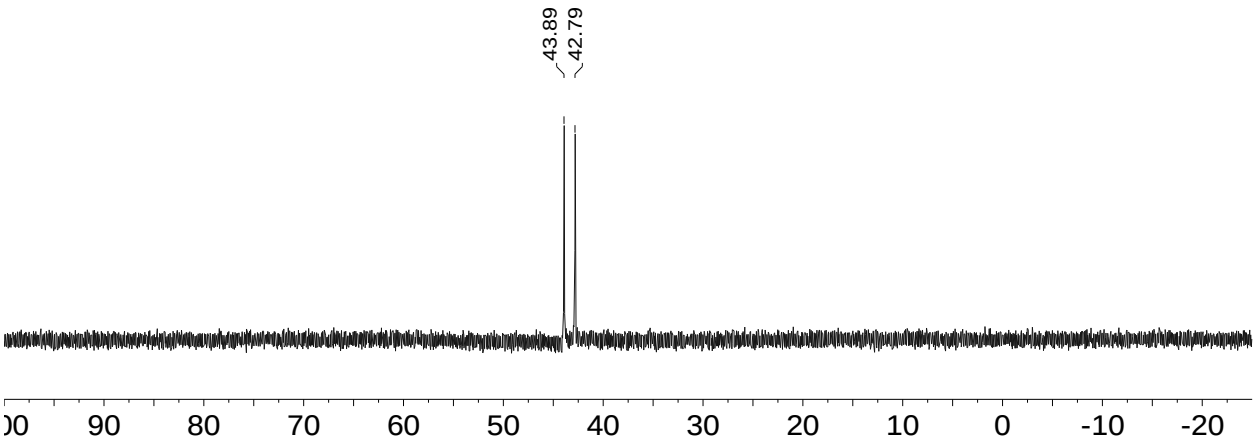

Figure C.64. ^{1}H NMR spectrum of 5-(tert-butyl)-1,3-diiodo-2-(methoxymethoxy)-benzene in $CDCl_3$.

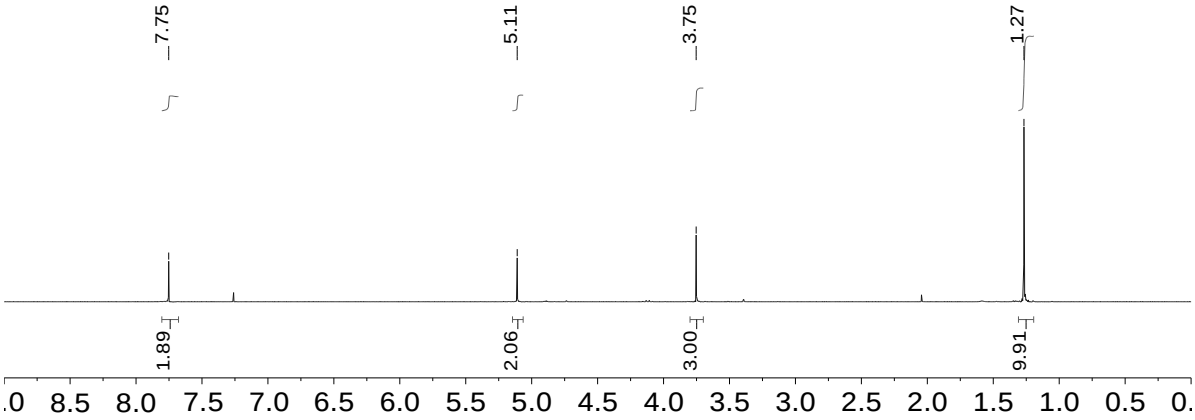

Figure C.65. $^{13}C\{^{1}H\}$ NMR spectrum of 5-(tert-butyl)-1,3-diiodo-2-(methoxy-methoxy)benzene in $CDCl_3$.

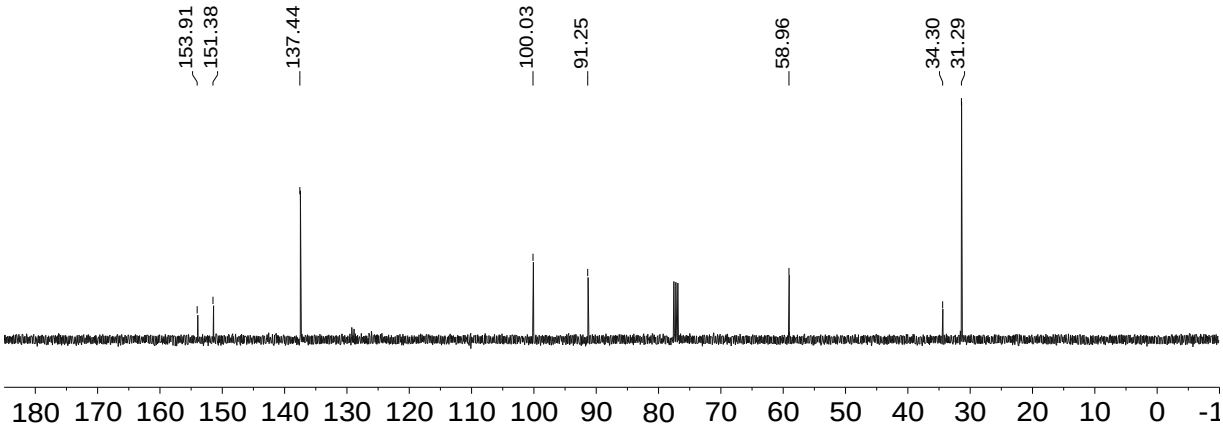

Figure C.66. ^{1}H NMR spectrum of 1,3-bis(2'-bromophenyl)-5-tert-butyl-2-(methoxy-methoxy)benzene in $CDCl_3$.

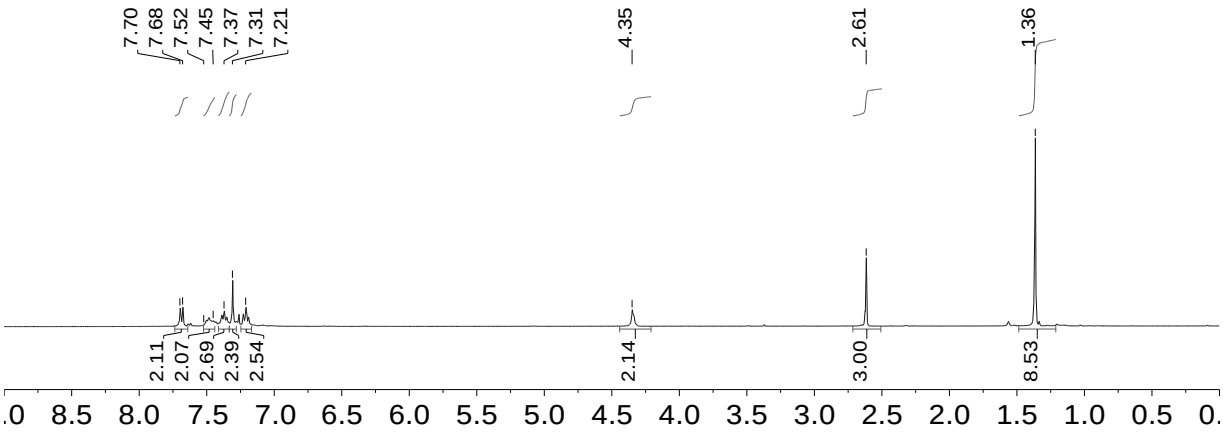

Figure C.67. ^{1}H NMR spectrum of **1f** at 25 °C in C_6D_6.

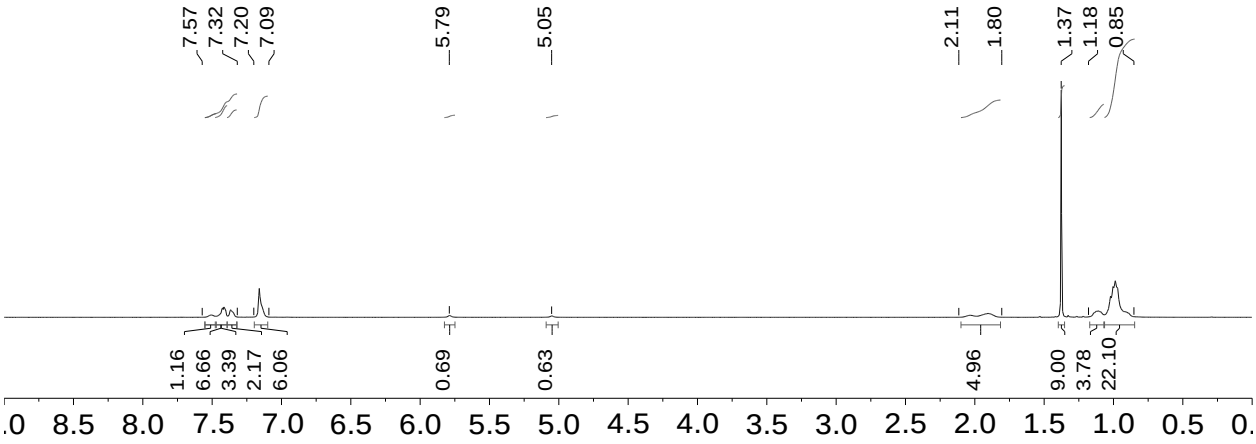

Figure C.68. $^{31}P\{^{1}H\}$ NMR spectrum of **1f** at 25 °C in C_6D_6. Note: Referenced to solvent residual.

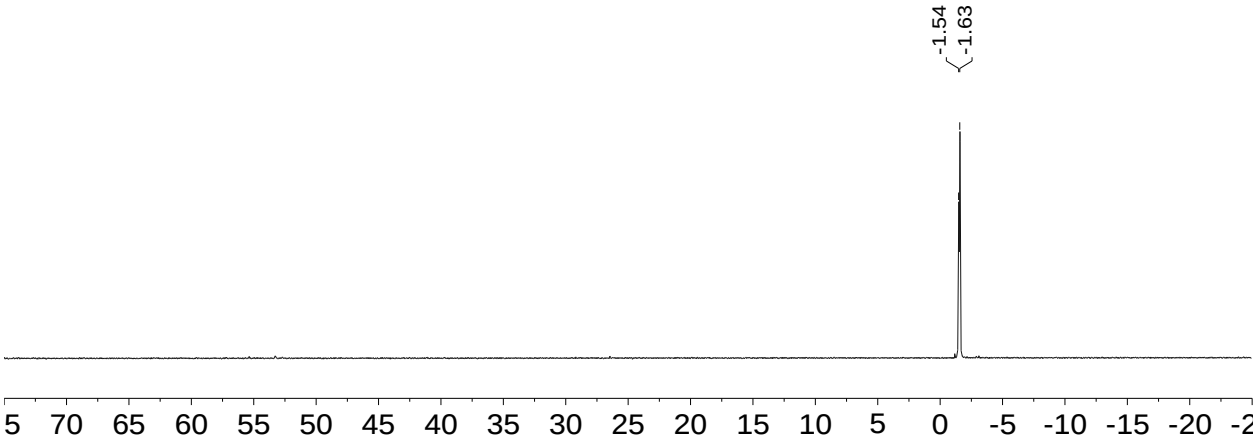

Figure C.69. ^{1}H NMR spectrum of **1f** at 70 °C.

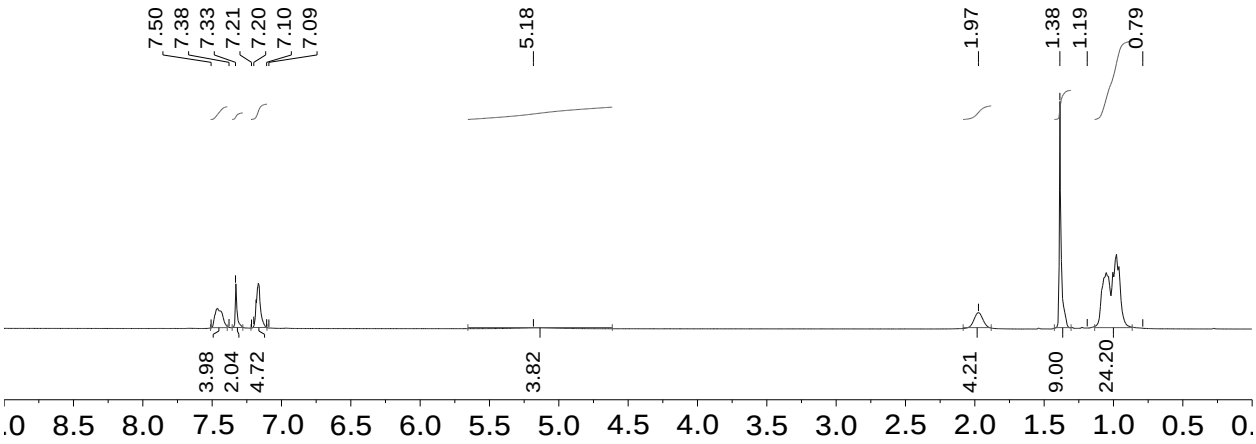

Figure C.70. $^{13}C\{^{1}H\}$ NMR spectrum of **1f** at 70 °C in C_6D_6.

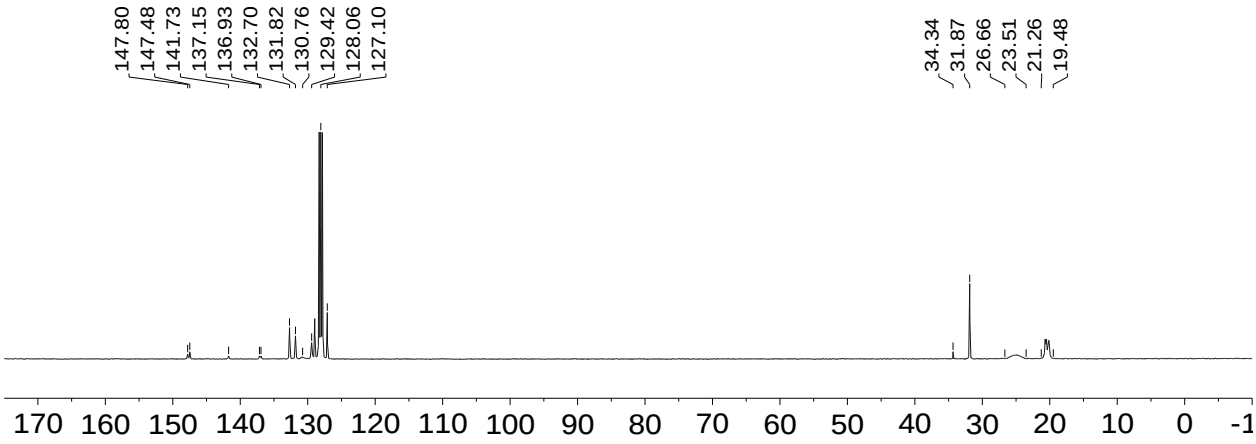

Figure C.71. $^{31}P\{^{1}H\}$ NMR spectrum of **1f** at 70 °C in C_6D_6. Note: Referenced to solvent residual.

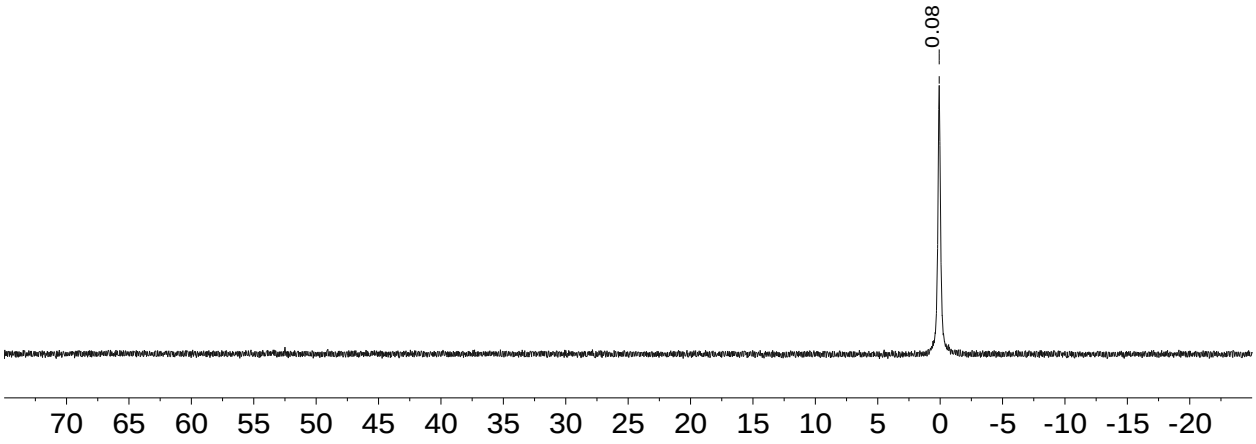

Figure C.72. ^{1}H NMR spectrum of **26a** in C_6D_6.

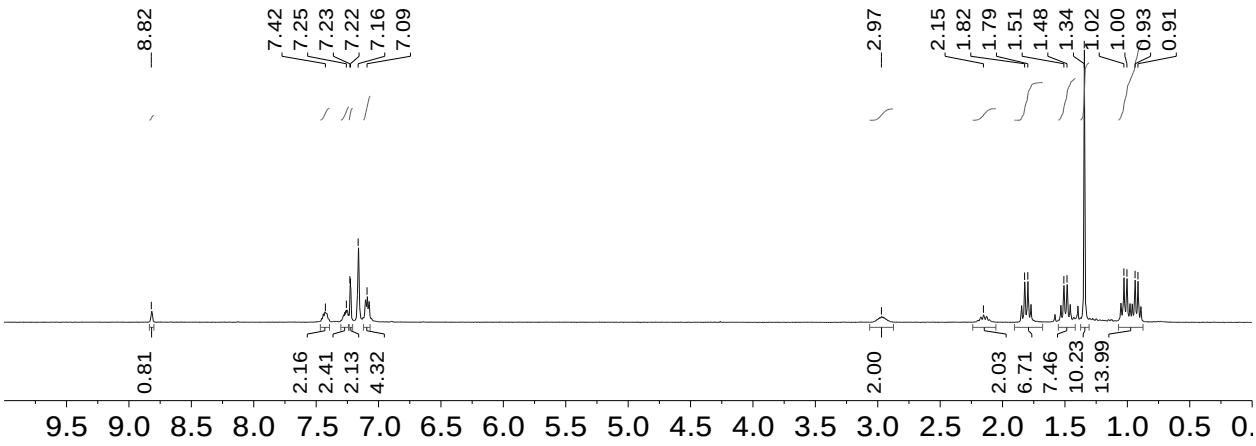

Figure C.73. $^{13}C\{^{1}H\}$ NMR spectrum of **26a** in C_6D_6.

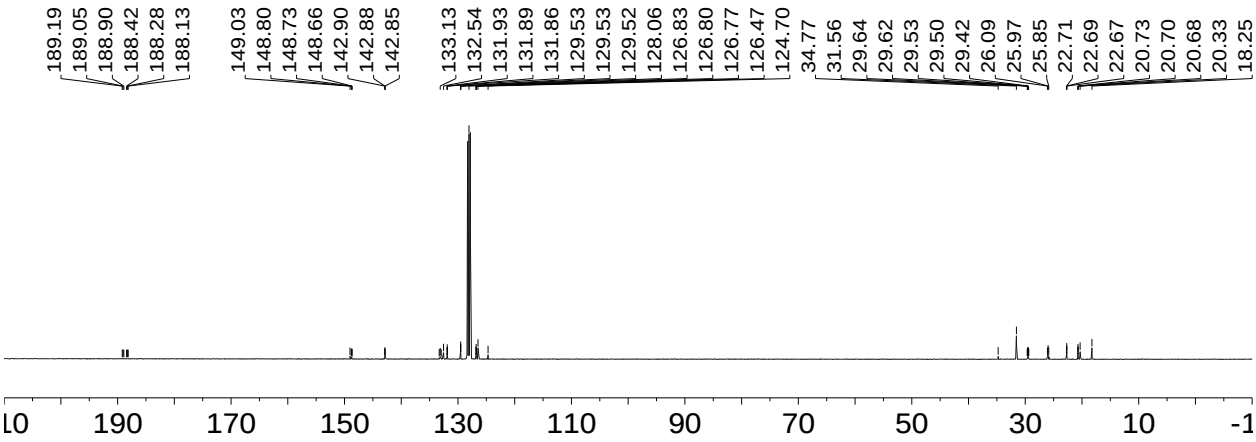

Figure C.74. $^{31}P\{^{1}H\}$ NMR spectrum of **26a** in C_6D_6.

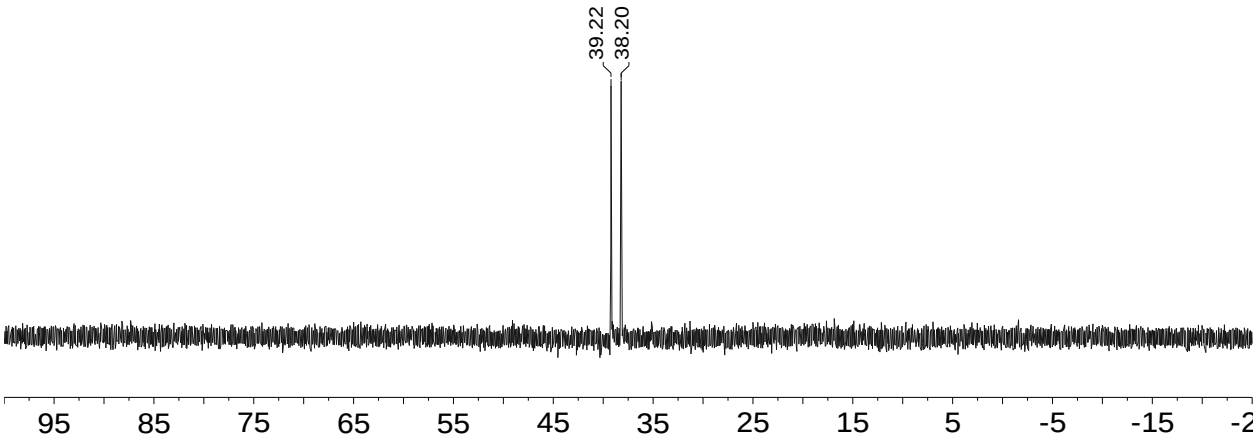

Figure C.75. ^{1}H NMR spectrum of **27a** in C_6D_6.

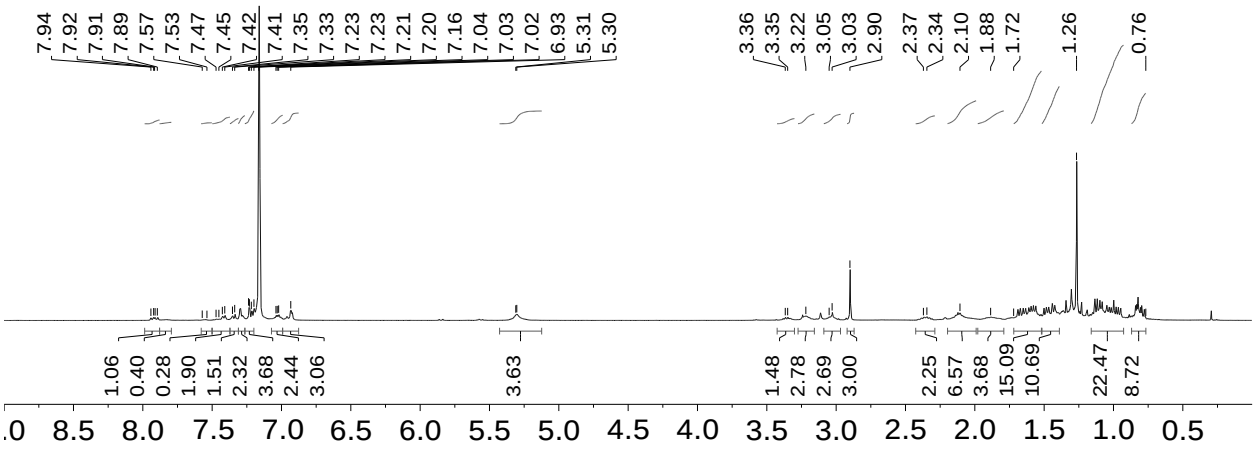

Figure C.76. $^{13}C\{^{1}H\}$ NMR spectrum of **27a** in C_6D_6.

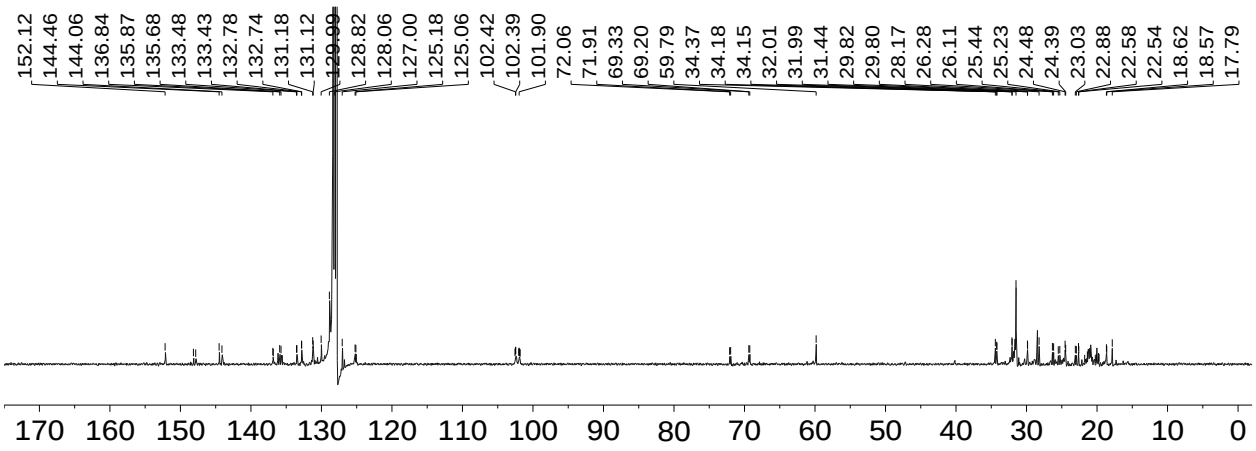

Figure C.77. $^{31}P\{^{1}H\}$ NMR spectrum of **27a** in C_6D_6.

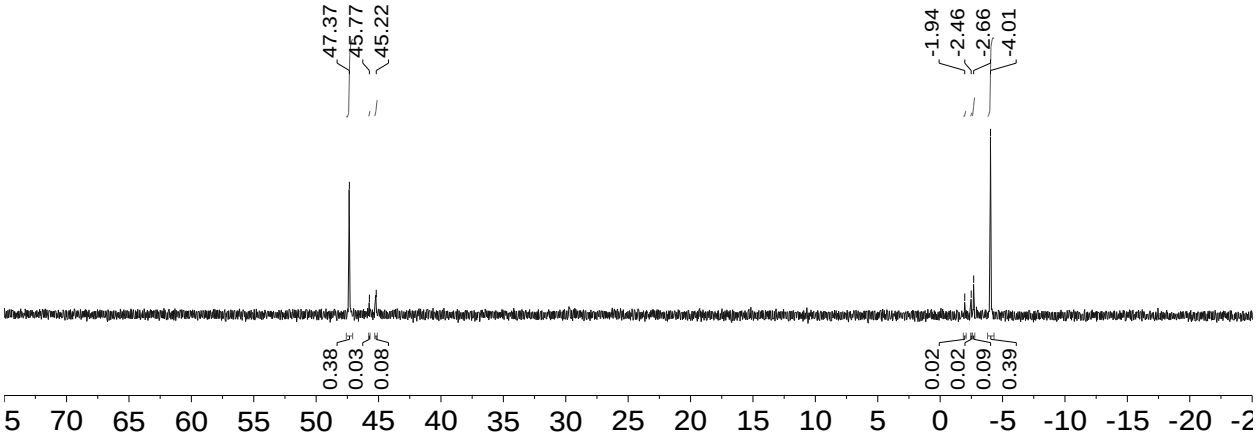

Figure C.78. ^{1}H NMR spectrum of **28a** in C_6D_6.

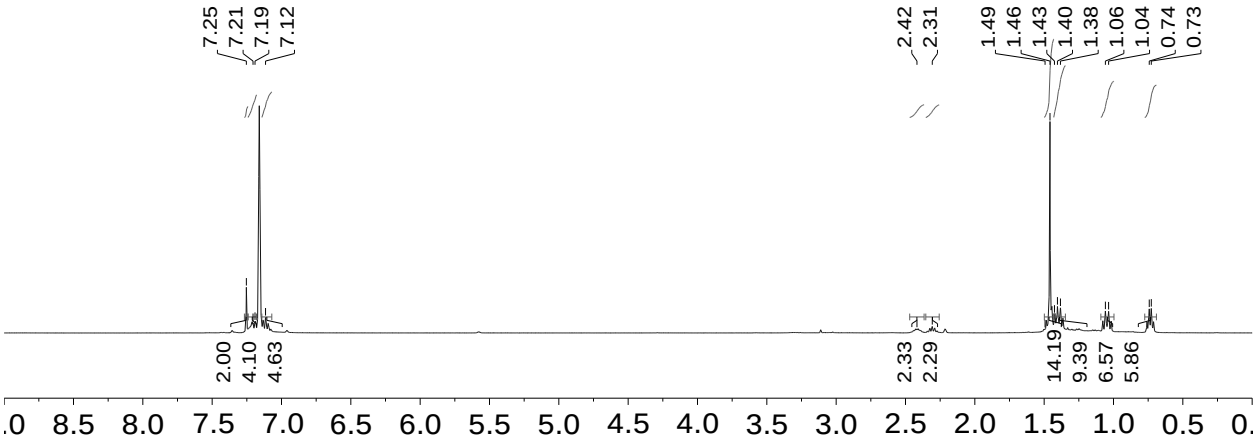

Figure C.79. $^{13}C\{^{1}H\}$ NMR spectrum of **28a** in C_6D_6.

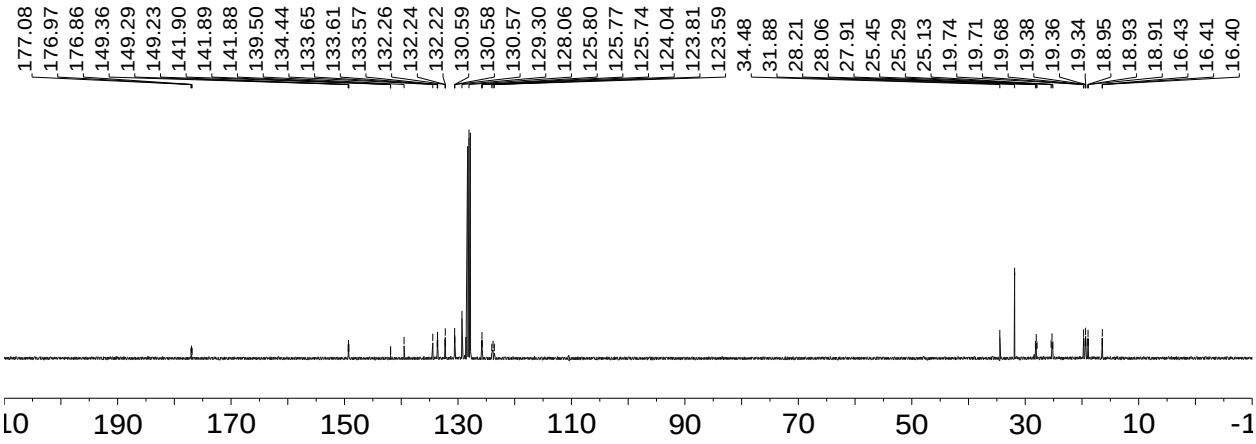

Figure C.80. $^{31}P\{^{1}H\}$ NMR spectrum of **28a** in C_6D_6.

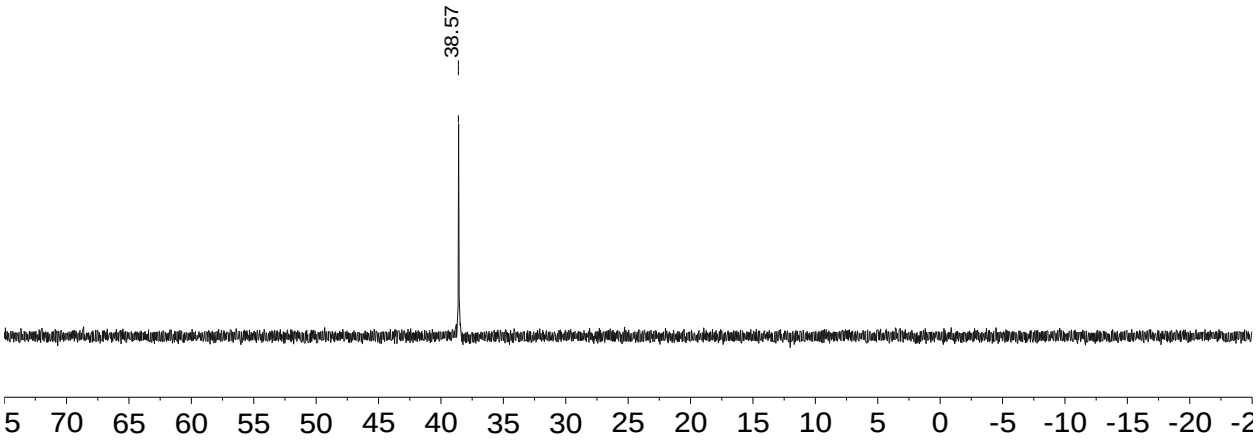

Figure C.81. ^{1}H NMR spectrum of **29a** in C_6D_6. Note: Residual 1,5-cyclooctadiene present.

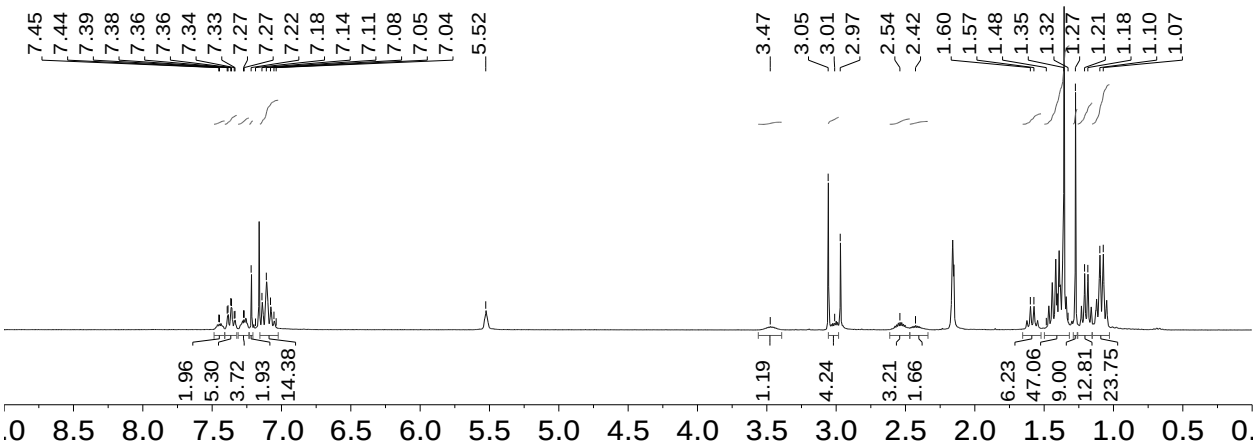

Figure C.82. $^{13}C\{^{1}H\}$ NMR spectrum of **29a** in C_6D_6. Note: Residual 1,5-cycloocta-diene present.

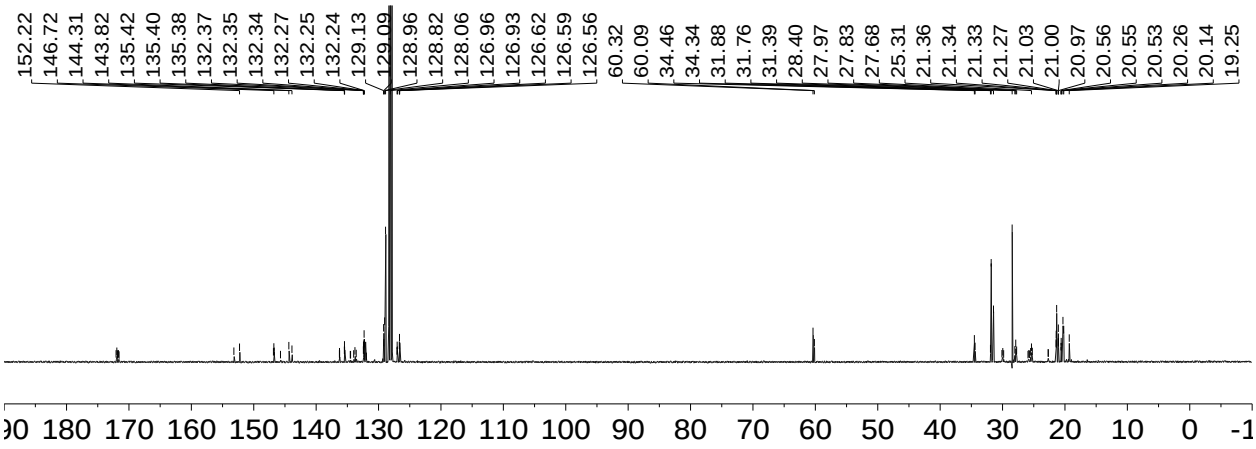

Figure C.83. $^{31}P\{^{1}H\}$ NMR spectrum of **29a** in C_6D_6.

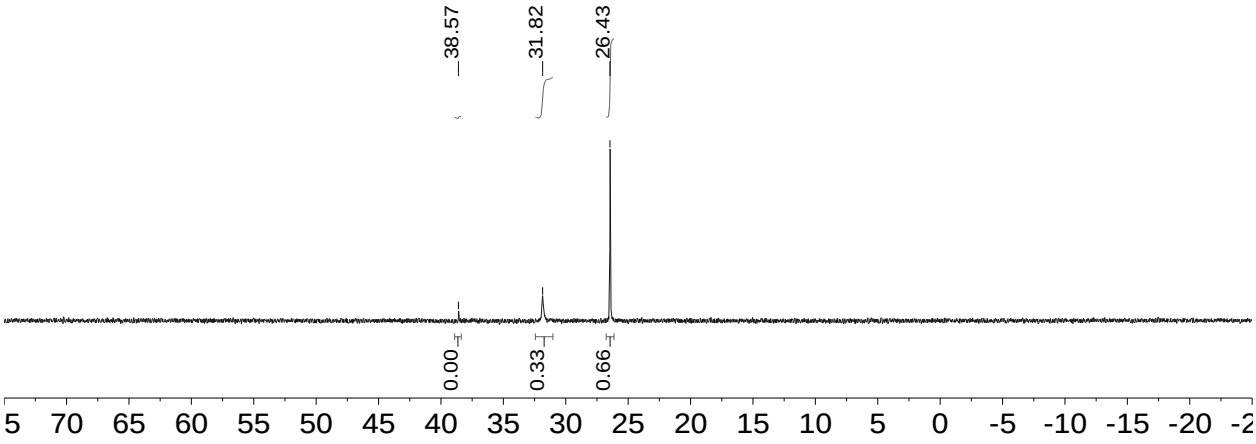

Figure C.84. ^{1}H NMR spectrum of **32a** in C_6D_6. Note: Residual toluene present.

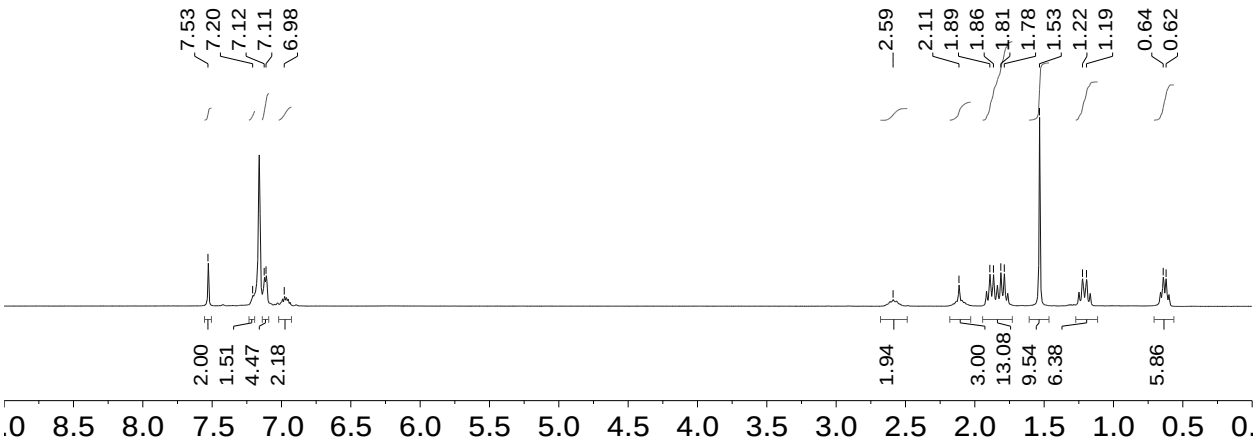

Figure C.85. $^{13}C\{^{1}H\}$ NMR spectrum of **32a** in C_6D_6. Note: Residual toluene present.

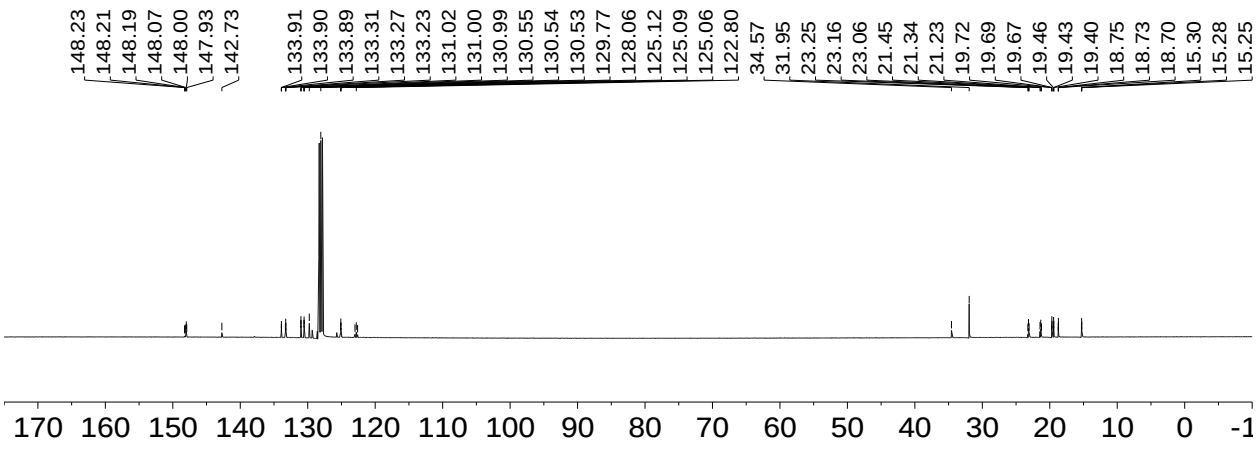

Figure C.86. $^{31}P\{^{1}H\}$ NMR spectrum of **32a** in C_6D_6.

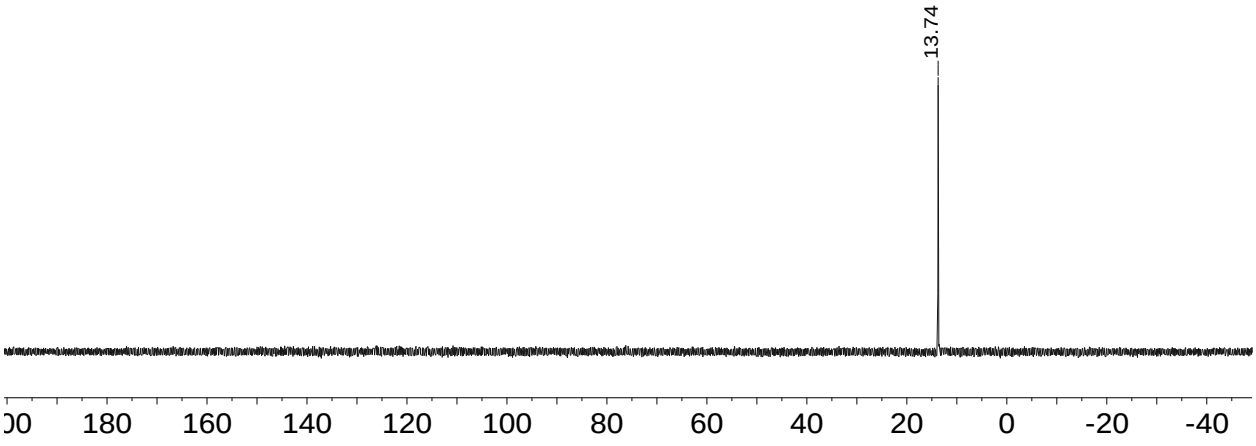

Figure C.87. ^{1}H NMR spectrum of **32b** in C_6D_6.

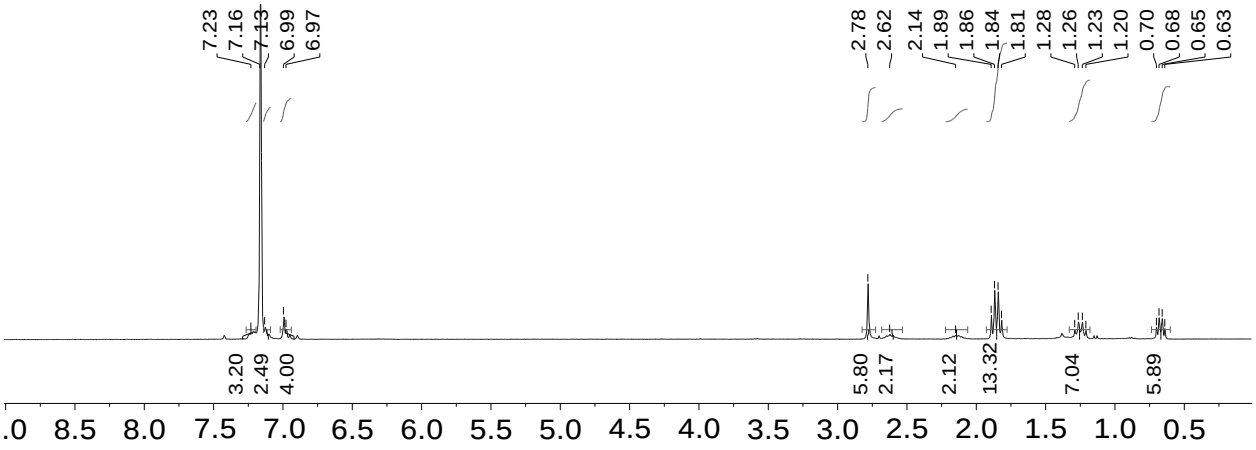

Figure C.88. $^{13}C\{^{1}H\}$ NMR spectrum of **32b** in C_6D_6.

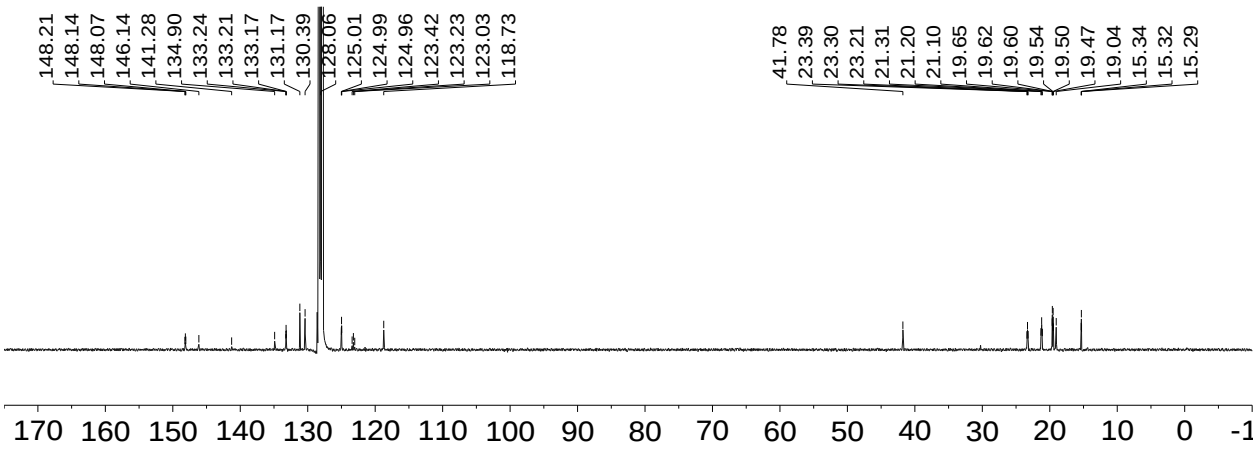

Figure C.89. $^{31}P\{^{1}H\}$ NMR spectrum of **32b** in C_6D_6.

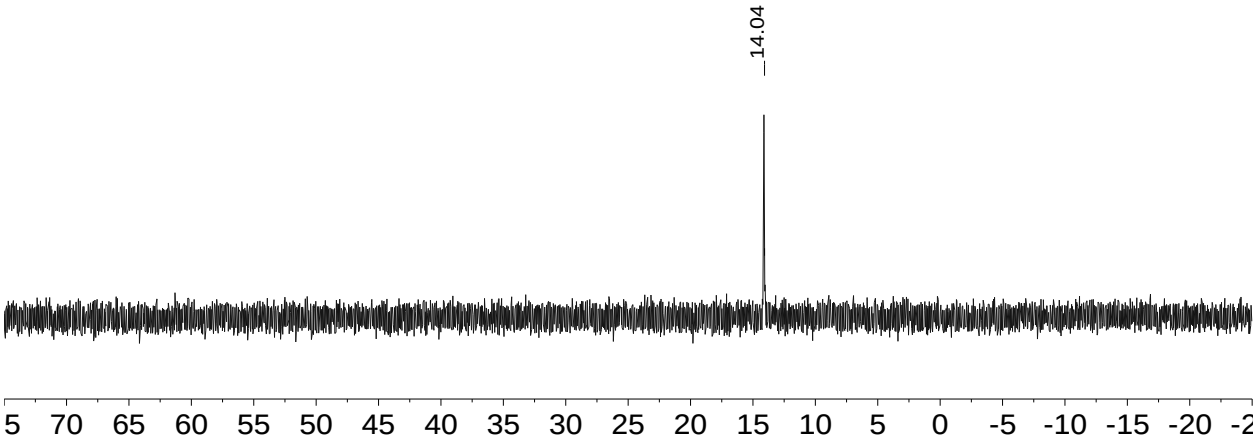

Figure C.90. ^{1}H NMR spectrum of **33a** in C_6D_6.

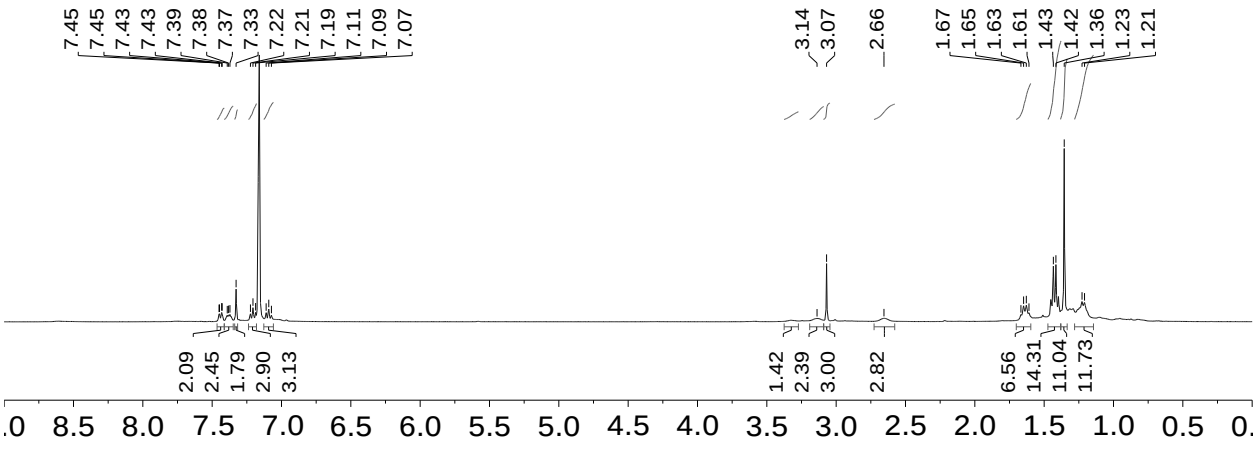

Figure C.91. $^{13}C\{^{1}H\}$ NMR spectrum of **33a** in C_6D_6.

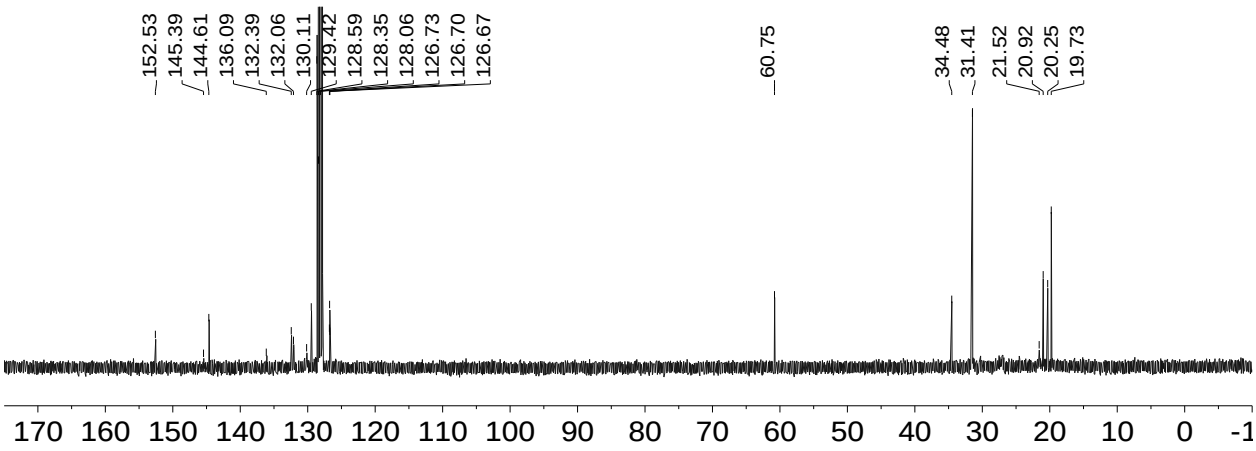

Figure C.92. $^{31}P\{^{1}H\}$ NMR spectrum of **33a** in C_6D_6.

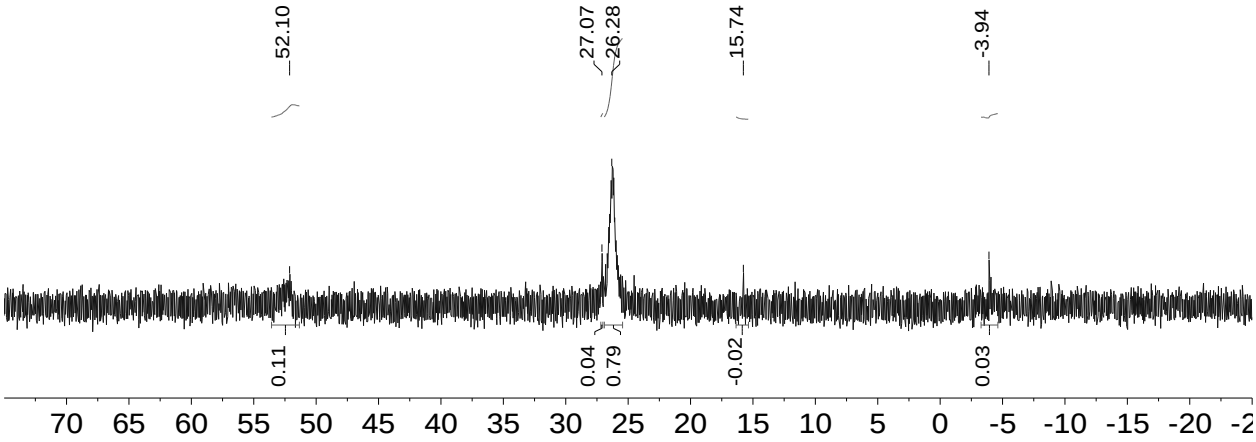

Figure C.93. ^{1}H NMR spectrum of **34a** in CD_3CN.

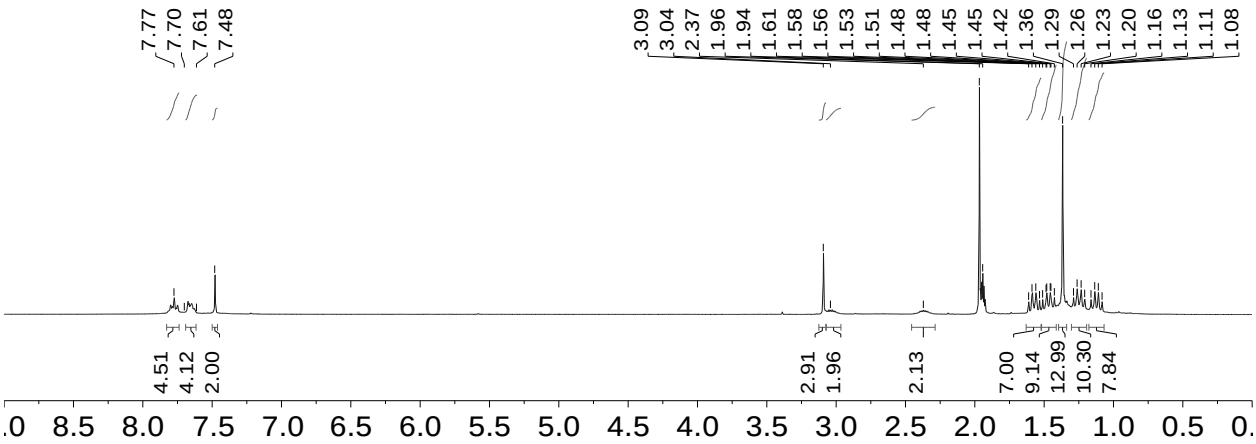

Figure C.94. $^{13}C\{^{1}H\}$ NMR spectrum of **34a** in CD_3CN.

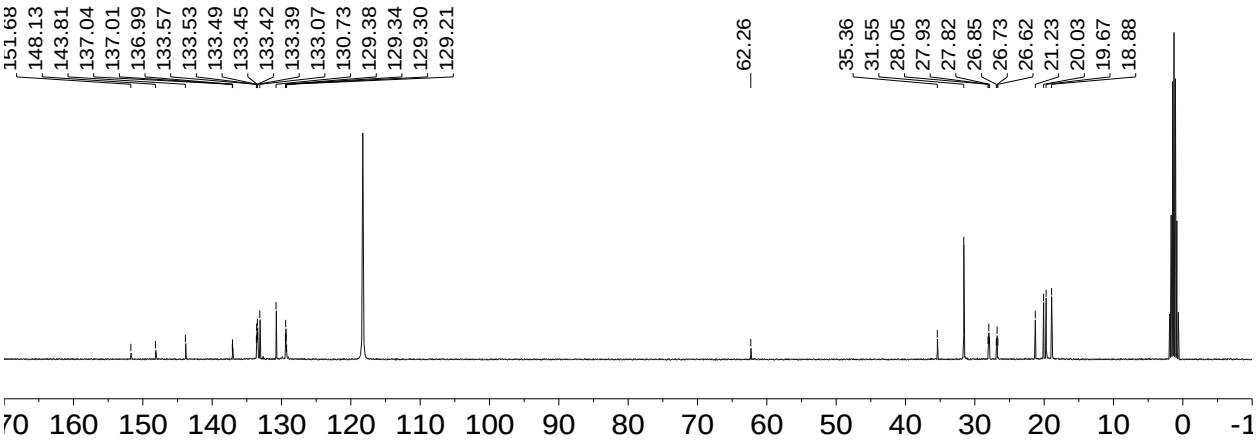

Figure C.95. ^{19}F NMR spectrum of **34a** in CD_3CN.

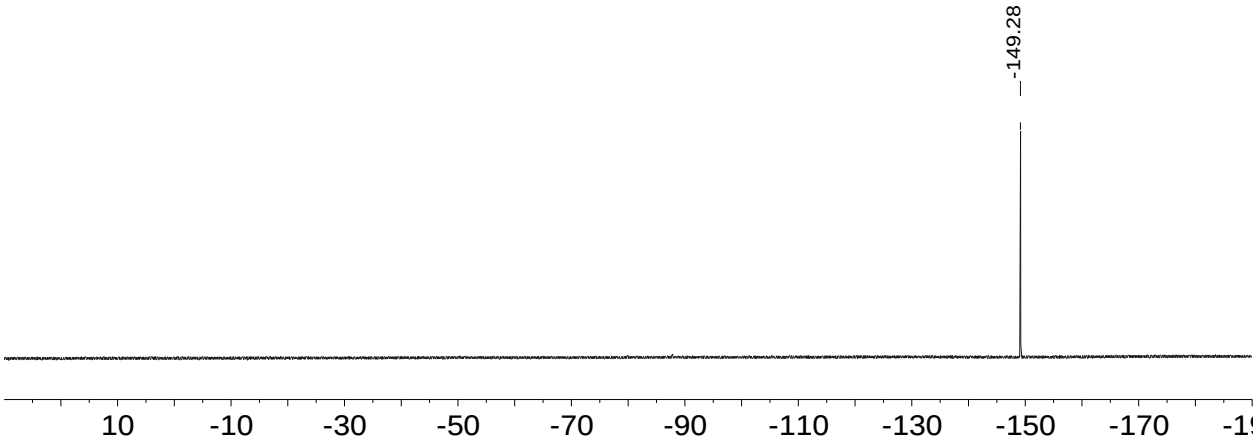

Figure C.96. $^{31}P\{^{1}H\}$ NMR spectrum of **34a** in CD_3CN.

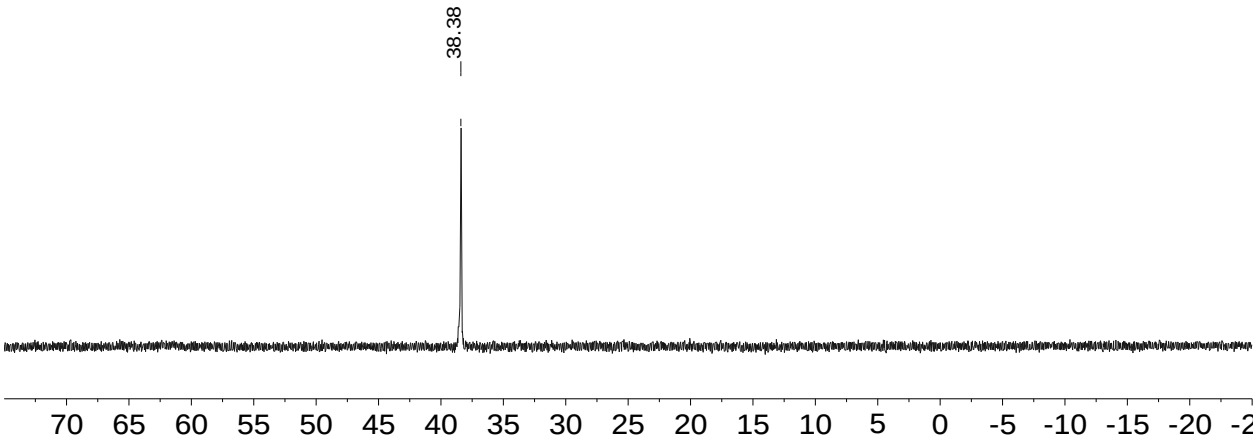

Figure C.97. ^{1}H NMR spectrum of **35a** in C_6D_6.

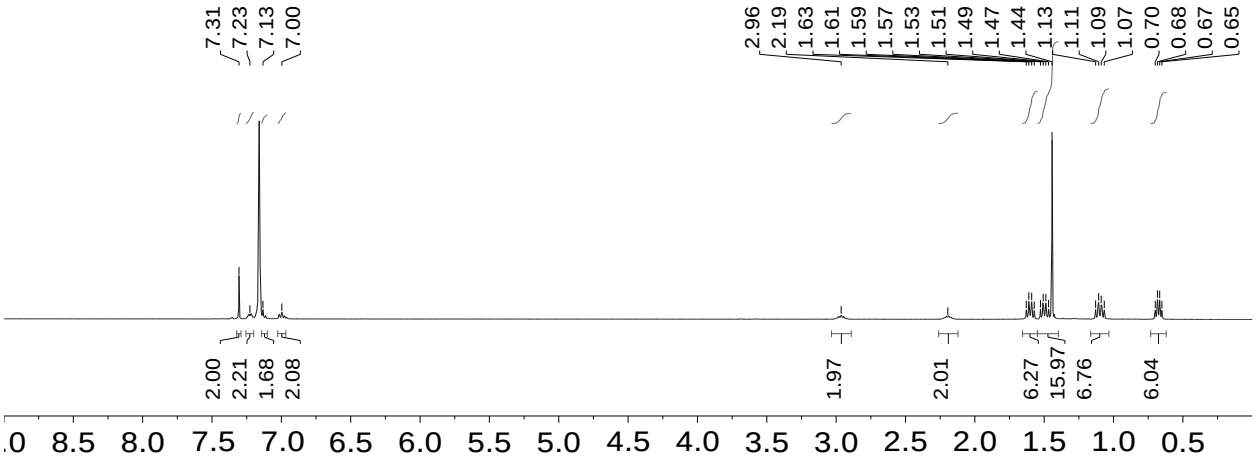

Figure C.98. $^{13}C\{^{1}H\}$ NMR spectrum of **35a** in C_6D_6.

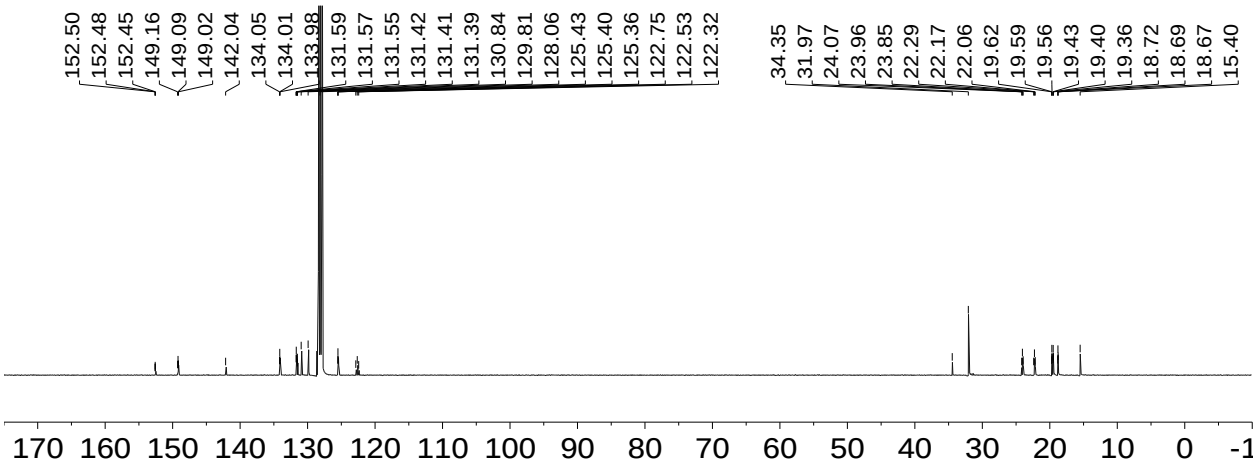

Figure C.99. $^{31}P\{^{1}H\}$ NMR spectrum of **35a** in C_6D_6.

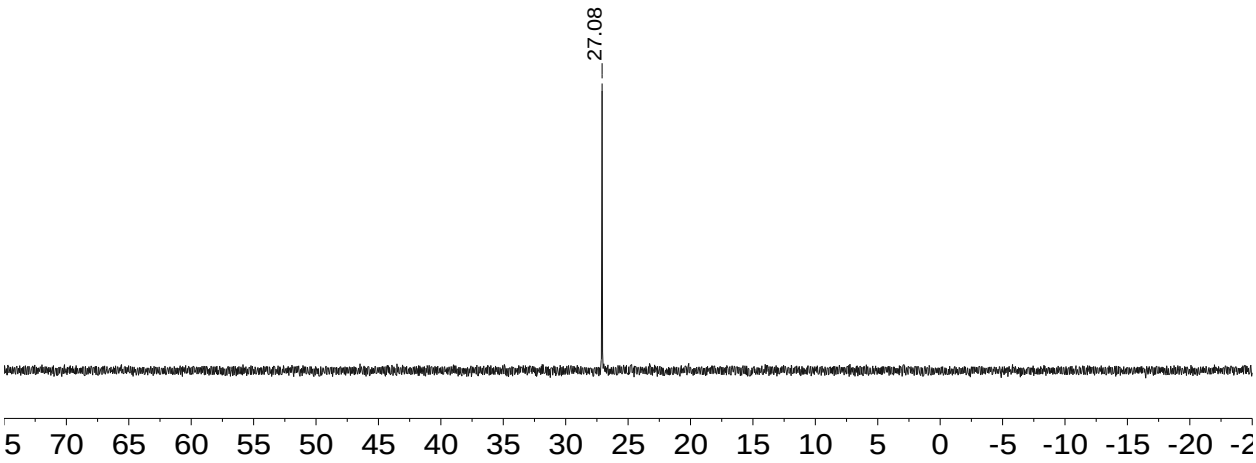

Figure C.100. ^{1}H NMR spectrum of **36a** in C_6D_6.

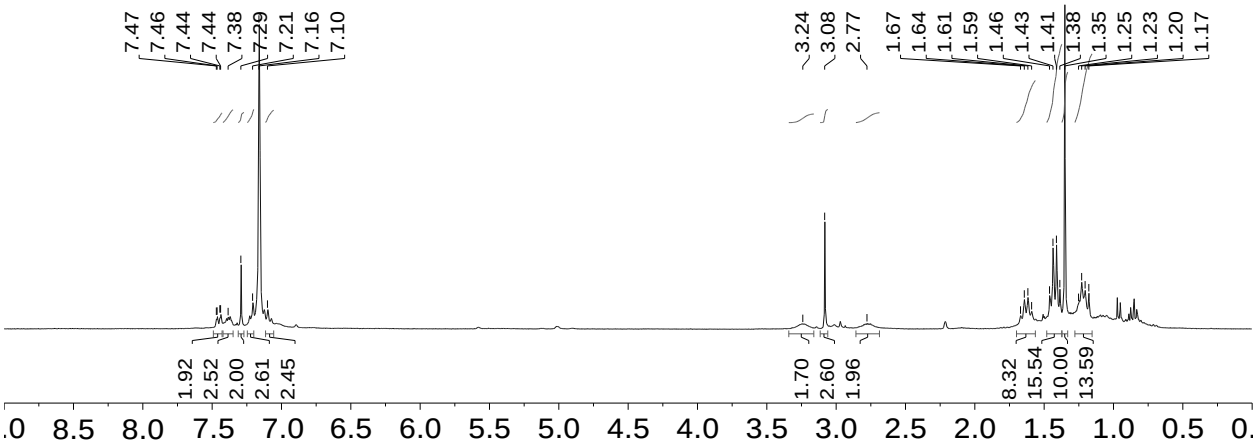

Figure C.101. $^{13}C\{^{1}H\}$ NMR spectrum of **36a** in C_6D_6.

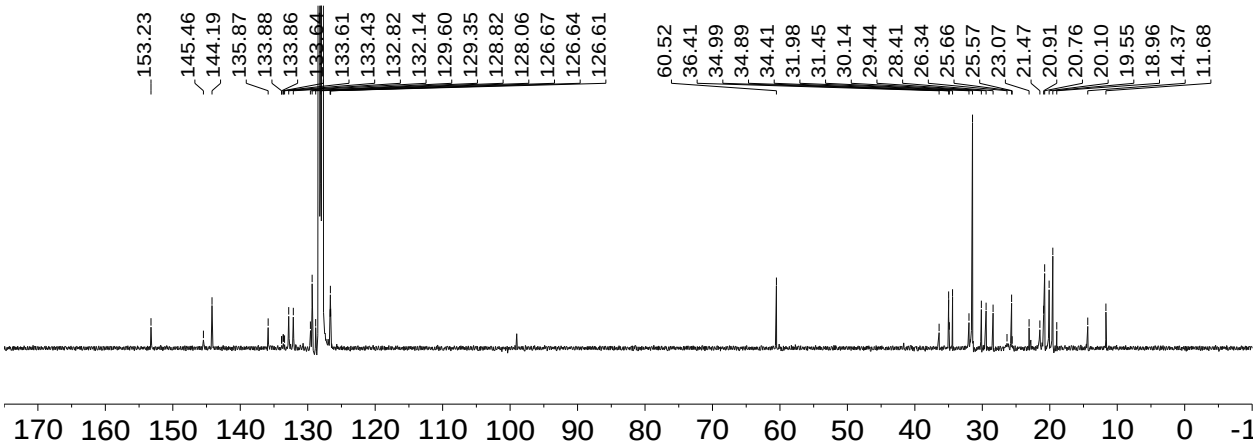

Figure C.102. $^{31}P\{^{1}H\}$ NMR spectrum of **36a** in C_6D_6.

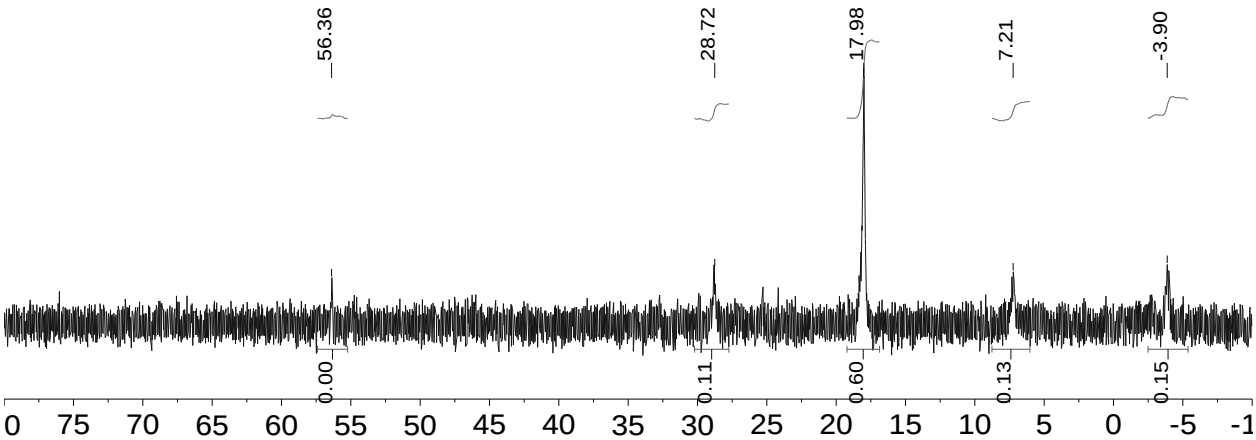

Figure C.103. ^{1}H NMR spectrum of **37a** in C_6D_6.

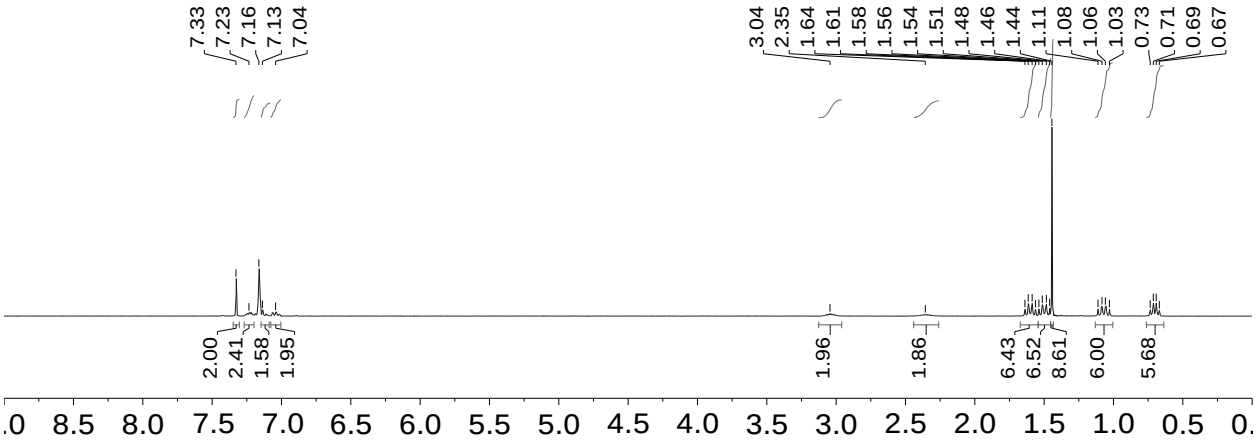

Figure C.104. $^{13}C\{^{1}H\}$ NMR spectrum of **37a** in C_6D_6.

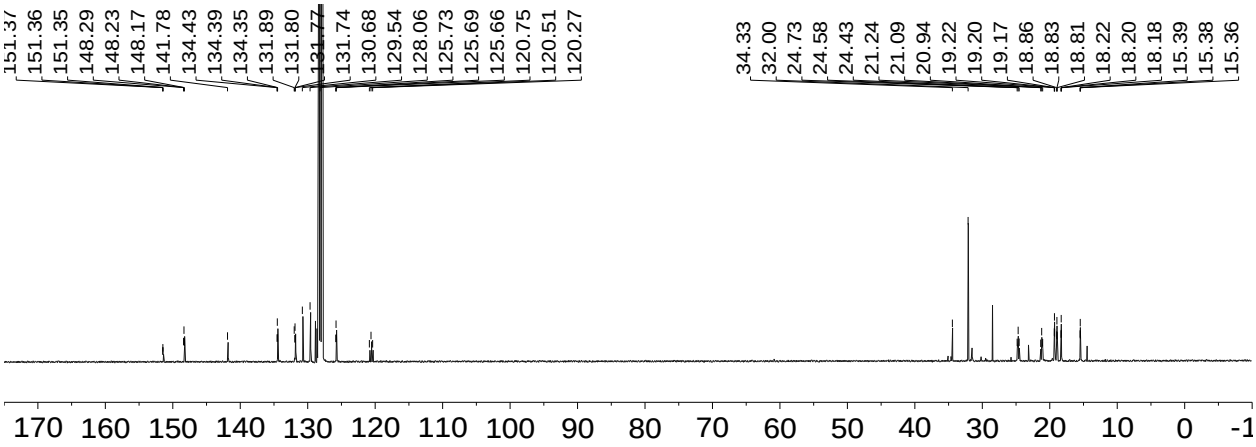

Figure C.105. $^{31}P\{^{1}H\}$ NMR spectrum of **37a** in C_6D_6.

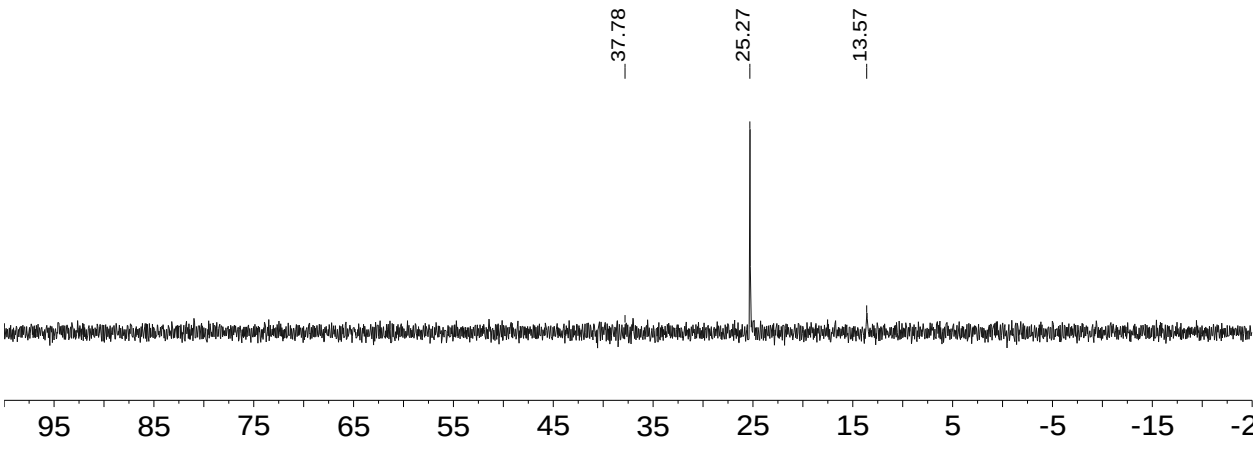

Figure C.106. ^{1}H NMR spectrum of **38a** in C_6D_6.

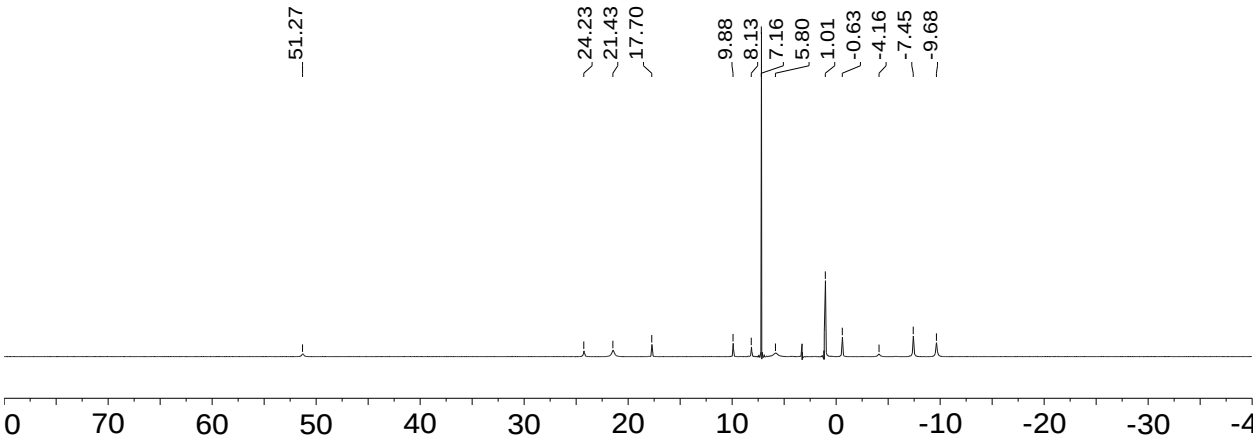

Figure C.107. ^{1}H NMR spectrum of **46** in $CDCl_3$.

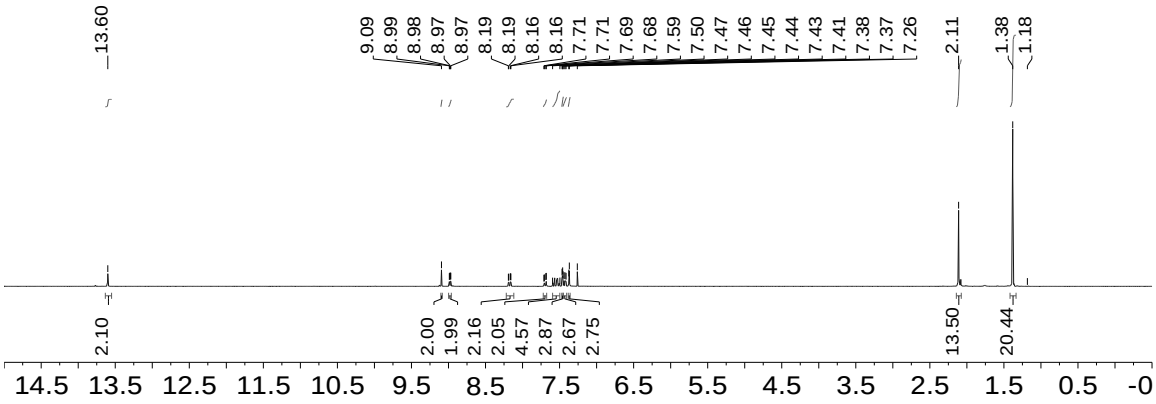

Figure C.108. ^{1}H NMR spectrum of **46** in C_6D_6.

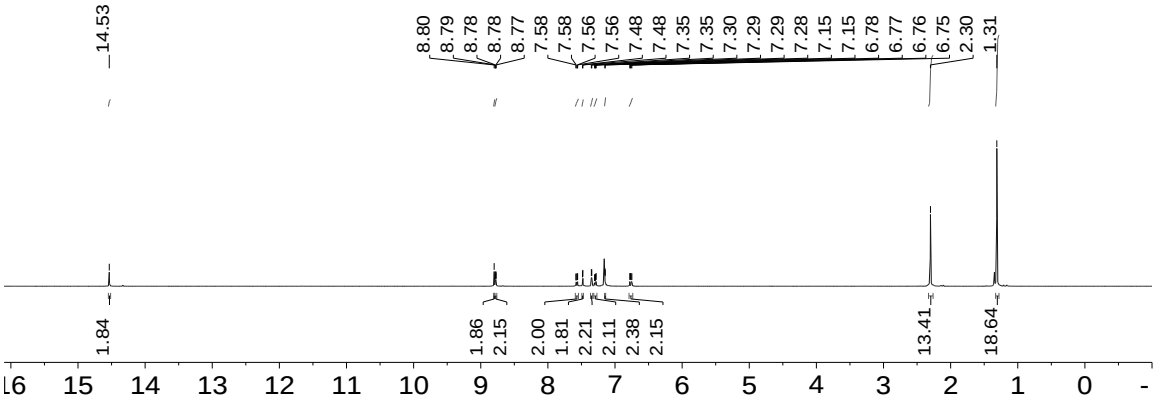

Figure C.109. $^{13}C\{^{1}H\}$ NMR spectrum of **46** in C_6D_6.

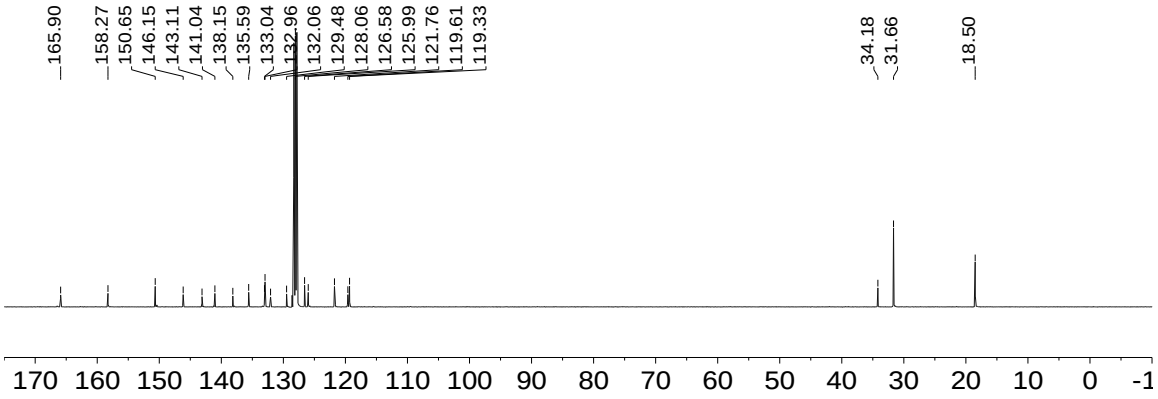

Figure C.110. ^{1}H NMR spectrum of **44** in $CDCl_3$.

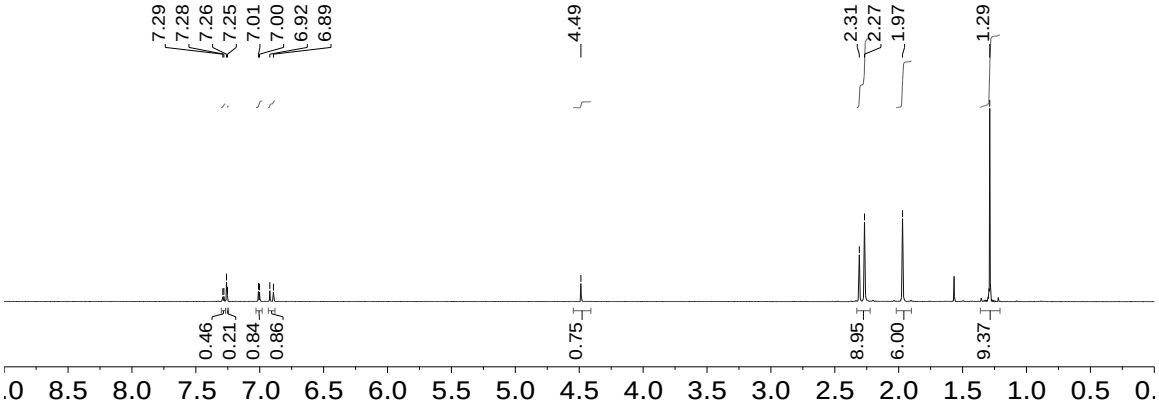

Figure C.111. ^{1}H NMR spectrum of **45** in $CDCl_3$.

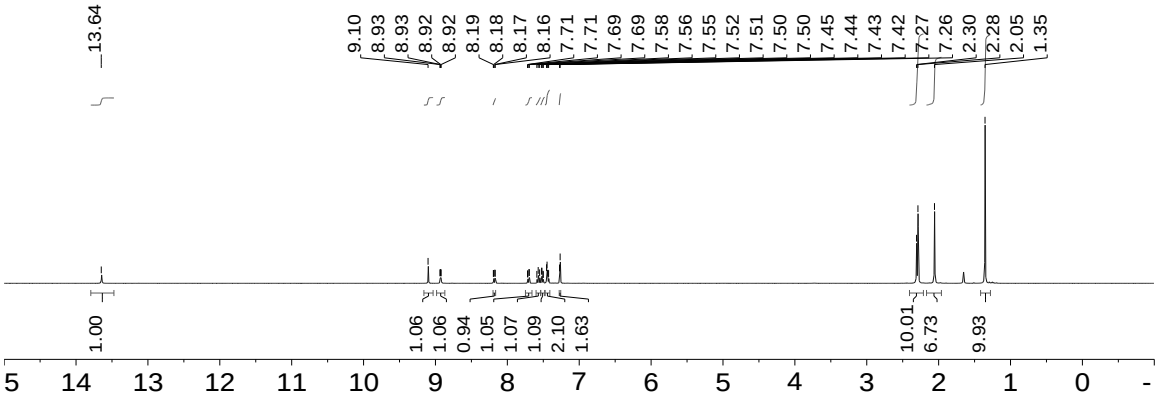

Figure C.112. $^{13}C\{^{1}H\}$ NMR spectrum of **45** in $CDCl_3$.

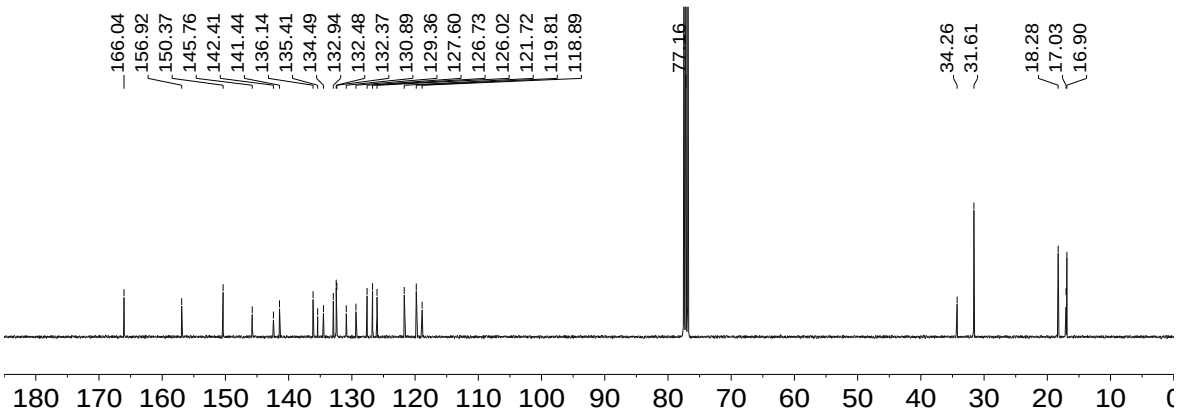

Figure C.113. ^{1}H NMR spectrum of **57** in CD_2Cl_2.

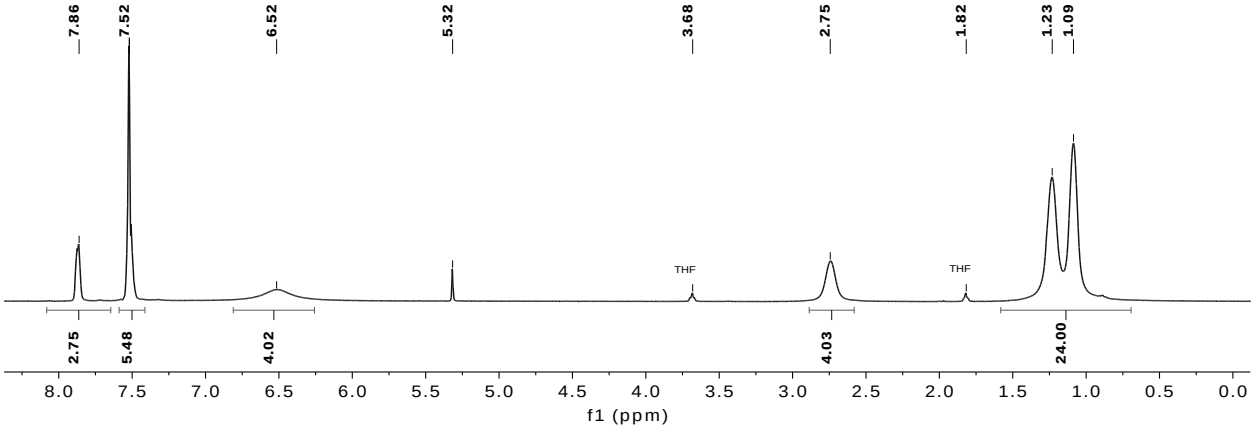

Figure C.114. $^{31}P\{^{1}H\}$ NMR spectrum of **57** in CD_2Cl_2.

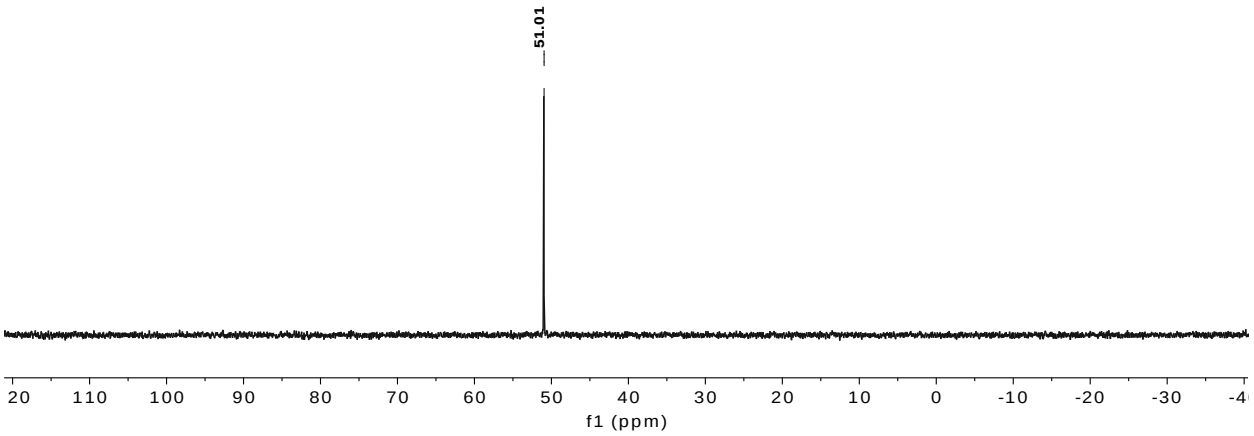

Figure C.115. $^{13}C\{^{1}H\}$ NMR spectrum of **57** in CD_2Cl_2.

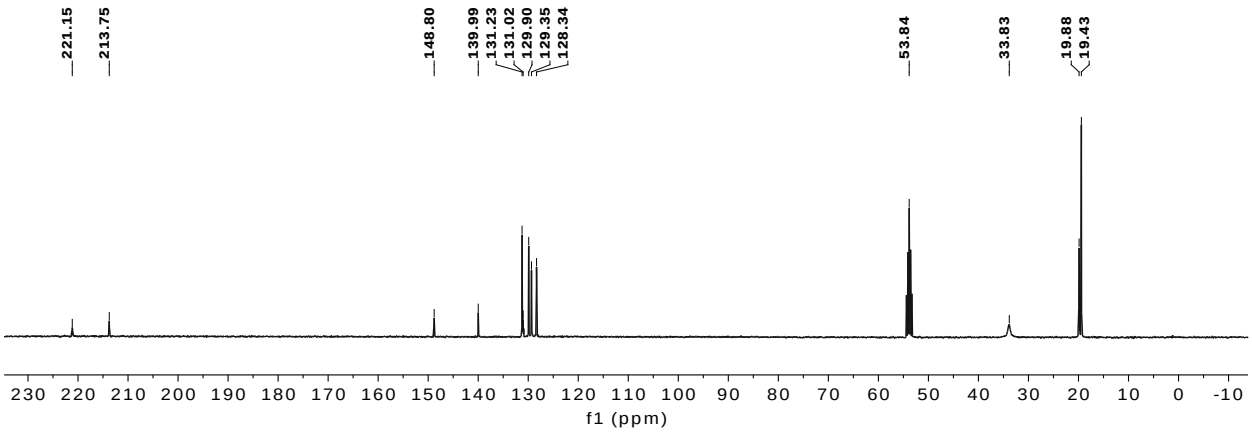

Figure C.116. ^{1}H NMR spectrum of **58** in CD_3CN.

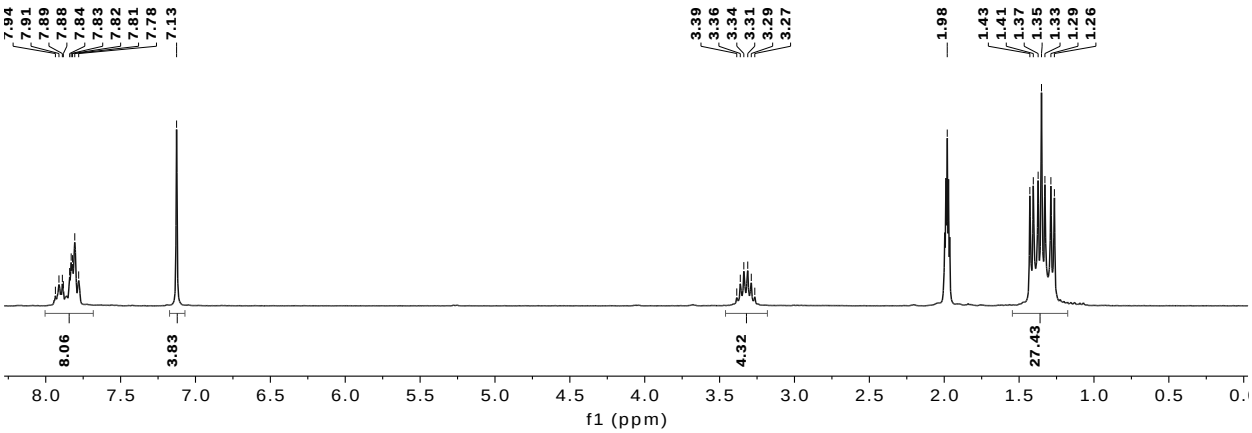

Figure C.117. $^{31}P\{^{1}H\}$ NMR spectrum of **58** in CD_3CN.

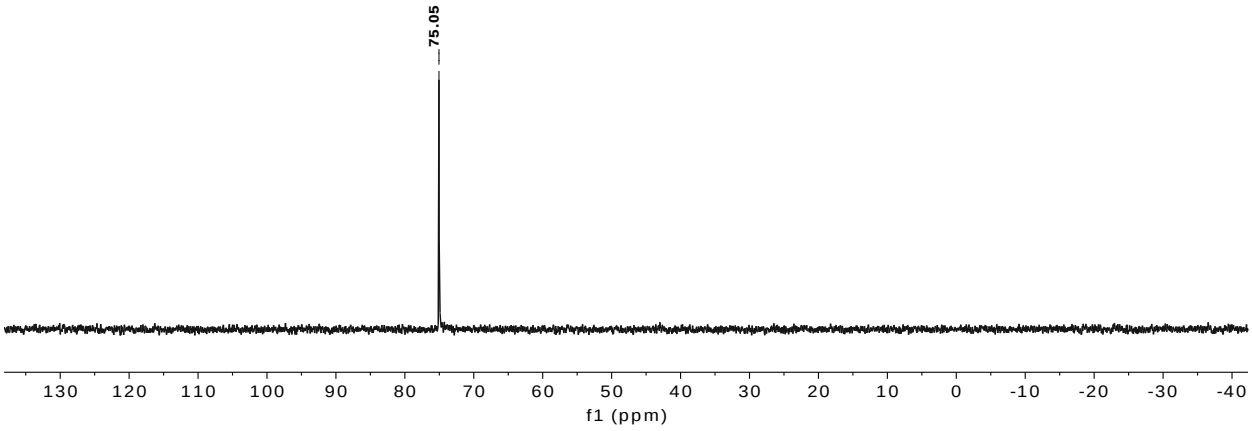

Figure C.118. $^{13}C\{^{1}H\}$ NMR spectrum of **58** in CD_3CN.

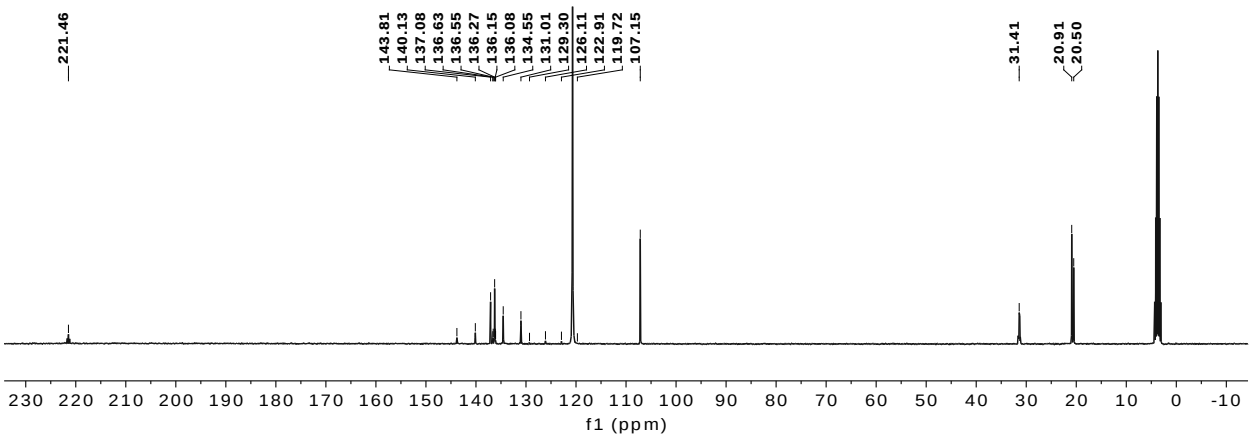

Figure C.119. ^{1}H NMR spectrum of **59** in CD_3CN.

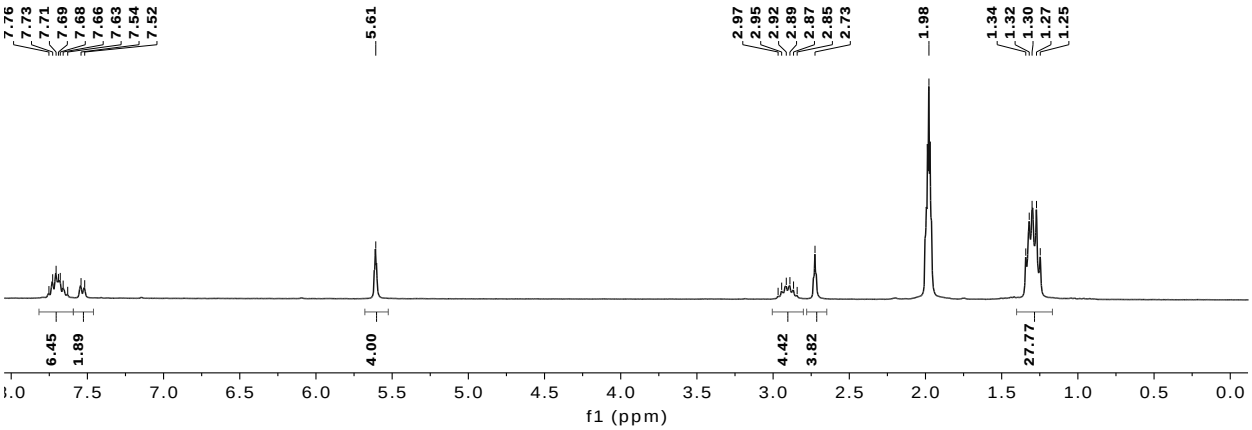

Figure C.120. $^{31}P\{^{1}H\}$ NMR spectrum of **59** in CD_3CN.

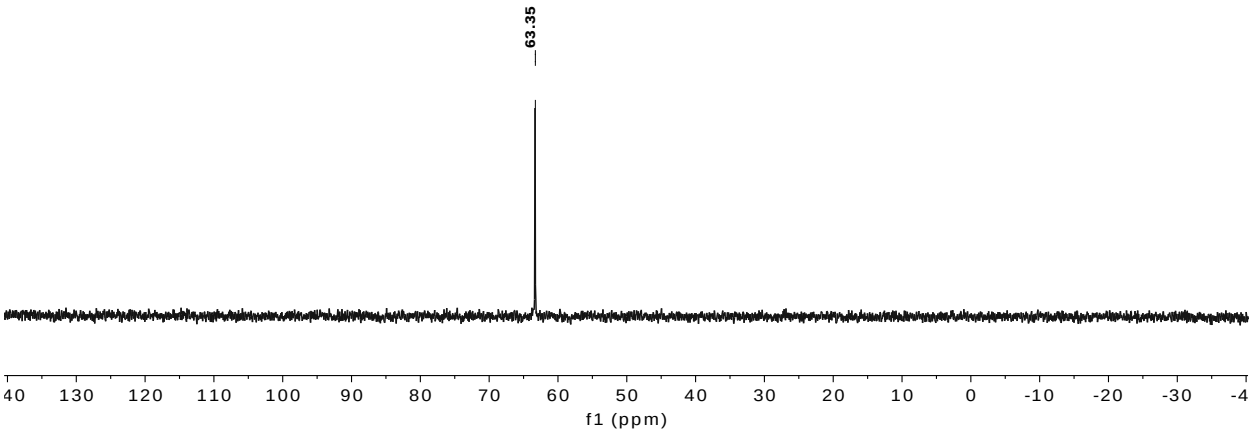

Figure C.121. $^{13}C\{^{1}H\}$ NMR spectrum of **59** in CD_3CN.

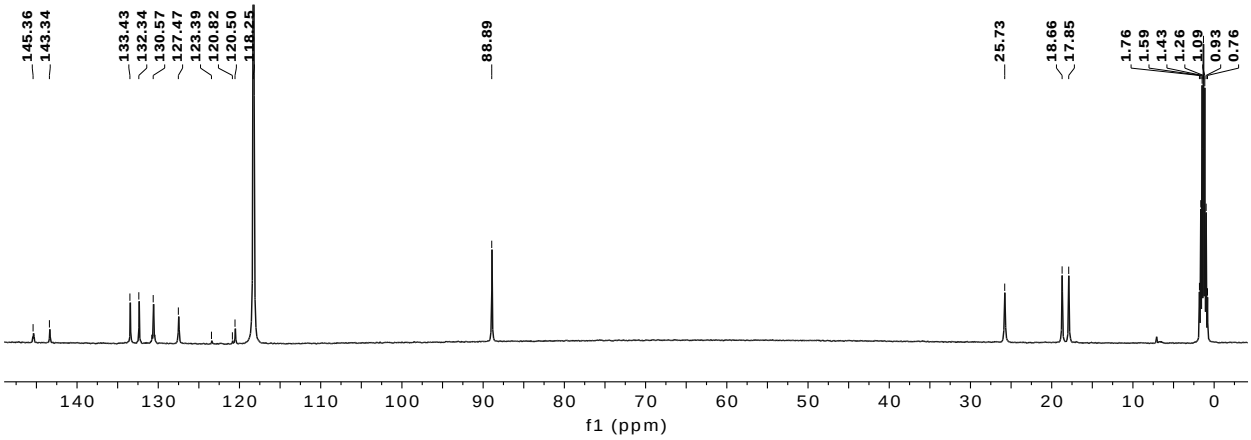

Figure C.122. ^{1}H NMR spectrum of **60** in C_6D_6.

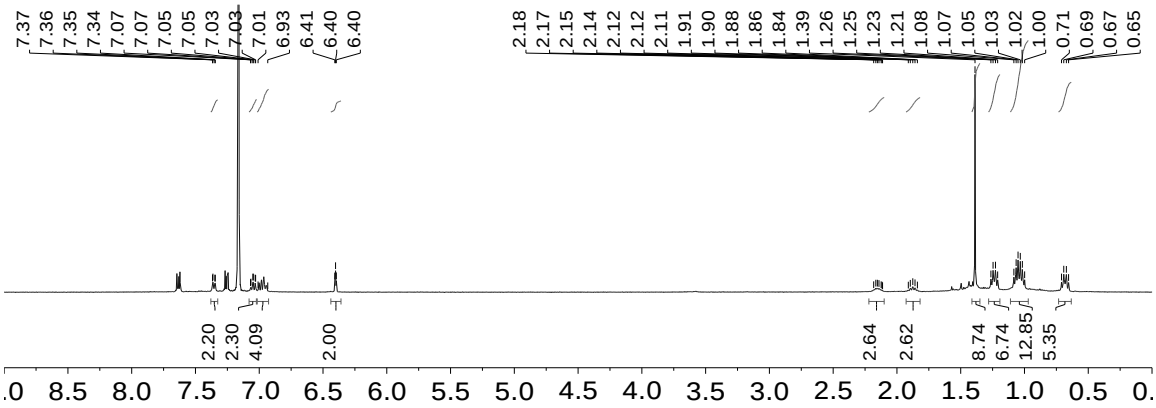

Figure C.123. $^{13}C\{^{1}H\}$ NMR spectrum of **60** in C_6D_6.

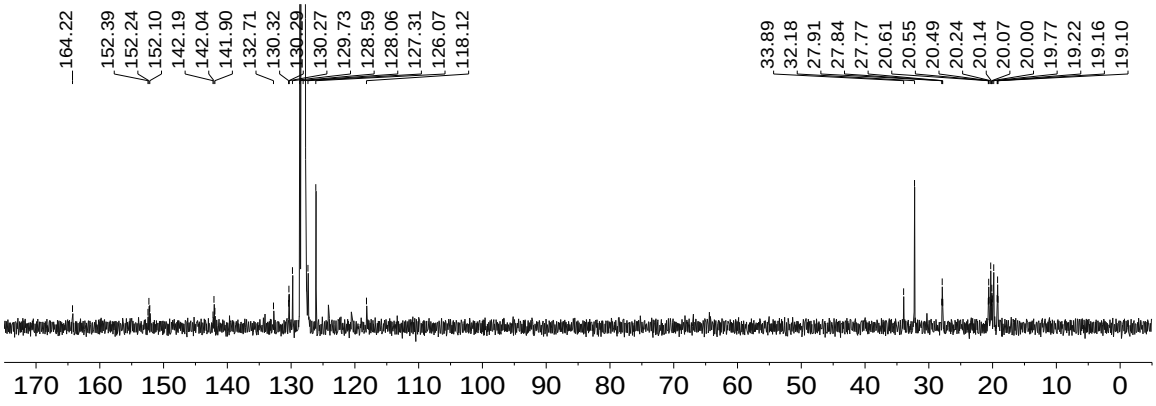

Figure C.124. $^{31}P\{^{1}H\}$ NMR spectrum of **60** in C_6D_6.

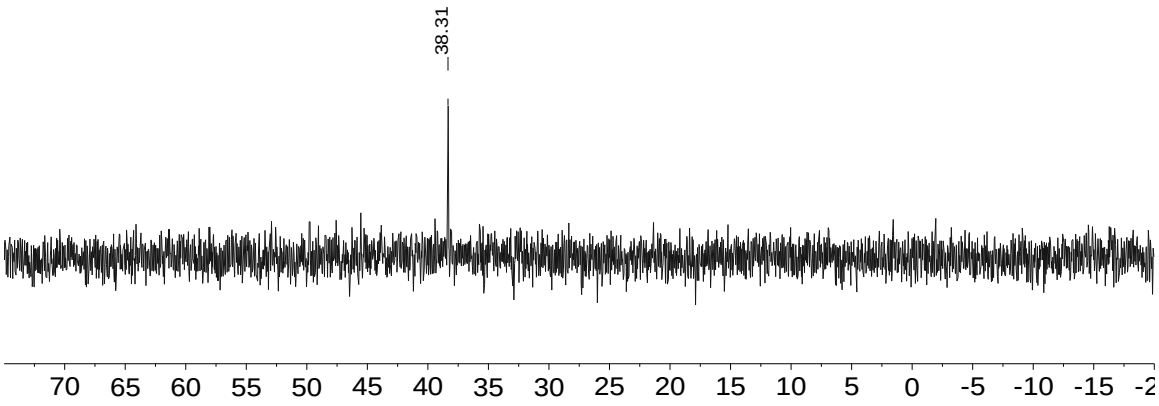

Figure C.125. ^{1}H NMR spectrum of **62** in C_6D_6.

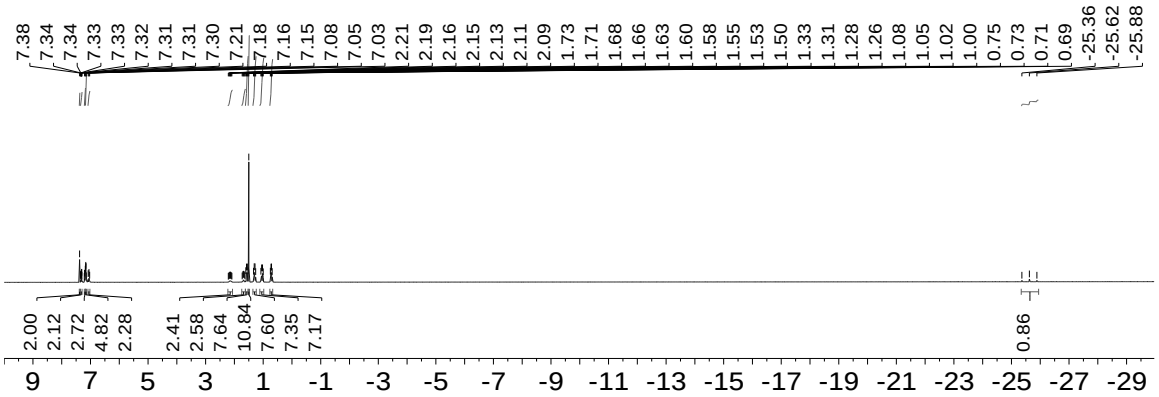

Figure C.126. $^{13}C\{^{1}H\}$ NMR spectrum of **62** in C_6D_6.

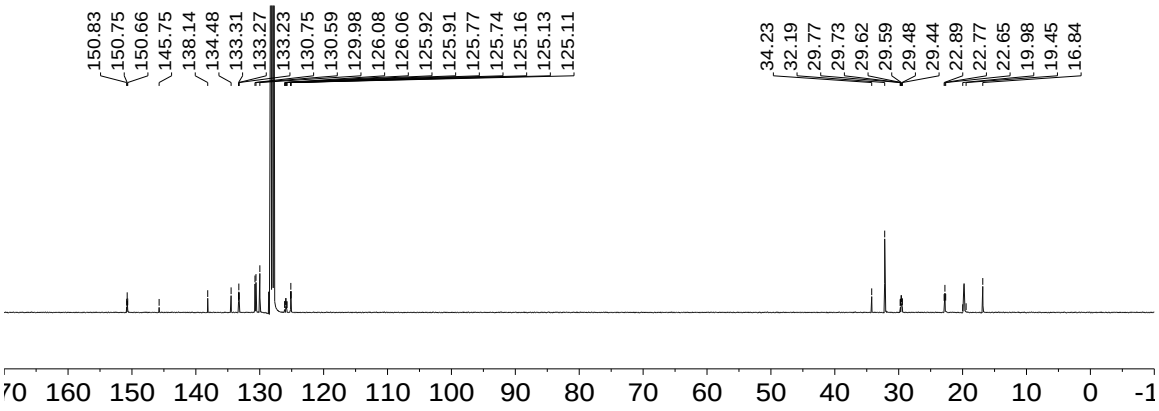

Figure C.127. $^{31}P\{^{1}H\}$ NMR spectrum of **62** in C_6D_6.

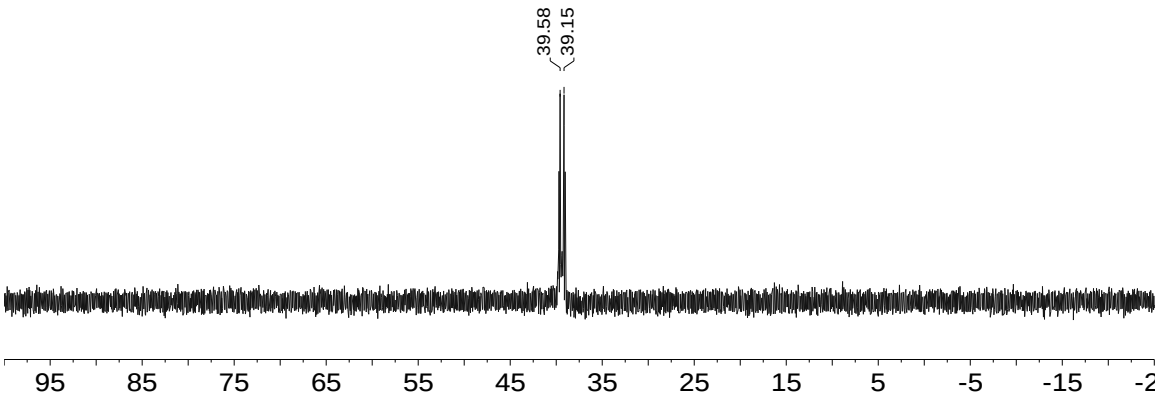

Figure C.128. ^{1}H NMR spectrum of 1-(2'-diisopropylphosphino)phenyl-2-methoxymethoxy-3,5-di-tert-butylbenzene in C_6D_6.

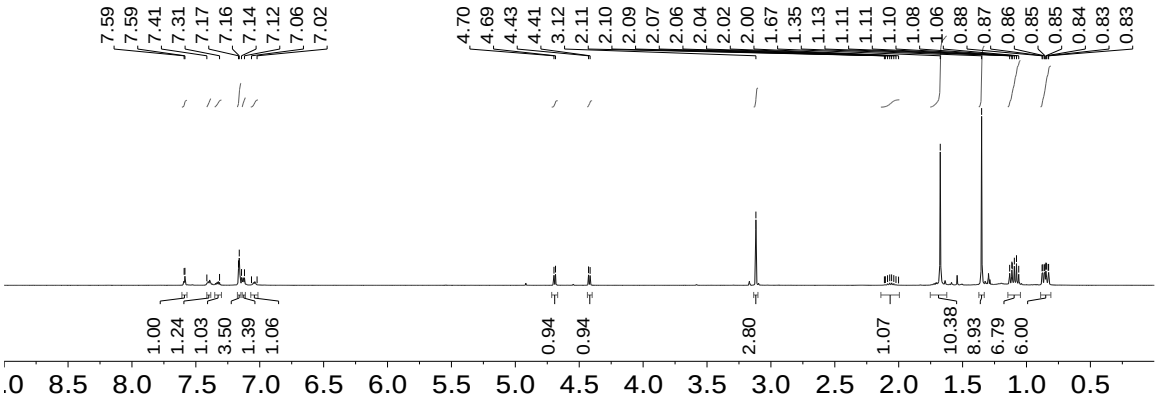

Figure C.129. $^{13}C\{^{1}H\}$ NMR spectrum of 1-(2'-diisopropylphosphino)phenyl-2-methoxymethoxy-3,5-di-tert-butylbenzene in C_6D_6.

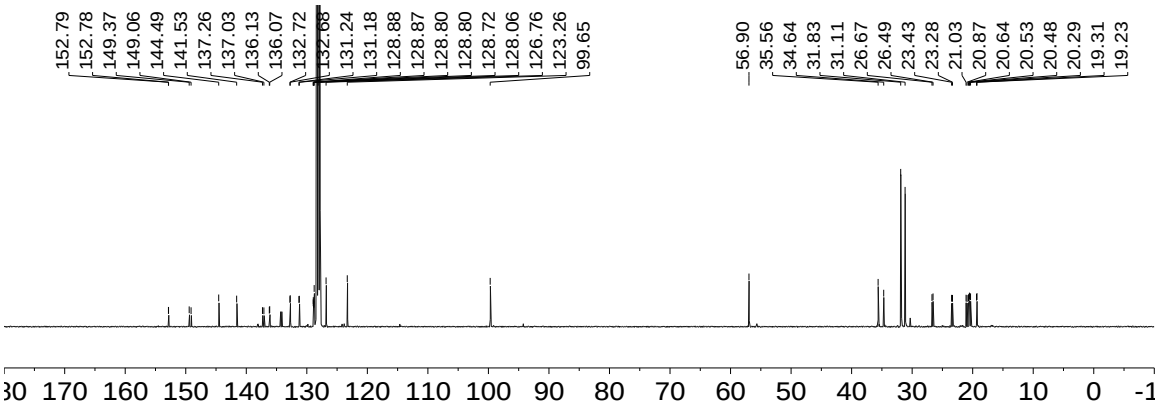

Figure C.130. $^{31}P\{^{1}H\}$ NMR spectrum of 1-(2'-diisopropylphosphino)phenyl-2-methoxymethoxy-3,5-di-tert-butylbenzene in C_6D_6.

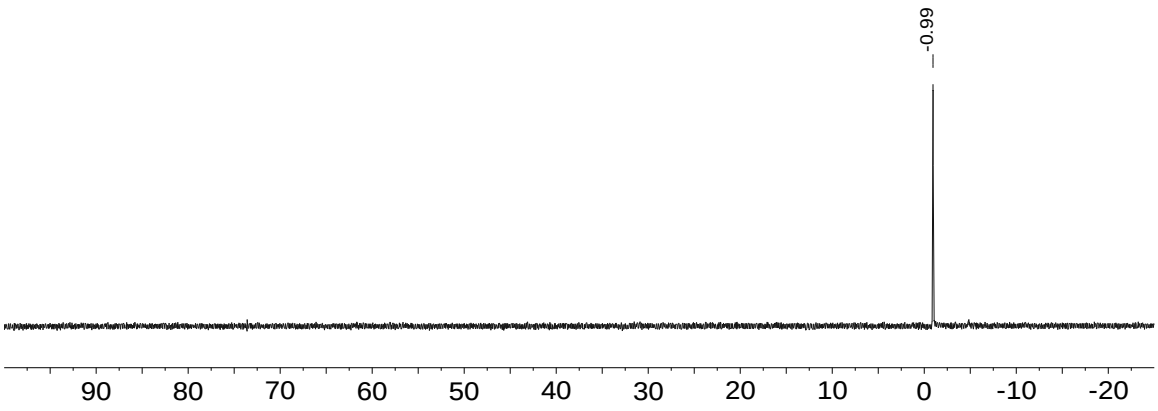

Figure C.131. ^{1}H NMR spectrum of **65** in C_6D_6.

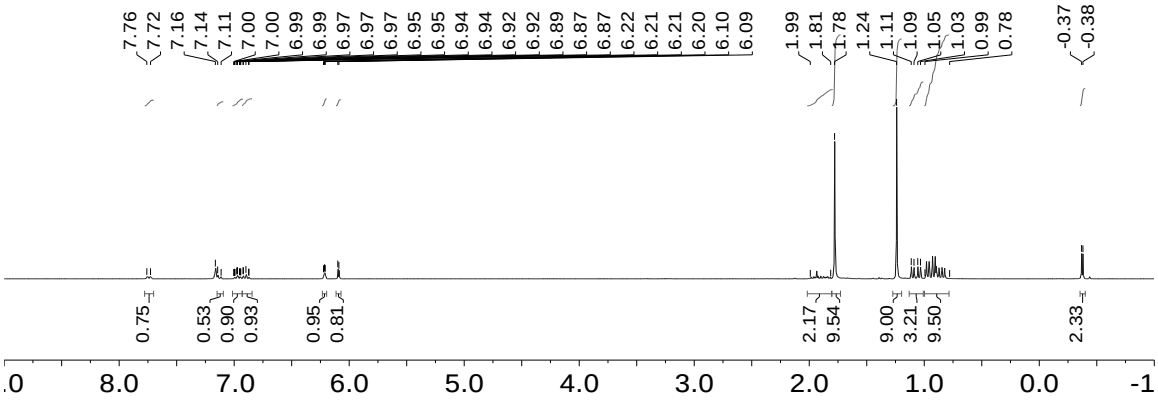

Figure C.132. $^{13}C\{^{1}H\}$ NMR spectrum of **65** in C_6D_6.

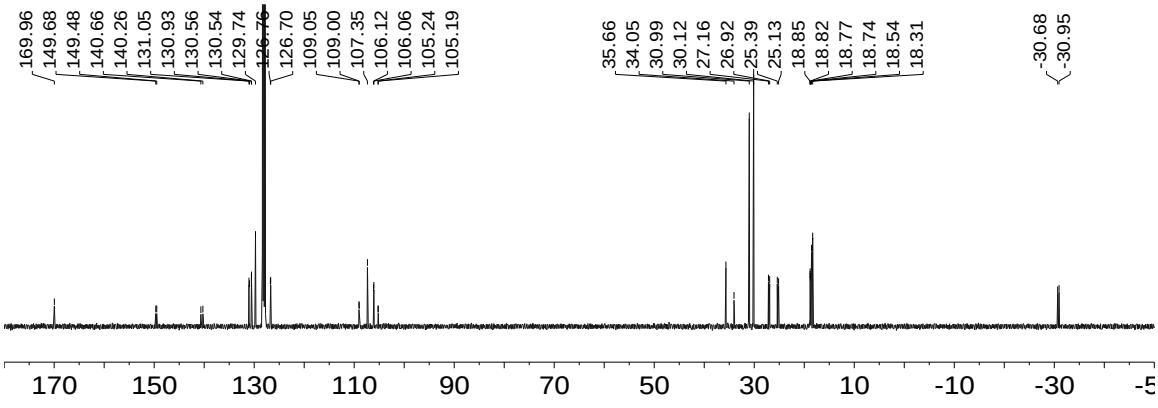

Figure C.133. $^{31}P\{^{1}H\}$ NMR spectrum of **65** in C_6D_6.

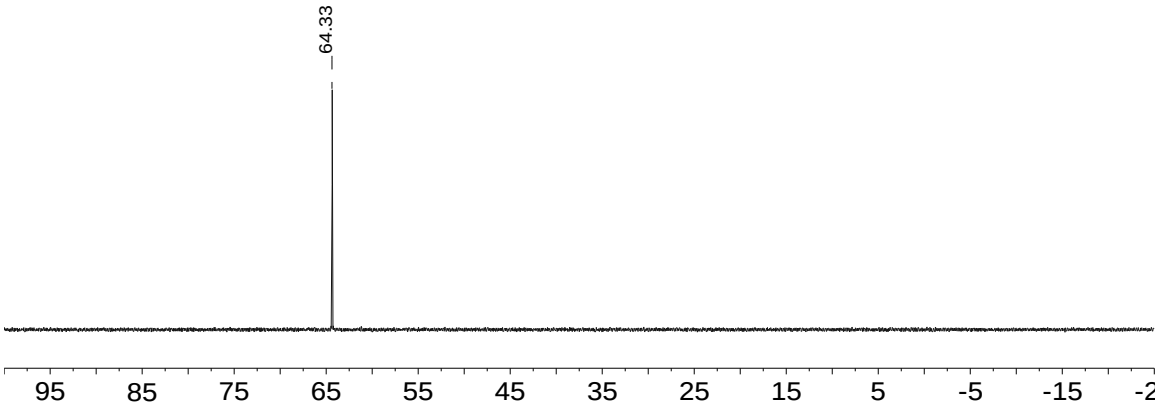

Figure C.134. ^{1}H NMR spectrum of **66** in C_6D_6. Note: Residual tetrahydrofuran present.

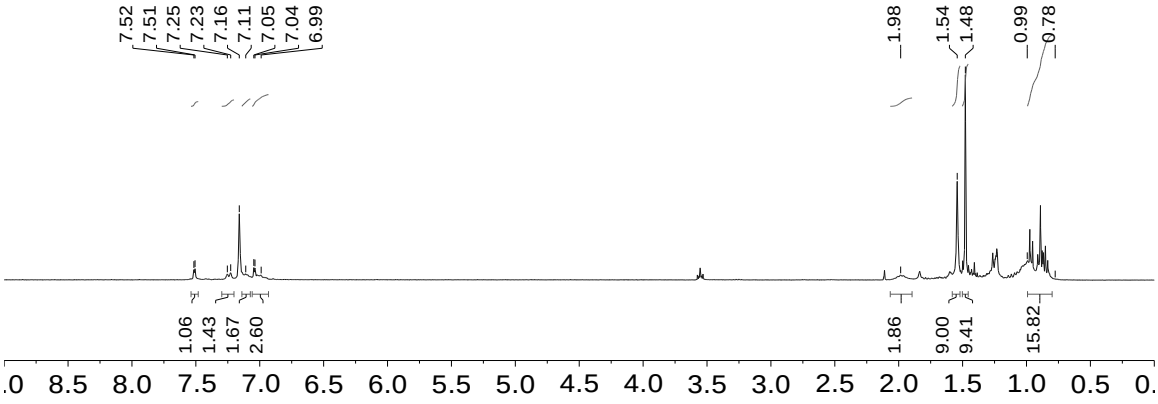

Figure C.135. $^{31}P\{^{1}H\}$ NMR spectrum of **66** in C_6D_6.

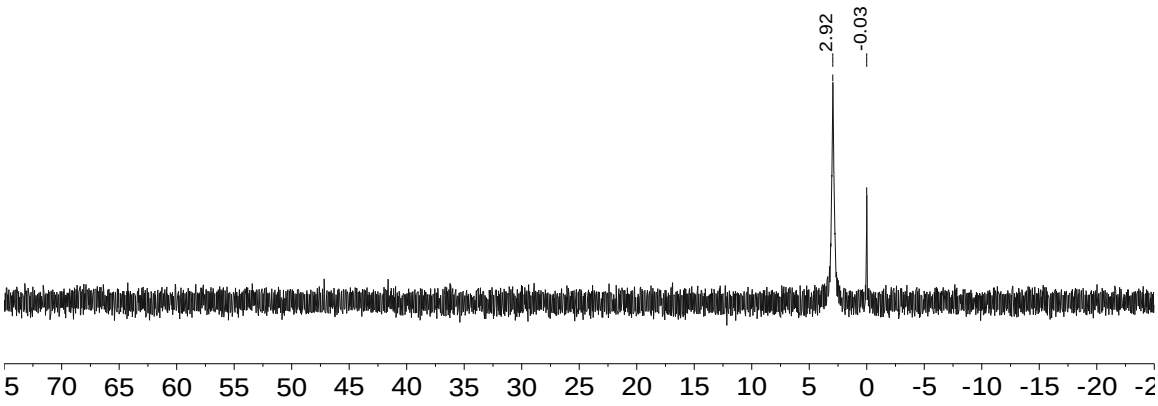

Figure C.136. ^{1}H NMR spectrum of **68** in $CDCl_3$. Note: Residual Et_2O and acetone present.

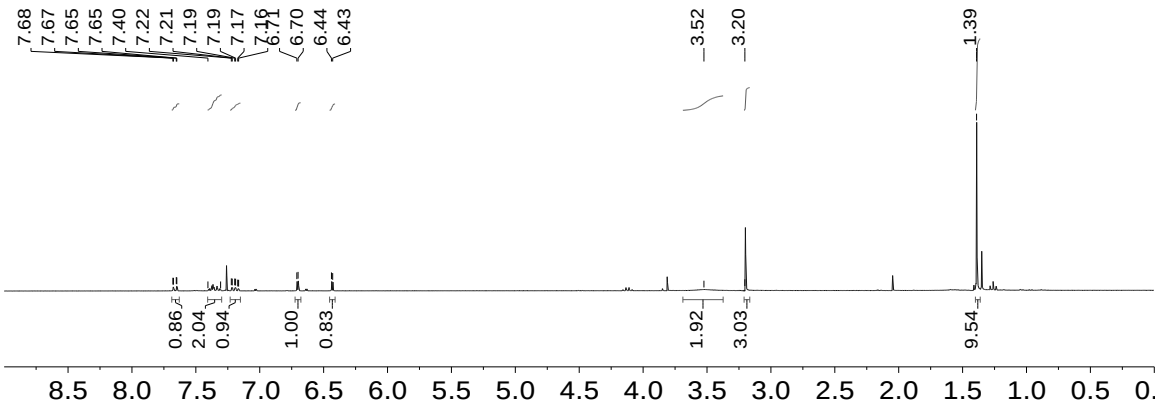

Figure C.137. ^{1}H NMR spectrum of **69** in $CDCl_3$.

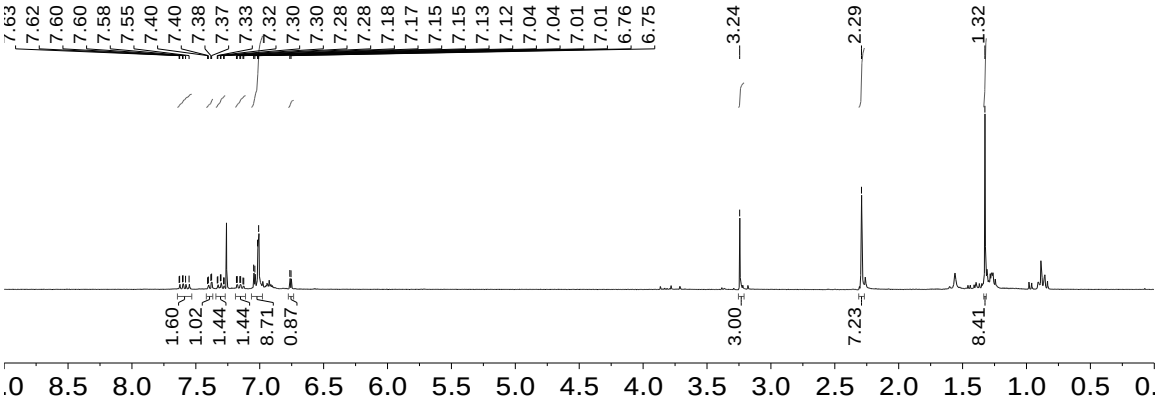

Figure C.138. ^{1}H NMR spectrum of **69** in C_6D_6.

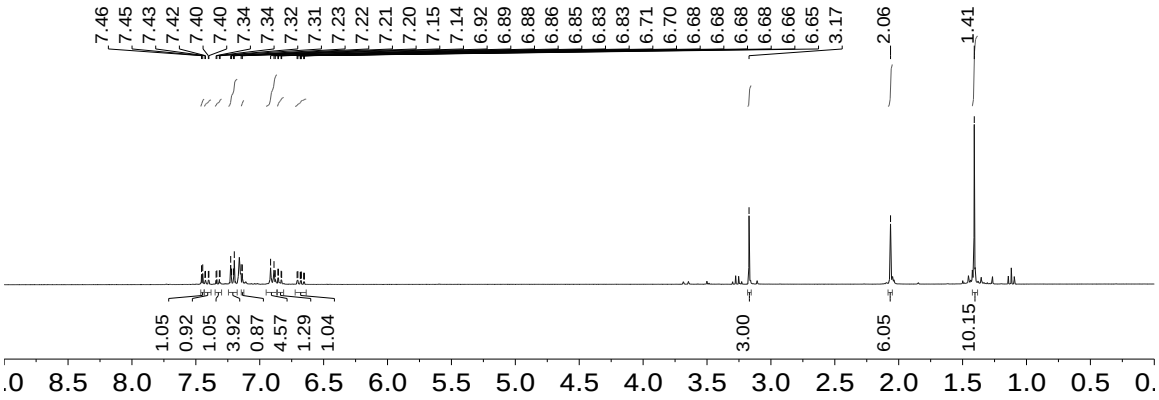

Figure C.139. ^{1}H NMR spectrum of **70** in C_6D_6. Note: Residual $(^{i}Pr)_2PCl$ present.

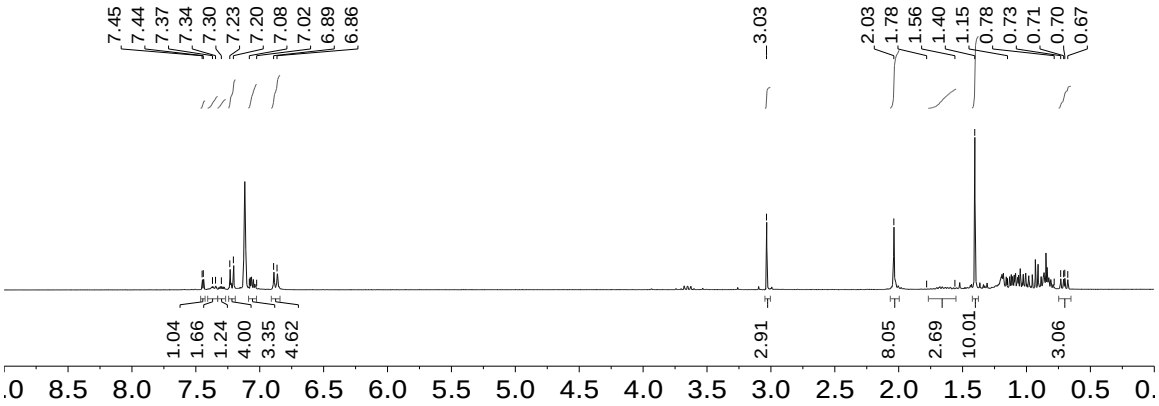

Figure C.140. $^{31}P\{^{1}H\}$ NMR spectrum of **70** in C_6D_6. Note: Residual $(^{i}Pr)_2PCl$ present.

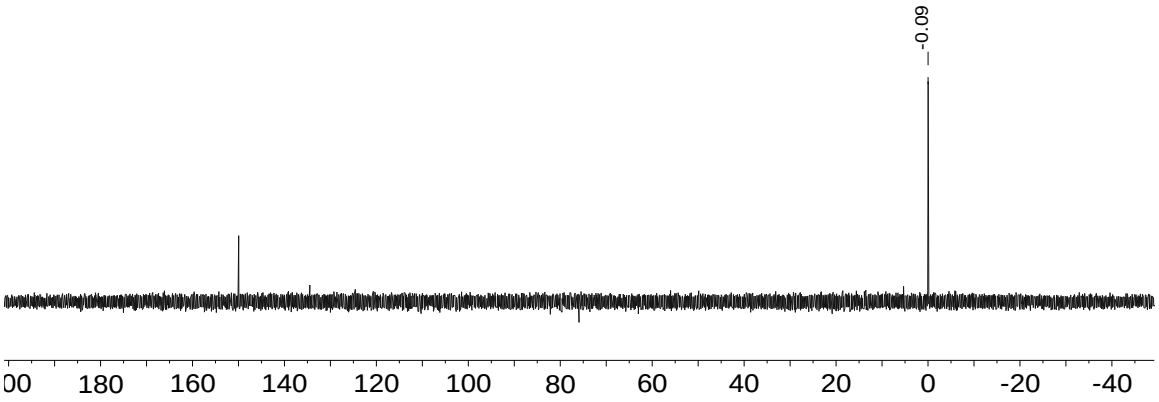

Figure C.141. ^{1}H NMR spectrum of **71** in $CDCl_3$.

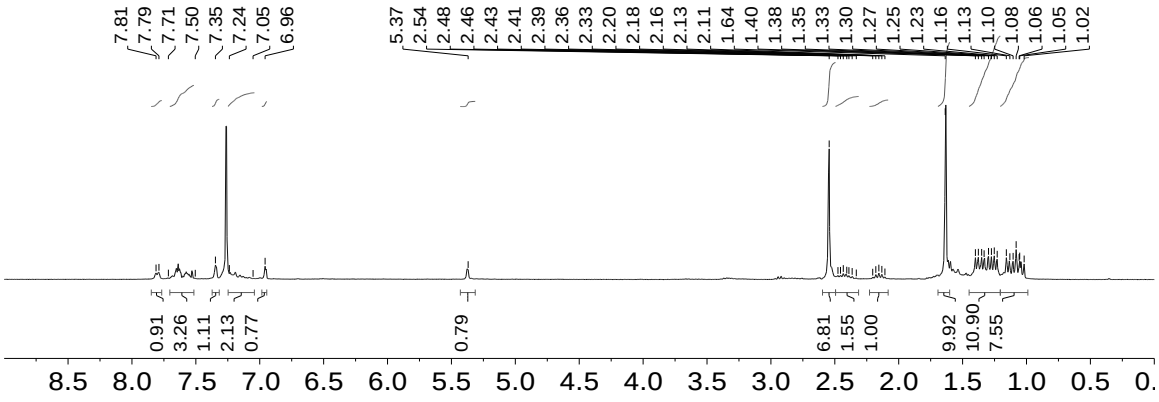

Figure C.142. $^{31}P\{^{1}H\}$ NMR spectrum of **71** in $CDCl_3$.

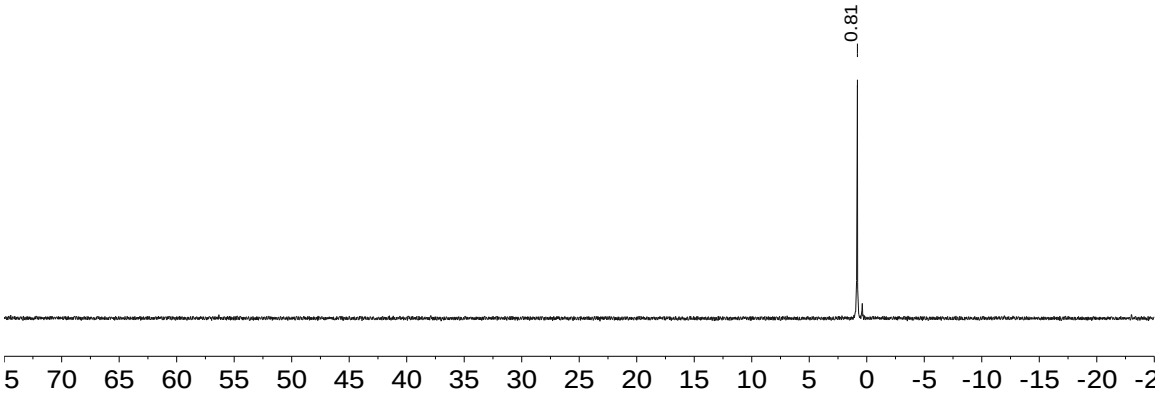

Figure C.143. ^{1}H NMR spectrum of **71** in C_6D_6.

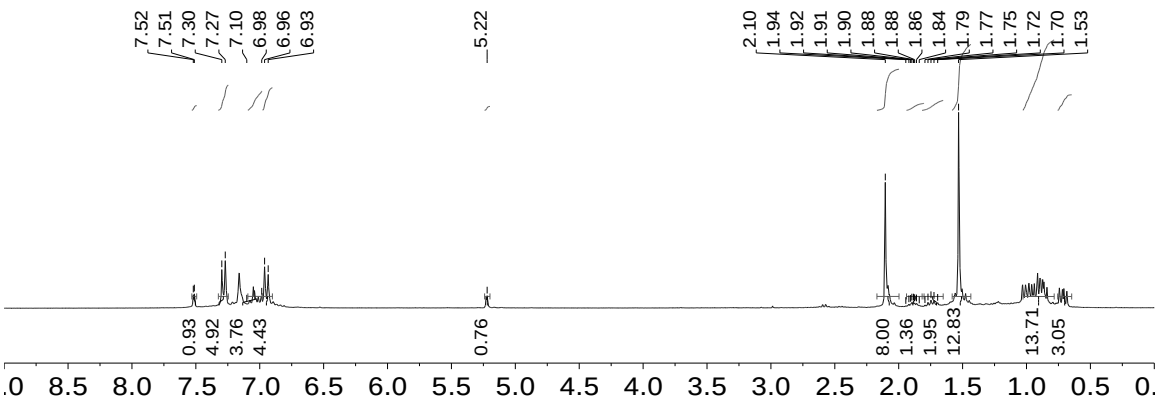

Figure C.144. $^{31}P\{^{1}H\}$ NMR spectrum of **71** in C_6D_6.

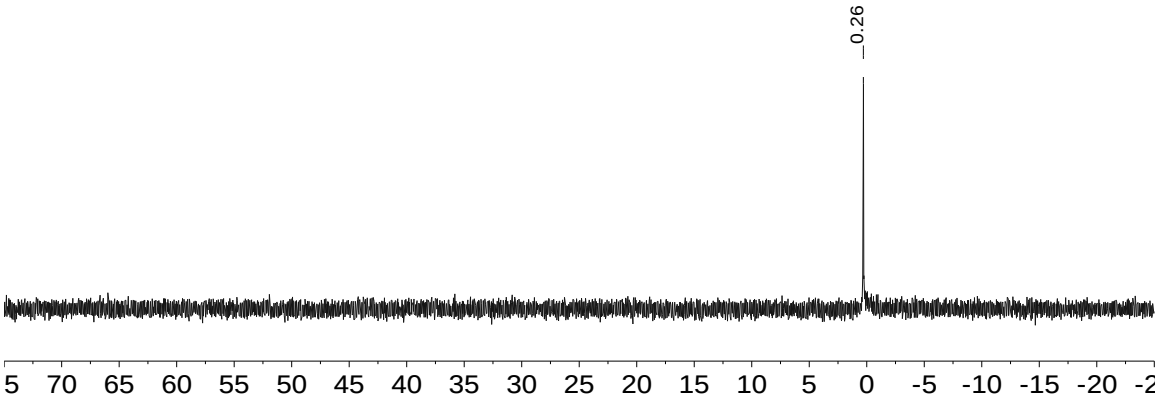

Figure C.145. ^{1}H NMR spectrum of **72** in C_6D_6. Note: Residual toluene and tetrahydrofuran present.

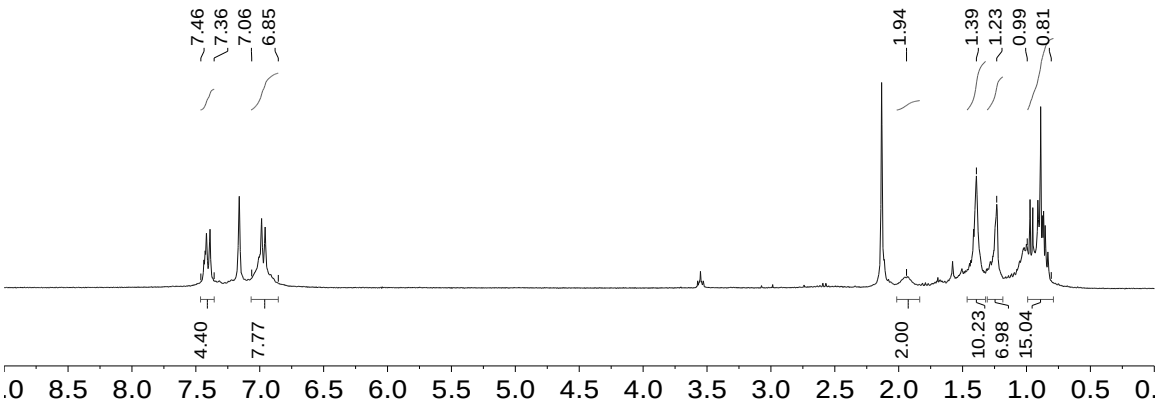

Figure C.146. $^{31}P\{^{1}H\}$ NMR spectrum of **72** in C_6D_6.

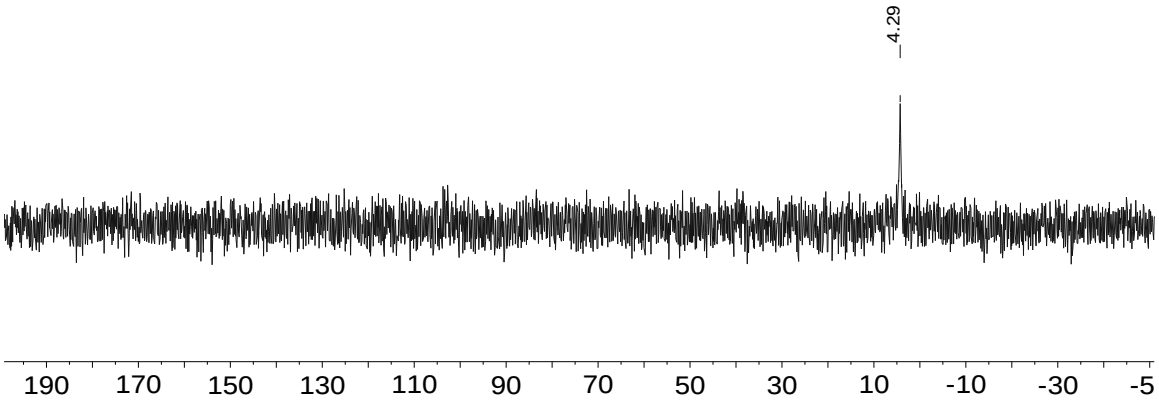

ABOUT THE AUTHOR

Guy Anthony Edouard was born in Boston, MA, on August 28, 1987, son of Marise Valbrun Edouard and Guy Milhaud Edouard, who met in their hometown of Cap Haïtien, Haiti. He was raised in Brockton, MA, with his two brothers, Rudy and Alan. In Brockton, he attended St. Edward's School and Cardinal Spellman High School. After high school, he graduated from Harvard College with a B. A. in Chemical and Physical Biology in 2010, where he performed research in the laboratory of Prof. Ted Betley. His Ph. D. studies were completed in the laboratory of Prof. Theo Agapie at the California Institute of Technology. In 2016, he left Pasadena to begin work as an engineer with Intel at their research and development facility in Hillsboro, OR. Guy's interests have long included but are not limited to: high school and college Mock Trial competitions and trial advocacy, Haitian food, standup comedy, playing basketball, and rooting for the Celtics and Patriots.

"When I picture him heading south in his own car with the top down, it always makes me laugh. Andy Dufresne... who crawled through a river of ---- and came out clean on the other side. Andy Dufresne... headed for the Pacific."

Red, *The Shawshank Redemption* (1994)